Synthesis, Characterization and Biological Properties of Schiff Base and Mixed ligand Complexes of Copper and Zinc

A

Thesis

Submitted to

For the award of

DOCTOR OF PHILOSOPHY (Ph.D)

in

Chemistry

By

Nidhi Aggarwal

(41300103)

Supervised By

Dr. Suman Maji

LOVELY FACULTY OF TECHNOLOGY AND SCIENCES
LOVELY PROFESSIONAL UNIVERSITY
PUNJAB
2019

ABSTRACT

Coordination chemistry is the chemistry of metal complexes where ligand is coordinated to the metal atom through coordinate covalent bond. Metal complexes are generally known for their easy preparation, extreme stability and chelating properties. Therefore they have attracted the attention of chemists all over the globe which resulted in the appearance of new branches of chemistry in recent past viz. biochemistry, organometallic chemistry and bioinorganic chemistry. These are fast developing fields as they help to understanding the role and structure of metal ions in living systems. Among them, Schiff bases and mixed ligand complexes with metal ions have shown fascinating results. Millions of people lost their lives every year due to microbial infections viz. bacterial and fungal infections. So there is dire need to develop promising medicines those can cure these infectious diseases. Schiff bases if designed with proper structural relationships can give potential compounds which can show potential therapeutic activity.

It is observed from literature that –C=N- based Schiff bases can be used in wide variety of therapeutic drug activities. The possibility of mixed ligand synthesis by the combination of Schiff bases with 2,2'-bipyridine and 1,10-phenonthroline provide a new platform to prepare better complexes with transition metal complexes. The ligands are synthesized with a new strategy of funtionalization of diketones rather than the usual approach of diamines as starting materials. The ligands should be able to provide a different coordination approach from the existing ones due to different stereo-chemical positioning of the ligating atoms. Also very few reports are available that check the interactions of mixed ligand complexes of this category with serum proteins. As per gap in literature it is expected that there is a good scope to prepare new combinations of mixed ligand complexes with Schiff bases and dinitrogen donor ligands (2,2'-bipyridine and 1,10-phenonthroline) with selected transition metals and they will show promising results in the directions of therapeutics activity and binding with serum albumin protein.

This work focused on the synthesis of new as well as previously reported mixed ligand complexes of copper and zinc (***1- 40***) with either Schiff bases (**L_1- L_8)** as primary ligands and diimines (1,10- phenanthroline or 2,2'-bipyridine) as secondary ligands or as simple mixed ligand chelates. The reactions were carried out between metal (II) chloride, synthesized Schiff base and diimines in the molar ratio 1:1:1 using methanol as solvent. The precipitates obtained were washed with methanol and dried in desiccator. The whole work was carried out in four series:

A) Synthesis of Schiff base of glyoxal and ortho / para - anisidine and their metal complexes with Cu(II) or Zn(II) and diimines

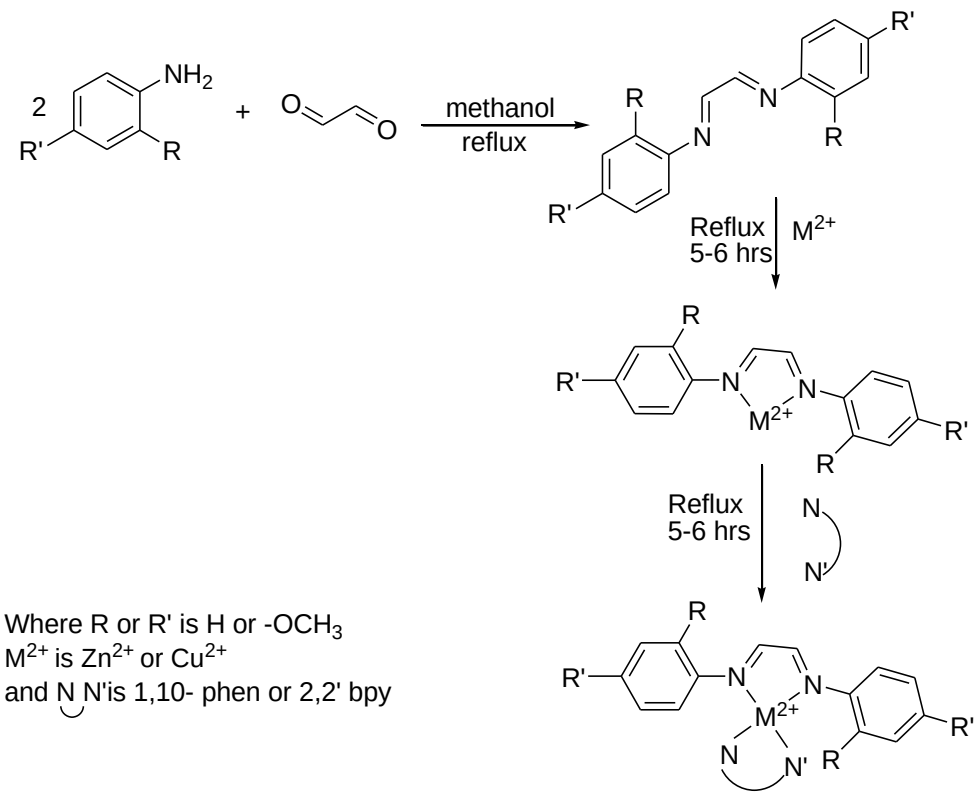

Where R or R' is H or -OCH_3
M^{2+} is Zn^{2+} or Cu^{2+}
and N N'is 1,10- phen or 2,2' bpy

B) Synthesis of Schiff base of benzil and ortho / meta / para - anisidine and their metal complexes with Cu(II) or Zn(II) and diimines

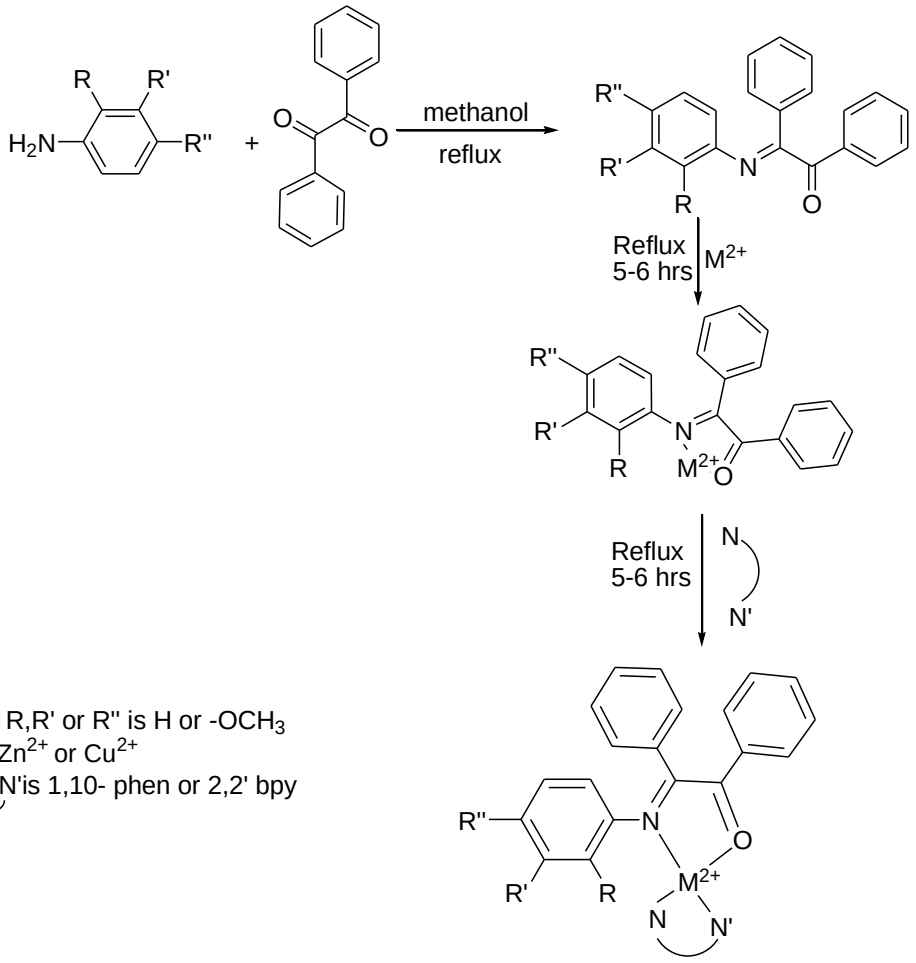

Where R,R' or R'' is H or -OCH_3
M^{2+} is Zn^{2+} or Cu^{2+}
and N N'is 1,10- phen or 2,2' bpy

C) Synthesis of Schiff base of *o*-aminophenol and glyoxal / diacetyl / benzil and their metal complexes with Cu(II) or Zn(II) and diimines

(i) Scheme for the synthesis Schiff base of *o*-aminophenol and glyoxal / diacetyl and their metal complexes with Cu(II) or Zn(II) and diimines

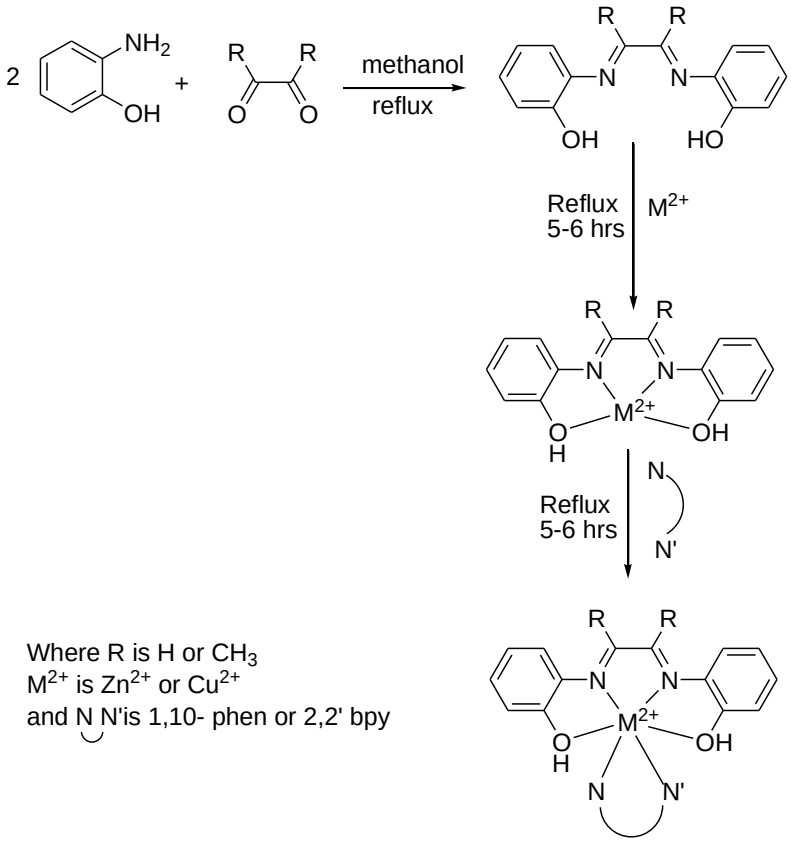

(ii) Scheme for the synthesis Schiff base of *o*-aminophenol and benzil and their metal complexes with Cu(II) or Zn(II) and diimines

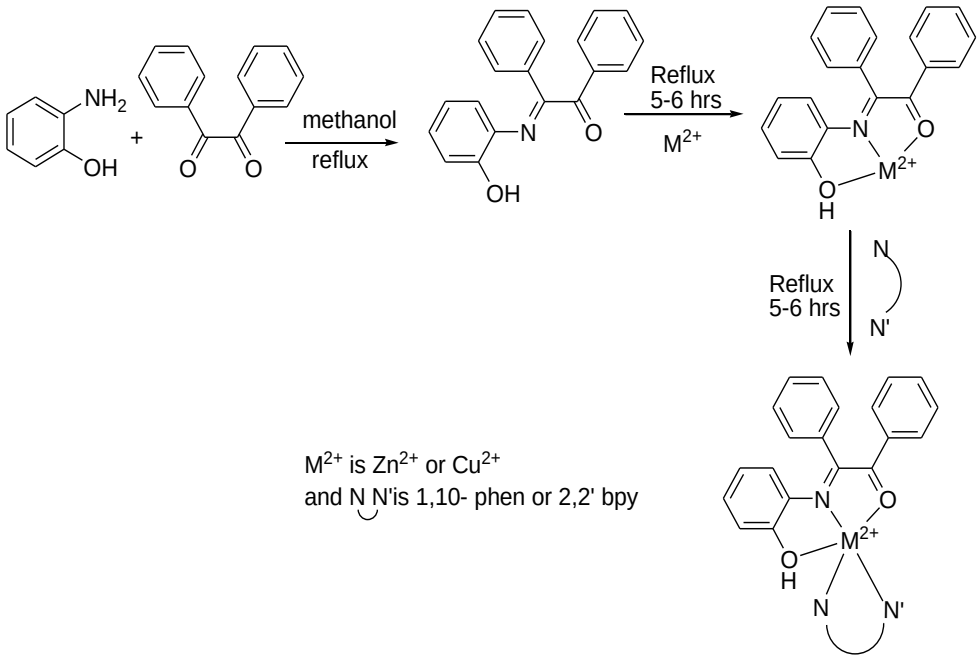

D) Scheme for the synthesis of mixed ligand complexes of copper and zinc with salicylic acid / 3,5-dinitrosalicylic acid as primary ligand and diimines as secondary ligand.

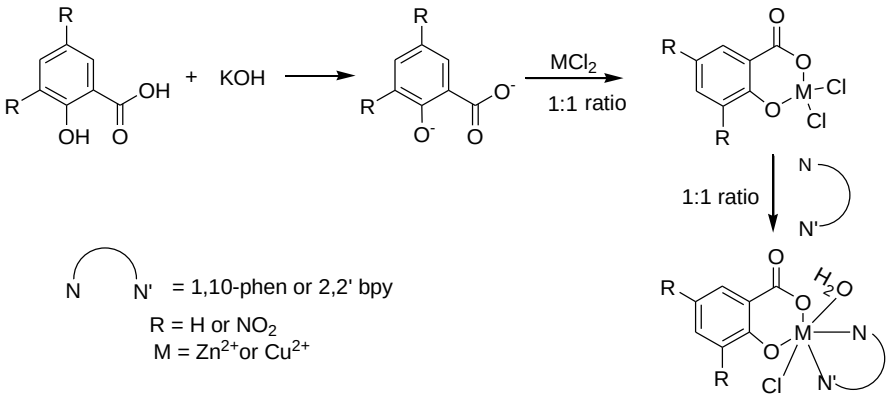

All the synthesized ligands and their metal complexes were characterized using different spectroscopic techniques i.e UV-vis, FTIR, ^{1}H NMR and Mass spectral techniques. Shifting in the peaks of the ligands in the UV-vis spectroscopy indicates coordination of ligand to metal ions. The analysis of IR spectrum further supports binding of ligand to metal ions through nitrogen and oxygen donor atoms. The formation of ligands and metal complexes were also confirmed by m/z values obtained by mass spectroscopy.

In vitro analysis of binding constants of ligands and their metal chelates were done with bovine serum albumin using UV-vis spectral technique. For analysis, the solutions of metal chelates (50 μM) and BSA (1000 μM) were prepared in tris buffer of pH 7.4. The UV-vis spectra were recorded by taking static concentration of metal complex (50 μM) vs. dynamic [BSA] concentrations in the array of 0 - 3 μM. The values of binding constants thus calculated come out in the range of 10^4 - 10^6. The moderate values of binding constants are consistent in determining the role of serum proteins as transporter for effective delivery of drugs to their target sites.

The antimicrobial assays of the ligands and their metal chelates were determined by agar well diffusion method against two bacterial species i.e *Escherichia coli and Staphylococcus aureus* and two fungal species i.e. *Aspergillus niger and Aspergillus fumigatus.* Antimicrobial activity of standard antibiotic drug amikacin against test bacteria and fluconazole against test fungi was evaluated by agar disc diffusion method. The results of antimicrobial assays indicate that mixed ligand metal chelates are more biologically active as compared to their Schiff base ligand.

DECLARATION

I hereby declare that the thesis entitled **"Synthesis, Characterization and Biological Properties of Schiff Base and Mixed ligand Complexes of Copper and Zinc"** submitted in fulfillment of the requirement for the award of degree of **Doctor of Philosophy in Chemistry** under the supervision of **Dr Suman Maji**, **Associate Professor in Chemistry, Lovely Professional University, Phagwara** is entirely my original work and all ideas and references have been duly acknowledged. It does not contain any work for the award of any other degree or diploma or fellowship at any other institute or university.

Nidhi Aggarwal

Regd. No: 41300103

Department of Chemistry

Lovely Professional University

Phagwara-144402

Date:

CERTIFICATE

This is to certify that Nidhi Aggarwal has completed her Ph.D thesis entitled **"Synthesis, Characterization and Biological Properties of Schiff Base and Mixed ligand Complexes of Copper and Zinc"** for the award of degree of **Doctor of Philosophy in Chemistry at Lovely Professional University, Phagwara** under my guidance and supervision. To the best of my knowledge, the present work is the result of her original investigation and study. No part of this thesis has ever been submitted for any other degree of fellowship previously at this or any other university or institute.

The thesis is fit for the submission and the partial fulfillment of the conditions for the award of degree of Doctor of Philosophy in Chemistry.

Dr. Suman Maji

UID: 18432

Associate Professor

Department of Chemistry

Lovely Professional University

Phagwara-144402

Date:

ACKNOWLEDGEMENT

The preparation of the thesis has been a long journey for me. The successful completion of this thesis was made possible by the support and encouragement of the many people. I take this opportunity to express my gratitude to them.

First of all my gratitude goes to Almighty for giving me this privilege and grace to go through the entire process of writing this thesis. Without his hidden guidance and support, it was not possible to complete the journey full of obstacles.

It would have been distant dream without the constant support and help of my supervisor **Dr. Suman Maji**, Associate Professor, Lovely Professional University, Phagwara. With his constant motivation and support, it was made possible to meet the deadlines and complete the research program. His untiring support, constant encouragement, enthusiastic approach, feeling of being there always whenever I needed him or approached him during the research work in time, always motivated me to fulfill his aspirations and to complete my task on time. He not only provided dexterous guidance but also shared his valuable thought provoking experiences in carrying out the research work timely. His scientific contributions blended with result oriented investigation in present work cannot be summed up in few words and I will not be fulfilling my duty without due acknowledgement to him. Sir, accept my heartiest thanks for shaping my raw knowledge in some concrete shape.

I would also like to extend my sincere thanks to **Dr. Sameena Mehtab** for her earlier guidance and initiating the process of getting enrolled to the program. Her guidance has been with me right from initial phase of writing synopsis till the final dissertation and has been a great help always.

I am also grateful to Dr. Ramesh Thakur, Dr. Rekha, Dr. Gurpinder Singh and Dr. Jandeep Singh, faculties at LPU Phagwara, who besides motivating also gave valuable suggestions during the course of my research work. I am also thankful to Dr. Gaurav, Assistant Professor, LPU and his student Ms. Charisma who have helped me in carrying out anti-microbial activities.

I owe my cordial thanks to all the lab staff particularly Mr. Manoj and Ms. Rinki for their assistance in the lab whenever needed.

I would also acknowledge Mr. Rishikant and Mr. Dharmendra, research scholars at LPU, for sharing their experiences during the interactions as part of my present study and providing valuable inputs.

I am thankful and express my love towards my husband **Mr. Pankaj Goel** (Asstt. Prof., GNIMT, Ludhiana) for his never ending unconditional support, enthusiasm and understanding throughout this phase of writing dissertation. This acknowledgement is incomplete without expressing my love to my son **Sourish** for his continuous motivation and love. I have no words to express my thanks to my mother **Ms. Kanchan** and brother **Rupesh Kumar** for their support and encouragement during the research work. I here, would like to acknowledge my father **Late Sh. Gulshan Kumar** who sayings are still a source of immense inspiration for me to achieve my dreams.

Last but not least I also thank all those people who have contributed directly or indirectly in my research work.

NIDHI AGGARWAL

TABLE OF CONTENTS

LIST OF TABLES

	Cu(II) mixed ligand chelates
15	Values of Binding constant values ($K_b M^{-1}$)
16	Antimicrobial activity of ligand and complexes (Concentration of 5 mg ml^{-1})
17	Selected bond frequencies (cm^{-1}) and UV-vis values of ligands, Zn(II) and Cu(II) mixed ligand chelates
18	Values of binding constant ($K_b M^{-1}$)
19	Antimicrobial activity of ligand and complexes (Concentration of 5 mg ml^{-1})
20	Selected bond frequencies (cm^{-1}) and UV-vis values of ligands, Zn(II) and Cu(II) mixed ligand chelates
21	Values of binding constant ($K_b M^{-1}$)
22	Antimicrobial activity of ligand and complexes (Concentration of 5 mg ml^{-1})
23	Selected bond frequencies (cm^{-1}) of synthesized complexes
24	Values of binding constant ($K_b M^{-1}$)
25	Antimicrobial activity of mixed ligand complexes (Concentration of 5 mg ml^{-1})

LIST OF FIGURES

81	(A) UV-vis titration graphs of complex $[Cu(L_3)(phen)]Cl_2$ (50 μM) with incremental [BSA] concentration in the range of 0 – 3 μM
	(B) Graph of {[BSA complex with $[Cu(L_3)(phen)]Cl_2$ – [Variant concentrations of [BSA]}
	(C) Graph of $1 / (A-A_0)$ vs. 1 / [BSA] concentration
82	(A) UV-vis titration graphs of complex $[Cu(L_3)(bpy)]Cl_2$ (50 μM) with incremental [BSA] concentration in the range of 0 – 3 μM
	(B) Graph of {[BSA complex with $[Cu(L_3)(bpy)]Cl_2$ – [Variant concentrations of [BSA]}
	(C) Graph of $1 / (A-A_0)$ vs. 1 / [BSA] concentration
83	(A) UV-vis titration graphs of complex $[Zn(L_4)phen]Cl_2$ (50 μM) with incremental [BSA] concentration in the range of 0 – 3 μM
	(B) Graph of {[BSA complex with $[Zn(L_4)phen]Cl_2$ – [Variant concentrations of [BSA]}
	(C) Graph of $1 / (A-A_0)$ vs. 1 / [BSA] concentration
84	(A) UV-vis titration graphs of complex $[Zn(L_4)bpy]Cl_2$ (50 μM) with incremental [BSA] concentration in the range of 0 – 3 μM
	(B) Graph of {[BSA complex with $[Zn(L_4)bpy]Cl_2$ – [Variant concentrations of [BSA]}
	(C) Graph of $1 / (A-A_0)$ vs. 1 / [BSA] concentration
85	(A) UV-vis titration graphs of complex $[Cu(L_4)(bpy)]Cl_2$ (50 μM) with incremental [BSA] concentration in the range of 0 – 3 μM
	(B) Graph of {[BSA complex with $[Cu(L_4)(bpy)]Cl_2$ – [Variant concentrations of [BSA]}
	(C) Graph of $1 / (A-A_0)$ vs. 1 / [BSA] concentration

86	(A) UV-vis titration graphs of complex $[Zn(L_5)(phen)]Cl_2$ (50 μM)with incremental [BSA] concentration in the range of 0 – 3 μM
	(B) Graph of {[BSA complex with $[Zn(L_5)(phen)]Cl_2$ – [Variant concentrations of [BSA]}
	(C) Graph of 1 / ($A-A_0$) vs. 1 / [BSA] concentration
87	(A) UV-vis titration graphs of complex $[Zn(L_5)bpy]Cl_2$ (50 μM) with incremental [BSA] concentration in the range of 0 - 3μM
	(B) Graph of {[BSA complex with $[Zn(L_5)bpy]Cl_2$ – [Variant concentrations of [BSA]}
	(C) Graph of 1 / ($A-A_0$) vs. 1 / [BSA] concentration
88	(A) UV-vis titration graphs of complex $[Cu(L_5)(phen)]Cl_2$ (50 μM) with incremental [BSA] concentration in the range of 0 – 3 μM
	(B) Graph of {[BSA complex with $[Cu(L_5)(phen)]Cl_2$ – [Variant concentrations of [BSA]}
	(C) Graph of 1 / ($A-A_0$) vs. 1 / [BSA] concentration
89	(A) UV-vis titration graphs of complex $[Cu(L_5)bpy]Cl_2$ (50 μM) with incremental [BSA] concentration in the range of 0 - 3μM
	(B) Graph of {[BSA complex with $[Cu(L_5)bpy]Cl_2$ – [Variant concentrations of [BSA]}
	(C) Graph of 1 / ($A-A_0$) vs. 1 / [BSA] concentration
90	Antimicrobial assay of Schiff base ligand (L_3) and its metal chelate (Alphabet levels are according to table 19.
91	Antimicrobial assay of Schiff base ligand (L_4) and its metal chelate (*13 - 16*) (Alphabet levels are according to table 19.
92	Antimicrobial assay of Schiff base ligand (L_5) and its metal chelate (*17 - 20*) (Alphabet levels are according to table 19).
93	Scheme for synthesis Schiff base (L_6)

126	(A) UV-vis titration graphs of complex $[Zn(L_7)(bpy)]Cl_2$ (50 μM) with incremental [BSA] concentration in the range of 0 – 3 μM
	(B) Graph of {[BSA complex with $[Zn(L_7)(bpy)]Cl_2$ – [Variant concentrations of [BSA]}
	(C) Graph of 1 / ($A-A_0$) vs. 1 / [BSA] concentration
127	(A) UV-vis titration graphs of complex $[Zn(L_8)(phen)]Cl_2$ (50 μM) with incremental [BSA] concentration in the range of 0 – 3 μM
	(B) Graph of {[BSA complex with $[Zn(L_8)(phen)]Cl_2$ – [Variant concentrations of [BSA]}
	(C) Graph of 1 / ($A-A_0$) vs. 1 / [BSA] concentration
128	(A) UV-vis titration graphs of complex $[Zn(L_8)(bpy)]Cl_2$ (50 μM) with incremental [BSA] concentration in the range of 0 – 3 μM
	(B) Graph of {[BSA complex with $[Zn(L_8)(bpy)]Cl_2$ – [Variant concentrations of [BSA]}
	(C) Graph of 1 / ($A-A_0$) vs. 1 / [BSA] concentration
129	Antimicrobial assay of Schiff base ligand (L_6) and its metal chelate (*21* - *24*) (Alphabet levels are according to table 22)
130	Antimicrobial assay of Schiff base ligand (L_7) and its metal chelate (*25* - *28*) (Alphabet levels are according to table 22)
131	Antimicrobial assay of Schiff base ligand (L_8) and its metal chelate (*29* - *32*) (Alphabet levels are according to table 22)
132	General scheme for the preparation of the complexes
133	Proposed geometry of [Zn(sal)(phen)Cl] *(33)*
134	Proposed geometry of [Zn(sal)(bpy)]Cl *(34)*
135	Proposed geometry of [Zn(DNSA)(phen)]Cl *(35)*

151	(A) UV-vis titration graphs of complex [Zn(DNSA)(bpy)]Cl (50 μM) with incremental [BSA] concentration in the range of 0 – 3 μM
	(B) Graph of {[BSA complex with [Zn(DNSA)(bpy)]Cl –[Variant concentrations of [BSA]}
	(C) Graph of 1 / (A-A_0) vs. 1 / [BSA] concentration
152	(A) UV-vis titration graphs of complex [Cu(sal)(phen)]Cl (50 μM) with incremental [BSA] concentration in the range of 0 – 3 μM
	(B) Graph of {[BSA complex with [Cu(sal)(phen)]Cl – [Variant concentrations of [BSA]}
	(C) Graph of 1 / (A-A_0) vs. 1 / [BSA] concentration
153	(A) UV-vis titration graphs of complex [Cu(sal)(bpy)]Cl (50 μM) with incremental [BSA] concentration in the range of 0 - 3 μM
	(B) Graph of {[BSA complex with [Cu(sal)(bpy)]Cl – [Variant concentrations of [BSA]}
	(C) Graph of 1 / (A-A_0) vs. 1 / [BSA] concentration
154	(A) UV-vis titration graphs of complex [Cu(DNSA)(phen)]Cl (50 μM) with incremental [BSA] concentration in the range of 0 – 3 μM
	(B) Graph of {[BSA complex with [Cu(DNSA)(phen)]Cl – [Variant concentrations of [BSA]}
	(C) Graph of 1 / (A-A_0) vs. 1 / [BSA] concentration
155	(A) UV-vis titration graphs of complex [Cu(DNSA)(bpy)]Cl (50 μM) with incremental [BSA] concentration in the range of 0 – 3 μM
	(B) Graph of {[BSA complex with [Cu(DNSA)(bpy)]Cl – [Variant concentrations of [BSA]}
	(C) Graph of 1 / (A-A_0) vs. 1 / [BSA] concentration

156	Antimicrobial activity of mixed ligand complexes of zinc (*33 - 36*) (Alphabetical levels are according to table 25)
157	Antimicrobial activity of mixed ligand complexes of copper *(37 - 40)* (Alphabetical levels are according to table 25)

LIST OF ANNEXURE

3g	IR of $[Cu(L_3)phen]Cl_2$
3h	IR of $[Cu(L_3)bpy]Cl_2$
3i	IR of (L_4)
3j	IR of $[Zn(L_4)phen]Cl_2$
3k	IR of $[Zn(L_4)bpy]Cl_2$
3l	IR of $[Cu(L_4)phen]Cl_2$
3m	IR of $[Cu(L_4)bpy]Cl_2$
3n	IR of (L_5)
3o	IR of $[Zn(L_5)phen]Cl_2$
3p	IR of $[Zn(L_5)bpy]Cl_2$
3q	IR of $[Cu(L_5)phen]Cl_2$
3r	IR of $[Cu(L_5)bpy]Cl_2$
3s	NMR spectra of L_3
3t	NMR spectra of L_4
3u	NMR spectra of L_5
4a	UV spectra of (L_6) Schiff base and its metal complexes
4b	UV spectra of (L_7) Schiff base and its metal complexes
4c	UV spectra of (L_8) Schiff base and its metal complexes
4d	IR spectra of (L_6)
4e	IR spectra of $[Zn(L_6)(phen)Cl_2]$
4f	IR spectra of $[Zn(L_6)(bpy)Cl_2]$
4g	IR spectra of $[Cu(L_6)(phen)Cl_2]$
4h	IR spectra of $[Cu(L_6)(bpy)Cl_2]$
4i	IR spectra of (L_7)
4j	IR spectra of $[Zn(L_7)(phen)Cl_2]$

4k	IR spectra of $[Zn(L_7)(bpy)Cl_2]$
4l	IR spectra of $[Cu(L_7)(phen)Cl_2]$
4m	IR spectra of $[Cu(L_7)(bpy)Cl_2]$
4n	IR of (L_8)
4o	IR spectra of $[Zn(L_8)(phen)Cl].H_2O$
4p	IR spectra of $[Zn(L_8)(bpy)Cl].H_2O$
4q	IR spectra of $[Cu(L_8)(phen)Cl].H_2O$
4r	IR spectra of $[Cu(L_8)(bpy)Cl].H_2O$
4s	NMR of (L_6)
4t	NMR of (L_7)
4u	NMR of (L_8)
5a	UV spectra of mixed ligand complexes of zinc
5b	UV spectra of mixed ligand complexes of copper
5c	IR spectra of [Zn(sal)(phen)]Cl
5d	IR spectra of [Zn(DNSA)(phen)]Cl
5e	IR spectra of [Zn(sal)(bpy)]Cl
5f	IR spectra of [Zn(DNSA)(bpy)]Cl
5g	IR spectra of [Cu(DNSA)(bpy)]Cl
5h	IR spectra of [Cu(sal)(phen)]Cl
5i	IR spectra of [Cu(DNSA)(phen))]Cl
5j	IR spectra of [Cu(DNSA)(bpy)]Cl

GLOSSARY OF ABBREVIATIONS

phen	1,10-phenanthroline
bpy	2,2'-bipyridine
HSA	Human Serum Albumin
BSA	Bovine serum albumin
MBS	Multi-metal Binding Site
ATCUN motif	Copper and Nickel binding site
HBAA	hydroxybenzalidineanthranillic acids
HQ	8-hydroxyquinoline
MIC	Minimum Inhibitory Concentration
IZ	Inhibition Zone
dppz	Dipyridophenazine
phen-dione	Phenanthroline - dione
DA	Dodecylamine
thr	DL - threonine
gly	Glycine
DL-ala	DL - alanine
c-dmg	2-dimethylglycine
Sar	Sarcosine
MS	5-methylsalicylaldehyde
gly	Glyoxal

o-andn	*o*-anisidine
m-andn	*m*-anisidine
p-andn	*p*-anisidine
o-amp	*o*-aminophenol
sal	Salicylic acid
3,5-DNSA	3,5-dinitrosalicylic acid
DMSO	Dimethylsulphoxide
DMF	Dimethylformamide
TMS	Tetramethylsilane

GENERAL INSTRUMENTATION AND MATERIAL USED

A) Materials

(i) Chemicals from Loba chemie: *o*-anisidine, *m*-anisidine, *p*-anisidine, benzil, diacetyl, o- aminophenol, salicylic acid, 3,5-dinitrosalicylic acid, potassium hydroxide, zinc chloride, copper chloride, 2,2'-bipyridine, 1,10-phenanthroline, tris buffer.

(ii) Chemicals from CDH: Glyoxal

(iii) Chemicals from SDFCL: BSA

(iv) Preparation of Tris buffer (pH-7.4): In double distilled water.

B) General Instrumentation

(i) UV-vis spectroscopy: SHIMADZU UV-1800 spectrophotometer has been used for recording UV-vis absorption spectra at Department of Chemistry, Lovely Professional University, Punjab.

(ii) Infra-red spectroscopy: SHIMADZU FTIR 8400S, Fourier Transform Infrared spectrophotometer has been used for recording Infra-red spectra at Department of Chemistry, Lovely Professional University, Punjab.

(iii) ^{1}H NMR: BRUCKER ADVANCE I.I 400 NMR Spectrometer has been used for recording ^{1}H NMR spectra using d^{6} – DMSO / $CDCl_3$ as solvents with TMS as the internal reference at Panjab University, Chandigarh.

(iv) Mass spectroscopy: XEVO G2-XS QTOF Mass Spectrometer has been used for recording mass spectra using DMSO / Chloroform as solvent at IIT Ropar.

(v) Antibacterial and antifungal activity: The anti - microbial tests were conducted on two bacterial species i.e. *Staphylococcus aureus* (gram positive) and *Escherichia coli* (gram negative) and two fungal strains i.e. *Aspergillus niger* and *Aspergillus fumigatus* by well diffusion method at Department of Biotechnology, Lovely Professional University, Punjab.

CHAPTER 1

Introduction and Review of Literature

1.1 Introduction

Coordination complexes have been used and are known since olden times. Now days it is a fast growing branch of chemistry. In 1869, Christian Wilhelm Blomstrand tried to explain the structure of coordination complexes through his complex ion chain theory [1]. Later on Danish scientist, Sophus Mads Jorgensen made certain amendments but the most accepted theory was by Alfred Werner (a Swiss chemist) in 1893 [2]. He got noble prize in 1913, for his commendable work on coordination compounds [3].

In coordination complexes, a ligand is attached to the metal ion through coordinate covalent bond [4]. The thermodynamic and kinetic properties of the metal complexes can be altered by varying the coordination number, design of ligand and steric environment around central metal ion [5]. Thus chelation brings radical changes both in metal and ligand moieties. Metal complexes which are redox active and have labile ligands interacts easily with biological systems and extensively taking part in biological reactions [6]. This makes them suitable and reliable candidates for numerous biological applications and lead to the development of new branch of chemistry known as bioinorganic chemistry [7].

1.2 Chemistry and biological importance of metal ions and ligands

1.2.1 Copper

Copper is a soft and ductile reddish metal with atomic number 29. It shows two biologically accessible oxidation states i.e. Cu(I) and Cu(II). Cu(I) is less stable and is readily oxidized to Cu(II) but further oxidation to Cu(III) is relatively difficult [8 – 10]. The lack of cubic symmetry, due to Jahn- Teller distortions, in $3d^9$ electronic configuration of Cu(II) makes it less prone to adopt regular tetrahedral and octahedral geometries [11]. A variety of applications of copper and its compounds ranging from industry to biological systems can be viewed historically. Around 3000 BC it was

used by Egyptians to sterilize water and around 400 BC it was used by Hippocrats to cure leg ulcers allied with varicose veins [12].

Being one of the essential trace elements, copper is present in most of the tissues of the body. A large number of copper dependent enzymes are found in biological systems e.g. Cytochrome C oxidase is required for cellular utilization of oxygen, Angigenin for stimulation of blood vessels construction etc. [13]. It also plays a key role in the normal functioning of liver, triggers vitamin C to synthesize a connective tissue called elastin [14, 15]. Its deficiency in blood can lead to pregnancy disorders, heart diseases in children and improper absorption of iron in the body [12].

1.2.2 Zinc

The element with atomic number 30 i.e. zinc exists as five isotopes i.e. ^{70}Zn (0.62%), ^{67}Zn (4.90%), ^{68}Zn (18.75%), ^{66}Zn (27.90%) and ^{64}Zn (48.63%). It is a redox stable metal as it mainly shows +2 oxidation state in most of its compounds. It acts as a Lewis acid and owing to its small radius to charge ratio it forms quite strong coordinate covalent bonds with ligands containing nitrogen and oxygen as donor atom [16, 17].

Zinc, next to iron, is essentially required to human body. It is present as an essential structural component in enzymes and can also be located at their active sites [18]. Nearly eighty Zn - containing metalloenzymes have been known so far which are known to cure tissue injury, inflammatory diseases etc. [14]. It plays an essential role in cell division, cell growth, wound healing, breakdown of carbohydrate, nucleic acid synthesis, glycolysis etc. [19, 20]. Its deficiency has severely affected approximately two billion people globally and leads to many diseases like growth retardation in children, hair loss, delayed sexual maturation, infection susceptibility etc. [21, 22]. Various skin ointment creams used for curing minor burns, diaper rash and other minor skin ailments contain zinc oxide [12]. The studies have shown Zn(II) complexes as suppressants in elimination of histaminic parts from extra cellular fluids or base cells. Thus they can be used in the treatment of anafilactidic shocks. Hence they are the subject of demanding biological evaluation [23].

1.2.3 1,10-phenanthroline and 2,2'-bipyridine

Diimines i.e 2,2'-bipyridine and 1,10-phenanthroline are biochemically active but π - electron deficient nitrogen containing chiral bidentate ligands [24]. They are rigid, hydrophobic, planar and heteroaromatic chelating ligands and act as powerful σ-donors and π - acceptors due to the presence of low energy π* antibonding orbitals [25 – 27]. These ligands can stabilize low oxidation state transition metal ions and endow complexes with hydrophobic properties with inbuilt M-N bond strength complemented by the chelate effect [28, 29]. Australian chemist Francis P. Dwyer first studied the complexes of ruthenium with 2,2'-bipyridine and 1,10-phenanthroline having considerable biological activity [30]. The specific pharmacological activity of transition metal complexes with these N, N' donor ligands can be characterized by their enhanced antibacterial, antiviral, antitumor, antifungal activities [18, 31 – 33]. These type of complexes are gaining great interest as they can act as catalytic ligands, stabilizing agents in the synthesis of nanoparticles, luminescent devices, potential probe for DNA interactive and cleavage studies and show enormous pharmacological activity.

1.2.4 Serum albumins

Albumin is the most copious and comprehensively studied protein in the blood serum of ample assortment of organisms. It is the chief soluble protein in circulatory system and performs several physiological functions like maintenance of blood pH and regulation of osmotic pressure. By reversible mode of binding it transports and delivers large number of exogenous and endogenous compounds like bilirubin, hormones, fatty acids, porphyrins, amino acids, drugs etc. [34 – 36]. Researches on the study of interaction of these serum proteins with drugs can help to attain pharmodynamic and pharmokinetic information [37 – 39]. Human Serum Albumin (HSA) is the most copious protein in human plasma. Since BSA not only closely resembles Human Serum Albumin (HSA) but is cost effective, readily available, extensively characterized and helps in many vitro studies [40].

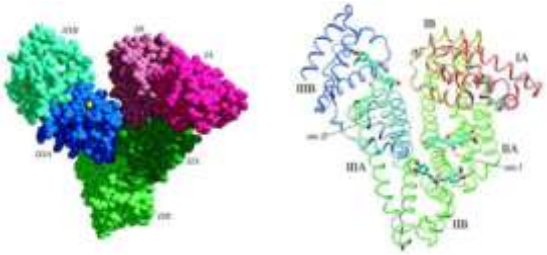

Fig. 1: Comparative structure of BSA and HSA [38]

Bovine serum albumin (BSA or Fraction V) is a large globular nonglycoprotein (65000 Daltons) having 583 amino acid residues in a single polypeptide chain in its primary structure while its secondary structure has 17 disulfide bridges and 67% α - helix which provides remarkable stability to the protein. It is alienated into three homologous, linear but structurally distinct domains (I - III), each of which is subsequently divided into two subdomains (A and B). There are mainly two binding regions namely Sudlow site I and site II located in subdomias IIA and IIIA which largely determines the binding capacity of serum albumin to heteroaromatic systems [23, 41 – 43]. BSA has two tryptophan residues i.e. Trp-212 (buried deep in hydrophobic pocket of domain IIA) and Trp-134 (on the surface of domain IB) which act as fluorophores and make the protein competent to fluorescence quenching [44, 45].

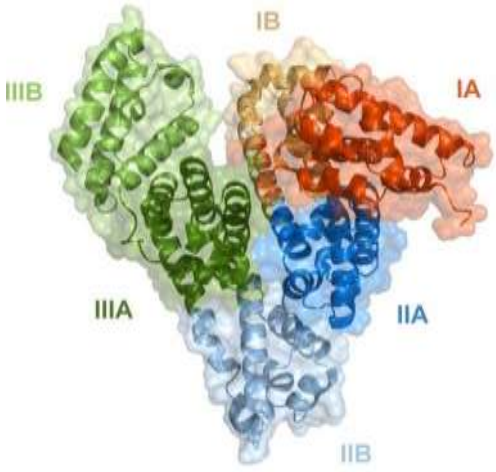

Fig. 2: A ribbon representation of BSA [41]

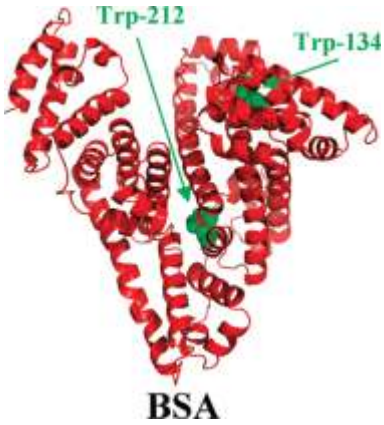

Fig. 3: Structure of Bovine Serum Albumin with tryptophan residues [45]

Albumin can swiftly acquire various configurations under the influence of a ligand. It can expand and contract rapidly owing to its flexibility. This rapid expansion and contraction of its major domains along with numerous amino acids is the root of its transport system as they facilitate the binding and release of transporting material. There are four metal binding sites on albumin have been identified so far and these are as follows:

- Multi - metal Binding Site (MBS) or Site A which binds primarily to M(II) ions particularly Zn^{+2}.
- The N - terminus or ATCUN motif (Copper and Nickel binding site).
- Platinum and gold complexes binding site on reduced thiol of Cys-34.
- Site B which binds primarily to Cd(II) and secondarily to Zn(II) [46].

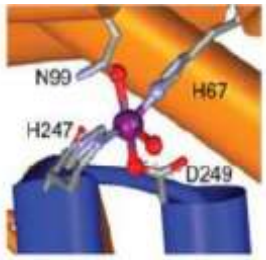

Fig. 4: Modeled structure of BSA representing inter-domain zinc site formed by His - 67 (Nε) and Asn - 99 (Oamide) from domain I and His – 247 (Nδ) and Asp - 249 (Ocarboxylate) from domain II [46]

1.2.5 Antimicrobial activity

Antimicrobials have been used around 2000 years back by ancient Egyptians and Greeks using molds and plant extracts to cure infections [47, 48]. They are the agents that can either kill (biostatic agent) or stop (microbiocidal agent) the growth of various microorganisms. These antimicrobial agents are categorized broadly on the basis of microorganisms on which they act e.g. antibiotics used for the treatment of bacteria and antifungals used for the treatment of fungi.

The era of antibiotics started in the year 1928 after the discovery of pencillin by Alexander Fleming but the term antibiotic was first used by Selman Waksman (discoverer of streptomycin) in the year 1941 [48 – 50]. The indiscriminate and hasty use of antibiotics not only poses a threat to human race across the globe by these single cell microorganisms but also put the mankind back to square. Gradually the bacteria are becoming more resistant to such antibiotics [51, 52]. The contest for their survival is making them more adaptive and powerful against the developments in the field of medicines. Keeping in mind the possible worst future scenario numerous alternate strategies are being kept handy. One of the possible alternatives is the production of metal based drugs as it has been demonstrated that antimicrobial activities of several compounds like Schiff bases have been enhanced on interaction with metal ions [53].

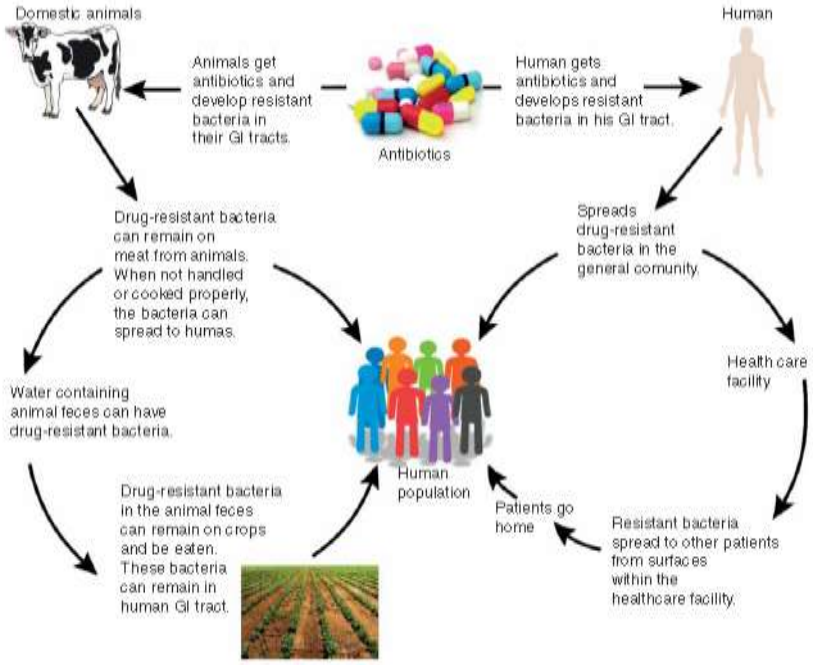

Fig. 5: Pathway of antibiotic resistance [54]

It is, therefore, considered worthwhile not only to synthesize, characterized new metal based mixed ligand complexes but also to determine the biological activity of these new complexes.

1.3 Schiff bases

Imines or Schiff bases were named after Italian naturalized chemist Hugo Schiff who first synthesized them in 1864 [55]. They are nitrogen analogs of aldehyde or ketone containing –C=N- group where nitrogen is attached to aryl or alkyl group and not to hydrogen atom. They are synthesized following condensation reaction amid a carbonyl compound (aldehyde or ketone) and a primary amine under varied solvents and reaction conditions [40, 56 – 58]. The reaction can be carried out either with or without acidic or basic conditions. In these reactions, hydrogen from amine and oxygen from carbonyl group react leading to formation of water molecule and another product known as Schiff base (Fig. 6) [59 – 61].

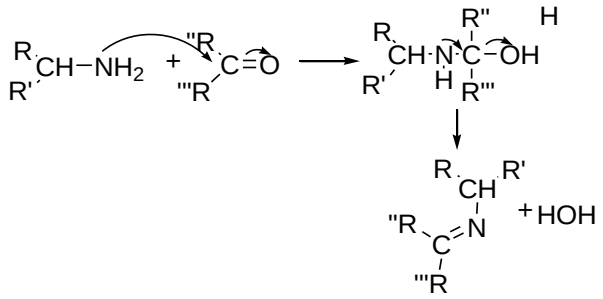

Fig. 6: Scheme for the synthesis of Schiff base [60]

This –C=N- imine bond is the main factor accountable for wide applicability of these azomethine compounds. There are generally three synthetic routes for their preparation:

- Direct synthesis of ligand followed by complexation [63]
- Template synthesis [62]
- Rearrangement of heterocycles [63]

Owing to their greater flexibility, sensitivity and selectivity, they appear as enzyme models and proved as effective reagents in trace analysis. There is also certain possibility of using Schiff bases as Acid - Base indicators. They have large number of widely accepted applications in the area of biological, analytical, nuclear, pharmacological, radio immunotherapy, clinical and biochemical fields [64, 65]. Their major applications are as follows:

- Biological models to elucidate the composition of biomolecules and biological procedures [66, 67]
- Electroluminescent materials owing to their good thermal stability and film forming capabilities [25]
- Fluorometric analytical reagents [68]
- Catalysts [69]
- Enzymatic intermediates having capability of providing synthetic models in metalloproteins [70]
- Medical substrates and fine chemicals [71]
- Organic blockers [72]
- Corrosion inhibitors [73]

- Tumor radio imaging agents [74]
- Optical, electrochemical and chemosensors [75, 76]
- Insecticides, herbicides, nematocides and rodenticides [77]
- Antibacterial, antifungal, antimalarial, anti-inflammatory, anticancerous and antidiabetic [13, 78 – 86]
- They also play significant role in transammination (transaminases are found in mitochondria), chemistry of vision and biosynthesis of porphyrins [78]

Schiff bases are also known to form complexes with "Metals of Life" like Zn, Cu, Ni, Co, Fe, Mn, Cr, V, Ca, Mg and Na [87, 88].

1.3.1 Types of Schiff bases

Extensive survey of literature makes us familiar with galaxy of Schiff bases and different methods either classical or others i.e. water suspension medium [89], infrared irradiation and no solvent [90, 91], ultrasound irradiation [92], one pot template synthesis [93], solvent free etc. [94] which are available today for their synthesis. The water produced during the reaction can be eliminated by dehydrating agents viz. $MgSO_4$, Na_2SO_4 or molecular sieves or by Dean Stark apparatus (while using benzene or toluene as a solvent) [74]. Schiff bases can be categorized as Salen, Salophen, Hydrazone, Semicarbazone or Thiosemicarbazone and Heterocyclic type.

1.3.2 Salen type ligand

The term salen refers to the N_2O_4 tetradentate ligand obtained by the condensation reaction between salicyladehyde and its derivatives with ethylenediamine in the molar ratio 2:1 (Fig.7) [95].

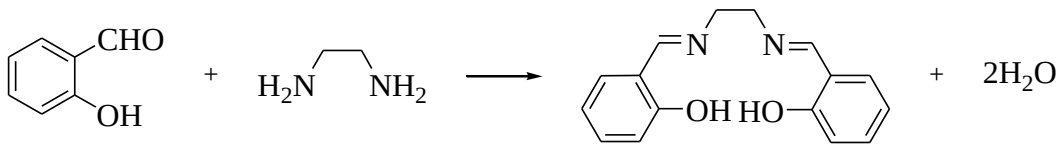

Fig. 7: General methodology for preparation of salen ligand [95]

A large variety of salen type ligands have been synthesized till date and they find large applications due to their convenient preparation, varied denticities and structural varieties [96 – 99].

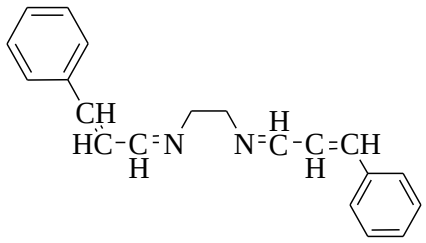

[96]

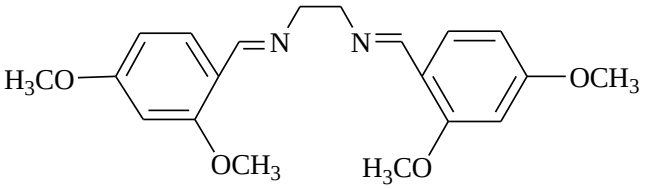

[98]

Fig. 8: Some examples of salen type ligands

1.3.3 Salophen type ligand

Like salen they are also tetradentate ligands with four donor atoms i.e. O, N, N, O synthesized by the reaction between salicyladehyde and its derivatives with 1,2-phenylenediamines.

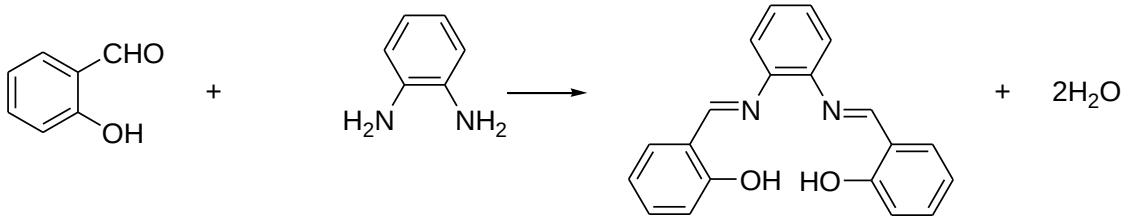

Fig. 9: General scheme for the synthesis of salophen type ligand

The captivating properties of these ligands can be unfolded from the huge content of literature. An enormous variety of their multimetallic complexes is available in literature to determine their coordination pattern with different metal ions [100 – 104].

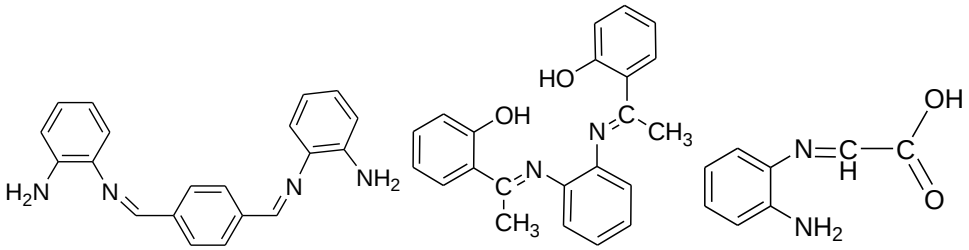

Fig. 10: Some examples of salophen type ligands

1.3.4 Hydrazone type ligand

These are another important class of ligands having general formula $R_1R_2C{=}NNHR_3$ having donor groups on R^n (where n ranges from 1 - 3) and are obtained by condensation reaction between carbonyl compounds (aldehyde or ketone) and hydrazine or its derivatives. They have engrossed the due consideration of chemists due to their large number of biological and pharmaceutical applications. These ligands have varied denticities ranging from monodentate to multidentate ligands [105 – 108].

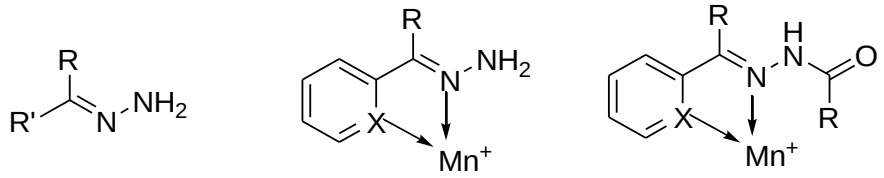

where R or R' = H, alkyl or aryl

X = OH, N, S or O

Fig. 11: General formula of hydrazone type ligands

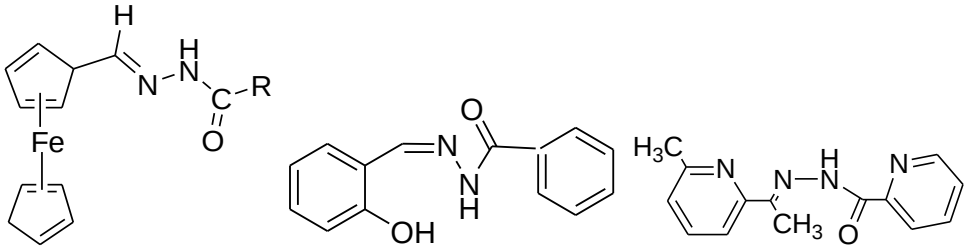

Fig. 12: Some examples of hydrazone type ligands

1.3.5 Thiosemicarbazone / Carbazone type ligand

Thiosemicarbazone ligands are an important class of nitrogen / sulphur compound which made their first emergence in literature in 1800 [62]. They form a novel class of biologically active compounds owing to their enhanced chelating capability and lipophilicity. They are obtained by the typical condensation reaction between an aliphatic, aromatic or heterocyclic aldehyde or ketone with thiosemicarbazide or carbazide.

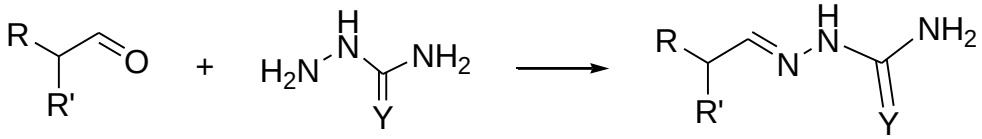

where R or R' = alkyl or aryl group

Y = Oxygen or Sulphur

Fig. 13: General scheme for the synthesis of thiosemicarbazone / carbazone type ligand

Large number of metal complexes with thiosemicarbazones has been recorded in the literature due to the presence of heteroatoms like nitrogen, oxygen and sulphur which shows remarkable chelating properties. Thus they can act either as bidentate or tridentate ligand by bonding metal ions both through the thiol sulfur atom (in thiosemicarbazones) or oxygen atom (in semicarbazones) or both and the hydrazine nitrogen atom [100, 109 – 113].

Fig. 14: Some examples of thiosemicarbazone / carbazone type ligands

1.3.6 Heterocyclic Schiff bases

Metal complexes with heterocyclic Schiff base are of substantial curiosity for the chemists. Ligand modifications are easily accessible due to preparative simplicity, structural variability and tunable electronic properties. Hetero atoms like N, O and S when incorporated in Schiff bases play a key role at binding sites in metallobiomolecules. Millions of people have to lose their lives every year owing to microbial infections. Moreover toxicity, side effects and drug resistance has strained the researchers to develop more compounds so as to reduce these drawbacks tethered with better efficiency. As transition metals form an integral part of biological system and become easily soluble in biological fluids, so they have been used in medicines for centuries [114, 115]. An overview of some of the Schiff bases containing N, O and S as heteroatom along with their metal complexes and activities has been listed below (Table1):

Table 1: List of some metal complexes of heterocyclic Schiff bases along with their biological activity

Compound 1	Compound 2	Schiff base	Metalion	Antimicrobial Activity	Reference No.
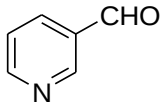 Pyridine-3-aldehyde	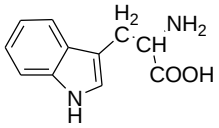 Tryptophan	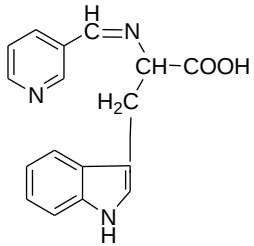	Zn(II) Cu(II) Ni(II) Co(II)	Antibacterial Antifungal	[116]
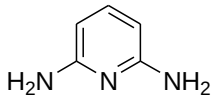 2,6-Diaminopyridine	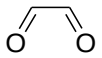 Glyoxal	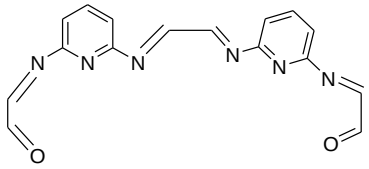	Co(II) Cu(II)	Antibacterial Antifungal	[117]
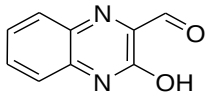 3-Hydroxyquinoxaline-2-carboxyaldehyde	 Ethylenediamine	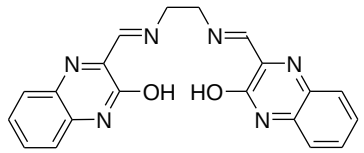	Ni(II) Co(II) Cu(II)	Catalytic	[118]

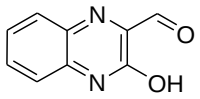 3-Hydroxyquinoxaline-2-carboxyaldehyde	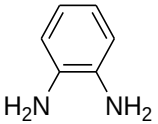 *o*-Phenylenediamine	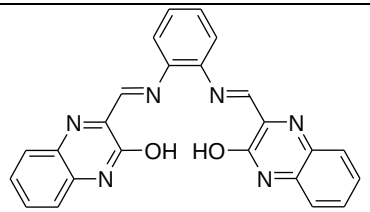	Cu(II) Co(II) Ni(II)	Catalytic	[118]
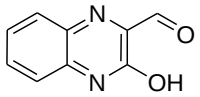 3-Hydroxyquinoxaline-2-carboxyaldehyde	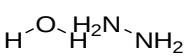 Hydrazine hydrate	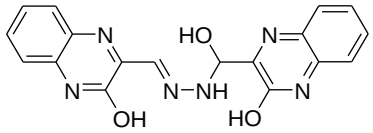	Cu(II) Co(II) Ni(II)	Catalytic	[118]
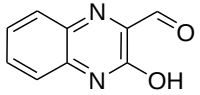 3-Hydroxyquinoxaline-2-carboxyaldehyde	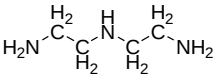 Diethylenetriamine	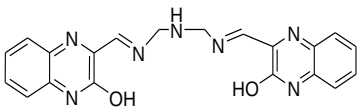	Co(II) Cu(II) Ni(II)	Catalytic	[118]
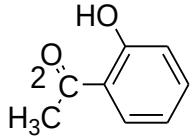 2-Hydroxyacetophenone	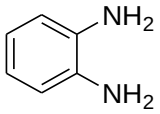 *o*-Phenylenediamine	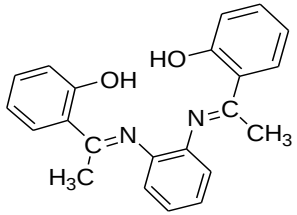	Co(II) Cu(II)	Antibacterial	[101]

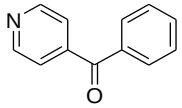 Phenyl(pyridine-4-yl)methanone	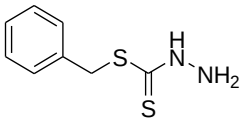 Benzylhydrazinecarbodithioate	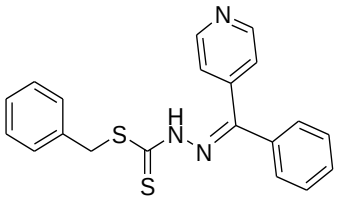	Cu(II) Ni(II) Zn(II)	-	[119]
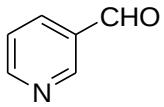 Pyridine-2 aldehyde	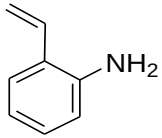 Vinyl aniline	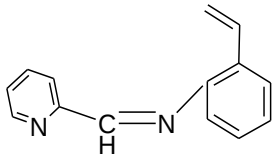	Cu(II) Ni(II) Co(II) Mn(II)	Antibacterial Antifungal	[120]
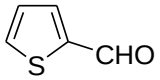 Thiophene-2-carboxyaldehyde	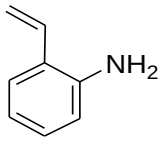 Vinyl alanine	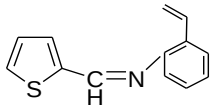	Cu(II) Ni(II) Co(II) Mn(II)	Antibacterial Antifungal	[120]
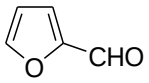 Furfuraldehyde	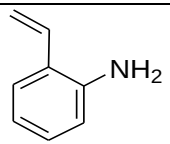 Vinyl alanine	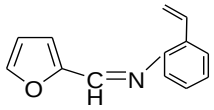	Cu(II) Ni(II) Co(II)	Antibacterial Antifungal	[120]

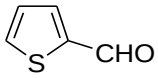 Thiophene-2-carboxyaldehyde	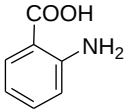 2-Aminobenzoic acid	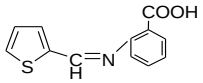	UO_2(II) Zn(II) Cu(II) Ni(II) Fe(III)	Antibacterial Antifungal	[121]
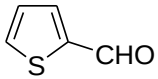 Thiophene-2-carboxyaldehyde	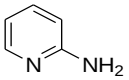 2-Aminopyridine	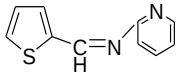	Zn(II) Cu(II) Ni(II) Co(II) Fe(II) Cd(II)	Antibacterial	[122]
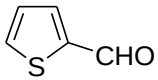 Thiophene-2-carboxyaldehyde	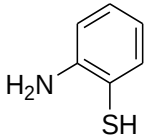 2-Aminothiophenol	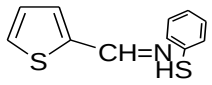	Zn(II) Cu(II) Ni(II) Cd(II)	Antibacterial	[123]

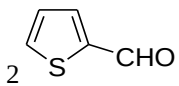 Thiophene-2-carboxyaldehyde	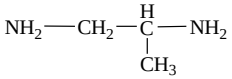 Propane-1,2-diamine	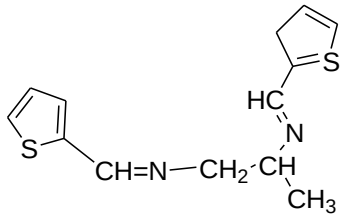	Cu(II) Cd(II) Ni(II) Zn(II)	Antibacterial	[71]
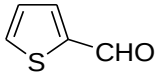 Thiophene-2-carboxyaldehyde	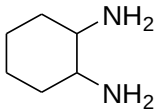 1,2-Diaminocyclohexane	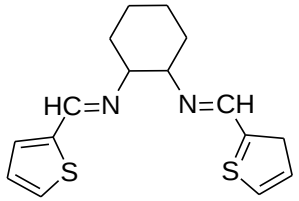	Cu(II) Salts	Anticancerous	[124]
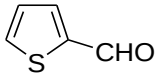 Thiophene-2-carboxyaldehyde	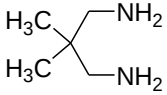 2,2-Dimethyl-1,3-propanediamine	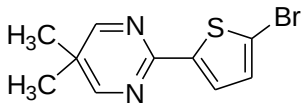	Cu(II) Salts	Anticancerous	[72]
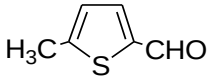 5-Methyl thiophene-2-carboxyaldehyde	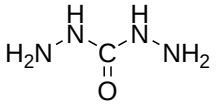 Carbohydrazide	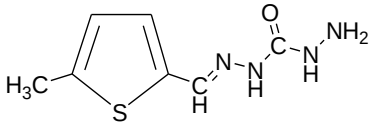	Cu(II) Cd(II) Ni(II) Zn(II)	Antibacterial Antifungal	[125]

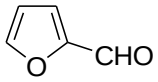 Furan-2-carbaldehyde	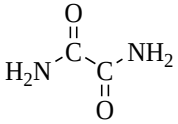 Oxamide	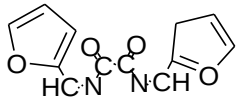	Mn(II) Co(II) Ni(II) Cu(II) Zn(II) Cd(II) Cr(III) Fe(III)	Antibacterial Antifungal Anticancerous	[126]
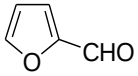 Furan-2-carbaldehyde	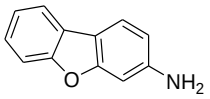 3-Aminodibenzofuran	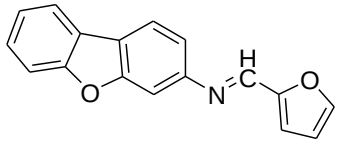	Co(II) Ni(II) Cu(II) Zn(II) Cd(II) Hg(II)	Antibacterial	[127]

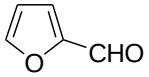 Furan-2-carbaldehyde	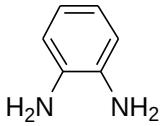 *o*-Phenylenediamine	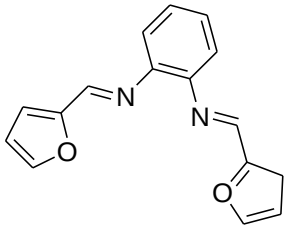	Pt(II)	Antibacterial Antifungal	[103]
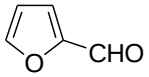 Furan-2-carbaldehyde	 *p*-phenylenediamine	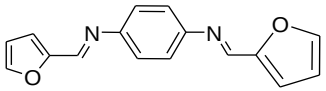	Pt(II)	Antibacterial Antifungal	[55]
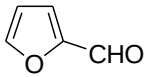 Furan-2-carbaldehyde	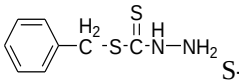 Benzyldithiocarbazic acid	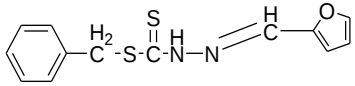	Ni(II) Co(II) Cu(II) Rh(II)	-	[128]

1.4 Mixed ligand metal complexes

Mixed ligand complexes are an important area of interesting metal based drug chemistry, where they are known for their extreme stability. Complexes of zinc and nickel with L-cysteine and D-pencilamine were the first mixed ligand complexes to be reported by Szazuchin O in 1965. These complexes showed noticeable therapeutical and biological activity [129, 130]. Due to their enormous bioinorganic applications, they have become the backbone in the progress of coordination, pharmaceutical and medicinal chemistry in the past few years [8, 131]. Several factors including radii, electronic structure and coordination geometry of central metal atom and donor properties of ligand determine the structure and geometry of complexes. They have the tendency to stabilize central metal atom in certain oxidation state in which otherwise it is unstable [5, 132]. Mixed ligand complexes which contain groups like aldehyde group are particularly of interest as after binding with metal ion these groups not only gets activated but also can undergo various transformations [133]. Many of these complexes are polymeric in nature and show high thermal stability and processibility [25]. They serve as models for metalloenzymes and act as novel reagents [134]. They not only possess the property of binding to DNA but these can also cause its cleavage by electrochemical and photochemical reactions. These complexes show numerous applications in biological, medicinal fields (like toxicology, pharmacology, biotechnology and biochemistry) and industries [130, 135, 136]. Some of the important applications of mixed ligand complexes are as

- In DNA foot printing studies [137]
- As sequence specific DNA binding agents [138, 139]
- As antibacterial, antifungal, antiviral, antidiabetic, anticancerous agents [90, 140 – 142]

1.4.1 Mixed ligand complexes as antimicrobial agents

A series of complexes of Cu with bidentate ligands i.e. acetylacetone and different derivatives of salicylic acids (5-chloro-, 3,5-dinitro-, 3,5-dibromo-, salicylic, thio- and acetylsalicylic acids) have been reported, characterized and assessed for their activities against selected strains of fungi and bacteria [143]. Results of the studies concluded that ternary complexes show enhanced antimicrobial activities with respect to their binary complexes (Fig. 15) (Table 2):

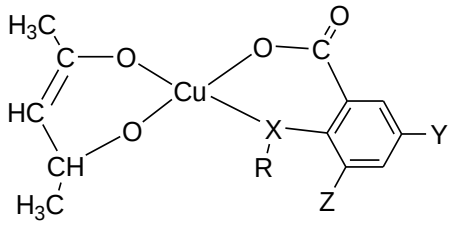

where X = O, R = H; Y = Z = H, Cl, Br, I, NO_2, SH, $COCH_3$

Fig. 15: Structure of Cu(II) complexes

Table 2: Antibacterial assays of Cu(II) complexes with acetylacetone and derivatives of salicylic acid

Antibacterial Activity (MIC in µ gm/ml)												
Complex	**Gram positive**					**Gram negative**						
	S. albus	***S. aureus***	***S. schmitzi***	***S. sonnei***	***P. pyrogens***	***S. sorrei***	***K. aerogenes***	***S. flexeneri***	***V. cholorae***	***S. typhii***	***S. paratyphii B***	***E. coli***
A	25.00	25.00	50.00	50.00	50.00	12.50	25.00	50.00	50.00	100.00	50.00	25.00
B	3.10	6.20	25.00	6.20	12.50	25.00	12.50	12.50	25.00	25.00	25.00	12.50
C	3.10	12.50	25.00	12.50	12.50	12.50	25.00	12.50	25.00	12.50	25.00	6.20
D	6.20	25.00	25.00	25.00	50.00	6.20	12.50	50.00	50.00	12.50	50.00	12.50
E	6.20	12.50	25.00	12.50	25.00	12.50	25.00	25.00	50.00	12.50	25.00	6.20
F	1.60	6.20	12.50	3.10	3.10	12.50	25.0	6.20	12.50	6.20	3.10	1.60
G	25.00	50.00	50.00	25.00	50.00	25.00	50.00	50.00	12.50	25.00	6.20	12.50
H	50.00	100.00	12.50	25.00	100.00	50.00	100.00	100.00	12.50	25.00	50.00	25.00

where complexes are numbered as **A.** Bis(acetylacetonato)copper(II), **B.** [Cu(acetylacetonato)(salicylato)],

C. [Cu(acetylacetonato)(5-chlorosalicylato)], **D.**[Cu(acetylacetonato)(3,5-dibromosalicylato)],

E. [Cu(acetylacetonato)(3,5diiodosalicylato], **F.**[Cu(acetylacetonato)(3,5-dinitrosalicylato)],

G. [Cu(acetylacetonato)(thiosalicylato)], **H.** [Cu(acetylacetonato)(acetyIsalicylato)].

The physiochemical studies of Zn(II) complex with 8-hydroxyquinoline and salicylic acid and its different derivatives (3,5-dinitro-, 3,5-dibromo-, 5-chloro-, 3,5-diiodo-, thio-, acetyl-) showed the ternary nature of the complexes **(**Fig. 16):

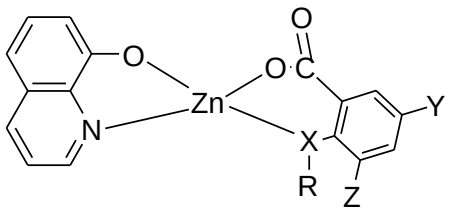

where X = O, S; R = H or $COCH_3$; Y = Z = H, Br, I, NO_2; Y = Cl

Fig. 16: Structure of Zn(II) complexes

In vitro, antimicrobial assays of complexes anticipatory to different strains of bacteria and fungi had shown that the activities were comparable to bis(8-hydroxyquinolinato)Zn(II) (Table 3) [144]:

Table 3: Antimicrobial activities of Zn (II) complexes with 8-hydroxyquinoline and different derivatives of salicylic acid

Complex	Antibacterial Activity (MIC in µ gm/ml)								Antifungal Activity		
	Gram positive				Gram negative				Average zone of inhibition (mm)		
	S. albus	***S. aureus***	***S. schmitzi***	***S. sonnei***	***P. morganii***	***V. cholerae***	***E. coli***	***P. spp***	***A. niger***	***T. rubrum***	***A. fumigatus***
I	25.00	50.00	50.00	25.00	50.00	100.00	50.00	8.00	8.00	9.00	8.00
J	12.50	25.00	50.00	50.00	50.00	25.00	50.00	10.00	12.00	12.00	12.00
K	25.00	50.00	50.00	25.00	50.00	50.00	50.00	10.00	12.00	10.00	10.00
L	25.00	50.00	50.00	50.00	50.00	50.00	50.00	8.00	10.00	7.00	8.00
M	25.00	50.00	50.00	50.00	50.00	50.00	50.00	8.00	10.00	7.00	7.00
N	6.25	12.50	25.00	12.50	25.00	25.00	50.00	12.00	14.00	14.00	13.00
O	12.50	12.50	25.00	12.50	25.00	50.00	12.50	10.00	13.00	10.00	12.00
P	25.00	50.00	50.00	25.00	50.00	25.00	50.00	7.00	8.00	-	7.00

where complexes are numbered as **I.** Bis(8-hydroxyquinolinato)Zn(II), **J.** (8- hydroxyquinolinato)(salicylato)Zn(II), **K**. (8-hydroxyquinolinato)(5-chlorosalicylato)Zn(II), **L.** (8-hydroxyquinolinato)(3,5-dibromo-salicylato)Zn(II), **M.** (8-hydroxyquinolinato)(3,5-diiodosalicylato)Zn(II), **N.** (8-hydroxyquinolinato)(3,5-dinitrosalicylato)Zn(II), **O.** (8- hydroxyquinolinato)(thiosalicylato)Zn(II), **P.** (8-hydroxyquinolinato)(acetylsalicylate)Zn(II).

The antimicrobial evaluation of mixed ligand complexes of Co(II), Cu(II) and Zn(II) with ligands viz. 2,2'-bipyridine and 1,10-phenanthroline have been determined against nine different stains i.e. *Salmonella typhi, Enterobacter choacae, Shigella flexneri, Citrobacter freundii, Klebsiella pneumonia, Escherichia coli, Morganella morganii, Pseudomonas aeruginosa and Staphylococcus aureus* (Table 4):

Table 4: Antibacterial activities of zinc, copper and cobalt mixed ligand complexes

Bacterial Strains	**Antibacterial Assays** **Diameter of Inhibition Zone (mm)**								
	Q	**R**	**S**	**T**	**U**	**V**	**W**	**X**	**RA**
E. choacae	32.00	-	11.00	22.00	-	30.00	9.00	18.00	28.00
S. aureus	31.00	9.00	10.00	24.00	7.00	30.00	8.00	20.00	30.00
E. coli	31.00	14.00	13.00	22.00	8.00	29.00	9.00	22.00	22.00
M. morganii	30.00	-	11.00	23.00	-	29.00	-	20.00	27.00
S. typhi	32.00	9.00	12.00	25.00	-	31.00	9.00	17.00	30.00
K. pneumonia	28.00	-	11.00	20.00	7.00	26.00	10.00	17.00	29.00
S. flexneri	31.00	13.00	13.00	22.00	8.00	30.00	10.00	20.00	22.00
C. freundii	30.00	10.00	-	16.00	-	26.00	-	16.00	21.00
P. aeruginosa	31.00	7.00	11.00	23.00	-	30.00	10.00	19.00	25.00

where IZ represents inhibition zone, **Q**. 1,10-phenanthroline, **R.** 2,2'-bipyridine, **S.** $Co(NO_3)_3.6H_2O$, **T.**$[Co(bpy)(phen)_2](NO_3)_2.2H_2O$, **U.** $CuCl_2.2H_2O$, **V.** $[Cu(bpy)(phen)]Cl_2.2H_2O$, **W.** $ZnCl_2$, **X.** $[Zn(bpy)_2(phen)]Cl_2.6H_2O$, **RA =** reference antibiotics (gentamycin)

The studies have concluded that the antibacterial assays of these water soluble complexes are elevated w.r.t. uncoordinated metals ions and 2,2'-bipyridine but lower than those of free 1,10-phenanthroline while Cu-mixed ligand show higher activity than Zn - mixed ligand complexes. The increasing order of activity is as $[Cu(bpy)(phen)H_2O]Cl_2.2H_2O$ > $[Co(bpy)(phen)_2](NO_3)_2.2H_2O$ > $[Zn(bpy)_2(phen)]Cl_2.6H_2O$ with inhibition zone (IZ) values in the range 16 - 31 mm [57].

The antimicrobial activities and spectrochemical studies have been done [145] on seven transition metal series viz. Zn(II), Cu(II), Ni(II), Co(II), Mn(II), Fe(III) and Cr(III) with 2-aminophenol as primary and 2-chloroaniline as secondary ligand. The characterized complexes were reported octahedral geometry having general formula $[M(C_{12}H_{12}Cl_3N_2O)]$ for M(II) ions i.e. M = Mn^{2+}, Co^{2+}, Ni^{2+}, Cu^{2+} and Zn^{2+} and $[M(C_{12}H_{12}Cl_3N_2O)].X$ for M(III) ions i.e. M = Cr^{2+}, Fe^{2+} and X is Cl^-. They were assessed for their antibacterial activity against *Bacillus subtilis, Staphylococcus aureus, Escherichia coli, Salmonella typhi* and antifungal activity against *Fusarium monilifore, Peniclilium chrysogenum, Aspergilllus niger, Aspergillus flavus* with Ni(II) complexes reportedly not showing any antifungal activity (Table 5 and 6):

Table 5: Antibacterial assessment of all the mixed ligand chelates of transition metal ions

Complex	Zone of inhibition (in mm)			
	E. coli	***S. typhi***	***S. aureus***	***B. subtilis***
$C_{12}H_{12}Cl_4CrN_2O$	Negative	14.00	19.00	13.00
$C_{12}H_{12}Cl_3MnN_2O$	12.00	16.00	19.00	16.00
$C_{12}H_{12}Cl_4FeN_2O$	14.00	19.00	20.00	19.00
$C_{12}H_{12}Cl_3CoN_2O$	22.00	20.00	30.00	19.00
$C_{12}H_{12}Cl_3N_2NiO$	15.00	15.00	13.00	11.00
$C_{12}H_{12}Cl_3CuN_2O$	17.00	20.00	17.00	30.00
$C_{12}H_{12}Cl_3ZnN_2O$	17.00	19.00	25.00	20.00
Penicillin	11.00	24.00	36.00	30.00
DMSO	Nil	Nil	Nil	Nil

Table 6: Antifungal activity of synthesized mixed ligand complexes of transition metal ions

Complex	***A. flavus***	***F. moneliforme***	***P. chrysogenum***	***A. niger***
$C_{12}H_{12}Cl_4CrN_2O$	Less Activity	Less Activity	Highest Activity	Less Activity
$C_{12}H_{12}Cl_3MnN_2O$	Less Activity	Less Activity	Highest Activity	Less Activity
$C_{12}H_{12}Cl_4FeN_2O$	No Activity	Less Activity	Less Activity	No Activity
$C_{12}H_{12}Cl_3CoN_2O$	Less Activity	Less Activity	Less Activity	Less Activity
$C_{12}H_{12}Cl_3N_2NiO$	No Activity	No Activity	No Activity	No Activity
$C_{12}H_{12}Cl_3CuN_2O$	Less Activity	Less Activity	Less Activity	Less Activity
$C_{12}H_{12}Cl_3ZnN_2O$	Less Activity	Highest Activity	Highest Activity	Reduced Growth
Griseofulvin	Highest Activity	Highest Activity	Highest Activity	Highest Activity
DMSO	No Activity	No Activity	No Activity	No Activity

To analyze the biological profile another mixed ligand complexes of Mn^{2+}, Co^{2+}, Ni^{2+}, Cu^{2+}, $Zn^{2+}$and Cr^{3+} ions using oxalic acid and trimethoprim as primary and secondary ligands have been prepared [146]. The scheme for the synthesis of complexes is as follows (Fig.17).

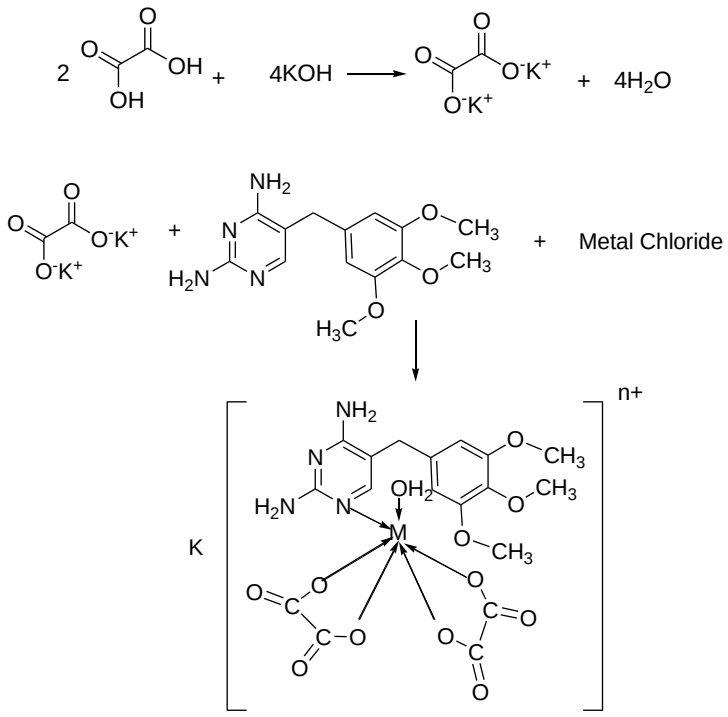

Fig. 17: Schematic procedure for the synthesis of various transition metal complexes

The characterized complexes were then analyzed for their antibacterial activities against four bacterial variety namely *Enterobacter cloacae, Staphylococcus aureus, Bacillus subtilis and Escherichia coli* where all the complexes had shown less activity as compared to trimethoprim but more than oxalic acid (Table 7):

Table 7: Antibacterial activity of different transition metal complexes

Ligand / Complex	***E. cloacae***	***B. subtilis***	***S. aureus***	***E.coli***
DMSO (Control)	5.00	4.00	4.00	5.00
Oxalic Acid	5.00	5.00	4.00	4.00
Trimethoprim (TM)	37.00	5.00	58.00	29.00
$K_2[Cr(C_2O_4)_2(TM)(H_2O)]$	5.00	5.00	4.00	4.00
$K_2[Mn(C_2O_4)_2(TM)(H_2O)]$	5.00	5.00	22.00	4.00
$K_2[Co(C_2O_4)_2(TM)(H_2O)]$	5.00	5.00	33.00	4.00
$K_2[Ni(C_2O_4)_2(TM)(H_2O)]$	5.00	5.00	44.00	4.00
$K_2[Cu(C_2O_4)_2(TM)(H_2O)]$	5.00	5.00	33.00	15.00
$K_2[Zn(C_2O_4)_2(TM)(H_2O)]$	5.00	5.00	23.00	4.00

Another series of the mixed ligand complexes of Co^{2+}, Ni^{2+} and Cu^{2+} with 2,2'-bipyridine and hydroxybenzalidine anthranillic acid (HBAA) with general formula ML_1L_2 (ligand is synthesized by the amalgamation amid anthranillic acid and salicyladehyde in the molar ratio 1:1) have been characterized by IR spectra, elemental technique, electronic spectral analysis and conductance measurements. The proposed structure of the complex is as follows (Fig. 18):

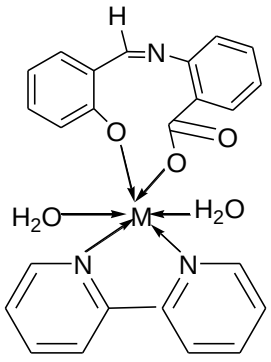

where M = Co^{2+}, $Ni^{2+}$and Cu^{2+}

Fig. 18: General representation of complexes of Co^{2+}, Ni^{2+} and Cu^{2+}

The complexes were then monitored for their antimicrobial properties against *Escherichia coli, Staphylococcus aureus, Aspergillus fumigatus, Aspergillus niger, Aspergillus flavus* (Table 8) [147]:

Table 8: Antimicrobial evaluation of ligands and their mixed ligand metal chelates

Ligand / Complex	**Bacteria**		**Fungi**		
	S. aureus	***E. coli***	***A. flavus***	***A. fumigatus***	***A. niger***
2,2'-bipyridine	Nil	Nil	Nil	Nil	Nil
HBAA	Highest Growth	Moderate	Moderate	Highest Growth	High
$Cu(bpy)HBAA(H_2O)_2$	Nil	Nil	Nil	Nil	Nil
$Ni(bpy)HBAA(H_2O)_2$	Nil	Nil	Nil	Nil	Poor
$Co(bpy)HBAA(H_2O)_2$	Nil	Nil	Nil	Nil	Nil

Two novel mixed ligand complexes of Co and Fe with 8-hydroxyquinoline and 1,10-phenanthroline were prepared and characterized by sophisticated spectral techniques. The complexes have been assigned the formula $[Co(HQ)(phen)](PF_6)_3$ and $[Fe(HQ)(phen)](PF_6)_2$ where HQ = 8-hydroxyquinoline and phen = 1,10-phenanthroline. The suggested structure of the complexes is as follows (Fig.19):

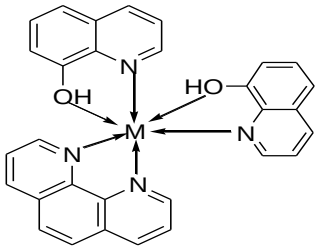

where M = Co(II) and Fe(II)

Fig. 19: General structure of mixed ligand complexes

Experimental results show that these complexes can intercalate DNA having K_b values of 26.64×10^6 M^{-1} (for Co complex) and 23.65×10^6 M^{-1} (for Fe complex) respectively. Their antimicrobial properties evaluated against four bacterial strains viz. *Proteus vulgaris, Staphylococcus aureus, Pseudomonas aeruginosa and Escherichia coli* and one fungal strain viz. *Aspergillus niger* show that complex $[Co(HQ)(phen)](PF_6)_3$ do not show any antimicrobial activity while the complex $[Fe(HQ)(phen)](PF_6)_2$ shows moderate antibacterial activity than the free ligand (Table 9) [148]:

Table 9: Antimicrobial activity of Co and Fe with 8-hydroxyquinoline and 1,10-phenanthroline

Ligand / Complex	**Concenteration (mg/ml)**	***P. aeruginosa***	***E. coli***	***P. vulgaris***	***S. aureus***	***A. niger***
8-hydroxyquinoline	0.50	8.00	0.00	0.00	0.00	0.00
	1.00	15.00	0.00	0.00	0.00	0.00
	1.50	16.00	0.00	0.00	0.00	0.00
	2.00	17.00	0.00	0.00	12.00	0.00
	2.50	19.00	0.00	0.00	15.00	0.00
1,10-phenanthroline	0.50	0.00	0.00	12.00	0.00	0.00
	1.00	10.00	0.00	15.00	10.00	0.00
	1.50	12.00	15.00	16.00	16.00	0.00
	2.00	15.00	22.00	21.00	19.00	0.00
	2.50	22.00	24.00	22.00	23.00	0.00
$[Co(HQ)(phen)](PF_6)_3$	0.50	0.00	0.00	0.00	0.00	0.00
	1.00	0.00	0.00	0.00	0.00	0.00
	1.50	0.00	0.00	0.00	0.00	0.00
	2.00	0.00	0.00	0.00	0.00	0.00

	2.50	0.00	0.00	0.00	0.00	0.00
[Fe(HQ)(phen)]$(PF_6)_2$	0.50	0.00	0.00	0.00	0.00	0.00
	1.00	10.00	0.00	0.00	0.0	0.00
	1.50	11.00	0.00	0.00	0.00	0.00
	2.00	15.00	0.00	0.00	16.00	0.00
	2.50	17.00	0.00	0.00	18.00	0.00
Antibiotic	0.50	24.00	21.00	21.00.	21.0	0.00
	1.00	22.00	21.00	22.00	20.00	0.00
	1.50	22.00	22.00	22.00	21.00	0.00
	2.00	24.00	24.00	24.00	24.00	0.00
	2.50	24.00	22.00	24.00	25.00	0.00
DMSO	0.50	0.00	0.00	0.00	0.00	0.00
	1.00	0.00	0.00	0.00	0.00	0.00
	1.50	0.00	0.00	0.00	0.00	0.00
	2.00	0.00	0.00	0.00	0.00	0.00
	2.50	0.00	0.00	0.00	0.00	0.00

Zn(II) and Cu(II) ternary complexes in slightly acidic media using glycine as primary and various hydroxy acids viz. salicylic acid, lactic acid and glycolic acid, as a secondary ligand have been characterized using UV-vis, IR, mass, thermal, magnetic measurements and ESR techniques. The complexes were then investigated for their antibacterial activities against various bacterial strains with inhibition zone range of 16.3 mm – 33.3 mm while ligands show inhibition zone range of 12.3 mm – 16.5 mm (Table 10) [149]:

Table 10: Antibacterial activity of Cu(II) complexes

Ligand / Complex	Inhibition Zone diameter (mm)		
	S. aureus **Mean+ RSD**	***P. aeruginosa*** **Mean+ RSD**	***E. coli*** **Mean+ RSD**
[Cu (L_1)(Gly)]	16.90 + 0.23	17.10+ 0.10	21.50+ 0.08
[Cu (L_2)(Gly)]	17.60+ 0.04	20.50+ 0.03	21.10+ 0.04
[Cu (L_3)(Gly)]	20.40+ 0.05	20.80+ 0.04	23.40+ 0.05
[Zn (L_1)(Gly)]	33.30+ 0.05	23.10+ 0.10	29.50+ 0.04
[Zn (L_2)(Gly)]	31.20+ 0.06	25.80+ 0.03	19.80+ 0.04
[Zn (L_3)(Gly)]	28.70+ 0.16	19.60+ 0.05	26.00+ 0.10
HL_1	15.00+ 0.16	14.30+ 0.09	16.50+ 0.11
HL_2	12.30+ 0.05	13.60+ 0.08	14.20+ 0.07
HL_3	13.60+ 0.04	14.10+ 0.03	14.70+ 0.17
Glycine	-----	-----	-----
Tetracycline HCl	35.50+0.01	37.20+0.03	36.50+0.02

where L_1 = Salicylate, L_2 = Lactate, L_3 = Glycolate, HL_1 = Salicylic acid, HL_2 = Lactic acid, HL_3 = Glycolic acid

Cu(II) complexes with twelve Schiff bases were synthesized followed by condensation between isoniazid, pyrazinamide, benzhydrazide, nicotinohydrazide with benzaldehyde, 2,3-dimethoxybenzaldehyde and 3,4-dimethoxybenzaldehyde. The scheme for the synthesis of the ligands is as follows (Fig. 20):

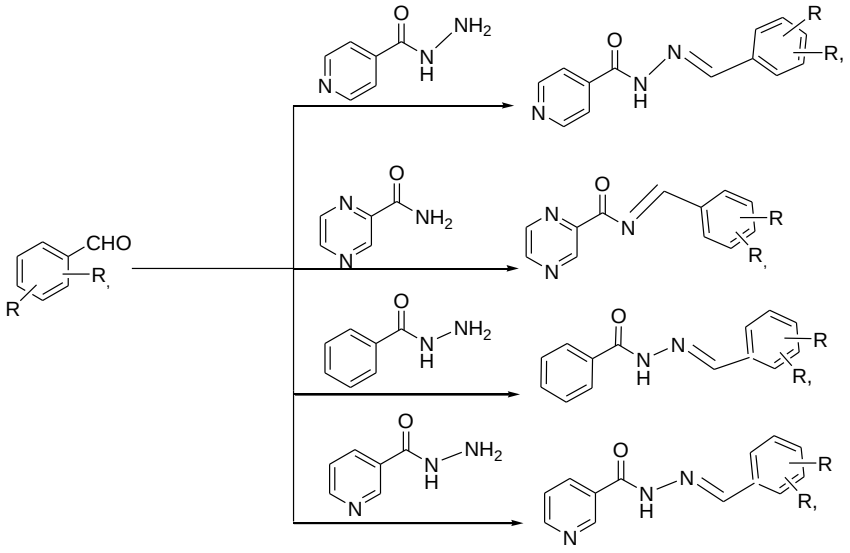

where R, R' = benzaldehyde, 2,3-dimethoxybenzaldehyde and 3,4- dimethoxybenzaldehyde.

Fig. 20: Scheme for the synthesis of different Schiff bases

The characterized complexes were then evaluated for their biological assays. All the tested complexes have been reportedly shown no antifungal activity while antibacterial activity was relatively comparable and antitubercular activity was less as compared to the standards (Table 11 and 12) [150]:

Table 11: Antibacterial assays of Cu(II) complexes

Cu(II) complexes	Zone of inhibition ± SD					
	Gram positive			Gram negative		
	B. subtilis	***S. aureus***	***S. pyogenes***	***E. faecalis***	***E. coli***	***K. pneumoniae***
$[(C_{13}H_{11}N_3O_3)_2CuClO_4]ClO_4$	15.00±0.63	15.00±0.27	11.40±1.60	17.00±3.10	16.20±2.00	13.00±0.18
$[(C_{15}H_{15}N_3O_3)_2CuClO_4]ClO_4$	13.00±0.18	14.00±0.44	12.00±0.18	14.00±2.00	16.00±1.40	16.50±1.02
$[(C_{15}H_{15}N_3O_3)_2CuClO_4]ClO_4$	14.00±0.66	12.00±1.88	14.00±0.50	18.00±2.11	10.00±2.44	17.00±0.11
$[(C_{12}H_9N_3O)_2CuClO_4]ClO_4$	15.30±2.70	13.00±1.64	15.00±0.30	18.00±2.40	13.00±0.10	18.00±3.20
$[(C_{14}H_{13}N_3O_3)_2CuClO_4]ClO_4$	16.00±1.77	19.00±2.90	22.00±0.42	15.40±2.40	19.00±1.03	16.00±2.90
$[(C_{14}H_{13}N_3O_3)_2CuClO_4]\ ClO_4$	10.00±1.60	16.00±1.95	14.00±0.54	18.00±1.30	15.40±3.00	17.00±2.40
$[(C_{14}H_9N_2O)_2CuClO_4]\ ClO_4$	15.00±0.29	14.30±0.30	15.50±1.50	18.00±1.32	18.00±0.16	18.00±0.10
$[(C_{16}H_{13}N_2O_3)_2CuClO_4]\ ClO_4$	14.00±0.82	18.00±0.16	13.00±0.10	16.40±1.39	15.50±1.30	16.50±1.30
$[(C_{16}H_{13}N_2O_3)_2CuClO_4]\ ClO_4$	11.00±0.38	15.00±0.52	15.00±2.50	17.00±0.10	14.00±0.13	16.00±1.30
$[(C_{13}H_{11}N_3O)_2CuClO_4]\ ClO_4$	19.00±0.02	20.00±0.33	20.50±2.60	10.00±1.22	15.00±0.22	20.50±2.60
$[(C_{15}H_{15}N_3O_3)_2CuClO_4]\ ClO_4$	13.00±0.18	12.00±0.62	14.40±0.20	18.50±1.20	17.00±0.98	15.30±1.20
$[(C_{15}H_{15}N_3O_3)_2CuClO_4]\ ClO_4$	10.00±0.24	10.50±0.50	13.00±0.21	15.30±1.25	16.00±0.27	18.00±0.10
Cu salt	12.00±1.62	16.00±1.12	11.00±0.31	17.00±0.10	16.00±1.30	11.00±0.31
Tetracycline	20.00±0.01	20.00±1.00	18.00±2.90	18.00±2.10	19.50±1.33	18.00±2.10

where zone of inhibition is in mm and SD is Standard Deviation

Table 12: Anti-tuberculosis activity of Cu^{2+} complexes against *M. tuberculosis*

Complex	**Minimum Inhibitory Concenteration (µg/mL)**	**% Inhibition**
$[(C_{15}H_{15}N_3O_3)_2CuClO_4]ClO_4$	250	93
$[(C_{14}H_{13}N_3O_3)_2CuClO_4]ClO_4$	250	68
$[(C_{16}H_{13}N_2O_3)_2CuClO_4]\ ClO_4$	250	49
$[(C_{15}H_{15}N_3O_3)_2CuClO_4]ClO_4$	250	79

Various complexes of Ni^{2+}, Cu^{2+} and Zn^{2+} with three Schiff bases (amalgamated by condensation between diphenylglyoxal and 1-amino-4-nitrobenzene / *o*-methoxy aniline / 1-amino-4-chlorobenzene) as primary and 1,10- phenanthroline as secondary ligand were prepared and characterized by sophisticated spectral methods. The scheme for the synthesis is as follows (Fig. 21):

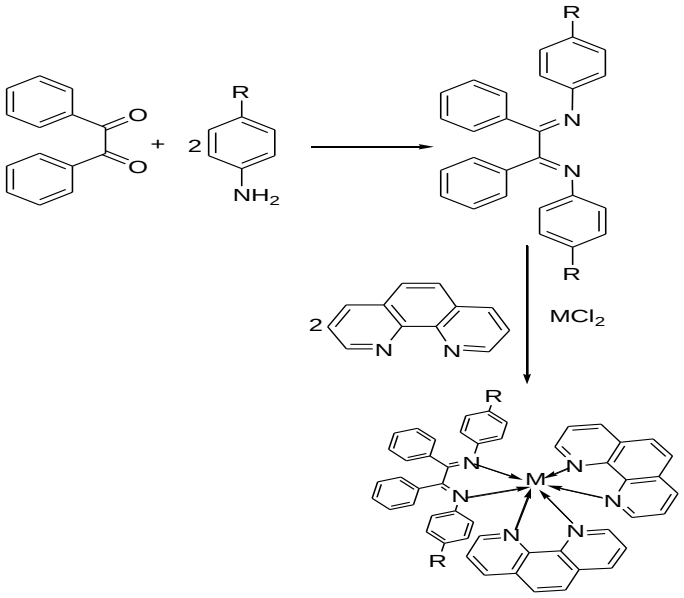

where M = Ni^{2+}, Cu^{2+} and Zn^{2+}

Fig. 21: Scheme for the synthesis of metal ligand complexes

The binding constant values (K_b) were analyzed to find mode of binding with calf thymus DNA and were found to be in the range of 2.8 - 7.5 × 10^5 M^{-1}. The minimum inhibitory concentration (MIC) was determined against various strains of bacteria and fungi whose results show better antifungal activities of the complexes than antibacterial activities. DNA cleavage studies were also demonstrated on pUC19DNA by gel electrophoresis techniques which confirm metal complexes as better cleavage agents [151].

1.4.2. DNA binding studies of mixed ligand complexes

Mixed ligand complexes having general formula $[M(phen)_2L]^{n+}$ (where M = Ni^{2+}, Co^{3+} or Ru^{2+}; L = phenanthroline - dione (phen - dione), 1,10-phenanthroline and dipyridophenazine (dppz) and *n* = 3 or 2) were synthesized having general structure (Fig. 22):

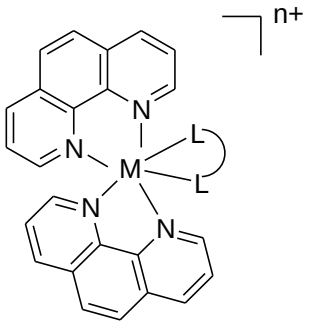

where M = Ni^{2+}, Co^{3+} or Ru^{2+}; and n+ = 2 or 3, L = phen - dione, phen or dppz

Fig. 22: General structure of mixed ligand complexes

Photocleavage and binding studies on DNA of these complexes have been analyzed by various physiochemical (UV-vis, fluorescence and viscometric titrations) and biochemical (thermal denaturation, and differential pulse voltametry) methods. The studies have been conducted by considering the effect of change of metal ion on ligand system and vice versa. Results of the studies have revealed that Ru(II) and Co(II) complexes in particular with dppz are better DNA intercalators while Ni(II) complexes are inactive. The better intercalation of dppz may be due to extended conjugation [152]

A novel Cr (III) mixed ligand complex having formula [CrCl(sal-gly)phen] $0.5H_2O$ with Schiff base (sal-gly) and 1,10-phenanthroline as different ligands. The composition of complex was characterized with UV, IR and crystallographic studies. CT - DNA and BSA binding studies of the complex had shown that it binds to DNA moderately by an intercalative mode and strongly to BSA with K_b and n values as $1.13 \times 10^5\ M^{-1}$ and 1.13 respectively. Approximately 1 value of n proposed that complex binds to BSA through one binding site only [40].

Eight new Ni(II) mixed ligand complexes with different Schiff bases (amalgamated by the fusion of 3-amino-5-methyl isoxazole with different salicylaldehydes) and 1,10-phenanthroline as ligands have been reported. The spectrochemical analysis proposed the octahedral geometries for the complexes (Fig. 23):

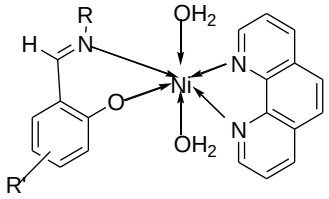

where R = 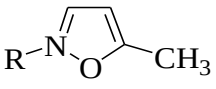 and R' = H, Cl, $-OC_2H_5$, $-NO_2$, $-CH_3$, Br, $-OCH_3$, -OH

Fig. 23: Mixed ligand complexes of Ni(II)

The synthesized complexes were then monitored for antibacterial and antifungal assays against some known drugs. The high value of $K_b = 2.5 \pm 0.2 \times 10^5\ M^{-1}$ suggests that complexes bind to DNA through groove binding or stacking. The complexes also show positive anticancerous activity against human promyelocytic leukemia (HL60 cells) with highest IC_{50} value of 82.30 ± 0.24 shown by $[Ni(phen)(BMIIMP)(H_2O)_2]Cl$ [67].

Various mixed ligand copper complexes having primary ligand as Schiff bases and secondary ligand as 1,10-phenanthroline have been reported in different reports like synthesis of $[Cu(o\text{-}van\text{-}ile)(phen)]1.5H_2O$ (where van-ile is obtained by the condensation of o-vanilline and L-isoleucine) [82], [Cu(naph-val)phen] (where naph-val is synthesized

by condensation of L-valine and 2-hydroxy-1-naphthaldehyde) [153] and of [Cu(sal-ala)(phen)(DA)] (where sal-ala = salicylalanine, DA = dodecylamine) [66]. All these complexes have shown binding to DNA through with K_b value of $2.13 \times 10^4\ M^{-1}$, $5.66 \times 10^3\ M^{-1}$ and $2 \times 10^5\ M^{-1}$ respectively.

DNA binding and anticancerous studies have been reported on two ternary Cu(II) complexes with DL- threonine and polypyridyl ligand (1,10-phenanthroline or 2,2'-bipyridine) having the formula $[Cu(thr)(bpy)Cl].H_2O$ and $[Cu(thr)(phen)H_2O]Cl\ .2H_2O$ and structure. Each complex depicts square pyramidal (4+1) geometry with slight distortion. The metal complexes with phenanthroline shows intercalation mode of binding with DNA and higher binding affinity than bipyridine metal complex which shows groove binding. This may be due to extended ring conjugation in phenanthroline. K_b values have been calculated as $5.55 \times 10^4\ M^{-1}$ for $[Cu(thr)(bpy)Cl].H_2O$ and $4.413 \times 10^5\ M^{-1}$ for $[Cu(thr)(phen)H_2O]Cl.2H_2O$. Dose dependent mild cytotoxicity against cell lines (HCT-116 and MCF-7) was shown by both complexes with bipyridine complex having relatively better cytotoxic effect [83].

The characterized ternary Cu(II) complexes with glycine and methylated glycine derivatives having formula $[Cu(phen)(aa)(H_2O)]NO_3.XH_2O$ where (aa) are amino acids i.e. sarcosine (sar), 2-dimethylglycine (c-dmg), DL-alanine (DL-ala), glycine (gly) and X = 0, 1.5, 2.5 were reported. On the basis of EPR, fluorescence quenching, gel electrophoresis and restriction enzyme assay they show that these complexes can bind to various B - forms of DNA duplexes and G-quadruplex. These complexes do not show any cell fatality in NP69 cells but cause apoptotic cell fatality in HK1 cells within percentage range of 41 - 60%. IC_{50} values for the complexes at 5 μM were in the range of 2.2 - 5.2 μM as compared to normal cell line NP69 where it is > 13.0 μM[86].

A copper(II) mixed ligand binuclear complex i.e. $[Cu(MS)(bpy)]_2.(ClO_4)_2$ having square bipyramidal geometry (where MS and bpy is 5-methylsalicylaldehyde and 2,2'-bipyridine) is confirmed by crystal structure determination, IR, EPR and magnetic moment studies. Binding studies have revealed the binding of complex binds to DNA

through intercalative mode with binding constant value of $5.2 \pm 1.7 \times 10^4$ M^{-1}. This value is lower than the reported values of classic intercalators (10^6 - 10^7 M^{-1}) [8].

Another series of mixed ligand complexes of copper i.e. $[Cu(L)(ClO_4)]$, $[Cu(L)(diimine)]ClO_4$, (where L is 4-chloro-2-((2-(phenylthio)phenylimino)methyl)phenol and diimine is 1,10-phenanthroline / 4,4'-dimethyl-2,2'-bipyridine / 2,2'-bipyridine). Spectral analysis of the complexes was evaluated using UV-vis, IR, ESI-mass, electrochemical studies and X-Ray crystallographic technique. The complexes depicted significant DNA cleavage activities in presence of ascorbic acid (reducing agent) and antitumor activity against A549 and Huh7 against lines of human tumor cell. Molecular docking techniques further supported the analysis [154]

The ternary complexes of Cr^{2+}, Mn^{2+}, Fe^{2+}, Co^{2+}, Ni^{2+}, Zn^{2+} and Fe^{3+} with lornoxicam as primary and 1,10 phenanthroline as primary and secondary ligands respectively. They have been proposed octahedral geometry. The proposed formula of the metal chelates is $[M(LOR)(phen)Cl_2]X_n.yH_2O$ where [M is (Ni^{2+}; n is 0 and y is 1) or (Cr^{2+}; n is 1and y is 2); $[M(LOR)(phen)(H_2O)_2](BF_4)_2$ where [M is Fe^{2+}; Co^{2+}, Ni^{2+} or Zn^{2+}] and $[M(LOR)_2(phen)]X_n.yH_2O$ where [M is (Mn^{2+}; n and y is 2) or (Fe^{3+}; n is 3; y is 0]. The ternary complexes show enhanced activity than parent ligand but reduced activity as compared to 1,10-phenanthroline. Cu^{2+} and Co^{2+} complexes do not show any anticancer activity while other complexes show IC_{50} values for anticancerous activities in the range of 9 - 23.1 μg/ml (Table 13) [5]:

Table 13: Anticancerous activity of lornoxicam ligand and its binary complexes

Complex / Ligand	**Concenteration (mg/ml)**					**IC_{50} (µg/ml)**
	0.00	5.00	12.50	25.00	50.00	
LOR	1.00	1.00	1.00	1.00	1.00	0.00
1,10-phenanthroline	1.00	0.48	0.32	0.32	0.30	4.73
$[Cr(LOR)(phen)Cl_2]Cl.2H_2O$	1.00	0.76	0.51	0.43	0.35	13.70
$[Mn(LOR)_2(phen)]Cl_2 \cdot 2H_2O$	1.00	0.52	0.51	0.35	0.35	12.70
$[Fe(LOR)_2(phen)]Cl_3$	1.00	0.78	0.59	0.37	0.34	17.20
$[Fe(LOR)(phen)2H_2O](BF_4)_2$	1.00	0.59	0.59	0.36	0.34	17.20
$[Ni(LOR)(phen)Cl_2].H_2O$	1.00	0.86	0.75	0.60	0.52	23.10
$[Zn(LOR)(phen)(H_2O)_2](BF_4)_2$	1.00	0.62	0.40	0.34	0.37	9.00

1.5 Bibliography

[1] Kauffman, G. B. Christian Wilhelm Blomstrand (1826 – 1897) Swedish chemist and mineralogist, *Annals of Science*. **1975**, *32*, 13-37.

[2] Kauffman, G. B. Pacific Southwest association of chemistry teachers Sophus Mads Jorgensen (1837 - 1914), *J. Chem. Educ.***1959**, *36*, 521-527.

[3] Morral, F. R. Alfred Werner and cobalt complexes, *Werner Centennial*. **2009**, 70–77.

[4] Amolegbe, S. A.; Yunus-Issa, M. T.; Elaigwu, S. E.; Lawal, A.; Shodeinde, A. S. Synthesis, characterization and antimicrobial activity of mixed transition metal complexes of salicylic acid with 1,10-phenanthroline, *J. Appl. Sci. Environ. Manag.* **2017**, *21*, 568–573.

[5] Mahmoud, W. H.; Mohamed, G. G.; El - Dessouky, M. M. I. M. Synthesis, characterization and in vitro biological activity of mixed transition metal complexes of lornoxicam with 1,10-phenanthroline, *Int. J. Electrochem. Sci.* **2014**, *9*, 1415–1438.

[6] Rajarajeswari, C.; Ganeshpandian, M.; Palaniandavar, M.; Riyasdeen, A.; Akbarsha, M. A. Mixed ligand copper(II) complexes of 1,10-phenanthroline with tridentate phenolate / pyridyl / (benz)imidazolyl Schiff base ligands: Covalent vs non - covalent DNA binding, DNA cleavage and cytotoxicity, *J. Inorg. Biochem.* **2014**, *140*, 255–268.

[7] Sivajiganesan, S.; Kadhiravansivasamy, K.; Chidhambram, S.; Manimekalai, R.; Periyathambi, T.; Nandhakumar, V. Synthesis and characterization of Schiff base Co(II), Ni(II) and Cu(II) complexes derived from 2-Hydroxy-1-naphthaldehyde and 2-Picolylamine, *Mod. Chem. Appl.* **2017**, *5*, 2–7.

[8] Gurumoorthy, P.; Ravichandran, J.; Rahiman, A. K. Mixed-ligand binuclear copper(II) complex of 5-methylsalicylaldehyde and 2,2′-bipyridyl: Synthesis, crystal structure, DNA binding and nuclease activity, *J. Chem. Sci.* **2014**, *126*, 783–792.

[9] Al Zoubi, W. Biological activities of Schiff bases and their complexes: A review of recent works, *Int. J. Org. Chem.* **2013**, *3*, 73–95.

[10] Melnik, M.; Kabesova, M.; Koman, M.; Macaskova, L.; Garaj, J.; Holloway, C. E. A valent copper(II) coordination compounds: Classification and analysis of crystallographic and structural data III. dimeric compounds, *J. Coord. Chem.* **1998**, *45*, 147–359.

[11] Hathaway, B. J.; Billing, D. E. The electronic properties and stereochemistry of mono-nuclear complexes of the copper(II) ion, *Coord. Chem. Rev.* **1970**, *5*, 143–207.

[12] Sekhon, B. S. Inorganics / bioinorganics: Biological, medicinal and pharmaceutical uses, *J. Pharm. Educ. Res.* **2011**, *2*, 1–20.

[13] Buczkowska, M. K. Synthesis, characterization, antitumor and antimicrobial activities of heterocyclic transition metal complexes. Ph.D. Dissertation, University of Greifswald, Greisfswald Mai, **2011.**

[14] K. Ni. Metal complexes of imidazole Schiff base and oxazine ligands: Synthesis and antimicrobial activity, Ph.D. Dissertation, N.U.I. Maynooth, **2012**.

[15] Aliyu, H.; Zayyan, R. Synthesis, analysis and bioactivity evaluation of copper(II) tetradentate Schiff base complex, *Int. J. Med. Chem. Anal.* **2014**, *4*, 150–154.

[16] Lux, A.; Broadley, M. R.; Hammond, J. P.; White, P. J.; Zelko, I. Zinc in plants, *New Phytol.* **2007**, *173*, 677–702.

[17] T. Carrette. Effect of natural complexing agents on zinc accumulation in Navy Beans, Ph.D. Dissertation, Universiteit Gent, **2013**.

[18] Adelaide, O. M.; James, O. O. Antimicrobial, DNA cleavage and antitumoral properties of some transition metal complexes of 1,10–phenanthroline and 2,2'–bipyridine: A review, *Int. J. Res. Pharm. Biomed. Sci.* **2013**, *4*, 1160–1171.

[19] Lukaski, H. C. Vitamin and mineral status: Effects on physical performance, *Nutrition.* **2004**, *20*, 632–644.

[20] Tsonev, T.; Lidon, F. J. C. Zinc in plants - An overview, *Emirates J. Food Agric.* **2012**, *24*, 322–333.

[21] Hambidge, K. M.; Krebs, N. F. Zinc deficiency: A special challenge, *J. Nutr.* **2018**, *137*, 1101–1105.

[22] Hafeez, B. Role of zinc in plant nutrition - A review, *Am. J. Exp. Agric.* **2014**, *3*, 374–391.

[23] Gunagi, S.; Nandibewoor, S.; Chimatadar, S. Interaction between a antiretroviral drug – Navirapine with bovine serum albumin: A fluorescence quenching and fourier transformation infrared spectroscopy study, *Res. J. Pharm. Biol. Chem. Sci.* **2011**, *2*, 814–826.

[24] Sieranski, T.; Kruszynski, R. Magnesium sulphate complexes with hexamethylenetetramine and 1,10-phenanthroline, *J. Therm. Anal. Calorim.* **2011**, *109*, 141–152.

[25] Kumar, S.; Sharma, T. R. Synthesis, structure and luminescent properties of Ti(III), V(III) transition metal polymeric macrocyclic complexes derived from phenanthroline and biphenyl groups, *Orient. J. Chem.* **2012**, *28*, 963–967.

[26] Accorsi, G.; Listorti, A.; Yoosaf, K.; Armaroli, N. 1,10-Phenanthrolines: Versatile building blocks for luminescent molecules, materials and metal complexes, *Chem. Soc. Rev.* **2009**, *38*, 1690–1700.

[27] Hosseini, M. W.; Kaes, C.; Katz, A. Bipyridine: the most widely used ligand. A review of molecules comprising at least two 2,2'-bipyridine units, *Chem. Rev.* **2000**, *100*, 3553–3590.

[28] Constable, E. C. Homoleptic complexes of 2,2′-bipyridine, *Adv. Inorg. Chem.* **1989**, 341–363.

[29] Devereux, M.; Kellett, A.; Kavanagh, K.; Santos, A. L. S.; McCann, M. Deciphering the antimicrobial activity of phenanthroline chelators, *Curr. Med. Chem.* **2012**, *19*, 2703–2714.

[30] Kilah, N. L.; Meggers, E. Sixty years young: The diverse biological activities of metal polypyridyl complexes pioneered by Francis P. Dwyer, *Aust. J. Chem.* **2012**, *65*, 1325-1332.

[31] Pal, T. K.; Alam, A.; Paul, S.; Sheikh, C.; Ahmad, H. Physico - chemical, antioxidant and antimicrobial investigation on new mixed ligand complexes containing bis(2,4,4-trimethylpentyl) dithiophosphinic acid and 2,2′-bipyridine, *Orient J. Chem.* **2018**, *34*, 1213–1221.

[32] Kannan, D.; Arumugham, M. N. Synthesis, characterisation, DNA - binding studies and antimicrobial activity of copper(II) complex with 1,10 phenanthroline, L-Tyrosine and thiourea as ligands, *Int. J. Res. Control Release.* **2012**, *2*, 10–17.

[33] Santhamakumar, P.; Arumugham, M. N. Synthesis, characterization of copper (II) complex with mixed ligands of 1,10-phenanthrolline, L-phenylalanine and ethylamine: studies on DNA binding, nuclease and biological activities, *Int. J. Recent Sci. Res.* **2012**, *3*, 459–466.

[34] Malhavan, V. M. K.; Boh, B. K.; Tayyab, S. Characterization of erythrosine B binding to bovine serum albumin and bilirubin displacement, *Indian J. Biochem. Biophys.* **2009**, *46*, 325–331.

[35] Wang, T.; Zhao, Z.; Hua, J.; Zhang, J. Characterization of the interaction between reserpine and bovine serum albumin: Spectroscopic approaches, *Indian J. Biochem. Biophys.* **2011**, *48*, 388–394.

[36] Chen, X.; Liu, Y.; Peng, M.; Shi, S.; Zhang, Y. Differential effects of Cu(II) and Fe(III) on the binding of omeprazole and pantoprazole to bovine serum albumin: Toxic effect of metal ions on drugs, *J. Pharm. Biomed. Anal.* **2011**, *56*, 1064–1068.

[37] Hu, Y. J.; Liu, Y.; Wang, J. B.; Xiao, X. H.; Qu, S. S. Study of the interaction between monoammonium glycyrrhizinate and bovine serum albumin, *J. Pharm. Biomed. Anal.* **2004**, *36*, 915–919.

[38] Naik, K. M.; Kolli, D. B.; Nandibewoor, S. T. Elucidation of binding mechanism of hydroxyurea on serum albumins by different spectroscopic studies, *Springerplus* **2014**, *3*, 1–13.

[39] Sułkowska, A. Interaction of drugs with bovine and human serum albumin, *J. Mol. Struct.* **2002**, *614*, 227–232.

[40] Liu, H.; Li, L.; Guo, Q.; Dong, J.; Li, J. Synthesis, crystal structure, DNA and albumin - binding properties of a chromium(III) complex with 1,10-phenanthroline and a Schiff base derived from glycine, *Transit. Met. Chem.* **2013**, *38*, 441–448.

[41] Yasseen, Z. G. On the interactions of bovine serum albumin with some surfactants: New insights from conductivity studies, *J. Chem. Pharm. Res.* **2012**, *4*, 3361–3367.

[42] Jha, N. S.; Kishore, N. Binding of streptomycin with bovine serum albumin: Energetics and conformational aspects, *Thermochim. Acta.* **2009**, *48*, *2*21–29.

[43] Peyrin, E.; Guillaume, Y. C.; Guinchard, C. Characterization of solute binding at human serum albumin site II and its geometry using a biochromatographic approach, *Biophys. J.* **1999**, *77*, 1206–1212.

[44] Trnkova, L.; Bousova, I.; Kubicek, V.; Drsata, Binding of naturally occurring hydroxycinnamic acids to bovine serum albumin, *J. Nat. Sci.* **2010**, *2*, 563–570.

[45] Bourassa, P.; Kanakis, C. D.; Tarantilis, P.; Pollissiou, M. G.; Tajmir - Riahi, H. A. Resveratrol, Genistein and Curcumin Bind Bovine Serum Albumin, *J. Phys. Chem. B.* **2010**, *114*, 3348–3354.

[46] Borovic, S. Copper complexes as therapeutic drugs. Use of analytical / spectroscopic methods for the evaluation of their transport in blood, Ph.D. Dissertation, University of Algarve, **2012**.

[47] Wainwright, M. Moulds in ancient and more recent medicine, *Top. Catal.* **1989**, *3*, 21–23.

[48] Sengupta, S.; Chattopadhyay, M. K.; Grossart, H. P. The multifaceted roles of antibiotics and antibiotic resistance in nature, *Front. Microbiol.* **2013**, *4*, 1–13.

[49] Kingston, W. Irish contributions to the origins of antibiotics, *Ir. J. Med. Sci.* **2008**, *177*, 87–92.

[50] Ventola, C. L. The antibiotic resistance crisis: Part 1: Causes and threats, *P T.* **2015**, *40*, 277–283.

[51] Tanwar, J.; Das, S.; Fatima, Z.; Hameed, S. Multidrug resistance: An emerging crisis, *Interdiscip. Perspect. Infect. Dis.* **2014**, *2014*, 1–7.

[52] Balouiri, M.; Sadiki, M.; Ibnsouda, S. K. Methods for in vitro evaluating antimicrobial activity: A review, *J. Pharm. Anal.* **2016**, *6*, 71–79.

[53] Santos, A. F.; Brotto, D. F.; Favarin, L. R. V.; Cabeza, N. A.; Andrade, G. R.; Batistote, M.; Cavalheiro, A. A.; Neves, A.; Rodrigues, D. C. M.; dos Anjos, A. Study of the antimicrobial activity of metal complexes and their ligands through bioassays applied to plant extracts, *Brazilian J. Pharmacogn.* **2014**, *24*, 309–315.

[54] Penchovsky, R.; Traykovska, M. Designing drugs that overcome antibacterial resistance: where do we stand and what should we do?, *Expert Opin. Drug Discov.* **2015**, *10*, 631–650.

[55] de Fatima, A.; Martins, C. V. B.; Modolo, L. V.; da Silva, C. M.; Alves, R. B.; da Silva, D. L.; de Resende, M. A. Schiff bases: A short review of their antimicrobial activities, *J. Adv. Res.* **2010**, *2*, 1–8.

[56] Selvi, E. T.; Mahalakshmi, S. Synthesis and characterisation of new heterocyclic Schiff base ligand derived from 4-amino antipyrine, *Int. J. Adv. Res. Dev.* **2017**, *2*, 51–56.

[57] Agwara, M. O.; Ndifon, P. T.; Ndosiri, N. B.; Paboudam, A. G.; Yufanyi, D. M.; Mohamadou, A. Synthesis, characterisation and antimicrobial activities of cobalt(II), copper(II) and zinc(II) mixed - ligand complexes containing 1,10-phenanthroline and 2,2′-bipyridine, *Bull. Chem. Soc. Ethiop.* **2010**, *24*, 383–389.

[58] El - Ajaily, M. M.; Maihub, A. A.; Mahanta, U. K.; Badhei, G.; Mohapatra, R. K.; Das, P. K. Mixed ligand complexes containing Schiff bases and their biological activities: A short review, *Rasayan J. Chem.* **2018**, *11*, 166–174.

[59] Kaura, A.; Kaura, M. Synthesis, spectral and comparative antimicrobial study of Schiff bases, *Int. J. Chem. Pharm. Sci.* **2012**, *3*, 24–29.

[60] Sahu, R.; Thakur, D. S.; Kashyap, P. Schiff base: An overview of its medicinal chemistry potential for new drug molecules, *Int. J. Pharm. Sci. Nanotechnol.* **2012**, *5*1, 757–1764.

[61] Ding, Y. Q.; Cui, Y. Z.; Li, T. D. New views on the reaction of primary amine and aldehyde from DFT study, *J. Phys. Chem. A.* **2015**, *119*, 4252–4260.

[62] Singh, D. P.; Kumar, R.; Malik, V.; Kumar, K. One pot template synthesis and characterization of trivalent transition metal ion complexes derived from diaminopyridine and glyoxal, *Rasayan J. Chem.* **2008**, *1*, 349–354.

[63] Sebastian, M. Transition metal complexes of quinoxaline based Schiff base ligands: Synthesis, characterization and catalytic activity study, Ph.D. Dissertation, Cochin University of Science and Technology, **2010**.

[64] Gaikwad, V. K.; Yadav, U. M. Metal complexes of Schiff bases, *Sch. Res. J. Interdiscip. Stud.* **2016**, *3*, 2225–2234.

[65] Singh, A.; Malik, S.; Mirza, A. S. Schiff base metal complexes of bioinorganic and medicinal relevance: A review, *Int. J. Chem. Pharm. Anal.* **2016**, *4*, 1–7.

[66] Nagaraj, K.; Sakthinathan, S.; Arunachalam, S. Synthesis, CMC determination, antimicrobial activity and nucleic acid binding of a surfactant copper(II) complex containing phenanthroline and alanine Schiff base, *J. Fluoresc.* **2014**, *24*, 589–598.

[67] Prashanthi, Y.; Kiranmai, K.; Kumar K. I. S.; Chityala, V. K.; Shivaraj. Spectroscopic characterization and biological activity of mixed ligand complexes of Ni(II) with 1,10-phenanthroline and heterocyclic Schiff bases, *Bioinorg. Chem. Appl.* **2012**, *2012*, 1–8.

[68] Ibrahim, M. N.; Sharif, S. Synthesis, characterization and use of Schiff bases as fluorimetric analytical reagents (Part II), *E - Journal Chem.* **2011**, *8*, 180–184.

[69] Kumar, S. P.; Dhar, D. N. Applications of metal complexes of Schiff bases - A review, *J. Sci. Ind. Res.* **2009**, *68*, 181–187.

[70] Al - Garawi, Z. S. M.; Tomi, I. H. R.; Al - Daraji, A. H. R. Synthesis and characterization of new amino acid- Schiff bases and studies their effects on the activity of ACP, PAP and NPA enzymes (in vitro), *E-Journal Chem.* **2012**, *9*, 962–969.

[71] Kumari, E.; Singh, S. K. Synthesis, characterisation and antimicrobial activity of some Schiff base metal chelates, *J. Chem. Pharm. Res.* **2017**, *9*, 180–184.

[72] Li, L.; Guo, Q.; Dong, J.; Xu, T.; Li, J. DNA binding, DNA cleavage and BSA interaction of a mixed - ligand copper(II) complex with taurine Schiff base and 1,10-phenanthroline, *J. Photochem. Photobiol. B Biol.* **2013**, *125*, 56–62.

[73] Gupta, N. K.; Quraishi, M. A.; Verma, C.; Mukherjee, A. K. Green Schiff's bases as corrosion inhibitors for mild steel in 1M HCl solution: Experimental and theoretical approach, *RSC Adv.* **2016**, *6*, 102076–102087.

[74] Wani, M. Y.; Malik, M. A.; Hashmi, A. A.; Dar, O. A.; Gull, P. Heterocyclic Schiff base transition metal complexes in antimicrobial and anticancer chemotherapy, *Med.Chem. Comm.* **2017**, *9*, 409–436.

[75] Yilmaz, H. A.; Dilimulati, K. M.; Zorlu, Y.; Andac, M. A new Co(III) complex of Schiff base derivative for electrochemical recognition of nitrite anion, *J. Chem. Sci.* **2017**, *129*, 1559–1569.

[76] Kim, M. S.; Lee, S. Y.; Jung, J. M.; Kim, C. A new Schiff - base chemosensor for selective detection of Cu^{2+} and Co^{2+} and its copper complex for colorimetric sensing of S^{2-} in aqueous solution, *Photochem. Photobiol. Sci.* **2017**, *16*, 1677–1689.

[77] Kiruthikajothi, K.; Chandramohan, G. Synthesis and evaluation of insecticide efficiency of copper complexes against eriophyid mite, Aceria guerreronis, *Int. J. Curr. Microbiol. App. Sci.* **2013**, *2*, 24–28.

[78] Anis, I.; Aslam, M.; Noreen, Z.; Afza, N.; Hussain, A.; Hanif, A.; Safder, M. A review (Part B) – Use of Schiff base transition metal complexes as a catalyst, *Int. J. Curr. Pharm. Res.* **2013**, *5*, 30–39.

[79] Katwal, R.; Kaur, H.; Kapur, B. K. Applications of copper - Schiff's base complexes: A review, *Sci. Rev. Chem. Commun.* **2013**, *3*, 1–15.

[80] Arulmurugan, S.; Kavitha, H. Biological activities of Schiff base and its complexes: A review, *Rasayan J. Chem.* **2010**, *3*, 385–410.

[81] Ejidike, I. P.; Ajibade, P. A. Transition metal complexes of symmetrical and asymmetrical Schiff bases as antibacterial, antifungal, antioxidant, and anticancer agents: Progress and prospects, *Rev. Inorg. Chem.* **2015**, *35*, 1-34.

[82] Jing, B.; Li, L.; Dong, J.; Li, J.; Xu, T. Synthesis, crystal structure, and DNA interaction studies of a mixed - ligand copper(II) complex of 1,10-phenanthroline and a Schiff base derived from isoleucine, *Transit. Met. Chem.* **2011**, *36*, 565–571.

[83] Han, T. Y.; Guan, T. S.; Iqbal, M. A.; Haque, R. A.; Rajeswari, K. S.; Ahamed, M. B. K. ; Majid, A. M. S. A. Synthesis of water soluble copper(II) complexes: Crystal structures, DNA binding, oxidative DNA cleavage, and in vitro anticancer studies, *Med. Chem. Res.* **2014**, *23*, 2347–2359.

[84] de Fatima, A.; Martins, C. V. B.; Modolo, L. V.; da Silva, C. M.; Alves, R. B.; da Silva, D. L.; de Resende, M. A. Schiff bases: A short review of their antimicrobial activities, *J. Adv. Res.* **2010**, *2*, 1–8.

[85] Vanco, J.; Marek, J.; Travnicek, Z.; Racanska, E.; Muselik, J.; Svajlenova, O. Synthesis, structural characterization, antiradical and antidiabetic activities of copper(II) and zinc(II) Schiff base complexes derived from salicylaldehyde and β-alanine, *J. Inorg. Biochem.* **2008**, *102*, 595–605.

[86] Seng, H. L.; Wang, W. S.; Kong, S. M.; Ong, H. K. A.; Win, Y.F.; Zaliha, R. N.; Chikira, M.; Leong, W. K.; Ahmad, M.; Khoo, A. S. B.; Ng, C. H. Biological and cytoselective anticancer properties of copper(II) - polypyridyl complexes modulated by auxiliary methylated glycine ligand, *BioMetals* **2012**, *25*, 1061–1081.

[87] Patel, V.; Trivedi, P.; Gohel, H.; Khetani, D. Synthesis and characterization of Schiff base of *p*-chloroaniline and their metal complexes and their evaluation for antibacterial activity, *Int. J. Adv. Pharmacy, Biol. Chem.* **2014**, *3*, 999–1003.

[88] Hussain, Z.; Khalaf, M.; Adil, H.; Zageer, D.; Hassan, F.; Mohammed, S.; Yousif, E. Metal complexes of Schiff's bases containing sulfonamides nucleus: A review, *Res.J. Pharm. Biol. Chem. Sci.* **2016**, *7*, 1008–1025.

[89] Tanaka, K.; Shiraishi, R. Clean and efficient condensation reactions of aldehydes and amines in a water suspension medium, *Green Chem.* **2000**, *2*, 272–273.

[90] Carballo, R.; Covelo, B.; Lopez, E. M. V.; Martinez, E.G.; Castineiras, A.; Niclos, J. Mixed - ligand complexes of zinc(II) with α-hydroxycarboxylates and aromatic N - N' donor ligands: Synthesis, crystal structures and effect of weak interactions on their crystal packing, *Z. Anorg. Allg. Chem.* **2005**, *631*, 785–792.

[91] Tong, J. Y.; Sun, N. B.; Wu, H. K. Grinding synthesis of Schiff bases combined with infrared irradiation, *Asian J. Chem.* **2013**, *25*, 5399–5401.

[92] Cella, R.; Stefani, H. A. Ultrasound in heterocycles chemistry, *Tetrahedron* **2009**, *65*, 2619–2641.

[93] Zheng, Y.; Ma, K.; Li, H.; Li, J.; He, J.; Sun, X.; Li, R.; Ma, J. One pot synthesis of imines from aromatic nitro compounds with a novel Ni / SiO_2 magnetic catalyst, *Catal. Letters* **2009**, *128*, 465–474.

[94] Varma, R. S.; Naicker, K. P.; Liesen, P. J. Selective nitration of styrenes with clayfen and clayan: A solvent - free synthesis of β-nitrostyrenes, *Tetrahedron Lett.* **1998**, *39*, 3977–3980.

[95] Shaabani, B.; Darbari, R. Synthesis and characterization of salen and thiocyanate complexes with Co^{2+}, *J.Org. Chem.* **2013**, *55*, 12764–12766.

[96] Radfard, R.; Abedi, A. Synthesis and characterization of new Schiff bases of ethylenediamine and benzaldehyde derivatives, along with their iron complexes, *J. Appl. Chem. Res.* **2015**, *9*, 59–65.

[97] Kotova, O. V.; Eliseeva, S. V.; Averjushkin, A. S.; Lepnev, L. S.; Vaschenko, A. A.; Rogachev, A. Y.; Vitukhnovskii, A. G.; Kuzmina, N. P. Zinc(II) complexes with Schiff bases derived from ethylenediamine and salicylaldehyde: The synthesis and photoluminescent properties, *Russ. Chem. Bull.* **2008**, *57*, 1880–1889.

[98] Desai, M. N.; Talati, J. D.; Shah, N. K. Schiff bases of ethylenediamine / triethylenetetramine with benzaldehyde / cinnamic aldehyde / salicylaldehyde as corrosion inhibitors of zinc in sulphuric acid, *Anti-Corrosion Methods Mater.* **2008**, *55*, 27–37.

[99] Zolezzi, S.; Decinti, A.; Spodine, E. Synthesis and characterization of copper(II) complexes with Schiff base ligands derived from ethylenediamine, diphenylethylenediamine and nitro, bromo and methoxy salicylaldehyde, *Polyhedron* **1999**, *18*, 897–904.

[100] Al - hamdani, A. A.; Mahmoud, M. A.; Bakir, S. R. Synthesis, structural studies of some new transition metals complexes of semicarbazide hydro chloride Schiff base derivatives, *J. Baghdad Sci.* **2013**, *10*, 583–596.

[101] Hamil, A. M.; Khalifa, K. M.; Al - Houni, A.; El - Ajaily, M. M. Synthesis, spectroscopic investigation and antiactivity activity of Schiff base complexes of cobalt(II) and copper(II) ions, *Rasayan J. Chem.* **2009**, *2*, 261–266.

[102] Nagajothi, A.; Kiruthika, A.; Chitra, S.; Parameswari, K. Synthesis and characterization of tetradentate Co(II) Schiff base complexes: Antimicrobial & DNA cleavage studies, *Int. J. Res. Pharm. Biomed. Sci.* **2012**, *3*, 1768–1778.

[103] Gaballa, A. S.; Asker, M. S.; Barakat, A. S.; Teleb, S. M. Synthesis, characterization and biological activity of some platinum(II) complexes with Schiff bases derived from salicylaldehyde, 2-furaldehyde and phenylenediamine, *Spectrochim. Acta - Part A Mol. Biomol. Spectrosc.* **2007**, *67*, 114–121.

[104] Fasina, T. M.; Ogundele, O. O.; Ayeni, I. Synthesis and biological properties of N_2O_2 Schiff bases derived from *o*-phenylenediamine and substituted salicylaldehydes, *J. Chem. Pharm. Res.* **2014**, *6*, 816–819.

[105] Krishnamoorthy, P.; Sathyadevi, P.; Butorac, R. R.; Cowley, A. H.; Bhuvanesh, N. S. P. Dharmaraj, N. Copper(I) and nickel(II) complexes with 1:1 vs. 1:2 coordination of ferrocenyl hydrazone ligands: Do the geometry and composition of complexes affect DNA binding / cleavage, protein binding, antioxidant and cytotoxic activities?, *Dalt. Trans.* **2012**, *41*, 4423–4436.

[106] Bagherzadeh, M.; Zare, M. Synthesis and characterization of NaY zeolite - encapsulated Mn - hydrazone Schiff base: An efficient and reusable catalyst for oxidation of olefins, *J. Coord. Chem.* **2012**, *65*, 4054–4066.

[107] Kitamura, F.; Sawaguchi, K.; Mori, A.; Takagi, S.; Suzuki, T.; Kobayashi, A.; Kato, M.; Nakajima, K. Coordination structure conversion of hydrazone – palladium(II) complexes in the solid state and in solution, *Inorg. Chem.* **2015**, *54*, 8436–8448.

[108] Chew, S. T.; Lo, K. M.; Sinniah, S. K.; Sim, K. S.; Tan, K. W. Synthesis, characterization and biological evaluation of cationic hydrazone copper complexes with diverse diimine co - ligands, *RSC Adv.* **2014**, *4*, 61232–61247.

[109] De Lima, R. L.; Regina, L.; Teixeira, D. S.; Carneiro, T. M. G.; Beraldo, H. Nickel (II), copper(I) and copper(II) complexes of bidentate heterocyclic thiosemicarbazones, *J. Braz. Chem. Soc.* **1999**, *10*, 184–188.

[110] Pelosi, G. Thiosemicarbazone metal complexes: from structure to activity, *Open Crystallogr. J.* **2010**, *3*, 16–28.

[111] Pelosi, G.; Re, M. C.; Casoli, C.; Schiavone, P.; Ronzi, P.; Pilotti, E.; Bisceglie, F.; Bignami, F. Antiretroviral activity of thiosemicarbazone metal complexes, *J. Med. Chem.* **2010**, *53*, 8765–8769.

[112] Sapna, K.; Sharma, N. K. Preparation and characterization of Ni(II) and Mn(II) complexes of semicarbazone and thiosemicarbazone of *m*-hydroxybenzaldehyde and *p*-hydroxybenzaldehyde, *Int. J. Sci. Eng. Res.* **2013**, *4*, 15–21.

[113] Padhye, S.; Kaufmann, G. Transition metal complexes of semicarbazones and thiosemicarbazones, *Coord. Chem. Rev.* **1985**, *63*, 127–160.

[114] Jesmin, M.; Islam, M. K.; Ali, S. M. M. Analgesic and anti - inflammatory activities of some transition metal Schiff base complexes, *Int. Lett. Chem. Phy. Astr.* **2014**, *8*, 64–72.

[115] Shiekh, R. A.; Rahman, I. A.; Malik, M. A.; Luddin, N.; Masudi, S. M.; Al -Thabaiti, S. A. Transition metal complexes with mixed nitrogen - sulphur (N - S) donor macrocyclic Schiff base ligand: Synthesis, spectral, electrochemical and antimicrobial studies, *Int. J. Electrochem. Sci.* **2013**, *8*, 6972–6987.

[116] Lovely, K. L. P. S.; Christudhas, M. Synthesis, characterization and biological activities of Schiff base complexes of Cu(II), Ni(II), and Co(II) with 4-pyridine carboxaldehyde and 3-aminopyridine, *J. Chem. Pharm. Res.* **2013**, *5*, 184–191.

[117] Jayalakshmi, R.; Rajavel, R. Elaborated studies on Schiff base homo - binuclear Cu(II) and Co(II) complexes, spectral, thermal, P - XRD and biocidal studies, *J. Adv. Appl. Sci. Res.* **2017**, *1*.

[118] Suja, N. Studies on some supported cobalt(II), nickel(II) and copper(II) complexes of *o*-phenylenediamine and Schiff bases derived from 3-hydroxyquinoxaline-2-carboxaldehyde, Cochin University of Science and Technology, Ph.D. Dissertation, **2002**.

[119] Shamkhy, E. T. Preparation and characterization of new Schiff base derived from pyridine and its metal complexes, *Int. J. Curr. Res. Chem. Pharm. Sci.* **2016**, *3*, 118–123.

[120] Mittal, P.; Joshi, S.; Panwar, V.; Uma, V. Biologically active Co(II), Ni(II), Cu(II) and Mn(II) complexes of Schiff bases derived from vinyl aniline and heterocyclic aldehydes, *Int. J. ChemTech Res.* **2009**, *1*, 225–232.

[121] Mohamed, G. G.; Omar, M. M.; Hindy, A. M. M. Synthesis, characterization and biological activity of some transition metals with Schiff base derived from 2-thiophenecarboxaldehyde and aminobenzoic acid, *Spectrochim. Acta - Part A Mol. Biomol. Spectrosc.* **2005**, *62*, 1140–1150.

[122] Spinu, C.; Pleniceanu, M.; Tigae, C. Biologically active transition metal chelates with a 2-thiophenecarboxaldehyde derived Schiff base: Synthesis, characterization, and antibacterial properties, *Turkish J. Chem.* **2008**, *32*, 487–493.

[123] Uddin, M. N. Metal complexes of Schiff bases derived from 2-thiophenecarboxaldehyde and mono / diamine as the antibacterial agents, *Mod. Chem.* **2014**, *2*, 6–14.

[124] Odeh, I. N. Synthesis, characterization, and CT - DNA interactions of novel complexes of (Copper(II) \ tetradentate SNNS Schiff bases), AN - Najah National University, Ph.D. Dissertation, **2016**.

[125] Apparao, C.; Seshaiah, K.; Reddy, D. H. K.; Kumar, B. N.; Harinath, Y. Synthesis, spectral characterization and antioxidant activity studies of a bidentate Schiff base, 5-methylthiophene-2-carboxaldehyde-carbohydrazone and its Cd(II), Cu(II), Ni(II) and Zn(II) complexes, S*pectrochim. Acta - Part A Mol. Biomol. Spectrosc.* **2012**, *101*, 264–272.

[126] Abd El - Halim, H. F.; Mohamed, G. G.; Khalil, E. A. M. Synthesis, spectral, thermal and biological studies of mixed ligand complexes with newly prepared Schiff base and 1,10-phenanthroline ligands, *J. Mol. Struct.* **2017**, *1146*, 153–163.

[127] Reiss, A.; Florea, S.; Caproiu, T.; Stanica, N. Synthesis, characterization, and antibacterial activity of some transition metals with the Schiff base N-(2-furanylmethylene)-3-aminodibenzofuran, *Turkish J. Chem.* **2009**, *33*, 775–783.

[128] Bose, R. N.; Ali, M. A. Transition metal complexes of furfural and benzil Schiff bases derived from s-benzyldithiocarbazate, *Polyhedron* **1984**, *3*, 517–522.

[129] Rosu, T.; Negoiu, M.; Circu, V. Complex combinations of Cu (II) with mixed ligands, *Analele Univ. Din Bucureşti – Chim.* **2005**, *I–II*, 153–159.

[130] Mihai, S.; Negoiu, M. Synthesis and characterization of Ni(II), Pt(IV), Pd(II), Co(II), Au(III), Cu(II) complexes with mixed ligands, *Rev. Chim.* **2009**, *60*, 222–225.

[131] Maurya, R. C.; Patel, P.; Rajput, S. Synthesis and characterization of mixed - ligand complexes of Cu(II), Ni(II), Co(II), Zn(II), Sm(III) and U(VI)O_2, with a Schiff base derived from the sulfa drug sulfamerazine and 2,2′-bipyridine, *Synth. React. Inorg. Met. Chem.* **2003**, *33*, 801–816.

[132] Boghaei, D. M.; Gharagozlou, M. Spectral characterization of novel ternary zinc(II) complexes containing 1,10-phenanthroline and Schiff bases derived from amino acids and salicylaldehyde-5-sulfonates, *Spectrochim. Acta - Part A Mol. Biomol. Spectrosc.* **2007**, *67*, 944–949.

[133] Sureshan, C. A.; Bhattacharya, P. K. Synthesis, characterization and electrochemical properties of Fe(III) binuclear complexes, *Indian J. Chem. - Sect. A Inorganic, Phys. Theor. Anal. Chem.* **2002,** *41*, 973–975.

[134] Reddy, P. R.; Radhika, M.; Manjula, P. Synthesis and characterization of mixed ligand complexes of Zn(II) and Co(II) with amino acids: Relevance to zinc binding sites in zinc fingers, *J. Chem. Sci.* **2005**, *117*, 239–246.

[135] Maihub, A. A.; Alassbaly, F. S.; El - Ajaily, M. M.; Etorki, A. M. Modification on synthesis of mixed ligand chelates by using di - and trivalent transition metal ions with Schiff base as primary ligand, *Green Sustain. Chem.* **2014**, *4*, 103–110.

[136] Gupta, M.; Srivastava, M. N. Synthesis and characterization of mixed ligand complexes of copper(II), nickel(II), cobalt(II) and zinc(II) with glycine and uracil or 2-thiouracil, *Polyhedron* **1985**, *4*, 475–479.

[137] Lian, W. J.; Wang, X. T.; Xie, C. Z.; Tian, H.; Song, X. Q.; Pan, H. T.; Qiao, X.; Xu, J. Y. Mixed - ligand copper(II) Schiff base complexes: The role of the co - ligand in DNA binding, DNA cleavage, protein binding and cytotoxicity, *Dalt. Trans.* **2016**, *45*, 9073–9087.

[138] Srinag, B. S.; Akbarsha, M. A.; Periasamy, V. S.; Palaniandavar, M.; Rajendiran, V.; Krishnamurthy, H.; Karthik, R. Mixed - ligand copper(II) - phenolate complexes: Effect of coligand on enhanced DNA and protein binding, DNA cleavage, and anticancer activity, *Inorg. Chem.* **2007**, *46*, 8208–8221.

[139] Lawrence, D.; Vaidyanathan, V. G.; Nair, B. U. Synthesis, characterization and DNA binding studies of two mixed ligand complexes of ruthenium(II), *J. Inorg. Biochem.* **2006**, *100*, 1244–1251.

[140] Poulter, N.; Donaldson, M.; Mulley, G.; Duque, L.; Waterfield, N.; Shard, A. G.; Spencer, S.; Jenkins, A. T. A.; Johnson, A. L. Plasma deposited metal Schiff - base compounds as antimicrobials, *New J. Chem.* **2011**, *35*, 1477–1484.

[141] Selvaganapathy, M.; Raman, N. Pharmacological activity of a few transition metal complexes: A short review, *J. Chem. Biol. Ther.* **2016**, *1*, 1–17.

[142] Mahalakshmi, R.; Raman, N. A therapeutic journey of mixed ligand complexes containing 1,10-phenanthroline derivatives: A review, *Int. J. Curr. Pharm. Rev. Res.* **2016**, *8*, 1–6.

[143] Anjaneyulu, Y.; Rao, R. P. Preparation, characterization and antimicrobial activity studies on some ternary complexes of Cu(II) with acetylacetone and various salicylic acids, *Synth. React. Inorg. Met. Chem.* **1986**, *16*, 257–272.

[144] Anjaneyulu, Y.; Raman, N.; Rao, R. Physicochemical and antimicrobial activity studies on the ternary complexes of Zn(II) with 8-hydroxyquinoline and salicylic acids, *Proc. Indian Natn. Sci. Acad.* **1987**, *53A*, 548–553.

[145] Wankhede, D. S.; Chavan, S. S. Synthesis, characterization and antimicrobial activities of mixed ligand complexes of transition metals using 2-aminophenol and 2-chloroaniline as ligands, *Asian J. Res. Chem.* **2017**, *10*, 639-645.

[146] Al - noor, T. H.; Shinan, G. T. Synthesis and characterization of mixed - ligand complexes of oxalic acid and trimethoprim with Mn(II), Co(II), Ni(II), Cu(II), Zn(II) and Cr(III) ions and antimicrobial activities, *Res. J. Pharm. Biol. Chem. Sci.* **2017**, *8*, 1375–1381.

[147] Prasad, B. B.; Sah, R. A biomimicing approach to the mixed ligand complexes of bivalent transition metal, *Int. J. Appl. Sci. Biotechnol.* **2013**, *1*, 16–20.

[148] Sreekanth, B.; Gopinath, S.; Pillai, V.; Shareef, I.; Reddy, J.; Vishnuvardhan, T.; Murali, K.; Sridhara, V. DNA binding and antimicrobial studies on Co(III) and Fe(II) metal complexes containing mixed ligands, *Res. J. Pharm. Biol. Chem. Sci.* **2013**, *4*, 217–225.

[149] Souaya, E. R.; Khalil, M. M. H.; Ismail, E. H.; Bendas, E. R.; Neaz, O. S. Synthesis and characterization of ternary complexes of certain hydroxyl acids and their biological applications, *Res. J. Pharm. Biol. Chem. Sci. Synth.* **2014**, *5*, 18–30.

[150] Tajudeen, S. S.; Kannappan, G. Schiff base – copper(II) complexes: Synthesis, spectral studies and anti-tubercular and antimicrobial activity, *Indian J. Adv. Chem. Sci.* **2016**, *4*, 40–48.

[151] Raman, N.; Mahalakshmi, R. Bio active mixed ligand complexes of Cu(II), Ni(II) and Zn(II): Synthesis, spectral, XRD, DNA binding and cleavage properties, *Inorg. Chem. Commun.* **2014**, *40*, 157–163.

[152] Arounaguiri, S.; Easwaramoorthy, D.; Kumar, A. A.; Dattagupta, A.; Maiya, B. G. Cobalt(III), nickel(II) and ruthenium(II) complexes of 1,10-phenanthroline family of ligands: DNA binding and photocleavage studies, *Proc. Indian Acad. Sci. Chem. Sci.* **2000**, *11*, 21–17.

[153] Li, J.; Dong, J.; Cui, H.; Xu, T.; Li, L. A copper(II) complex of the Schiff base from L-valine and 2-hydroxy-1-naphthalidene plus 1,10-phenanthroline: Synthesis, crystal structure, and DNA interaction, *Transit. Met. Chem.* **2012**, *37*, 175–182.

[154] Kathiresan, S.; Mugesh, S.; Murugan, M.; Ahamed, F.; Annaraj, J. Mixed ligand copper(II) - phenolate complexes: Structure and studies on DNA / protein binding profiles, DNA cleavage, molecular docking and cytotoxicity, *RSC Adv.* **2016**, *6*, 1810–1825.

Chapter 2

Synthesis, characterization and biological evaluation studies of Cu(II) and Zn(II) complexes with Schiff base formed by reaction between glyoxal and ortho / para - anisidine and N, N' donor ligands

2.1 Introduction

The present chapter concerns with the aim to synthesize metal complexes of zinc and copper with Schiff base (obtained by the condensation of glyoxal with ortho and para anisidine) as primary and N, N' donor molecules as secondary ligands. The ligand and their complexes were characterized with the help of various spectroscopic techniques viz. UV-vis, FTIR, NMR and mass spectral techniques. They were then analyzed for their antimicrobial activities against two bacterial strains i.e. *Staphylococcus aureus* (gram positive) and *Escherichia coli* (gram negative) and two fungal strains i.e. *Aspergillus niger* and *Aspergillus fumigatus* by agar well diffusion method. The complexes were also analyzed for their interaction with BSA by UV titration method.

2.2 Methodology

2.2.1 Methodology for the synthesis of (gly-*o*-andn) Schiff base (L_1)

In hot methanolic solution (35 ml) of glyoxal (4 mmol, 0.232 g) was added drop wise a hot methanolic solution (35 ml) of *o*-anisidine (8 mmol, 0.985 g or 0.9 ml). The whole set up was placed into an oil bath for 5 h at 70°C. The clear solution thus obtained was allowed to evaporate slowly. After 82 h, brown colored crystalline product separates out; this was filtered and dried in desiccators. Yield: 79 %, Color: Brown, M.P. 72°C, UV (λ_{max}): 239 nm, 284 nm, MS: $[M]^+$ 268, Main IR peaks (cm^{-1}): υ(C_6H_5 stretch) 3045, υ(C=N) 1599, υ(C–C) 1506, ^{1}H NMR (400 MHz, $CDCl_3$), δ = 8.15 (s, 2H, -CH=N), 7.66 (d, 4H, Ar-H), 7.53 (d, 4H, Ar-H), 3.85 (s, 6H, -OCH_3).

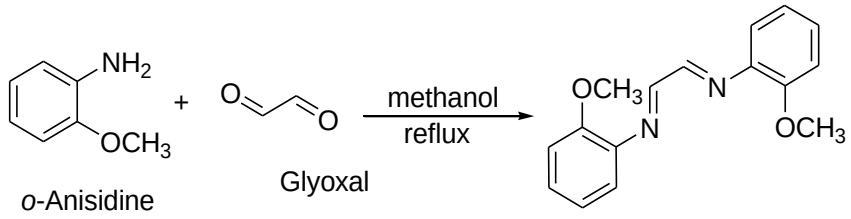

Fig. 24: Scheme for synthesis of Schiff base (L_1)

2.2.2 Methodology for the synthesis of $[Zn(L_1)phen]Cl_2$ *(1)*

In hot methanolic solution (30 ml) of Schiff base (1 mmol, 0.268 g) **(L_1)** was added methanolic solution (30 ml) of $ZnCl_2$ (1 mmol, 0.136 g) with constant stirring at 70°C. The solution was refluxed for 10 h. A hot methanolic solution of 1,10-phenanthroline (1 mmol or 0.198 g) was added drop wise to above solution with refluxing continuing for further 8 h. White precipitates were collected after filtration. Several washings were made with cold methanol. Yield: 54 %, Color: White, M.P. Above 280°C, UV (λ_{max}): 221 nm, 265 nm, MS: $[M]^+$ 620, Main IR peaks (cm^{-1}): υ(OH) 3200 - 3400, υ(C_6H_5 stretch) 3047, υ(C=N) 1581, υ(C–C) 1516, υ(M-N) 426.

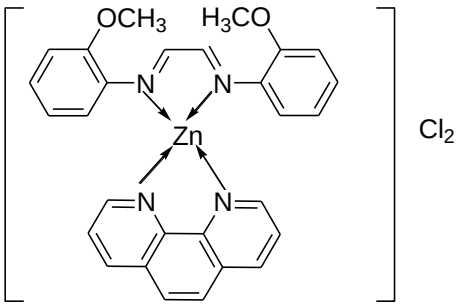

Fig. 25: Proposed geometry of $[Zn(L_1)phen]Cl_2$ *(1)*

2.2.3 Methodology for the synthesis of $[Zn(L_1)bpy]Cl_2$ *(2)*

In hot methanolic solution (30 ml) of Schiff base (1 mmol, 0.268 g) **(L_1)** was added methanolic solution (30 ml) of $ZnCl_2$ (1 mmol, 0.136 g) with constant stirring at 70°C. The solution was refluxed for 10 h. A hot methanolic solution of 2,2'-bipyridine (1 mmol or 0.156 g) was added drop wise to above solution with further refluxing for 8 h. White precipitates were collected after filtration. Several washings were made with cold methanol. Yield: 52 %, Color: White, M.P. Above 280°C, UV

(λ_{max}): 239 nm, 291 nm, MS: $[M]^+$ 578, Main IR peaks (cm^{-1}): υ(OH) 3200-3400, υ(C_6H_5 stretch) 3061, υ(C=N) + υ(C–C) 1595, υ(M-N) 412.

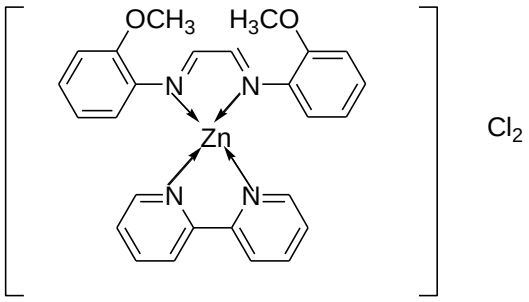

Fig. 26: Proposed geometry of [Zn(L_1)bpy]Cl_2 *(2)*

2.2.4 Methodology for the synthesis of [Cu(L_1)phen]Cl_2 *(3)*

In hot methanolic solution (30 ml) of Schiff base (1 mmol, 0.268 g) **(L_1)** was added methanolic solution (30 ml) of $CuCl_2.2H_2O$ (1 mmol, 0.170 g) with constant stirring at 70°C. The solution was refluxed for 10 h. A hot methanolic solution of 1,10-phenanthroline (1 mmol or 0.198 g) was added drop wise to above solution with refluxing continuing for further 8 h. Green precipitates were collected after filtration. Several washings were made with cold methanol. Yield: 49 %, Color: Green, M.P. Starts decomposing at 262°C, UV (λ_{max}): 269 nm, MS: $[M]^+$ 602, Main IR peaks (cm^{-1}): υ(OH) 3200-3400, υ(C_6H_5 stretch) 3048, υ(C=N) 1581, υ(C–C) 1512, υ(M-N) 428.

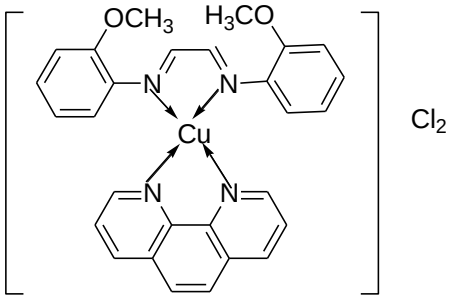

Fig. 27: Proposed geometry of [Cu(L_1)phen]Cl_2 *(3)*

2.2.5 Methodology for the synthesis of $[Cu(L_1)bpy]Cl_2$ *(4)*

In hot methanolic solution (30ml) of Schiff base (1 mmol, 0.268 g) **(L_1)** was added methanolic solution (30 ml) of $CuCl_2.2H_2O$ (1 mmol, 0.170 g) with constant stirring at 70°C. The solution was refluxed for 10 h. A hot methanolic solution of 2,2'-bipyridine (1 mmol or 0.156 g) was added drop wise to above solution with refluxing continuing for further 8 h. Green precipitates were collected after filtration. Several washings were made with cold methanol. Yield: 55 %, Color: Green, M.P. Starts decomposing at 248°C, UV (λ_{max}): 292 nm, MS: $[M]^+$ 558, Main IR peaks (cm^{-1}): υ(OH) 3200-3400, υ(C_6H_5 stretch) 3051, υ(C=N) 1595, υ(C–C) 1510, υ(M-N) 416.

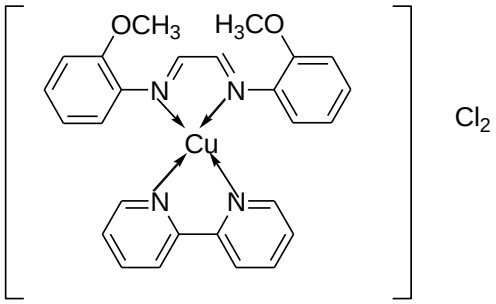

Fig. 28: Proposed geometry of $[Cu(L_1)bpy]Cl_2$ *(4)*

2.2.6 Methodology for the synthesis of (gly-*p*-andn) Schiff base (L_2)

To a stirred and refluxed solution of glyoxal (4 mmol, 0.232 g) in hot methanol (35 ml) was added drop wise a hot methanolic solution (35 ml) of *p*-anisidine (8 mmol, 0.985 g or 0.9 ml). The whole set up was placed into an oil bath for 5 h at 70°C. Yellow colored precipitates were formed immediately. The solution is further refluxed for 3 h to ensure complete precipitation. The precipitates thus obtained were filtered, washed many times with methanol. They were recrystallized using hot methanol as solvent. Yield: 80 %, Color: Yellow, M.P. 125^{0}C, UV (λ_{max}): 236 nm, 373 nm, Main IR peaks (cm^{-1}): υ(OH) 3300-3400, υ(C_6H_5 stretch) 3062, υ(C=N) 1600, υ(C–C) 1583. ^{1}H NMR (400 MHz, d^6 - DMSO) δ = 8.39 (s, 2H, -CH=N), 7.36 (d, 4H, Ar-H), 6.95 (d, 4H, Ar-H), 3.79 (s, 6H, -OCH_3).

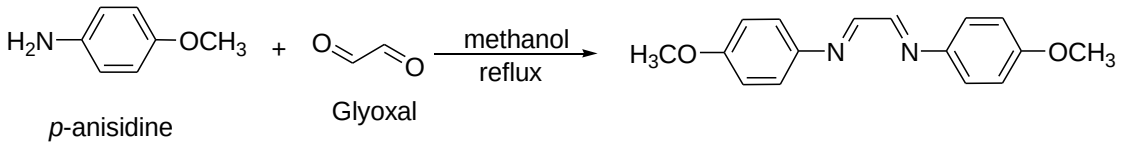

Fig. 29: Scheme for synthesis of Schiff base (L_2)

2.2.7 Methodology for the synthesis of $[Zn(L_2)phen]Cl_2$ *(5)*

In hot methanolic (30ml) of Schiff base (1mmol, 0.268g) **(L_2)** was added methanolic solution (30 ml) of $ZnCl_2$ (1 mmol, 0.136 g) with constant stirring at 70°C. The solution was refluxed for 10 h. A hot methanolic solution of 1,10-phenanthroline (1 mmol or 0.198 g) was added drop wise to above solution with refluxing continuing for further 8 h. White precipitates were collected after filtration. Several washings were made with cold methanol. Yield: 63 %, Color: White, M.P. Above 280°C, UV (λ_{max}): 223 nm, 267 nm, MS: $[M]^+$ 566, Main IR peaks (cm^{-1}): υ(C_6H_5 stretch) 3049, υ(C=N) 1583, υ(C–C) 1512, υ(M-N) 405.

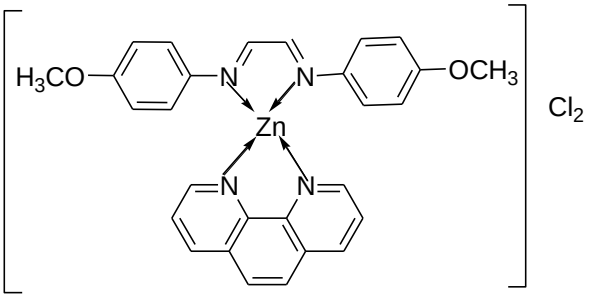

Fig. 30: Proposed geometry of $[Zn(L_2)phen]Cl_2$ *(5)*

2.2.8 Methodology for the synthesis of $[Zn(L_2)bpy]Cl_2$ *(6)*

In hot methanolic (30ml) of Schiff base (1mmol, 0.268g) **(L_2)** was added methanolic solution (30 ml) of $ZnCl_2$ (1 mmol, 0.136 g) with constant stirring at 70°C. The solution was refluxed for 10 h. A hot methanolic solution of 2,2'-bipyridine (1 mmol or 0.156 g) was added drop wise to above solution with refluxing continuing for further 8 h. White precipitates were collected after filtration. Several washings

were made with cold methanol. Yield: 62 %, Color: White, M.P. Above 280°C, UV (λ_{max}): 222 nm, 267 nm, MS: $[M]^+$ 542, Main IR peaks (cm^{-1}): υ(C_6H_5 stretch) 3064, υ(C=N) 1589, υ(C–C) 1491, υ(M-N) 414.

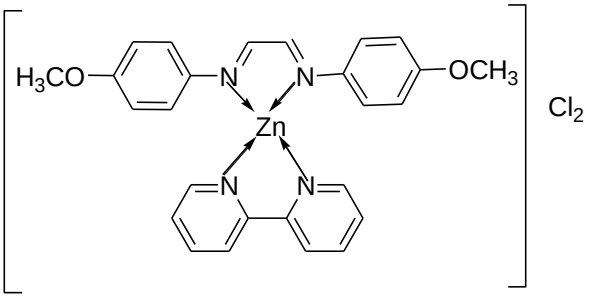

Fig. 31: Proposed geometry of [Zn(L_2)bpy]Cl_2 *(6)*

2.2.9 Methodology for the synthesis of [Cu(L_2)phen]Cl_2 *(7)*

In hot methanolic (30 ml) of Schiff base (1 mmol, 0.268 g) **(L_2)** was added methanolic solution (30 ml) of $CuCl_2.2H_2O$ (1 mmol, 0.170 g) with constant stirring at 70°C. The solution was refluxed for 10 h. A hot methanolic solution of 1,10-phenanthroline (1 mmol or 0.198 g) was added drop wise to above solution with refluxing continuing for further 8 h. Green precipitates were collected after filtration. Several washings were made with cold methanol. Yield: 55 %, Color: Green, M.P. Starts decomposing at 264°C, UV (λ_{max}): 296 nm, MS: $[M]^+$ 600, Main IR peaks (cm^{-1}): υ(C_6H_5 stretch) 3041, υ(C=N) 1577, υ(C–C) 1514, υ(M-N) 430.

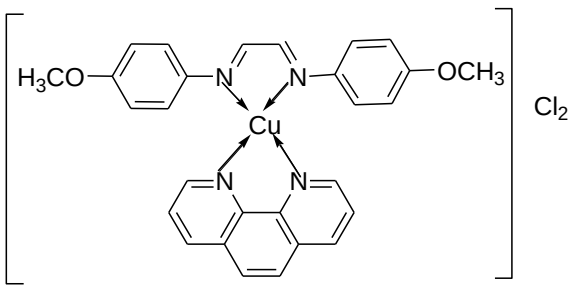

Fig. 32: Proposed geometry of [Cu(L_2)phen]Cl_2 *(7)*

2.2.10 Methodology for the synthesis of $[Cu(L_2)bpy]Cl_2$ *(8)*

In hot methanolic (30ml) of Schiff base (1 mmol, 0.268 g) **(L_2)** was added methanolic solution (30 ml) of $CuCl_2.2H_2O$ (1 mmol, 0.170 g) with constant stirring at 70°C. The solution was refluxed for 10 h. A hot methanolic solution of 2,2'-bipyridine (1 mmol or 0.156 g) was added drop wise to above solution with further refluxing for 8 h. Green precipitates were collected after filtration. Several washings were made with cold methanol. Yield: 54 %, Color: Green, M.P. Starts decomposing at 254°C, UV (λ_{max}): 296 nm, MS: $[M]^+$ 541, Main IR peaks (cm^{-1}): υ(OH) 3200-3400, $\upsilon(C_6H_5$ stretch) 3034, υ(C=N) 1566, υ(C–C) 1491, υ(M-N) 416.

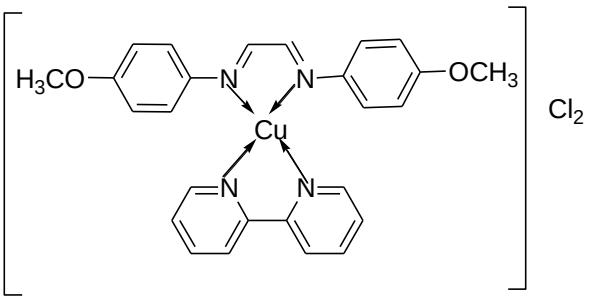

Fig. 33: Proposed geometry of $[Cu(L_2)bpy]Cl_2$ *(8)*

2.3 Results and discussions

The ligands and Cu^{2+} mixed ligand chelates appear as colored precipitates while Zn^{2+} complexes appear as white precipitates. All of them were found to be thermally stable and were non hygroscopic solids. They do not show any signs of decomposition in air and moisture even after months and were having fair solubility in water, DMSO, DMF and Tris buffer (pH 7.4).

2.3.1 UV-vis analysis

The UV-vis absorption spectroscopic results of Schiff bases and metal complexes were recorded in the range of 200 - 800 nm at low concentrations using water as solvent. The bands observed indicates π to π* transitions confirming binding

of metal centers with Schiff base, 1,10-phenanthroline / 2,2'-bipyridine. The UV–vis spectral peaks of the ligands and their chelates have been shown in Table 14.

2.3.2 FTIR analysis

In the uncoordinated ligand a strong band appears at 1599 cm^{-1} for $\mathbf{L_1}$ and 1600 cm^{-1} for $\mathbf{L_2}$ attributing to free azomethine group, but a negative shift up to 1566 cm^{-1} in metal chelates proposes coordination of the imine nitrogen to metal centers. This may occurs due to decrease in bond strength of imine bond and simultaneous increase in bond strength between azomethine nitrogen and metal centre. All the metal complexes show absorption peaks at 414 - 429 cm^{-1} region corresponding to M-N vibrations confirming the bond formation between azomethine nitrogen and metal ion. Absorption bands at 3200 - 3400 cm^{-1} range in some complexes marks the existence of coordinated or lattice water. IR analysis with selected bond frequencies of all Schiff bases and their corresponding mixed ligand chelates are as follows (Table14):

Table 14: Selected bond frequencies (cm^{-1}) and UV-vis values of ligand and Zn(II) and Cu(II) mixed ligand chelates

Complex	**$\nu_{(M-N)}$ (cm^{-1})**	**C_6H_5 stretch (cm^{-1})**	**ν(-C=N-) stretch (cm^{-1})**	**Lattice water**	**π to π^* transition (nm)**
(L_1)	-	**3045**	**1599**	-	**239, 284**
[Zn(L_1)phen]Cl_2 ***(1)***	426	3047	1581	3200-3400	221, 265
[Zn(L_1)bpy]Cl_2 ***(2)***	412	3061	1595	3200-3400	239, 291
[Cu(L_1)phen]Cl_2 ***(3)***	428	3048	1581	3200-3400	269
[Cu(L_1)bpy]Cl_2 ***(4)***	416	3051	1595	3200-3400	292
(L_2)	-	**3062**	**1600**	**3300-3400**	**236, 373**
[Zn(L_2)phen]Cl_2 ***(5)***	405	3049	1583	-	223, 267
[Zn(L_2)bpy]Cl_2 ***(6)***	414	3064	1589	-	222, 267
[Cu(L_2)phen]Cl_2 ***(7)***	430	3041	1577	-	296
[Cu(L_2)bpy]Cl_2 ***(8)***	416	3034	1566	3200-3400	296

2.3.3 Mass spectral analysis

The molecular ion peaks in mass spectra of ligands (**L_1** and **L_2**) was observed at m/z 269 which is the parent ion peak of both ortho and para isomers, thus confirming there formation. The mass fragmentation pattern of the complexes has been tabulated as follows:

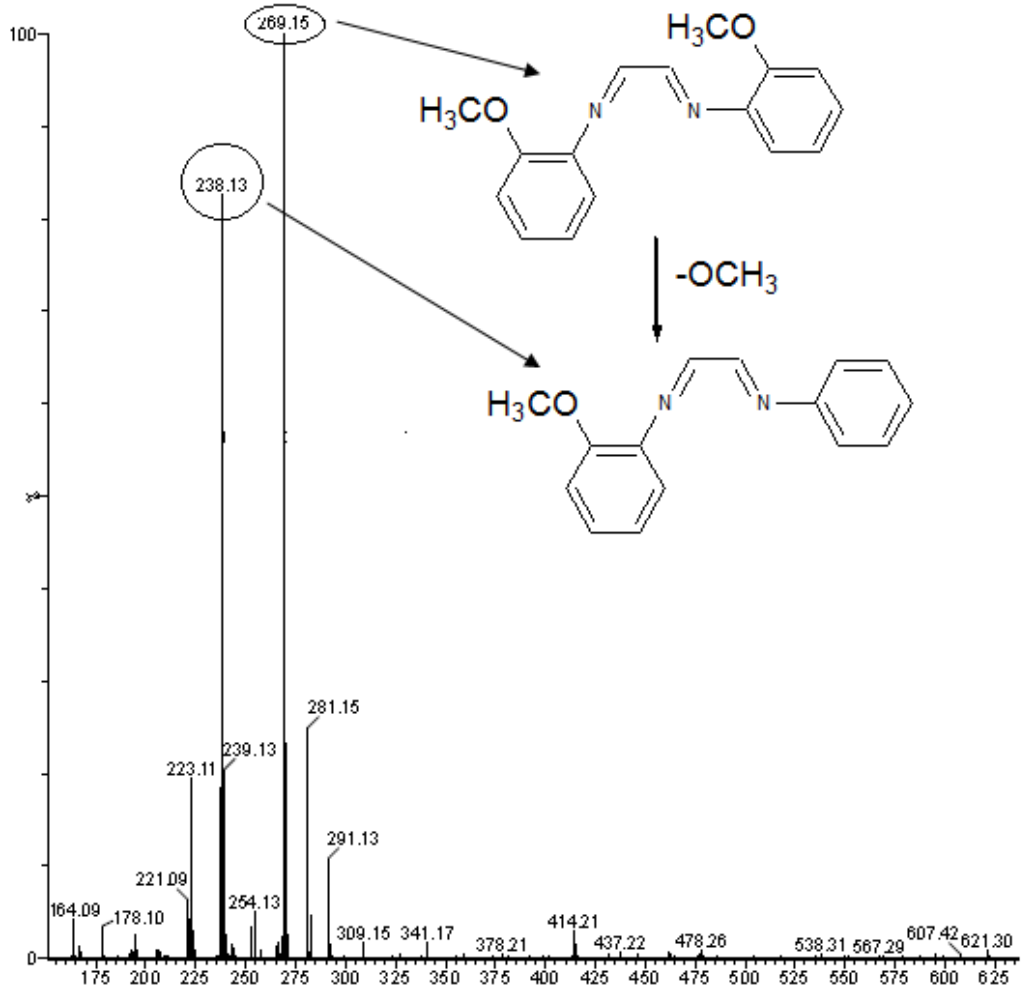

Fig. 34: Mass spectra of L_1 (Mol. Mass = 268 g)

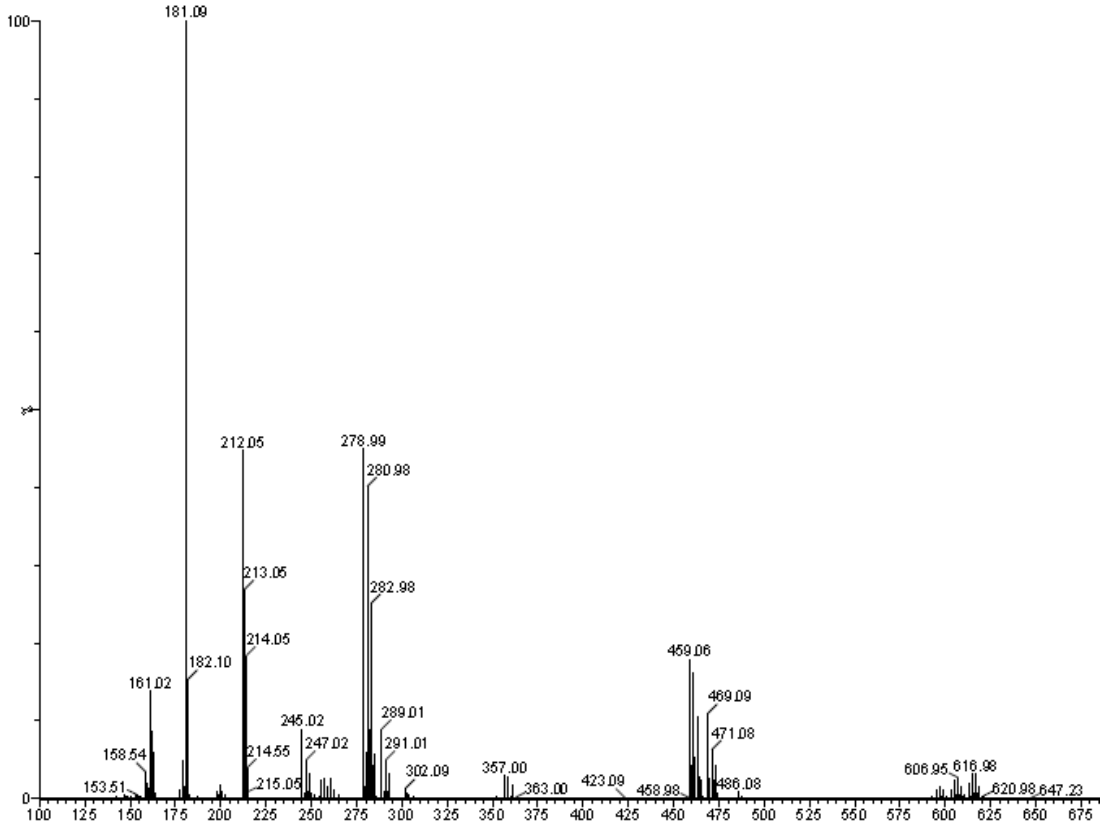

Fig. 35: Mass spectra of $[Zn(L_1)phen]Cl_2$ *(1)*

m/z	**Loss of**	**Fragment**
620		$[Zn(L_1)phen]Cl_2.2H_2O$
602	H_2O	$[Zn(L_1)phen]Cl_2.H_2O$
460		$[Zn(phen)_2Cl]$
281	L_1, Cl	[Zn(phen)Cl]
245	Cl	[Zn(phen)]
181	Zn	Free phen

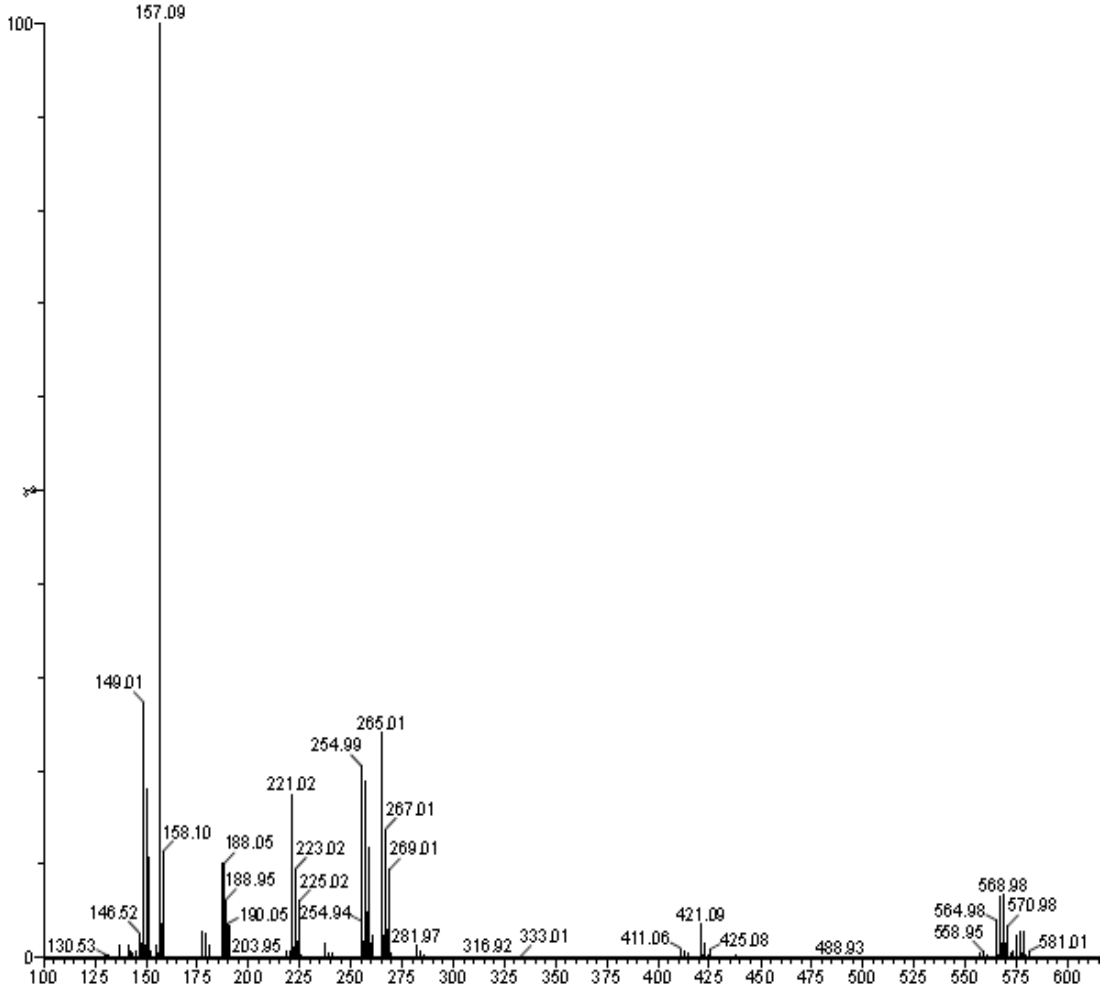

Fig. 36: Mass spectra of $[Zn(L_1)bpy]Cl_2$ *(2)*

m/z	**Loss of**	**Fragment**
578		$[Zn(L_1)bpy]Cl_2.H_2O$
256	L_1, Cl, H_2O	[Zn(bpy)Cl]
223	Cl	[Zn(bpy)]
157	Zn	Free bpy

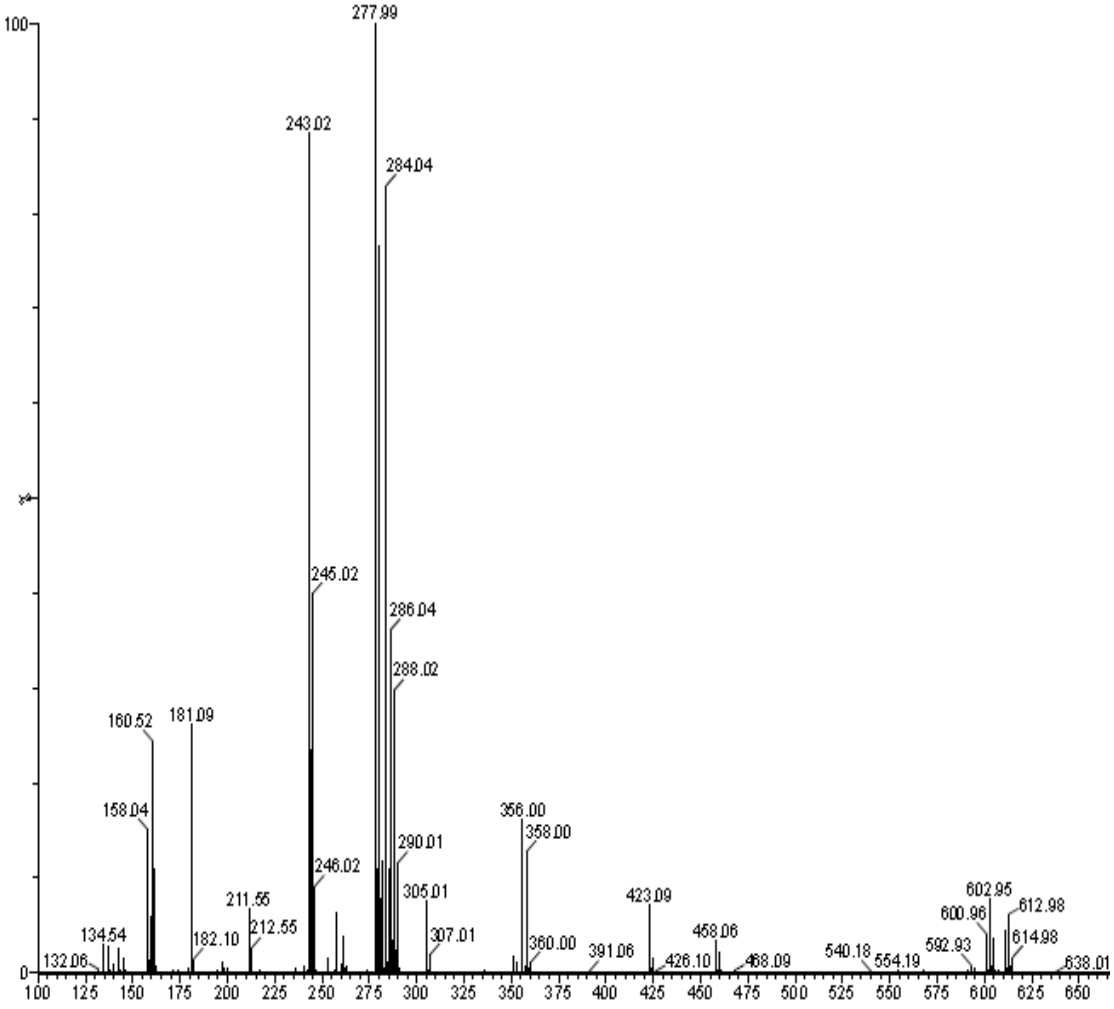

Fig. 37: Mass spectra of [Cu(L_1)phen]Cl_2 *(3)*

m/z	**Loss of**	**Fragment**
602		[Cu(L_1)phen]$Cl_2.H_2O$
279	L_1, Cl, H_2O	[Cu(phen)Cl]
243	Cl	[Cu(phen)]
180	Cu	Free phen

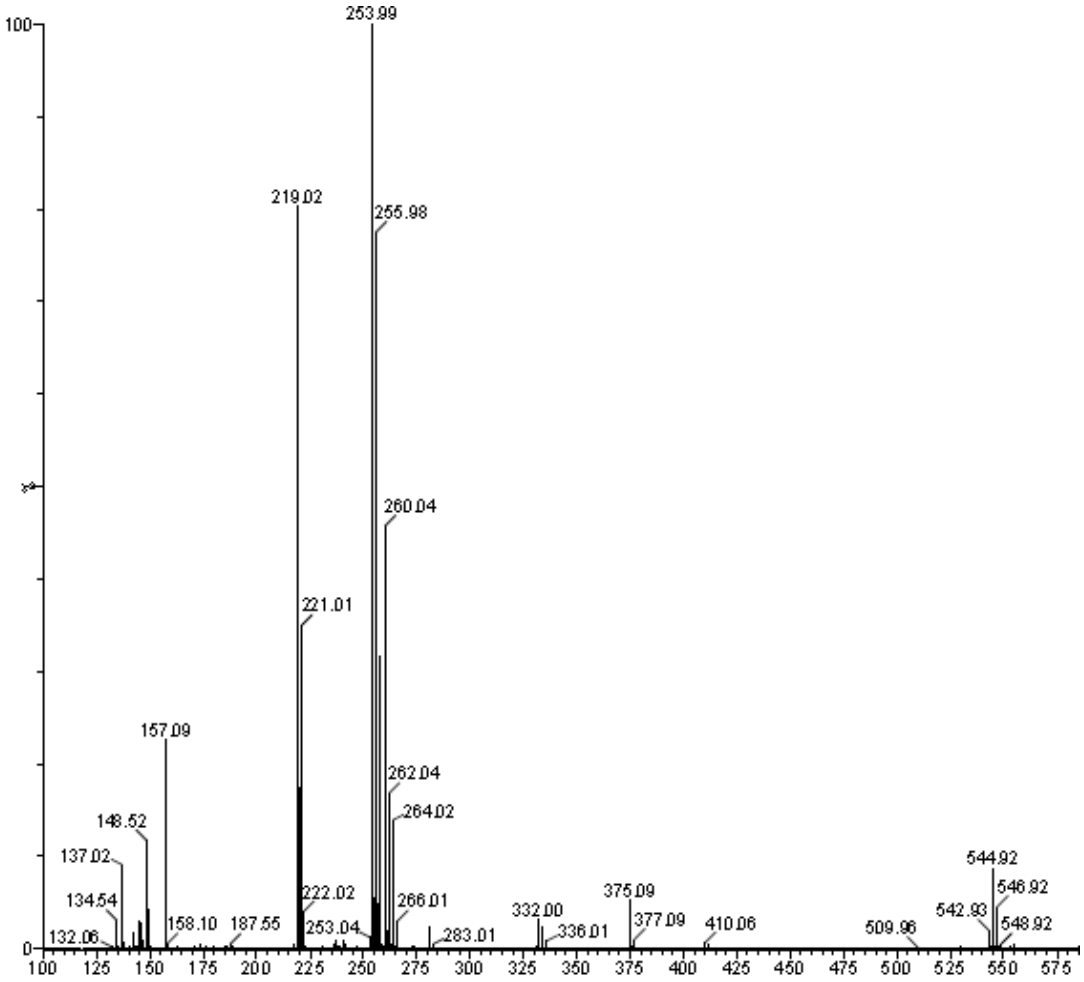

Fig. 38: Mass spectra of [Cu(L_1)bpy]Cl_2 *(4)*

m/z	**Loss of**	**Fragment**
558 (Not recorded)	-	[Cu(L_1)bpy]Cl_2
332	bpy, Cl_2	[Cu(L_1)]
255		[Cu(bpy)Cl]
219	Cl	[Cu bpy]
157	Cu	Free bpy

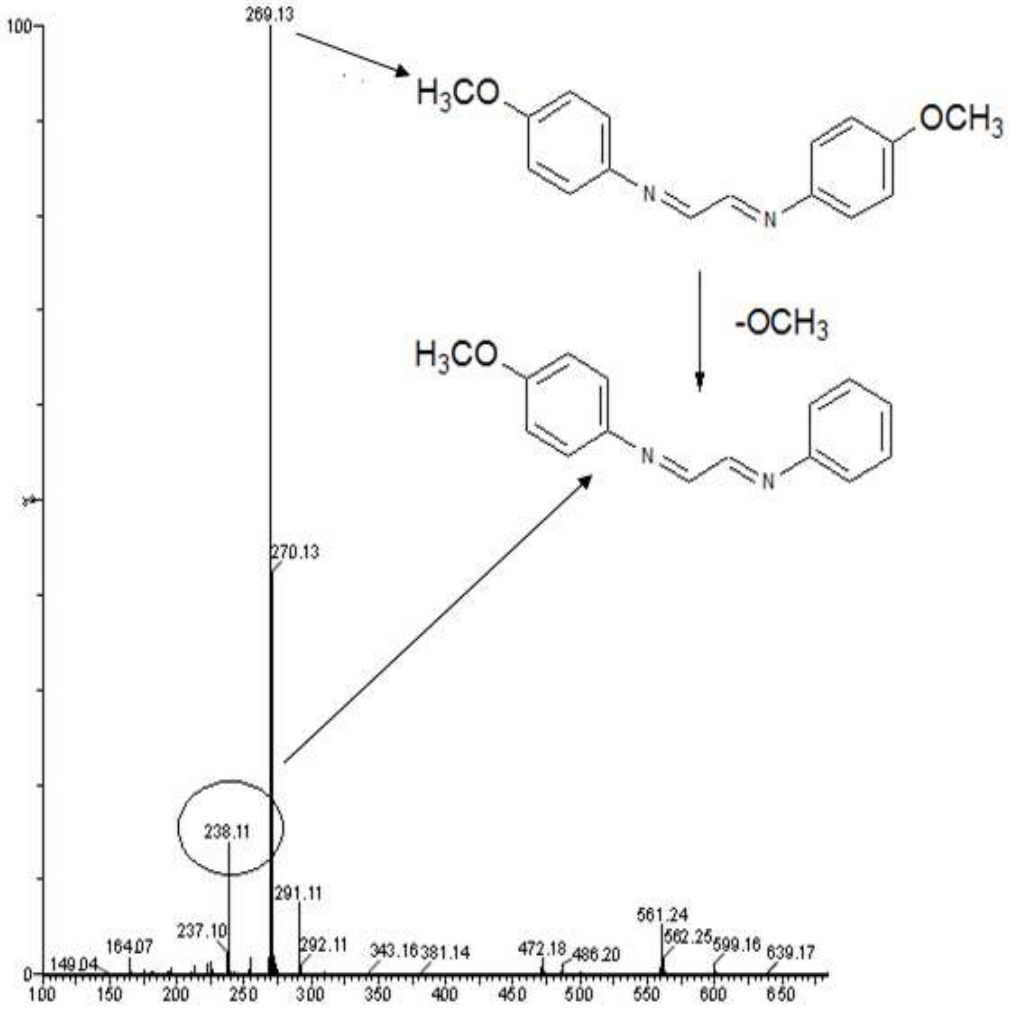

Fig. 39: Mass spectra of L_2 (Mol. Mass = 268 g)

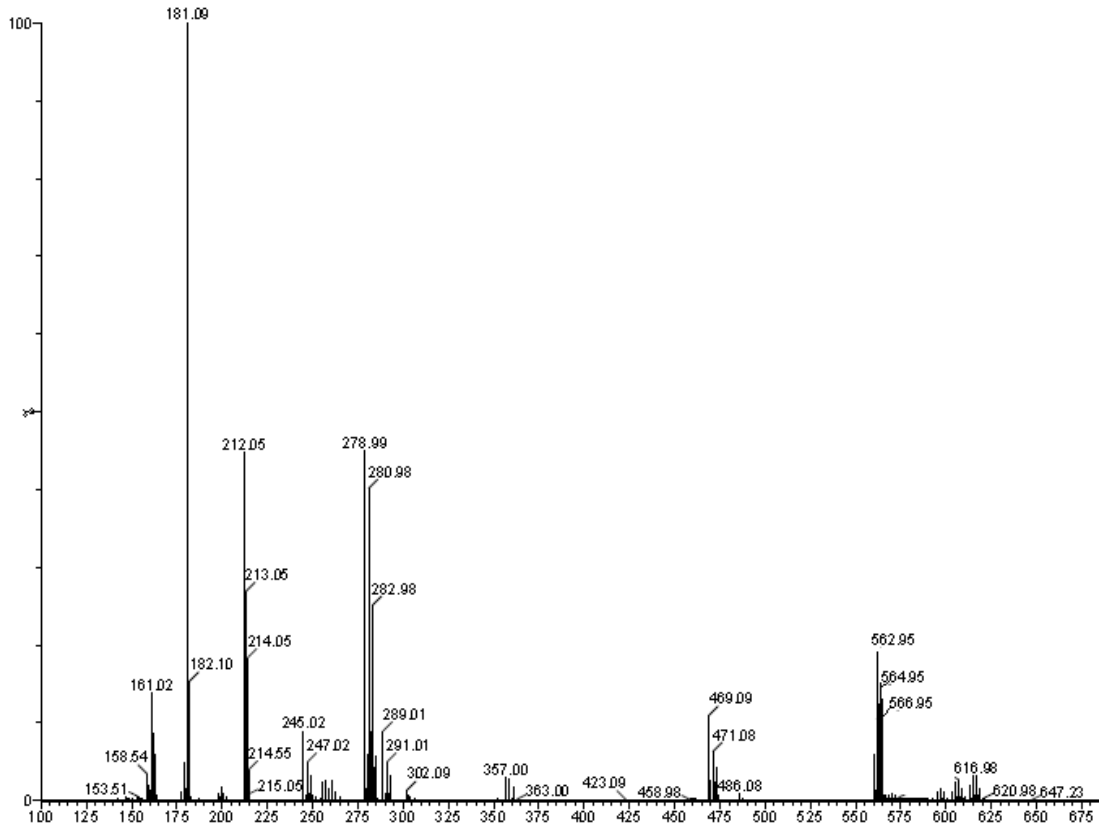

Fig. 40: Mass spectra of $[Zn(L_2)phen]Cl_2$ *(5)*

m/z	**Loss of**	**Fragment**
566		$[Zn(L_2)phen]Cl.H_2O$
280	L_2	[Zn(phen)Cl]
180	Zn, Cl	Free phen

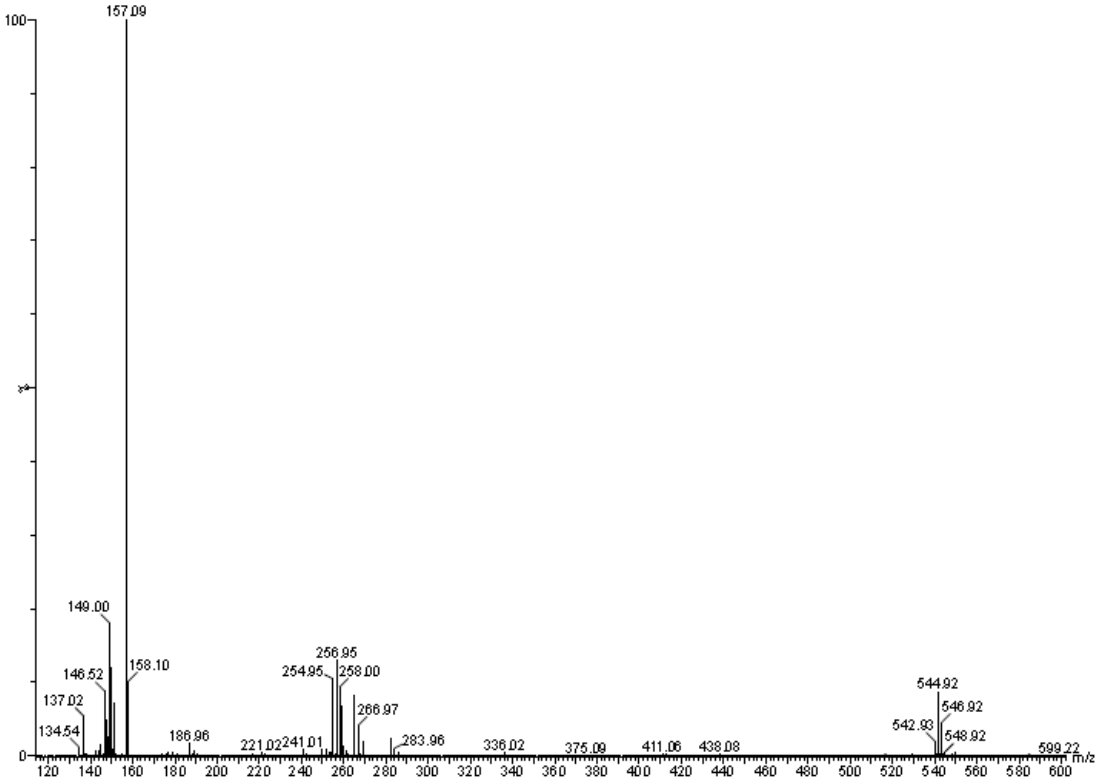

Fig. 41: Mass spectra of $[Zn(L_2)bpy]Cl_2$ *(6)*

m/z	**Loss of**	**Fragment**
542	-	$[Cu(L_2)bpy]Cl.H_2O$
256	L_2	[Cu(bpy)Cl]
157	Cu, Cl	Free bpy

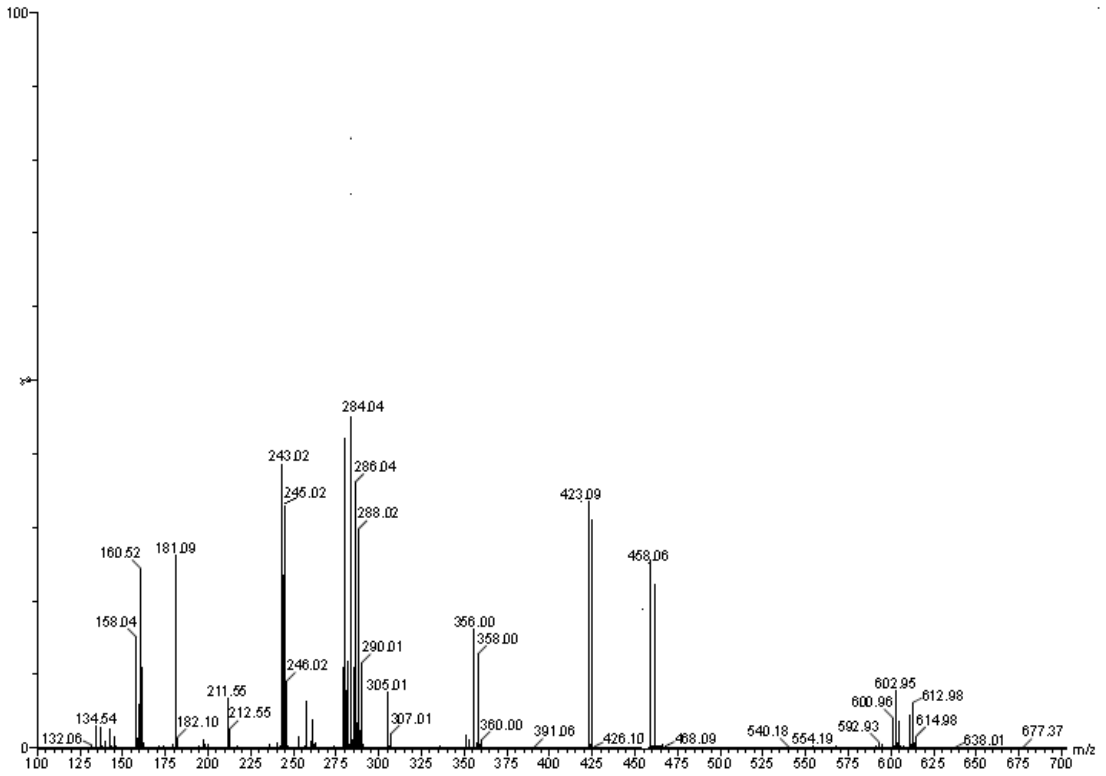

Fig. 42: Mass spectra of $[Cu(L_2)phen]Cl_2$ *(7)*

m/z	**Loss of**	**Fragment**
600	-	$[Cu(L_2)phen]Cl_2.H_2O$
460	L_2, Cl	$[Cu(phen)_2Cl]$
423	Cl	$[Cu(phen)_2]$
280	phen	[Cu(phen)Cl]
243	Cl	[Cu(phen)]
180	Cu	Free phen

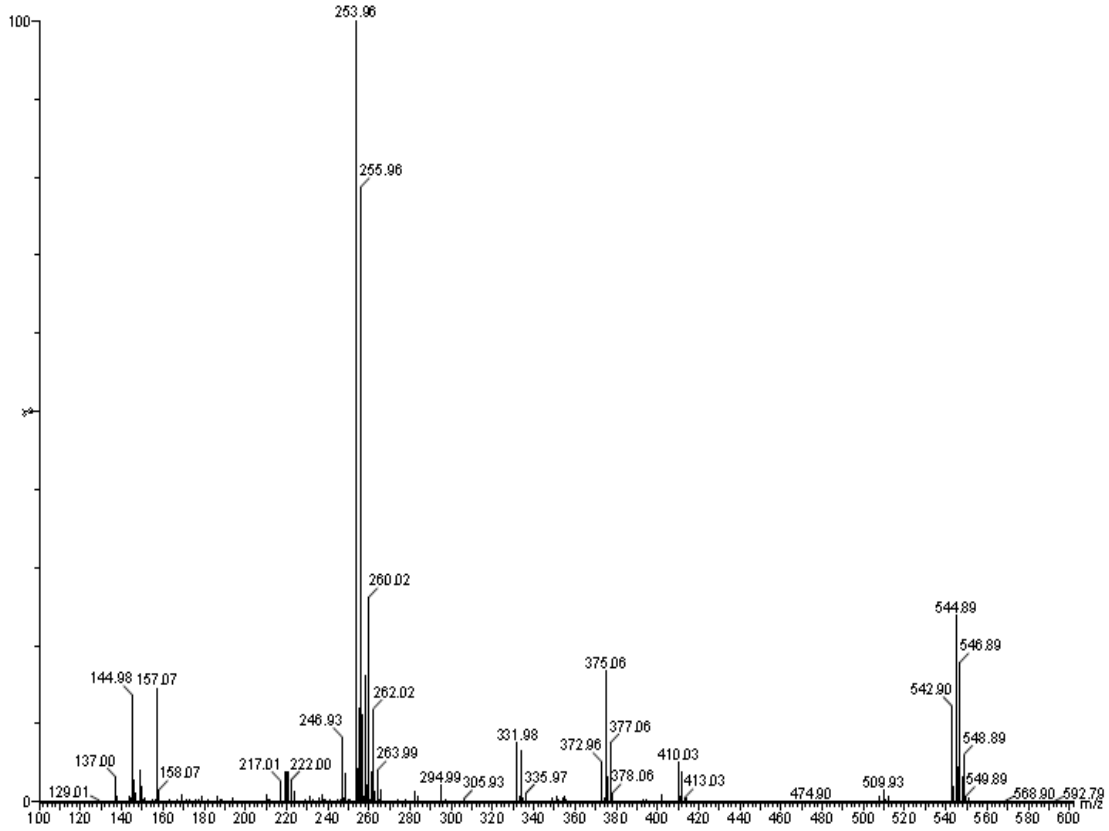

Fig. 43: Mass spectra of $[Cu(L_2)bpy]Cl_2$ *(8)*

m/z	**Loss of**	**Fragment**
541	-	$[Cu(L_2)bpy]Cl.H_2O$
331	bpy	$[Cu(L_2)]$
255	L_2	[Cu(bpy)Cl]
157	Cu, Cl	Free bpy

2.3.4 ^{1}H NMR spectrum analysis

The ^{1}H NMR of the **L_1** was recorded in chloroform while that of **L_2** was recorded in d^6 - DMSO. TMS was used as internal reference. A signal at 8.1 - 8.4 ppm in ligand spectra was due to azomethine protons. The multiplet in the range of 6.9 - 7.6 was assigned to protons of aromatic protons of benzene rings while a singlet at 3.7 - 3.8 was due to methoxy group. The ^{1}H NMR spectra of the Schiff bases is as follows:

^{1}H NMR of **L_1**: (400 MHz, $CDCl_3$), δ = 8.15 (s, 2H, -CH=N), 7.66 (d, 4H, Ar-H), 7.53 (d, 4H, Ar-H), 3.85 (s, 6H, $-OCH_3$)

^{1}H NMR of **L_2**: (400 MHz, d^6 - DMSO) δ = 8.39 (s, 2H, -CH=N), 7.36 (d, 4H, Ar-H), 6.95 (d, 4H, Ar-H), 3.79 (s, 6H, $-OCH_3$).

2.4 UV-vis absorption studies of BSA

UV-vis absorption spectroscopy acts as quite handy and reliable technique to scrutinize the interactive behaviour and structural changes of metal complexes with serum albumins. Firstly the solution of tris buffer (0.1 M) was prepared using doubly distilled water. Then BSA solution of 1000 μM concentration and metal complexes of 50 μM concentrations were prepared using tris buffer as solvent. The UV-vis spectra were recorded by taking static concentration of metal complex (50 μM) vs. dynamic [BSA] concentrations in the array of 0 - 3 μM. There is a direct proportional relationship between the concentration of [BSA] and the intensity of band. Then their binding constants were calculated:

(A) By UV-vis titration graphs of metal complexes (50 μM) with incremental [BSA] concentration in the range of 0 - 3 μM,

(B) By plotting graph of BSA complex with metal chelates subtracting corresponding signal for different concentrations of [BSA],

(C) By plotting graph of 1 / [BSA] (on X - axis) vs. 1 / ($A-A_0$) (on Y - axis) concentration, where A is the absorption signal of bounded complex at variant complex – [BSA] concentrations while A_0 is an absorption signal of unbound complex.

Then the values of binding constants for each metal complex were determined. The interaction between substrate (S) and BSA concenteration (L) is presumed to be of ratio 1:1, resulting into formation of a single complex (S_L).

The relationship amid the pragmatic absorbance (cm^{-1}) alteration, different parameters and system variables can be calculated as follows:

$$\frac{\Delta A}{b} = \frac{S_t K_{11} \Delta \epsilon_{11} [L]}{1 + K_{11} [L]} (1)$$

where S_t is total concenteration of substrate,

$\Delta A = A - Ao$,

$\Delta \varepsilon_{11} = \varepsilon_{11} - \varepsilon_S - \varepsilon_L$

Where ε_{11} signifies molar absorptivity of BSA - metal complex,

ε_s signifies molar absorptivity of unbound metal complex,

ε_L signifies molar absorptivity of the BSA.

From the mass balance expression $S_t = [S] + [SL]$,

And $[S] = S_t / (1 + K_{11} [L])$.

Where [S] signifies concentration of unbound metal complex,

[L] signifies concentration of unbound BSA,

[SL] signifies concentration of BSA – metal complex

Equation (1) shows that there is hyberbolic dependence on the concenteration of unbound BSA, thus it signifies binding isotherms.

Therefore double reciprocal plot of $1 / (A–A_0)$ vs. $1 / [BSA]$ comes out to be linear and the values of binding constant (K_b in M^{-1}) can be calculated as:

$$K_b = \frac{\text{Intercept}}{\text{Slope}}$$

where A: absorption signal at variant complex - [BSA] concentrations

A_0: absorption signal of unbound metal chelate.

Table15: Values of Binding constant values (K_b M^{-1})

Complex	**K_b M^{-1}**
$[Zn(L_1)phen]Cl_2$ ***(1)***	4.46×10^6
$[Zn(L_1)bpy]Cl_2$ ***(2)***	-
$[Cu(L_1)phen]Cl_2$ ***(3)***	-
$[Cu(L_1)bpy]Cl_2$ ***(4)***	6.9×10^6
$[Zn(L_2)phen]Cl_2$ ***(5)***	-
$[Zn(L_2)bpy]Cl_2$ ***(6)***	1.20×10^5
$[Cu(L_2)phen]Cl_2$ ***(7)***	1.08×10^6
$[Cu(L_2)bpy]Cl_2$ ***(8)***	4.18×10^6

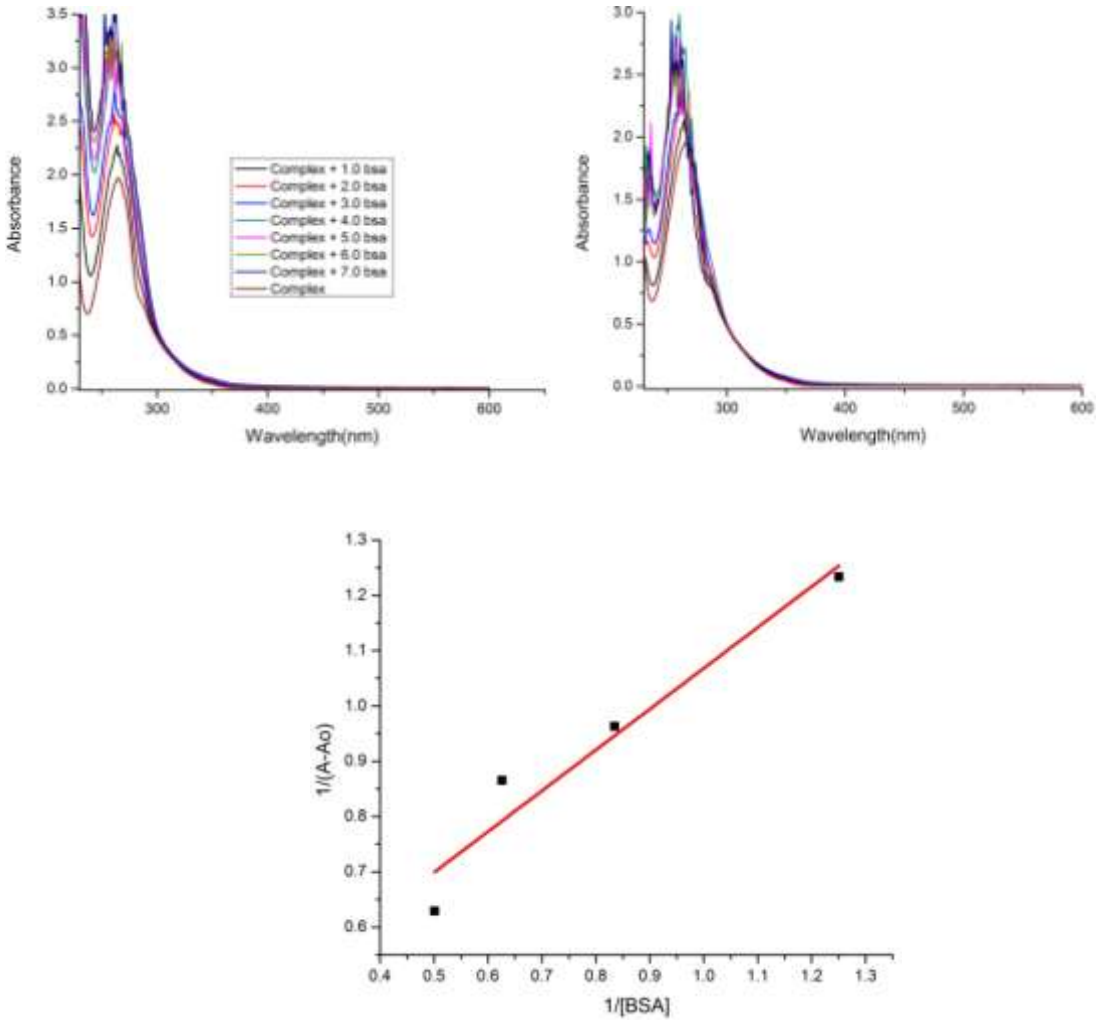

Fig. 44: (A) UV-vis titration graphs of complex $[Zn(L_1)phen]Cl_2$ (50 μM) with incremental [BSA] concentration in the range of 0 – 3 μM,

(B) Graph of {[BSA complex with $[Zn(L_1)phen]Cl_2$] – [Variant concentrations of [BSA]},

(C) Graph of $1 / (A-A_0)$ vs. $1 / [BSA]$ concentration

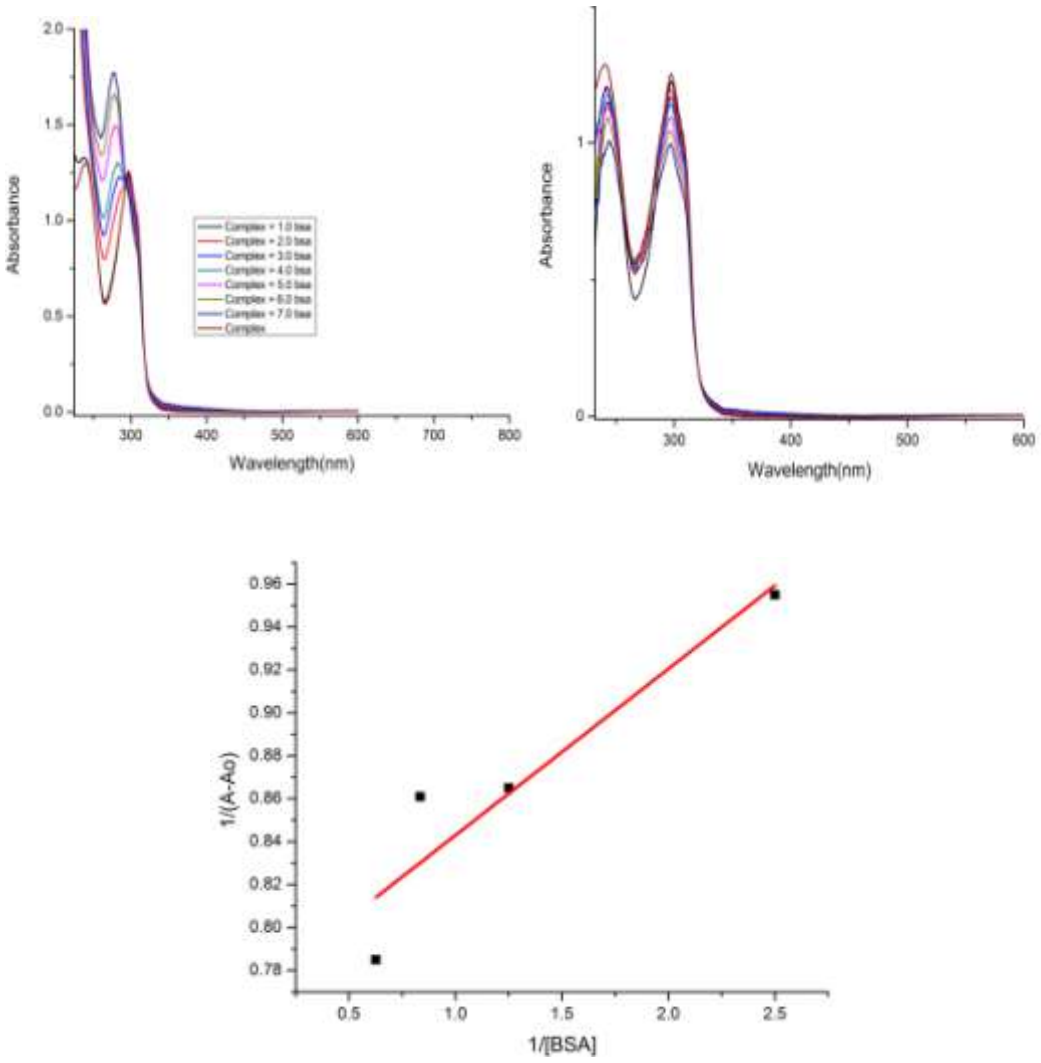

Fig. 45: (A) UV-vis titration graphs of $[Cu(L_1)bpy]Cl_2$ complex (50 μM) with incremental [BSA] concentration in the range of 0 – 3μM,

(B) Graph of {[BSA complex with $[Cu(L_1)bpy]Cl_2$] – [Variant concentrations of [BSA]},

(C) Graph of 1 / ($A-A_0$) vs. 1 / [BSA] concentration

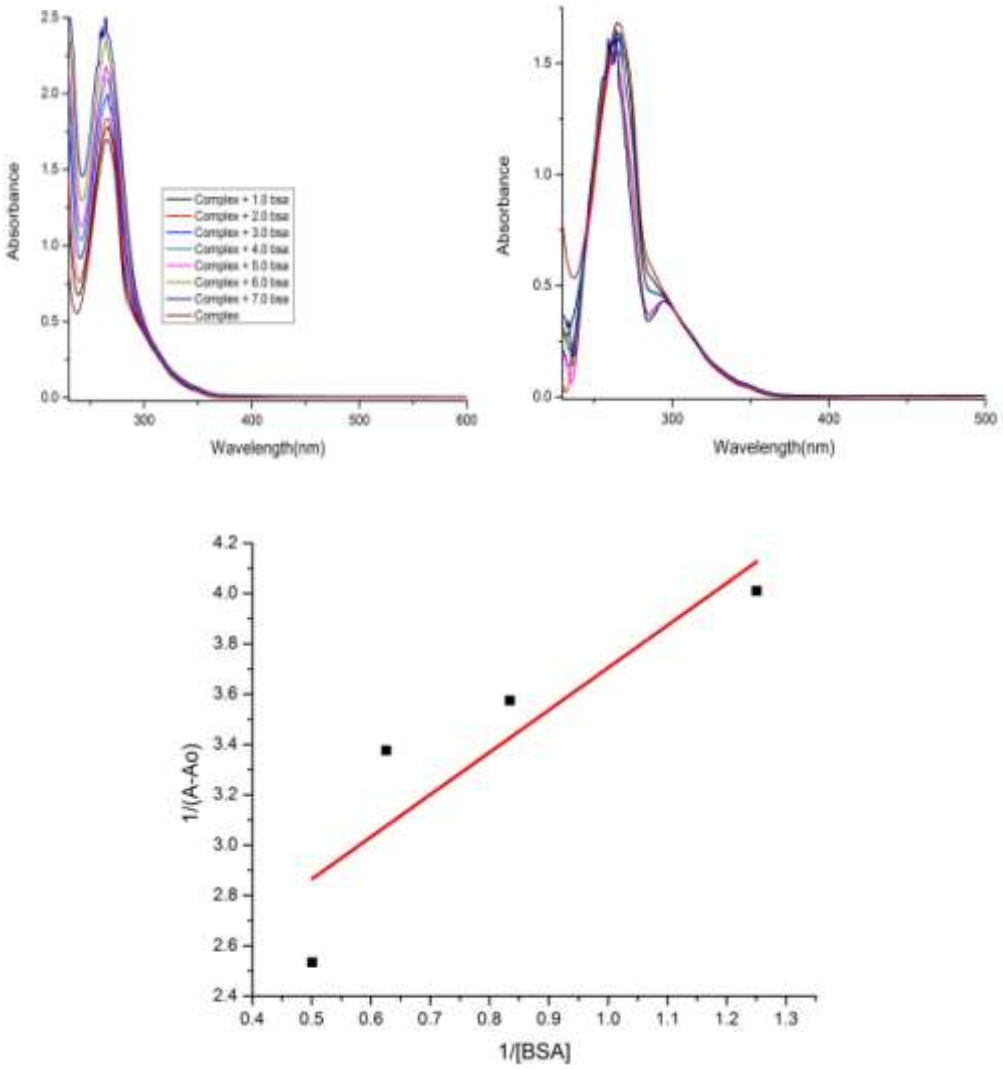

Fig. 46: (A) UV-vis titration graphs of complex $[Zn(L_2)bpy]Cl_2$ (50 μM) with incremental [BSA] concentration in the range of 0 – 3μM,

(B) Graph of {[BSA complex with $[Zn(L_2)bpy]Cl_2$] – [Variant concentrations of [BSA]},

(C) Graph of $1 / (A-A_0)$ vs. $1 / [BSA]$ concentration

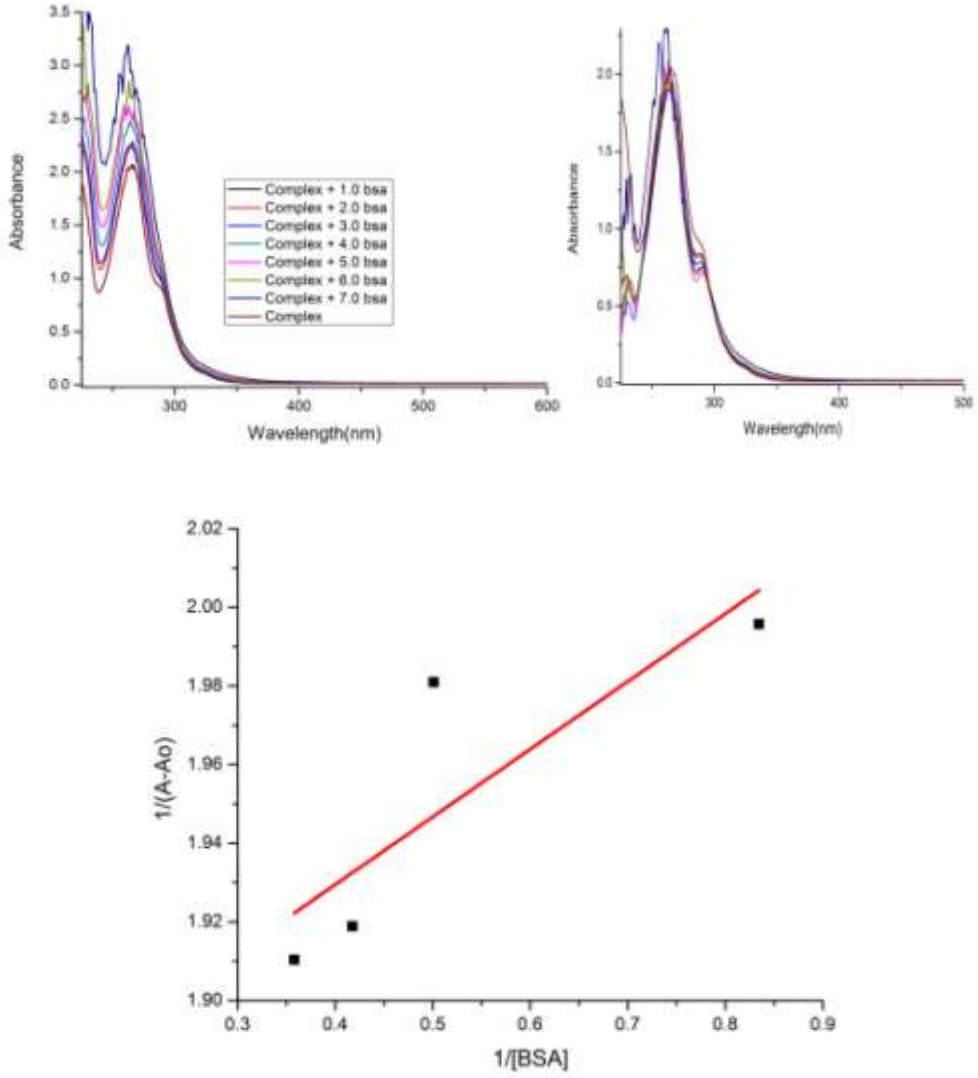

Fig. 47: (A) UV-vis titration graphs of complex $[Cu(L_2)phen]Cl_2$ (50 µM) with incremental [BSA] concentration in the range of 0 – 3µM,

(B) Graph of {[BSA complex with $[Cu(L_2)phen]Cl_2$ – [Variant concentrations of [BSA]},

(C) Graph of $1 / (A-A_0)$ vs. $1 / [BSA]$ concentration

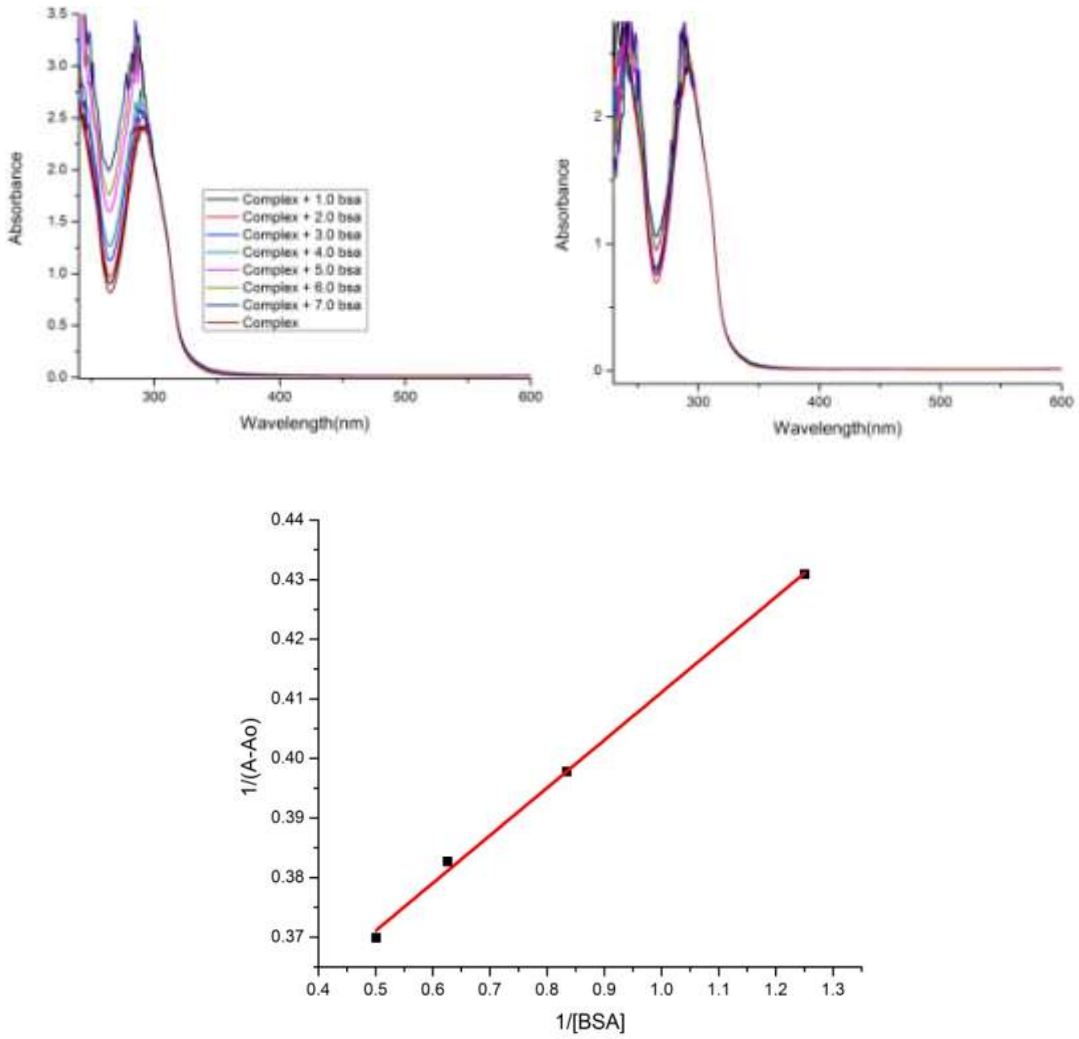

Fig. 48: (A) UV-vis titration graphs of complex $[Cu(L_2)bpy]Cl_2$ (50 µM) with incremental [BSA] concentration in the range of 0 – 3µM,

(B) Graph of {[BSA complex with $[Cu(L_2)bpy]Cl_2$ – [Variant concentrations of [BSA]},

(C) Graph of $1 / (A-A_0)$ vs. $1 / [BSA]$ concentration

2.5 Antimicrobial Assays

Agar well diffusion process is used to evaluate the antimicrobial behaviour of ligands along with their metal chelates. The concentrations of the solutions were made by dissolving 5 mg of sample in 1 ml of solvent (DMSO). The bacterial and fungal cultures were homogeneously applied with sterile cotton swabs on mueller hinton agar (MHA) and potato dextrose agar (PDA) respectively. Sterilized cork borer of 7mm diameter was employed for cutting of wells in agar plates. Micropipette was used to add 100 µl of each sample to the wells. The plates were incubated at 37°C for 24 h and 48 h for bacteria and fungi respectively. DMSO was used as negative control in well diffusion method. Antimicrobial activity of standard antibiotic drug amikacin against test bacteria and fluconazole against test fungi was evaluated by agar disc diffusion method. Zone of inhibition surrounding each well / disc was measured to determine the antimicrobial activities. Each experiment was performed three times to minimize the deviations (Table 16).

Test Organisms: A) Bacteria: *Escherichia coli and Staphylococcus aureus*

B) Fungi: *Aspergillus niger and Aspergillus fumigatus*

Table 16: Antimicrobial activity of ligand and complexes (Concentration of 5 mg ml^{-1})

Complex	Average Inhibition Zone in diameter (mm) ± SD			
	Antibacterial Activity		Antifungal Activity	
	E. coli **(A)**	***S. aureus*** **(B)**	***A. niger*** **(C)**	***A. fumigatus*** **(D)**
(L_1)	-	-	10.33±0.29	-
[Zn(L_1)phen]Cl_2 ***(1)***	-	16.66±0.58	35.16±0.29	-
[Zn(L_1)bpy]Cl_2 ***(2)***	11.00±0.58	25.33±0.58	22.50±0.50	-
[Cu(L_1)phen]Cl_2 ***(3)***	18.33±0.58	28.50±0.50	38.16±0.29	30.33±0.29
[Cu(L_1)bpy]Cl_2 ***(4)***	-	17.66±0.58	21.50 ±0.50	10.16±0.29
(L_2)	10.66±0.58	-	11.50±0. 29	-
[Zn(L_2)phen]Cl_2 ***(5)***	10.33±0.58	15.33±0.58	37.30±0.57	-
[Zn(L_2)bpy]Cl_2 ***(6)***	12.66±0.58	-	-	-
[Cu(L_2)phen]Cl_2 ***(7)***	22.00±0.36	30.40±0.36	38.16±0.29	33.50±0.50
[Cu(L_2)bpy]Cl_2 ***(8)***	14.00±0.50	15.33±0.29	18.500±0.50	21.50±0.50
Amikacin	21.50±0.50	24.83±0.76	-	-
Fluconazole	-	-	23.66±0.57	22.66±0.29
DMSO	Nil	Nil	Nil	Nil

where SD is Standard Deviation

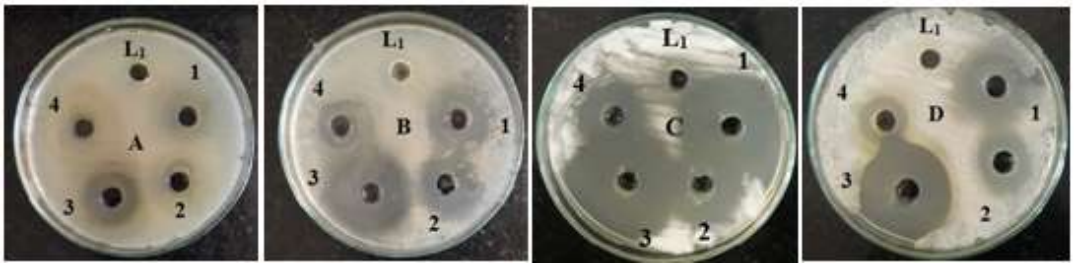

Fig. 49: Antimicrobial assay of Schiff base ligand (L_1) and its metal chelate (*1 - 4*) (Alphabet levels are according to table 16)

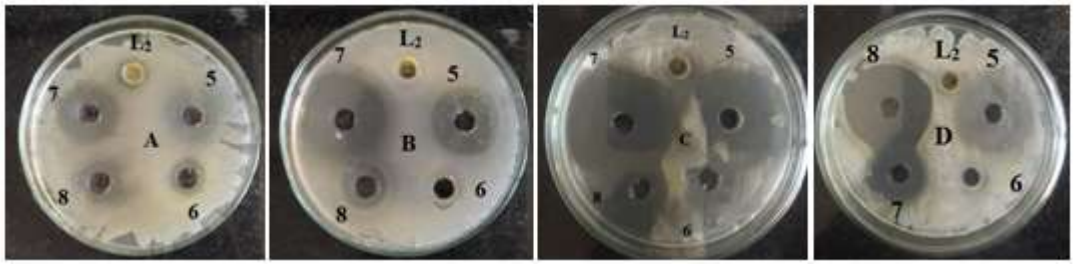

Fig. 50: Antimicrobial assay of Schiff base ligand (L_2) and its metal chelate (*5 - 8*) (Alphabet levels are according to table 16)

2.6 Conclusion

This chapter details about the synthesis of two Schiff bases **(L_1)** and **(L_2)** as primary ligand and their mixed ligand complexes with zinc(II) and copper(II) metal ions and 1,10-phenanthroline or 2,2'-bipyridine as the secondary ligand. The reactants for the synthesis of ligands are selected as dialdehydes with different isomers of primary amine instead of conventional method of reaction between diamines and aldehyde or ketone. Schiff base of para isomer of primary amine precipitates readily while ortho isomer precipitates in a longer time span. The reaction with meta isomer resulted in a tar and the product could not be isolated despite several attempts. Both the ligands appear as bidentate, coordinating to metal centers through imine nitrogen. Absence of peaks in the 500 cm^{-1} suggests the absence of M-O bond. Molecular mass of ligand and metal complexes are in consistence with their mass spectral data. Octahedral geometry has been proposed for all the complexes on the basis of evidences shown by their spectral studies with primary and secondary ligands at their equatorial position while axial positions may be occupied by weak coordinating

anions or water molecules. Serum protein interactions of complexes were studied by determining the values of binding constants using UV-vis titration technique. The complexes show binding constants in the range of 10^4 - 10^5 M^{-1}. It is worth mentioning that moderate values of binding constants further strengthen the task of serum proteins in drug delivery at targeted sites as carrier molecules. In antimicrobial assays, pure ligands show least activity while metal complexes show moderate to high activity as compared to standard drug. The zone of inhibition with *Staphylococcus aureus* and *Aspergillus fumigatus* is the highest. The better activities of metal complexes as compared to ligands could be due to the manipulation of the hydrophobicity of the metal complexes over the hydrated metal ions by different ligands. This change in polarity of metal on coordination with the ligand may result in easy penetration of the complexes through the cell membrane of the microbes.

2.7 Bibliography

[1] Singh, P.; Das, S.; Dhakarey, R. Bioinorganic relevance of some cobalt (II) complexes with thiophene-2-glyoxal derived Schiff bases, *E - J. Chem.* **2009**, *6*, 99–105.

[2] Akila, E.; Usharani, M.; Ramachandran, S.; Jayaseelan, P.; Velraj, G. Tetradentate-arm Schiff base derived from the glyoxal / diacetyl and 2-aminophenol: Designing, structural elucidation and properties of their binuclear metal (II) complexes, *Arab. J. Chem.* **2017**, *10*, S2950–S2960.

[3] Shirmohammadzadeh, L. K. L. Synthesis of Co(II) and Cr(III) salicylidenic Schiff base complexes derived from thiourea as precursors for nano-sized Co_3O_4 and Cr_2O_3 and their catalytic, antibacterial properties, *J. Nanostructure Chem.* **2017**, *7*, 179–190.

[4] Adamu, F.; Upadhyay, S.; Upadhyay, R. K. Antimicrobial relevance of Cu(II) complexes of thiophene-2-glyoxal-*p*-halogen substituted anils, *Orient. J. Chem.* **2014**, *30*, 1031–1036.

[5] Karmakar, I.; Mandal, S.; Mitra, A. Evaluation of antimicrobial and insect repellent properties of two novel zinc(II) and nickel(II) complexes containing a tetradentate Schiff base, *J. Integr. Sci. Technol* **2015**, *3*, 60–67.

[6] Jayalakshmi, R.; Rajavel, R. Elaborated studies on Schiff base homo-binuclear Cu(II) and Co(II) complexes, spectral, thermal, P - XRD and biocidal studies, *J. Adv. Appl. Sci. Res.* **2017**, *1*, 1-16.

[7] Prakash, A.; Adhikari, D. Application of Schiff bases and their metal complexes - A review, *Int. J. Chem Tech Res.* **2011**, *3*,1891–1896.

[8] Heatley, N. G. A method for the assay of penicillin, *Biochem. J.* **1944**, *38*, 61-65.

[9] Ganeshpandian, M.; Loganathan, R.; Ramakrishnan, S.; Riyasdeen, A.; Akbarsha, M. A.; Palaniandavar, M. Interaction of mixed ligand copper(II) complexes with CT DNA and BSA: Effect of primary ligand hydrophobicity on DNA and protein binding and cleavage and anticancer activities, *Polyhedron* **2013**, *52*, 924–938.

[10] Trnkova, L.; Bousova, I.; Kubi, V.; Drsata, J. Binding of naturally occurring hydroxycinnamic acids to bovine serum albumin, *Nat. Sci.* **2010**, *2*, 563–570.

[11] Jha, N. S.; Kishore, N. Binding of streptomycin with bovine serum albumin: Energetics and conformational aspects, *Thermochim. Acta.* **2009**, *482*, 21–29.

[12] Bonev, B.; Hooper, J.; Parisot, J. Principles of assessing bacterial susceptibility to antibiotics using the agar diffusion method. *J. Antimicrob. Chemother.* **2008**, *61*, 1295-1301.

2.8 Annexure

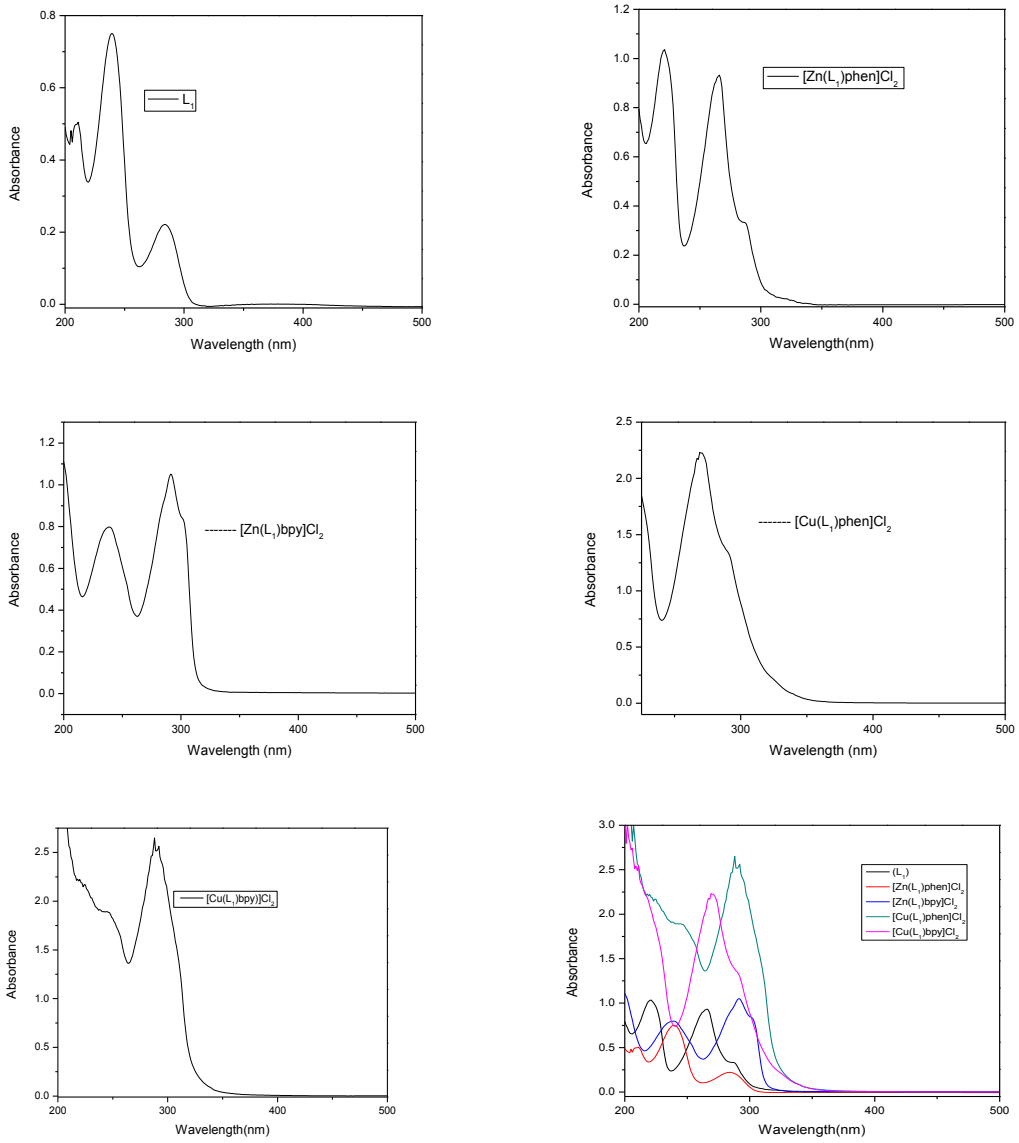

Annexure 2a: UV-vis spectra of (L_1) Schiff base and its metal complexes

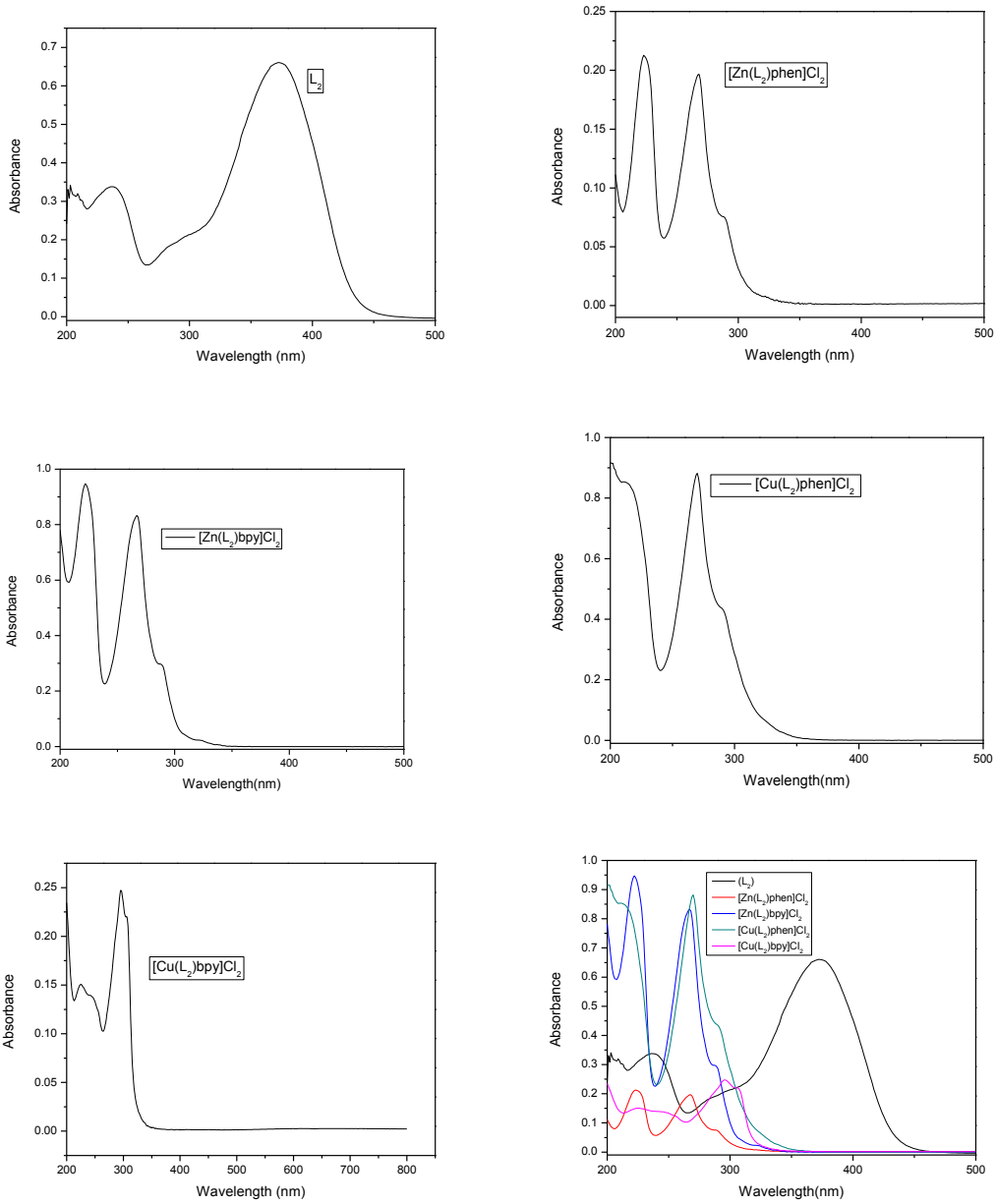

Annexure 2b: UV-vis spectra of (L_2) Schiff base and its metal complexes

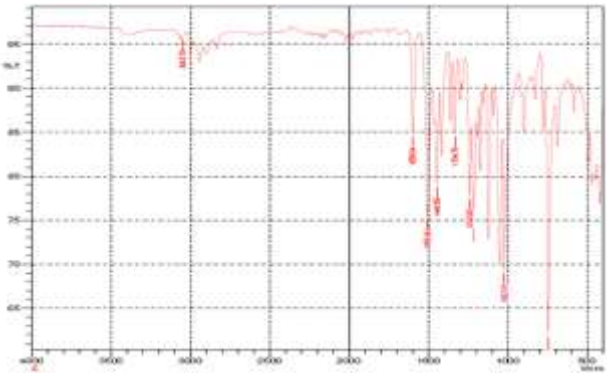

Annexure 2c: IR of (L_1)

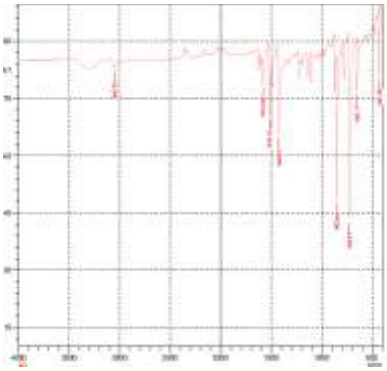

Annexure 2d: IR of [Zn(L_1)phen]Cl_2

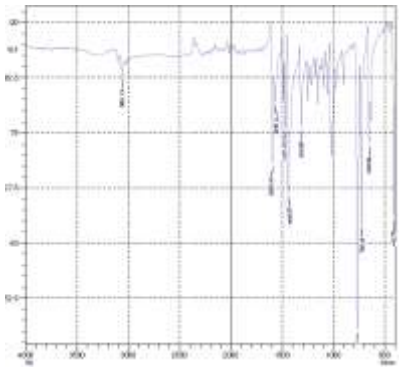

Annexure 2e: IR of [Zn(L_1)bpy]Cl_2

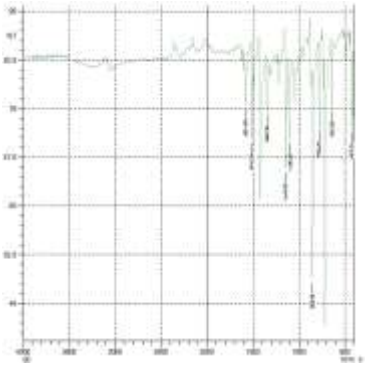

Annexure 2f: IR of [Cu(L_1)phen]Cl_2

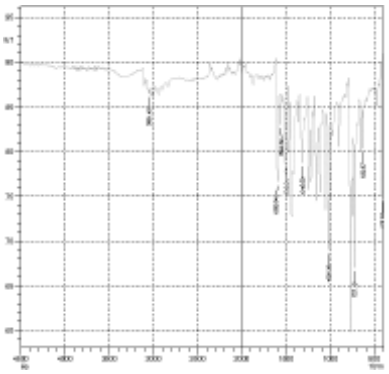

Annexure 2g: IR of [Cu(L_1)bpy]Cl_2

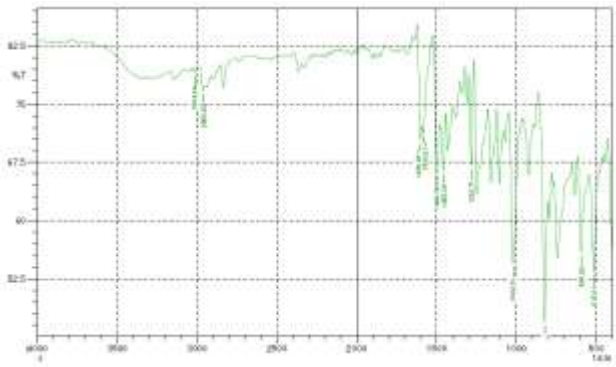

Annexure 2h: IR of (L_2)

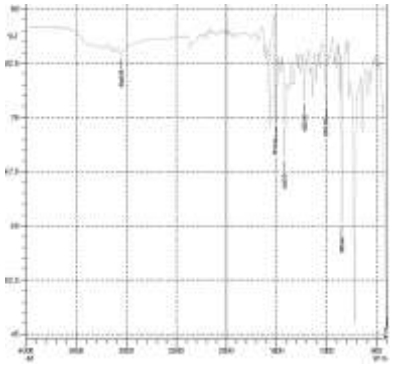

Annexure 2i: IR of [Zn(L_2)phen]Cl_2

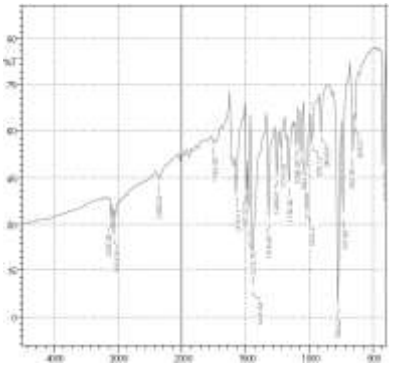

Annexure 2j: IR of [Zn(L_2)bpy]Cl_2

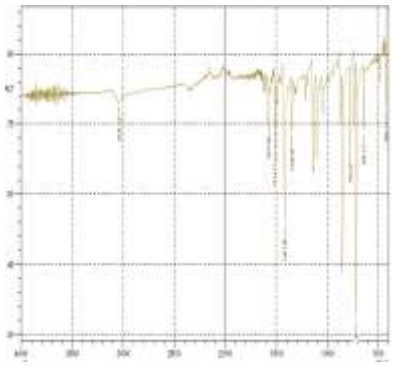

Annexure 2k: IR of [Cu(L_2)phen]Cl_2

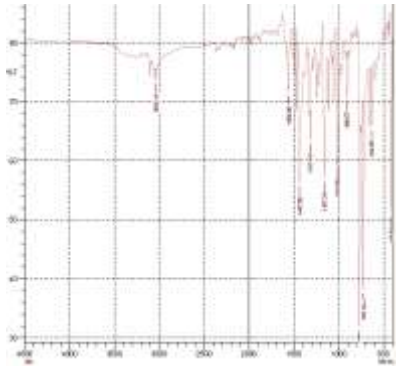

Annexure 2l: IR of [Cu(L_2)bpy]Cl_2

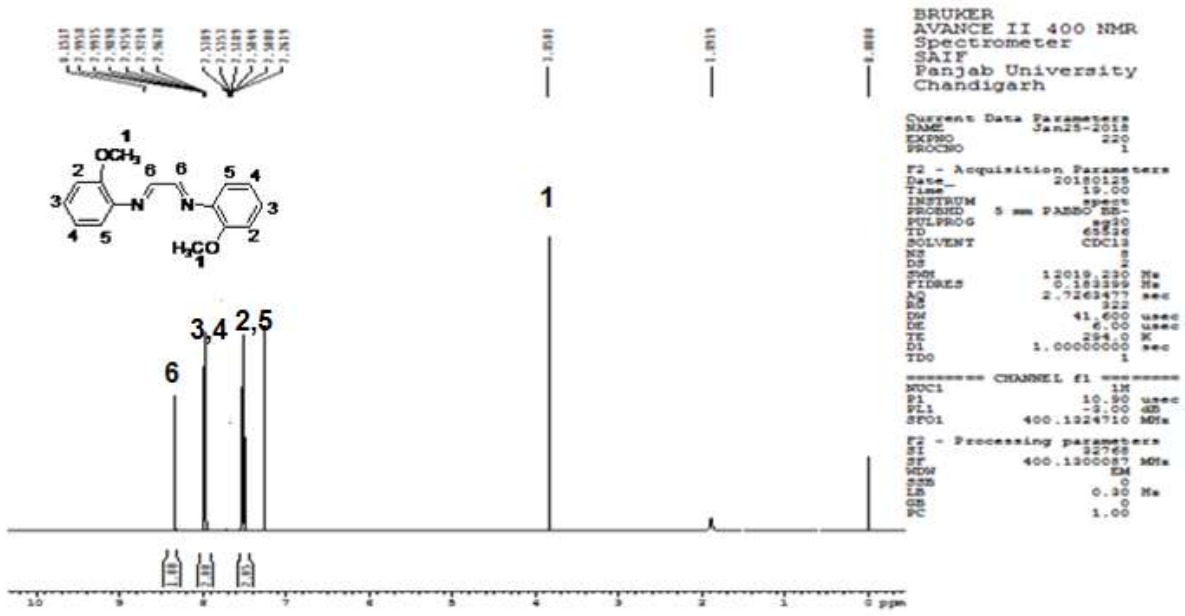

Annexure 2m: NMR of (L_1)

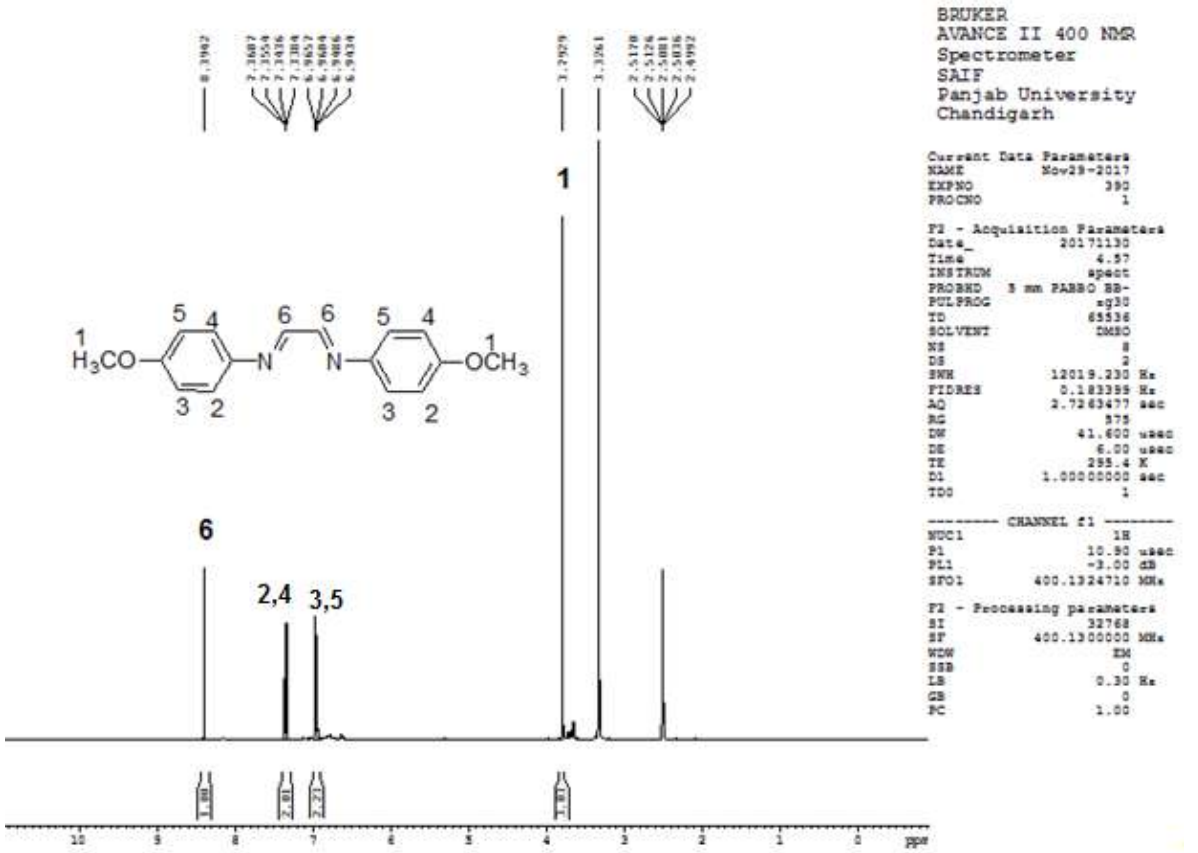

Annexure 2n: NMR of (L_2)

CHAPTER 3

Synthesis, characterization and biological evaluation studies of Cu(II) and Zn(II) complexes with Schiff base formed by reaction between benzil and ortho / meta / para - anisidine and N, N' donor ligands

3.1 Introduction

This chapter concerns with the aim to synthesize metal complexes of zinc and copper with Schiff base (obtained by the condensation of benzil with ortho, meta and para anisidine) as primary and N, N' donor molecules as secondary ligands. The ligand and their complexes were then characterized with the help of various spectroscopic techniques viz. UV-vis, FTIR, NMR and mass spectral techniques. They were then analyzed for their biological activities against two bacterial strains i.e. *Staphylococcus aureus* (gram positive) and *Escherichia coli* (gram negative) and two fungal strains i.e. *Aspergillus niger* and *Aspergillus fumigatus* by agar well diffusion method. The complexes were also analyzed for their interaction with BSA by UV titration method.

3.2 Methodology

3.2.1 Methodology for the synthesis of Schiff base (benzil-*o*-andn) (L_3)

To a stirred and refluxed solution of benzil (4 mmol, 0.232 g) in hot methanol (35 ml) was added dropwise a hot methanolic solution (35 ml) of *o*-anisidine (4 mmol, 0.493 g or 0.45 ml. The whole set up was kept in an oil bath for 5 h at 70°C. The clear solution thus obtained was allowed to evaporate slowly. After 82 hours, brown colored crystalline product separates out, this was filtered and dried in a dessicator. Yield: 82 %, Color: Light yellow, M.P. 60°C, UV (λ_{max}): 256 nm, MS: $[M]^+$ 316, Main IR peaks (cm^{-1}): $\upsilon(C_6H_5$ stretch) 3061, υ(C=N) 1656, υ(C=O) 1577, ^{1}H NMR (400 MHz, $CDCl_3$), δ = 7.28 (d, 1H, Ar-H), 7.15(d, 1H, Ar-H), 6.99 (t, 2H, Ar-H), 6.86 - 6.72 (m, 9H, Ar-H), 3.86 (s, 3H, -OCH_3).

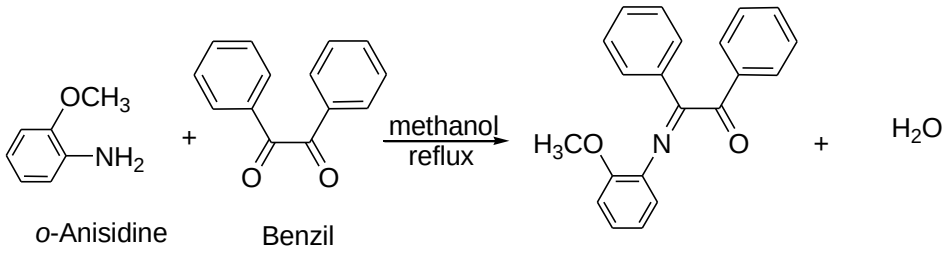

Fig. 51: Scheme for synthesis of benzil-*o*-andn Schiff base (L_3)

3.2.2 Methodology for the synthesis of $[Zn(L_3)phen]Cl_2$ *(9)*

To a hot methanolic solution (30 ml) of Schiff base (1 mmol, 0.268 g) **(L_3)** was added methanolic solution (30 ml) of $ZnCl_2$ (1 mmol, 0.136 g) with constant stirring at 70°C. The solution was refluxed for 10 h. Then a hot methanolic solution of 1,10-phenanthroline (1 mmol or 0.198 g) was added drop wise to above solution with refluxing continuing for further 8 h. White precipitates were collected after filtration. Several washings were made with cold methanol. Yield: 79 %, Color: White, M.P. Above 280°C, UV (λ_{max}): 223, 267 nm, MS: $[M]^+$ 316, Main IR peaks (cm^{-1}): υ(C_6H_5 stretch) 3055, υ(C=N) 1579, υ(C=O) 1514, υ(M-O) 642, υ(M-N) 422.

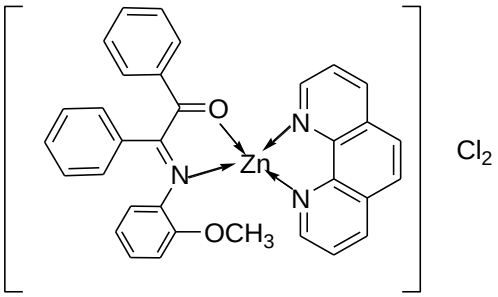

Fig. 52: Proposed geometry of $[Zn(L_3)phen]Cl_2$ *(9)*

3.2.3 Methodology for the synthesis of $[Zn(L_3)bpy]Cl_2$ *(10)*

To a hot methanolic solution (30 ml) of Schiff base (1 mmol, 0.268g) **(L_3)** was added methanolic solution (30 ml) of $ZnCl_2$ (1 mmol, 0.136 g) with constant stirring at 70°C. The solution was refluxed for 10 h. Then a hot methanolic solution of 2,2'-bipyridine (1 mmol or 0.156 g) was added drop wise to above solution with refluxing continuing for further 8 h. White precipitates were collected after filtration. Several

washings were made with cold methanol. Yield: 80 %, Color: White, M.P. Above 280°C, UV (λ_{max}): 237, 291 nm, MS: $[M]^+$ 316, Main IR peaks (cm^{-1}): υ(OH) 3200-3400, υ(C_6H_5 stretch) 3057, υ(C=N) 1600, υ(C=O) 1514, υ(M-O) 655, υ(M-N) 414.

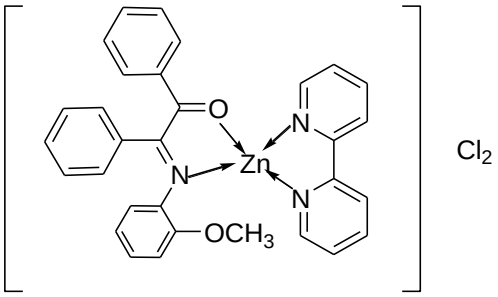

Fig. 53: Proposed geometry of $[Zn(L_3)bpy]Cl_2$ *(10)*

3.2.4 Methodology for the synthesis of $[Cu(L_3)phen]Cl_2$ *(11)*

To a hot methanolic solution (30 ml) of Schiff base (1 mmol, 0.268g) **(L_3)** was added methanolic solution (30 ml) of $CuCl_2.2H_2O$ (1 mmol, 0.170 g) with constant stirring at 70°C. The solution was refluxed for 10 h. Then a hot methanolic solution of 1,10-phenanthroline (1 mmol or 0.198 g) was added drop wise to above solution with refluxing continuing for further 8 h. Green precipitates were collected after filtration. Several washings were made with cold methanol. Yield: 84 %, Color: Green, M.P. Decomposes at 260°C, UV (λ_{max}): 270 nm, MS: $[M]^+$ 316, Main IR peaks (cm^{-1}): υ(C_6H_5 stretch) 3041, υ(C=N) 1581, υ(C=O) 1512, υ(M-O) 642, υ(M-N) 428.

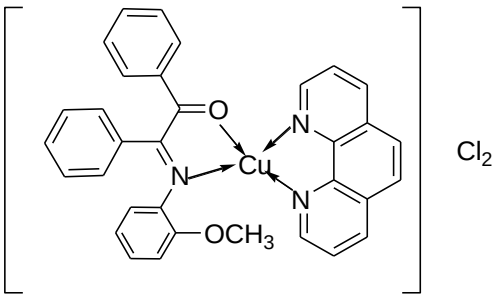

Fig. 54: Proposed geometry of $[Cu(L_3)phen]Cl_2$ *(11)*

3.2.5 Methodology for the synthesis of $[Cu(L_3)bpy]Cl_2$ *(12)*

To a hot methanolic solution (30 ml) of Schiff base (1 mmol, 0.268g) **(L_3)** was added methanolic solution (30 ml) of $CuCl_2.2H_2O$ (1 mmol, 0.170 g) with constant stirring at 70°C. The solution was refluxed for 10 h. Then a hot methanolic solution of 2,2'-bipyridine (1 mmol or 0.156 g) was added drop wise to above solution with refluxing continuing for further 8 h. Green precipitates were collected after filtration. Several washings were made with cold methanol. Yield: 82 %, Color: Green, M.P. Decomposes at 250°C, UV (λ_{max}): 296 nm, MS: $[M]^+$ 316, Main IR peaks (cm^{-1}): υ(OH) 3200-3400, υ(C_6H_5 stretch) 3034, υ(C=N) 1600, υ(C=O) 1566, υ(M-O) 632, υ(M-N) 416.

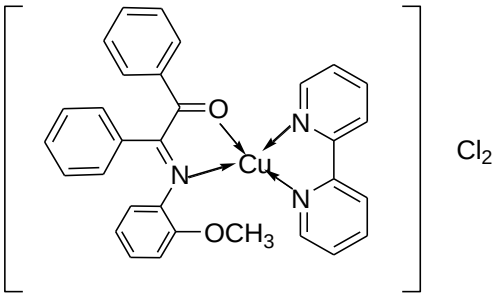

Fig. 55: Proposed geometry of $[Cu(L_3)bpy]Cl_2$ *(12)*

3.2.6 Methodology for the synthesis of Schiff base (benzil-*m*-andn) (L_4)

To a stirred and refluxed solution of benzil (4 mmol, 0.232 g) in hot methanol (35 ml) was added drop wise a hot methanolic solution (35 ml) of *m*-anisidine (4 mmol, 0.493 g or 0.45 ml). The whole set up was kept in an oil bath for 5 h at 70°C. The clear solution thus obtained was allowed to evaporate slowly. After 82 h, brown colored crystalline product separates out, this was filtered and dried in dessicator. Yield: 83 %, Color: Light yellow, M.P. 58°C, UV (λ_{max}): 255 nm, MS: $[M]^+$ 316, Main IR peaks (cm^{-1}): υ(C_6H_5 stretch) 3061, υ(C=N) 1658, υ(C=O) 1597, ^{1}H NMR (400 MHz, $CDCl_3$), δ = 7.86 (d, 2H, Ar-H), 7.78 (d, 2H, Ar-H), 7.48 (m, 4H, Ar-H), 7.37 (t, 2H, Ar-H), 7.02 (t, 1H, Ar-H), 6.47 (t, 3H, Ar-H), 3.65 (s, 3H, -OCH_3).

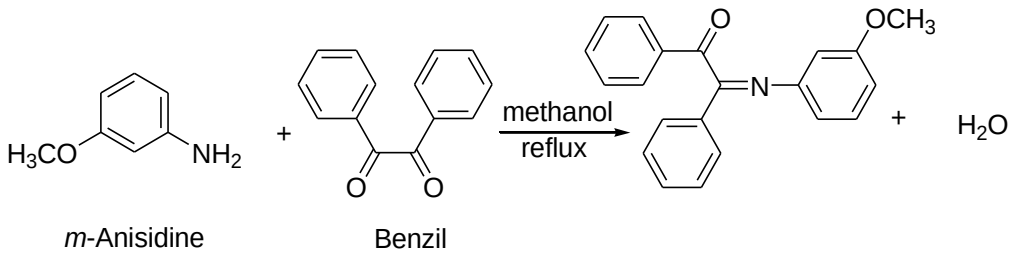

Fig. 56: Scheme for synthesis of benzil-*m*-andn Schiff base (L_4)

3.2.7 Methodology for the synthesis of [Zn(L_4)phen]Cl_2 *(13)*

To a hot methanolic solution (30 ml) of Schiff base (1 mmol, 0.268 g) **(L_4)** was added methanolic solution (30 ml) of $ZnCl_2$ (1 mmol, 0.136 g) with constant stirring at 70°C. The solution was refluxed for 10 h. Then a hot methanolic solution of 1,10-phenanthroline (1 mmol or 0.198 g) was added drop wise to above solution with refluxing continuing for further 8 h. White precipitates were collected after filtration. Several washings were made with cold methanol. Yield: 80 %, Color: White, M.P. Above 280°C, UV (λ_{max}): 223, 267 nm, MS: $[M]^+$ 316, Main IR peaks (cm^{-1}): υ(C_6H_5 stretch) 3059, υ(C=N) 1600, υ(C=O) 1570, υ(M-O) 640, υ(M-N) 416.

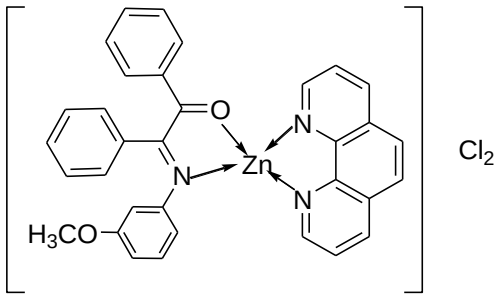

Fig. 57: Proposed geometry of Zn(L_4)phen]Cl_2 *(13)*

3.2.8 Methodology for the synthesis of [Zn(L_4)bpy]Cl_2 *(14)*

To a hot methanolic solution (30 ml) of Schiff base (1 mmol, 0.268 g) **(L_4)** was added methanolic solution (30 ml) of $ZnCl_2$ (1 mmol, 0.136 g) with constant stirring at 70°C. The solution was refluxed for 10 h. Then a hot methanolic solution of 2,2'-bipyridine (1 mmol or 0.156 g) was added drop wise to above solution with refluxing continuing for further 8 h. White precipitates were collected after filtration.

Several washings were made with cold methanol. Yield: 80 %, Color: White, M.P. Above 280°C, UV (λ_{max}): 237, 291 nm, MS: $[M]^+$ 316, Main IR peaks (cm^{-1}): υ(OH) 3200-3400, υ(C_6H_5 stretch) 3061, υ(C=N) 1597, υ(C=O) 1570, υ(M-O) 644, υ(M-N) 428.

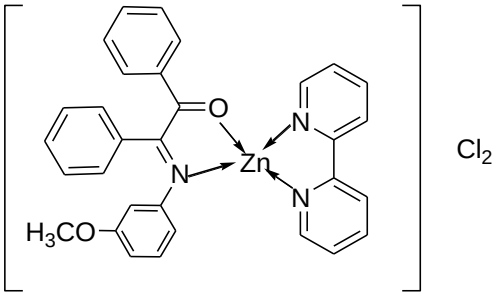

Fig. 58: Proposed geometry of $[Zn(L_4)bpy]Cl_2$ *(14)*

3.2.9 Methodology for the synthesis of $[Cu(L_4)phen]Cl_2$ *(15)*

To a hot methanolic solution (30 ml) of Schiff base (1 mmol, 0.268 g) **(L_4)** was added methanolic solution (30 ml) of $CuCl_2.2H_2O$ (1 mmol, 0.170 g) with constant stirring at 70°C. The solution was refluxed for 10 h. Then a hot methanolic solution of 1,10-phenanthroline (1 mmol or 0.198 g) was added drop wise to above solution with refluxing continuing for further 8 h. Dark green precipitates were collected after filtration. Several washings were made with cold methanol. Yield: 75 %, Color: Dark green, M.P. Above 280°C, M.P. Decomposes at 263°C, UV (λ_{max}): 270 nm, MS: $[M]^+$ 316, Main IR peaks (cm^{-1}): υ(C_6H_5 stretch) 3055, υ(C=N) 1582, υ(C=O) 1515, υ(M-O) 644, υ(M-N) 428.

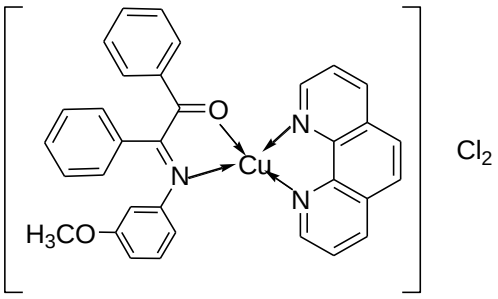

Fig. 59: Proposed geometry of $[Cu(L_4)phen]Cl_2$ *(15)*

3.2.10 Methodology for the synthesis of $[Cu(L_4)bpy]Cl_2$ *(16)*

To a hot methanolic solution (30 ml) of Schiff base (1 mmol, 0.268 g) **(L_4)** was added methanolic solution (30 ml) of $CuCl_2.2H_2O$ (1 mmol, 0.170 g) with constant stirring at 70°C. The solution was refluxed for 10 h. Then a hot methanolic solution of 2,2'-bipyridine (1 mmol or 0.156 g) was added drop wise to above solution with refluxing continuing for further 8 h. Light green precipitates were collected after filtration. Several washings were made with cold methanol. Yield: 79 %, Color: Light green, M.P. Starts decomposing at 273°C, UV (λ_{max}): 296 nm, MS: $[M]^+$ 316, Main IR peaks (cm^{-1}): υ(OH) 3200-3400, υ(C_6H_5 stretch) 3053, υ(C=N) 1600, υ(C=O) 1564, υ(M-O) 632, υ(M-N) 416.

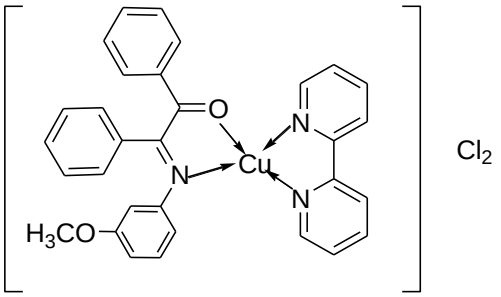

Fig. 60: Proposed geometry of $[Cu(L_4)bpy]Cl_2$ *(16)*

3.2.11 Methodology for the synthesis of Schiff base (benzil-*p*-andn) (L_5)

To a stirred and refluxed solution of benzil (4 mmol, 0.232 g) in hot methanol (35ml) was added drop wise a hot methanolic solution (35 ml) of *p*-anisidine (4 mmol, 0.493 g or 0.45 ml). The whole set up was kept in an oil bath for 5 h at 70°C. Immediately yellow colored precipitates were formed. The solution is further refluxed for 3 h. The precipitates thus obtained were filtered, washed many times with cold methanol. They were recrystallized using hot methanol as solvent. Yield: 83 %, Color: Yellow, M.P. 80°C, UV (λ_{max}): 247 nm, MS: $[M]^+$ 316, Main IR peaks (cm^{-1}): υ(C_6H_5 stretch) 3053, υ(C=N) 1664, υ(C=O) 1595, ^{1}H NMR (400 MHz, $CDCl_3$), 7.99 (d, 2H, Ar-H), 7.78 (d, 2H, Ar-H), 7.47 (m, 6H, Ar-H), 6.88 (d, 2H, Ar-H), 6.65 (d, 2H, Ar-H), 3.68 (s, 3H, -OCH_3).

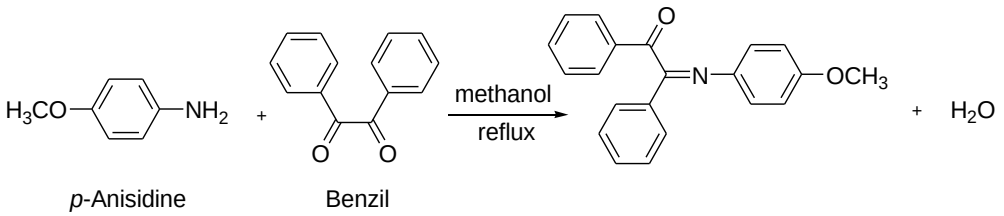

Fig. 61: Scheme for synthesis of benzil-*p*-andn Schiff base (L_5)

3.2.12 Methodology for the synthesis of $[Zn(L_5)phen]Cl_2$ *(17)*

To a hot methanolic solution (30 ml) of Schiff base (1 mmol, 0.268 g) **(L_5)** was added methanolic solution (30 ml) of $ZnCl_2$ (1 mmol, 0.136 g) with constant stirring at 70°C. The solution was refluxed for 10 h. Then a hot methanolic solution of 1,10-phenanthroline (1 mmol or 0.198 g) was added drop wise to above solution with refluxing continuing for further 8 h. White precipitates were collected after filtration. Several washings were made with cold methanol. Yield: 80 %, Color: White, M.P. Above 280°C, UV (λ_{max}): 223 nm, 267 nm, MS: $[M]^+$ 316, Main IR peaks (cm^{-1}): υ(C_6H_5 stretch) 3047, υ(C=N) 1581, υ(C=O) 1514, υ(M-O) 646, υ(M-N) 426.

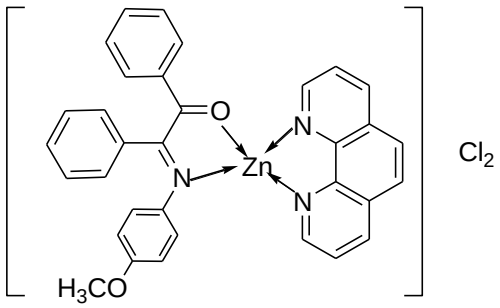

Fig. 62: Proposed geometry of $[Zn(L_5)phen]Cl_2$ *(17)*

3.2.13 Methodology for the synthesis of $[Zn(L_5)bpy]Cl_2$ *(18)*

To a hot methanolic solution (30 ml) of Schiff base (1 mmol, 0.268 g) **(L_5)** was added methanolic solution (30 ml) of $ZnCl_2$ (1 mmol, 0.136 g) with constant stirring at 70°C. The solution was refluxed for 10 h. Then a hot methanolic solution of 2,2'-bipyridine (1 mmol or 0.156 g) was added drop wise to above solution with refluxing continuing for further 8 h. White precipitates were collected after filtration. Several washings were made with cold methanol. Yield: 80 %, Color: White, M.P.

Above 280°C, UV (λ_{max}): 230 nm, 282 nm, MS: $[M]^+$ 316, Main IR peaks (cm^{-1}): υ(OH) 3300, υ(C_6H_5 stretch) 3061, υ(C=N) 1595, υ(C=O) 1570, υ(M-O) 636, υ(M-N) 412.

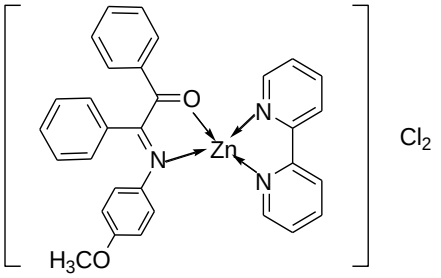

Fig. 63: Proposed geometry of $[Zn(L_5)bpy]Cl_2$ *(18)*

3.2.14 Methodology for the synthesis of $[Cu(L_5)phen]Cl_2$ *(19)*

To a hot methanolic solution (30 ml) of Schiff base (1 mmol, 0.268 g) **(L_5)** was added methanolic solution (30 ml) of $CuCl_2.2H_2O$ (1 mmol, 0.170 g) with constant stirring at 70°C. The solution was refluxed for 10 h. Then a hot methanolic solution of 1,10-phenanthroline (1 mmol or 0.198 g) was added drop wise to above solution with refluxing continuing for further 8 h. Green precipitates were collected after filtration. Several washings were made with cold methanol. Yield: 79 %, Color: Green, M.P. Above Decomposes at 260°C, UV (λ_{max}): 270 nm, MS: $[M]^+$ 316, Main IR peaks (cm^{-1}): υ(C_6H_5 stretch) 3061, υ(C=N) 1602, υ(C=O) 1570, υ(M-O) 642, υ(M-N) 428.

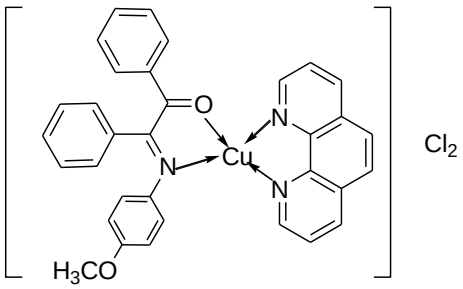

Fig. 64: Proposed geometry of $[Cu(L_5)phen]Cl_2$ *(19)*

3.2.15 Methodology for the synthesis of $[Cu(L_5)bpy]Cl_2$ *(20)*

To a hot methanolic solution (30 ml) of Schiff base (1 mmol, 0.268 g) **(L_5)** was added methanolic solution (30 ml) of $CuCl_2.2H_2O$ (1 mmol, 0.170 g) with constant stirring at 70°C. The solution was refluxed for 10 h. Then a hot methanolic solution of 2,2'-bipyridine (1 mmol or 0.156 g) was added drop wise to above solution with refluxing continuing for further 8 h. Dark green precipitates were collected after filtration. Several washings were made with cold methanol. Yield: 78 %, Color: Dark green, M.P. Decomposes at 248°C, UV (λ_{max}): 296 nm, MS: $[M]^+$ 316, Main IR peaks (cm^{-1}): υ(C_6H_5 stretch) 3034, υ(C=N) 1600, υ(C=O) 1566, υ(M-O) 634, υ(M-N) 416.

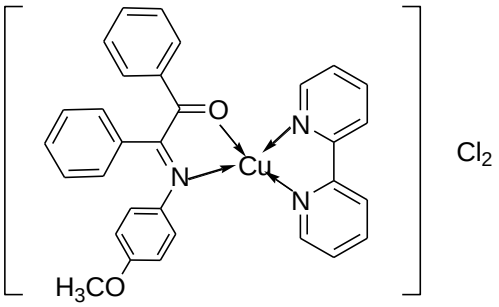

Fig. 65: Proposed geometry of $[Cu(L_5)bpy]Cl_2$ *(20)*

3.3 Results and discussions

The ligands and Cu^{2+} mixed ligand chelates appear as colored precipitates while Zn^{2+} complexes appear as white precipitates. All of them were found to be thermally stable, non hygroscopic solids which do not decomposes even after months of their synthesis and under varied conditions of temperature. They were having fair solubility in water, DMSO, DMF and Tris buffer (pH 7.4).

3.3.1. UV-vis analysis

The results of the UV-vis absorption studies of Schiff base ligands and their complexes were recorded in the range of 200 - 800 nm at low concentrations using water as solvent. The bands observed indicates π to π* transitions confirming binding of metal centers with Schiff base, 1,10-phenanthroline / 2,2'-bipyridine. The UV–vis spectral data of the Schiff base along with its chelates are tabulated in table 17.

3.3.2 FTIR analysis

In the uncoordinated ligand a strong band appears at 1656 cm^{-1} for $\mathbf{L_3}$, 1658 cm^{-1} for $\mathbf{L_4}$ and 1664 cm^{-1} for $\mathbf{L_5}$ attributing to free azomethine group, but in metal complexes a negative shift up to 1579 cm^{-1} suggests coordination of the imine nitrogen to metal centers. This may occurs due to decrease in bond strength of imine bond and simultaneous increase in bond strength between azomethine nitrogen and metal center. Another absorption bands in the region of 1575 - 1595 cm^{-1} are due to (-C=O-) stretch of free carbonyl group in the ligand and shows negative up to 60 cm^{-1} in metal complexes suggesting coordination in metal complexes. All the metal complexes show absorption peaks in the region 414 - 429 cm^{-1} corresponding to M-N and 637 - 659 cm^{-1} corresponding to M-O vibrations confirming the bond formation between azomethine nitrogen, carbonyl oxygen and metal ion. Another absorption bands in the range of 3200 - 3400 cm^{-1} in some complexes marks the presence of coordinated or lattice water. The IR spectra of all Schiff base ligand and their complexes are as follows (Table 17):

Table 17: Selected bond frequencies (cm^{-1}) and UV-vis values of ligands, Zn(II) and Cu(II) mixed ligand chelates

Complex	**$\nu_{(M-N)}$ (cm^{-1})**	**$\nu_{(M-O)}$ (cm^{-1})**	**C_6H_5 stretch (cm^{-1})**	**ν(-C=N-) stretch (cm^{-1})**	**ν(-C=O-) stretch (cm^{-1})**	**Coordinated / Lattice Water**	**π to π^* transition (nm)**
(L_3)	**-**	**-**	**3061**	**1656**	**1577**	**-**	**256**
[Zn(L_3)phen]Cl_2 ***(9)***	422	642	3055	1579	1514	-	223, 267
[Zn(L_3)bpy]Cl_2 ***(10)***	414	655	3057	1600	1514	3200-3400	237, 291
[Cu(L_3)phen]Cl_2 ***(11)***	428	642	3041	1581	1512	428	270
[Cu(L_3)bpy]Cl_2 ***(12)***	416	632	3034	1600	1566	3200-3400	296
(L_4)	**-**	**-**	**3061**	**1658**	**1597**	**-**	**255**
[Zn(L_4)phen]Cl_2 ***(13)***	416	640	3059	1600	1570	-	223, 267
[Zn(L_4)bpy]Cl_2 ***(14)***	414	636	3061	1597	1570	3200-3400	237, 291
[Cu(L_4)phen]Cl_2 ***(15)***	428	644	3055	1582	1515	-	270
[Cu(L_4)bpy]Cl_2 ***(16)***	416	632	3053	1600	1564	3200-3400	296
(L_5)	**-**	**-**	**3053**	**1664**	**1595**	**-**	**247**
[Zn(L_5)phen]Cl_2 ***(17)***	426	646	3047	1581	1514	-	223, 267
[Zn(L_5)bpy]Cl_2 ***(18)***	412	636	3061	1595	1570	3300	230, 282
[Cu(L_5)phen]Cl_2 ***(19)***	428	642	3061	1602	1570	-	270
[Cu(L_5)bpy]Cl_2 ***(20)***	416	634	3034	1600	1566	-	296

3.3.3 Mass spectral analysis

The molecular ion peaks in mass spectra of ligands (**L_3, L_4** and **L_5**) was observed at m/z 316 corresponds to the parent ion peak of all the three isomers thus confirming there formation. The mass fragmentation pattern of the complexes has been tabulated as follows:

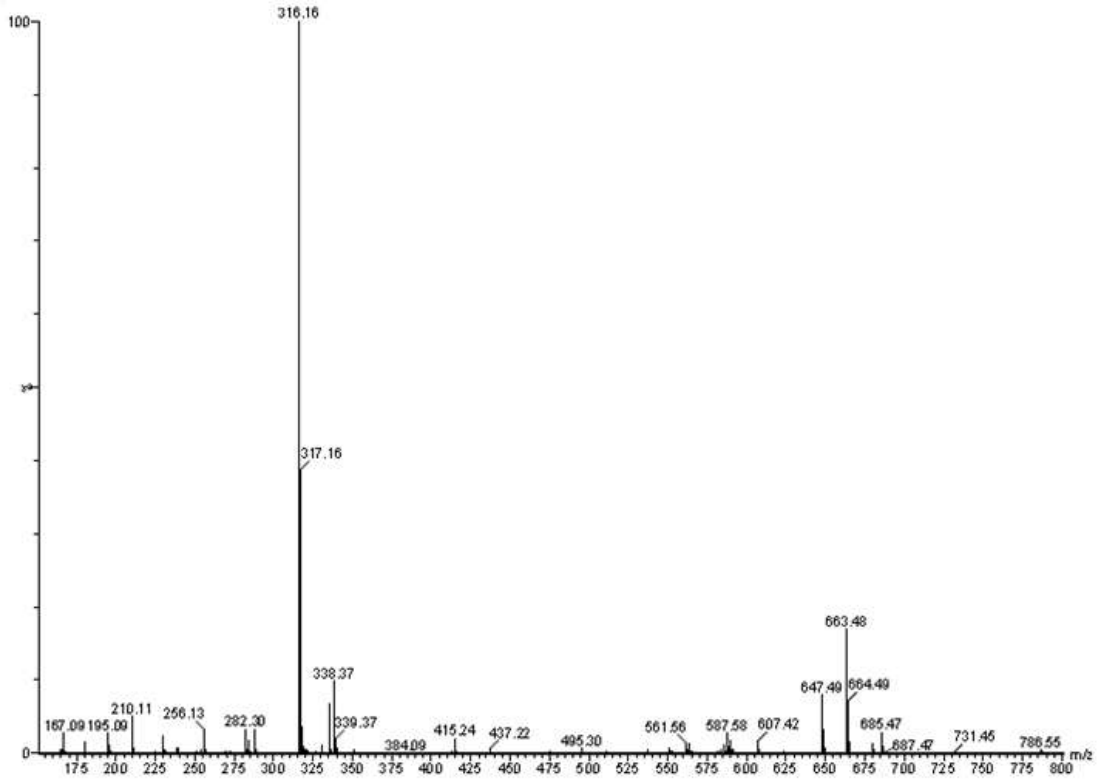

Fig. 66: Mass spectra of (L_3) (Mol. Mass = 315 g)

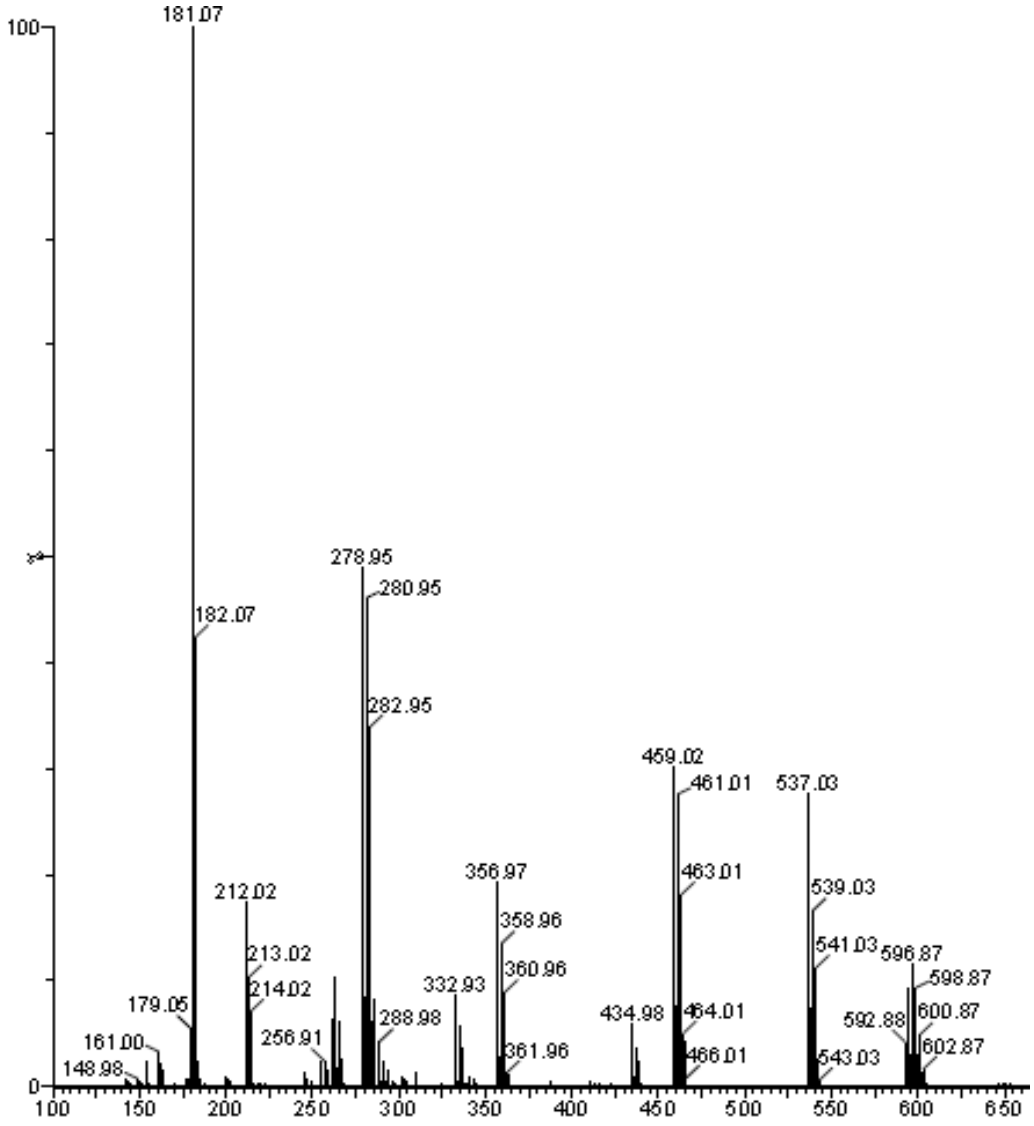

Fig. 67: Mass spectra of [Zn(L_3)phen]Cl_2 *(9)*

m/z	**Loss of**	**Fragment**
595		[Zn(L_3)phen]Cl
459	C_6H_5CO, -OCH_3	
280		[Zn(phen)Cl]
180	Zn, Cl	Free phen

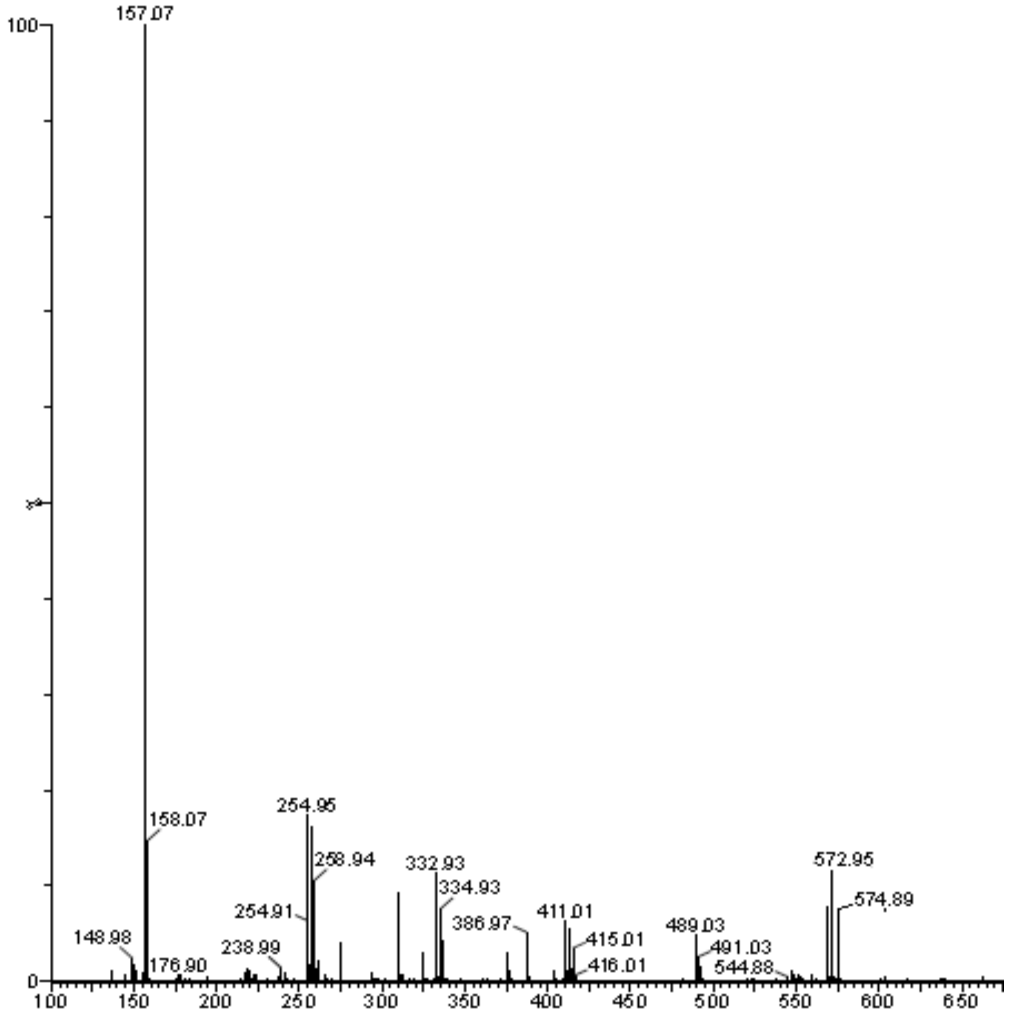

Fig. 68: Mass spectra of [Zn(L_3)bpy]Cl_2 *(10)*

m/z	**Loss of**	**Molecular Ion**
571		[Zn(L_3)bpy] Cl
410	C_6H_5CO, -OCH_3	
256		[Zn(bpy)Cl]
156	Zn, Cl	Free bpy

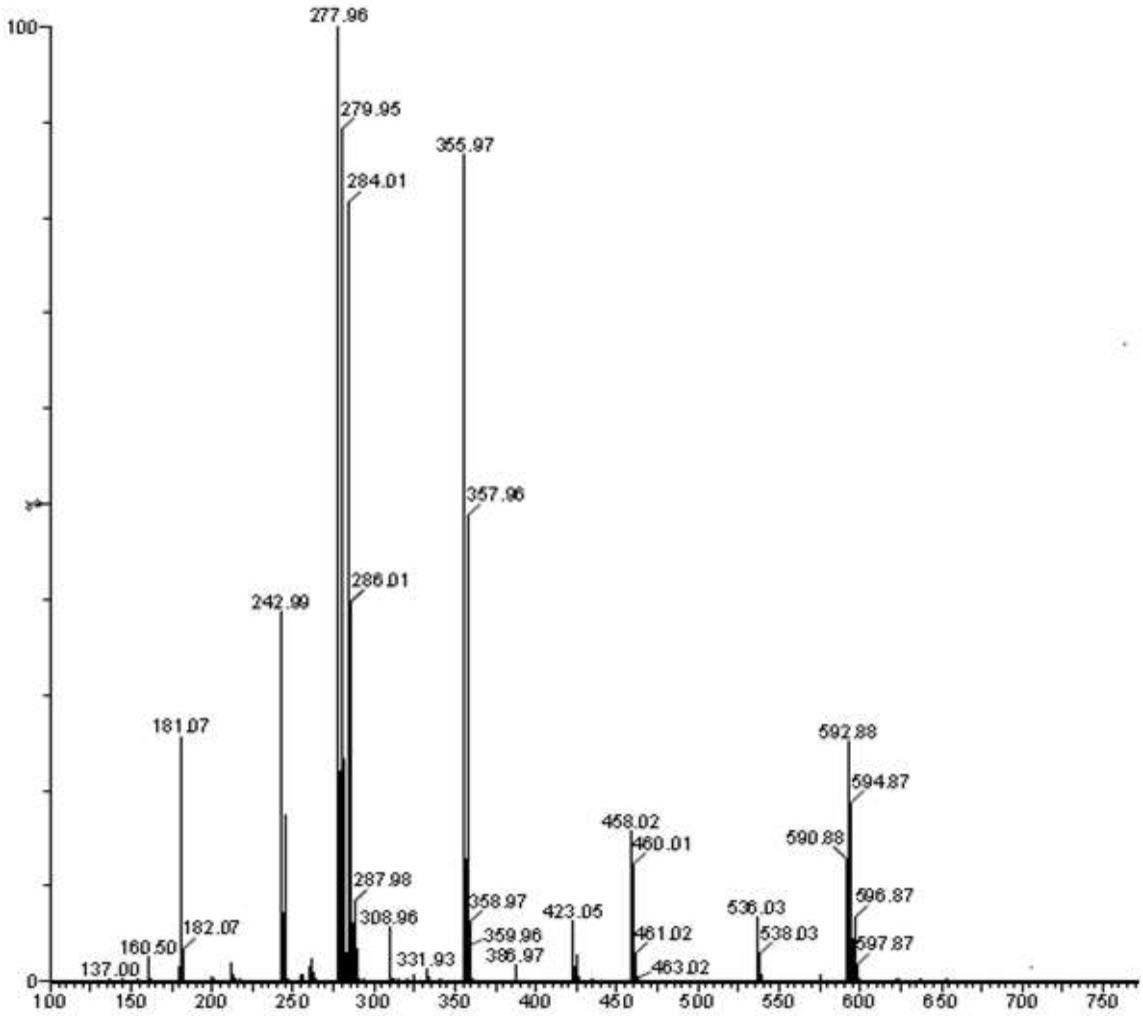

Fig. 69: Mass spectra of [Cu(L_3)phen]Cl_2 (*11*)

m/z	**Loss of**	**Fragment**
594		[Cu(L_3)phen]Cl
458	C_6H_5CO, -OCH_3	
270		[Cu(phen)Cl]
180	Cu, Cl	Free phen

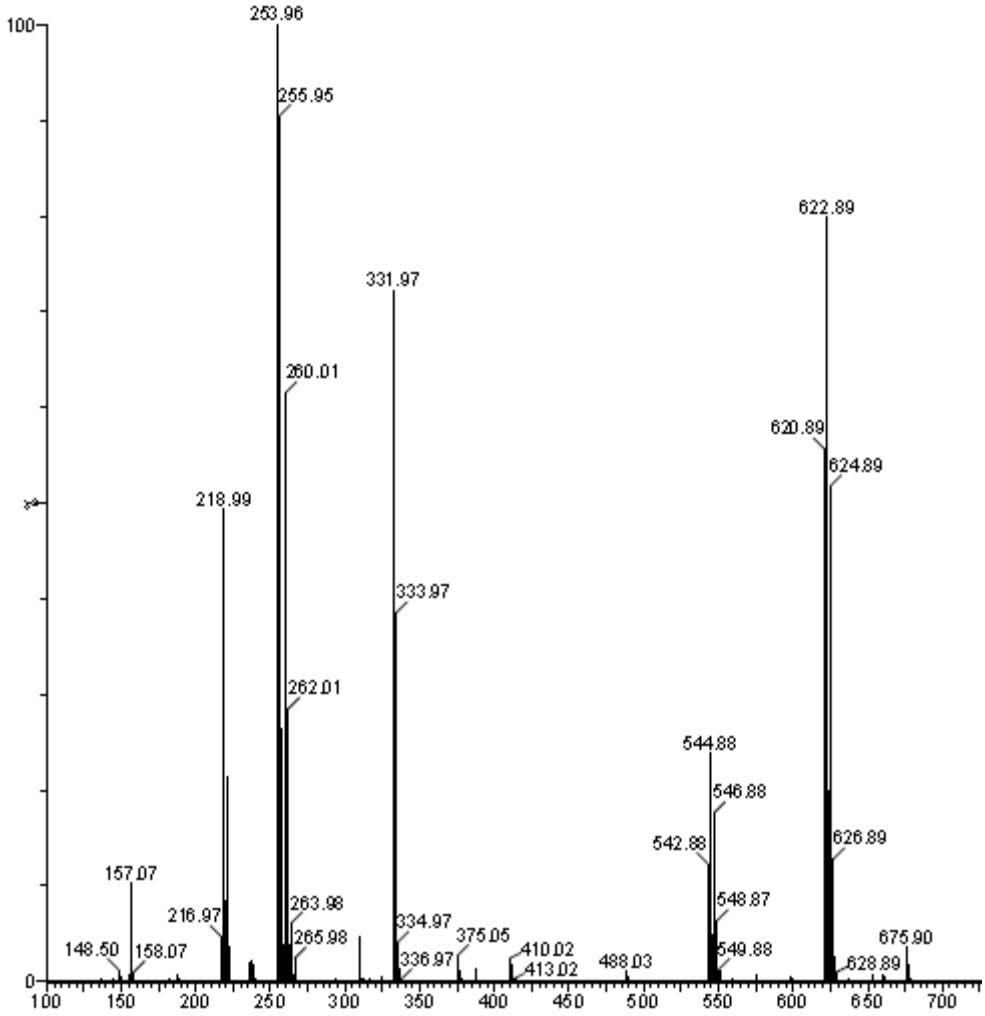

Fig. 70: Mass spectra of $[Cu(L_3)bpy]Cl_2$ (*12*)

m/z	**Loss of**	**Fragment**
623		$[Cu(L_3)bpy]Cl_2.H_2O$
255	L_3	[Cu(bpy)Cl]
219	Cl	[Cu(bpy)]
156	Cu	Free bpy

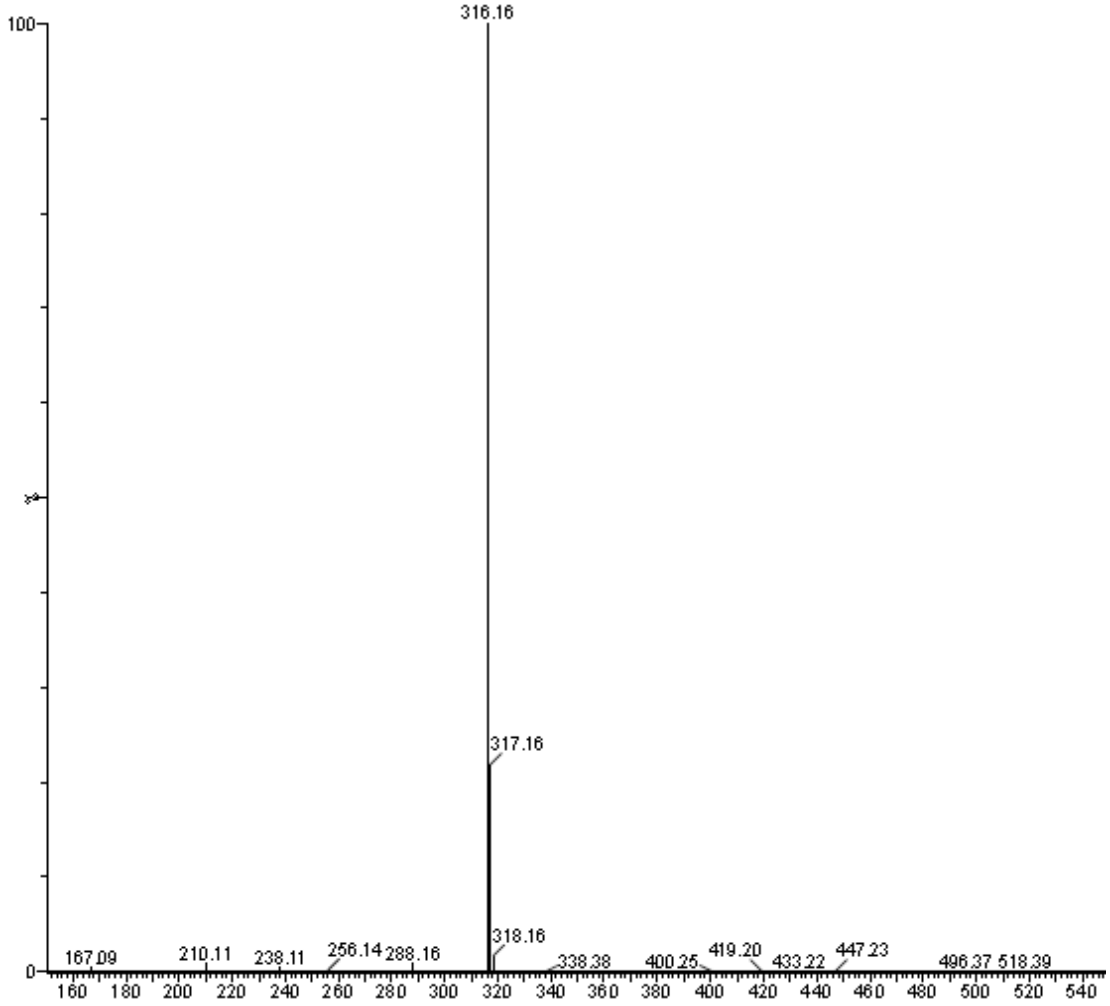

Fig. 71: Mass spectra of (L_4) (Mol. Mass = 315 g)

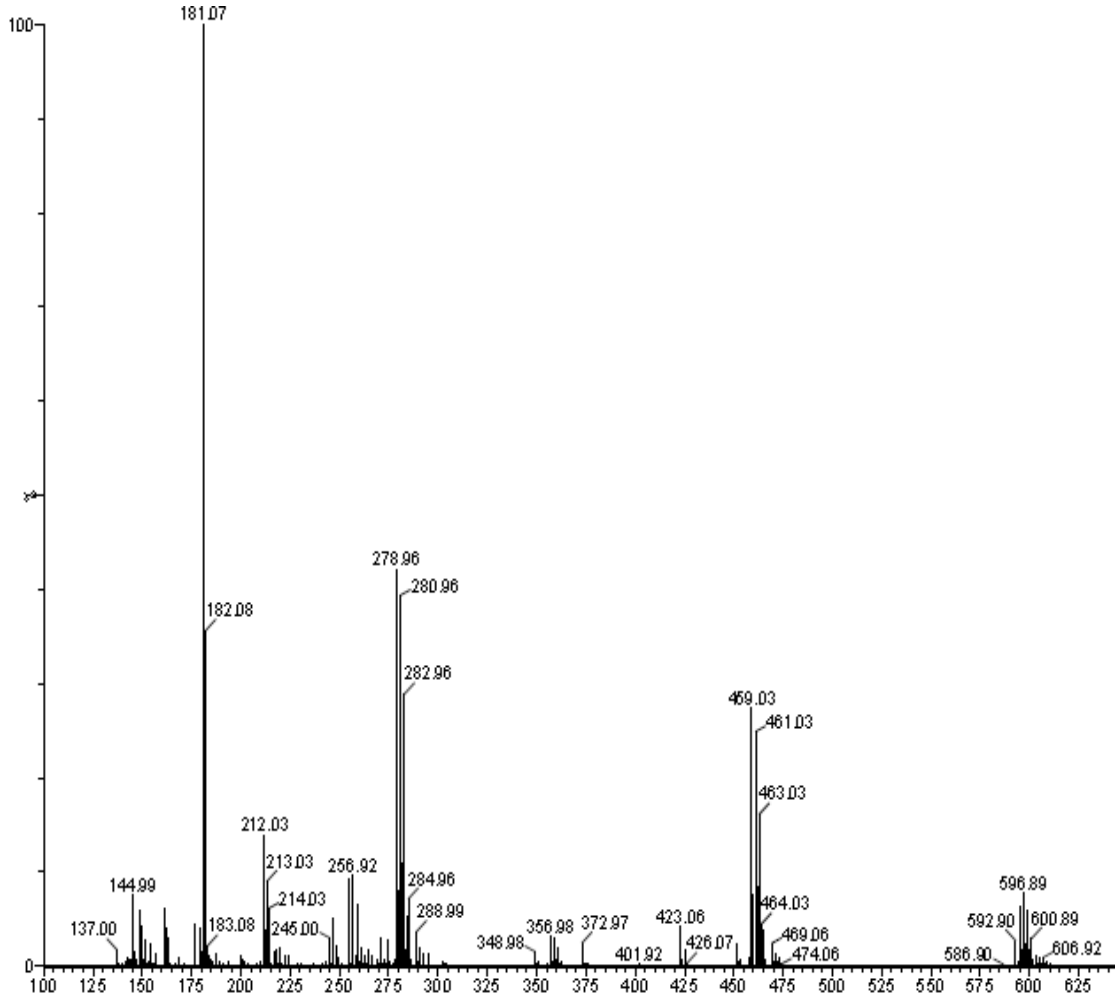

Fig. 72: Mass spectra of [Zn(L_4)phen]Cl_2 (*13*)

m/z	**Loss of**	**Fragment**
596		[Zn(L_4)phen]Cl
461	C_6H_5CO, -OCH_3	
281	L_4	[Zn(phen)Cl]
246	Cl	[Zn(phen)]
180	Zn	Free phen

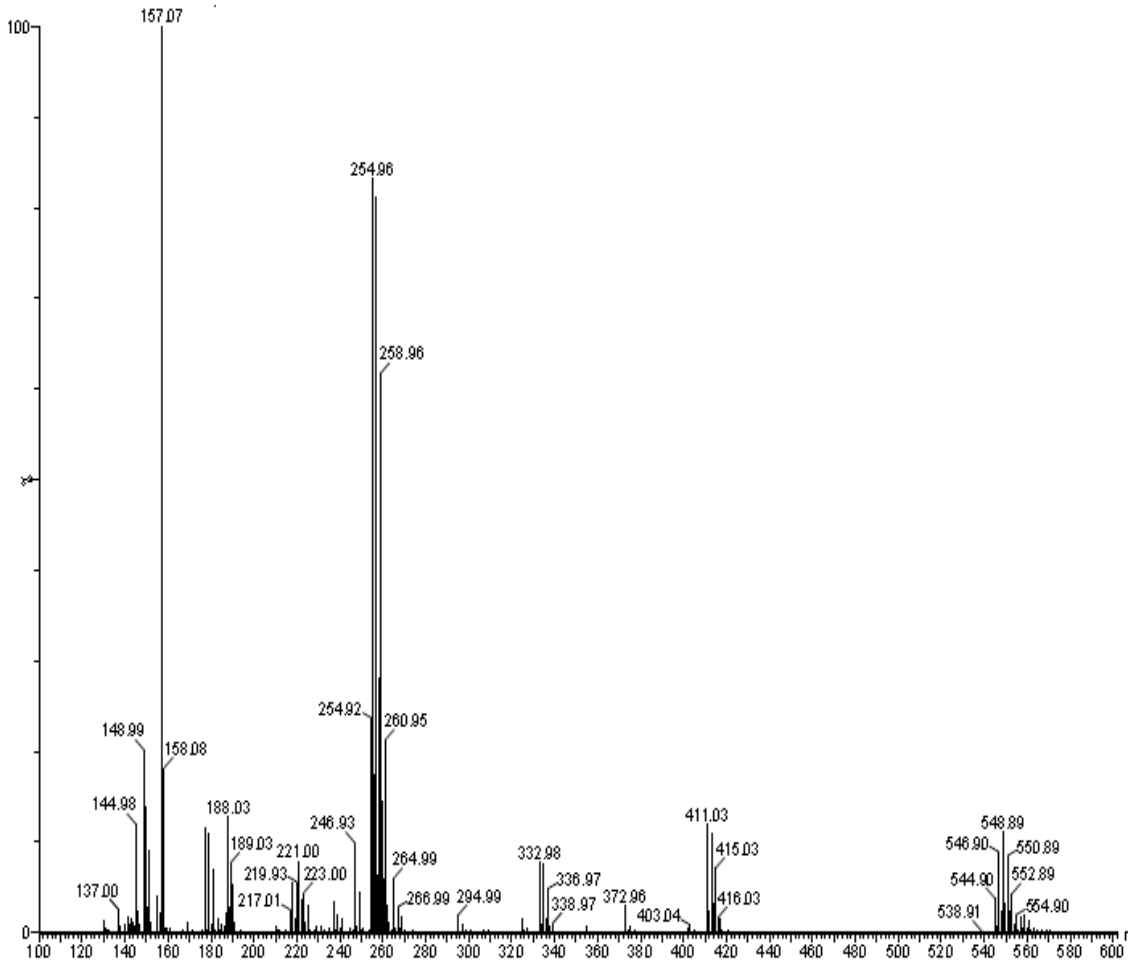

Fig. 73: Mass spectra of $[Zn(L_4)bpy]Cl_2$ (*14*)

m/z	**Loss of**	**Fragment**
625(Not recorded)		$[Zn(L_4)bpy]Cl_2.H_2O$
554		$[Zn(L_4)bpy]H_2O$
411	C_6H_5CO, $-OCH_3$	
257	L_4	[Zn(bpy)Cl]
222	Cl	[Zn(bpy)]
156	Zn	Free bpy

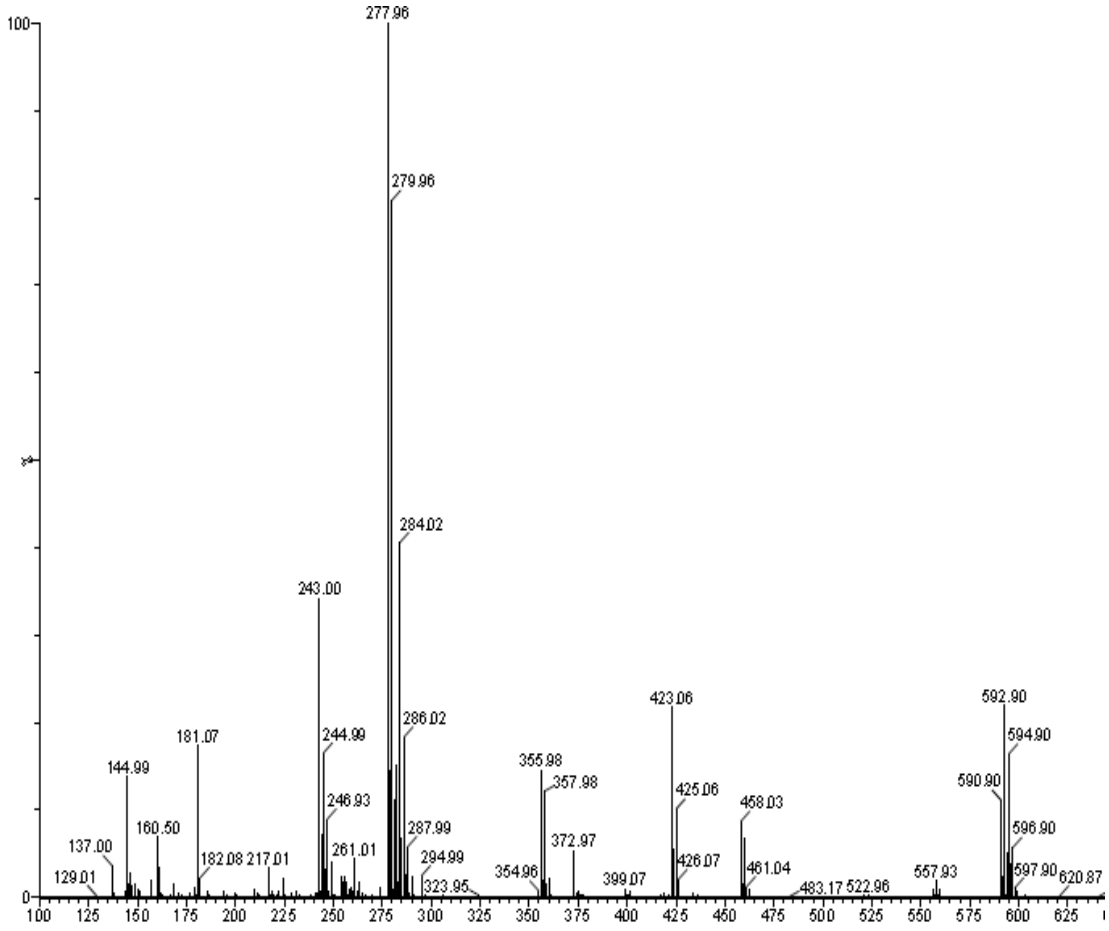

Fig. 74: Mass spectra of [Cu(L_4)phen]Cl_2 (*15*)

m/z	**Loss of**	**Fragment**
594		[Cu(L_4)phen]Cl
460	C_6H_5CO, -OCH_3	
280	L_4	[Cu(phen)Cl]
243	Cl	[Cu(phen)]
180	Cu	Free phen

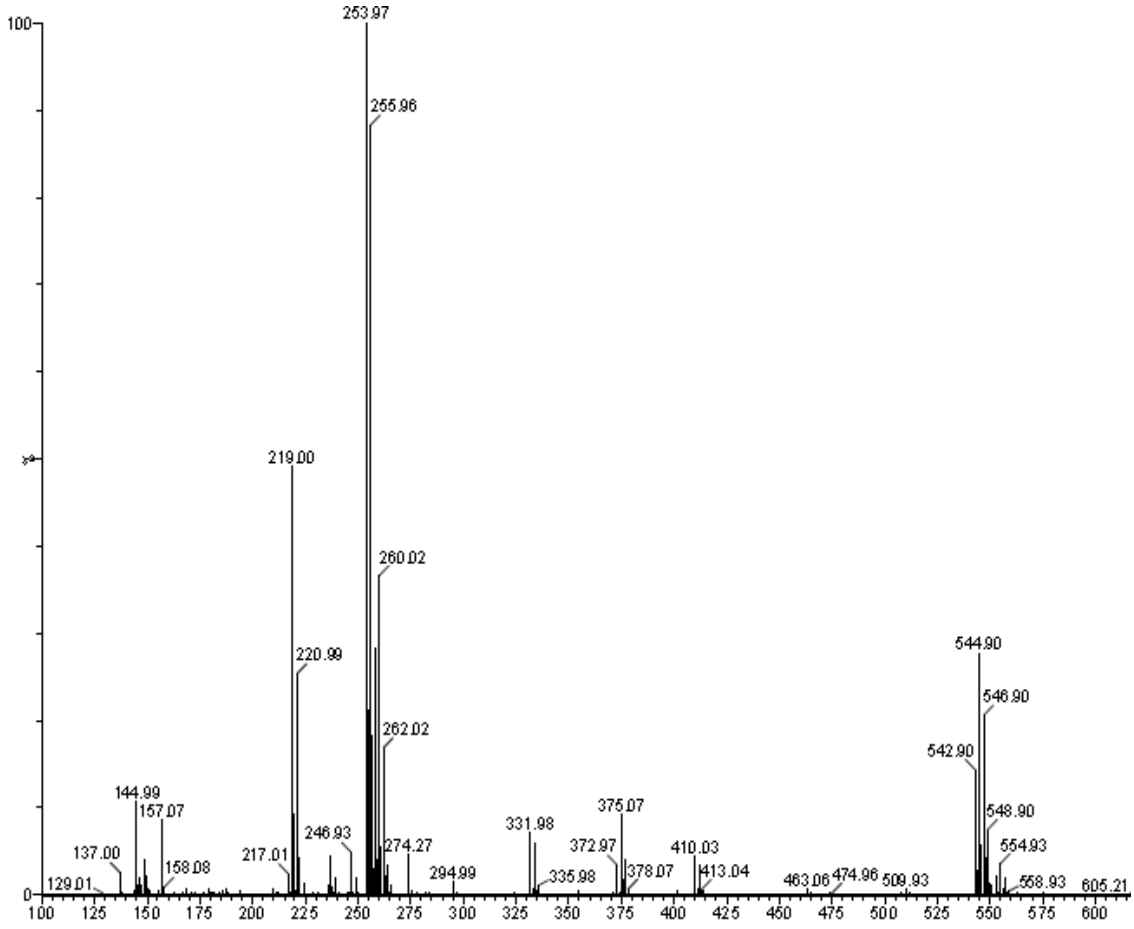

Fig. 75: Mass spectra of $[Cu(L_4)bpy]Cl_2$ (*16)*

m/z	**Loss of**	**Fragment**
623(Not recorded)		$[Cu(L_4)bpy]Cl_2.H_2O$
553	2 Cl	$[Cu(L_4)bpy]H_2O$
255	L_4	[Cu(bpy)Cl]
220	Cl	[Cu(bpy)]
156	Cu	Free bpy

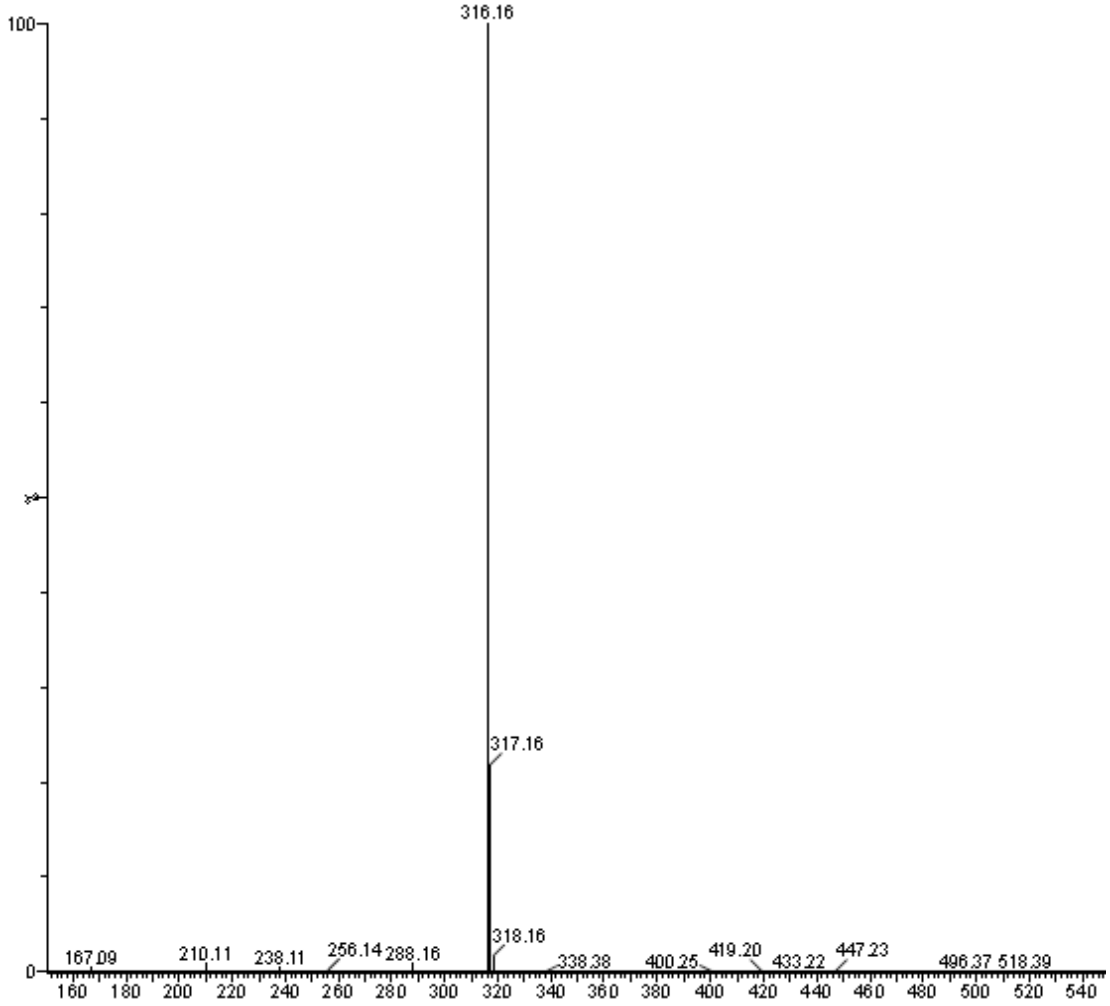

Fig. 76: Mass spectra of (L_5) (Mol. Mass = 315 g)

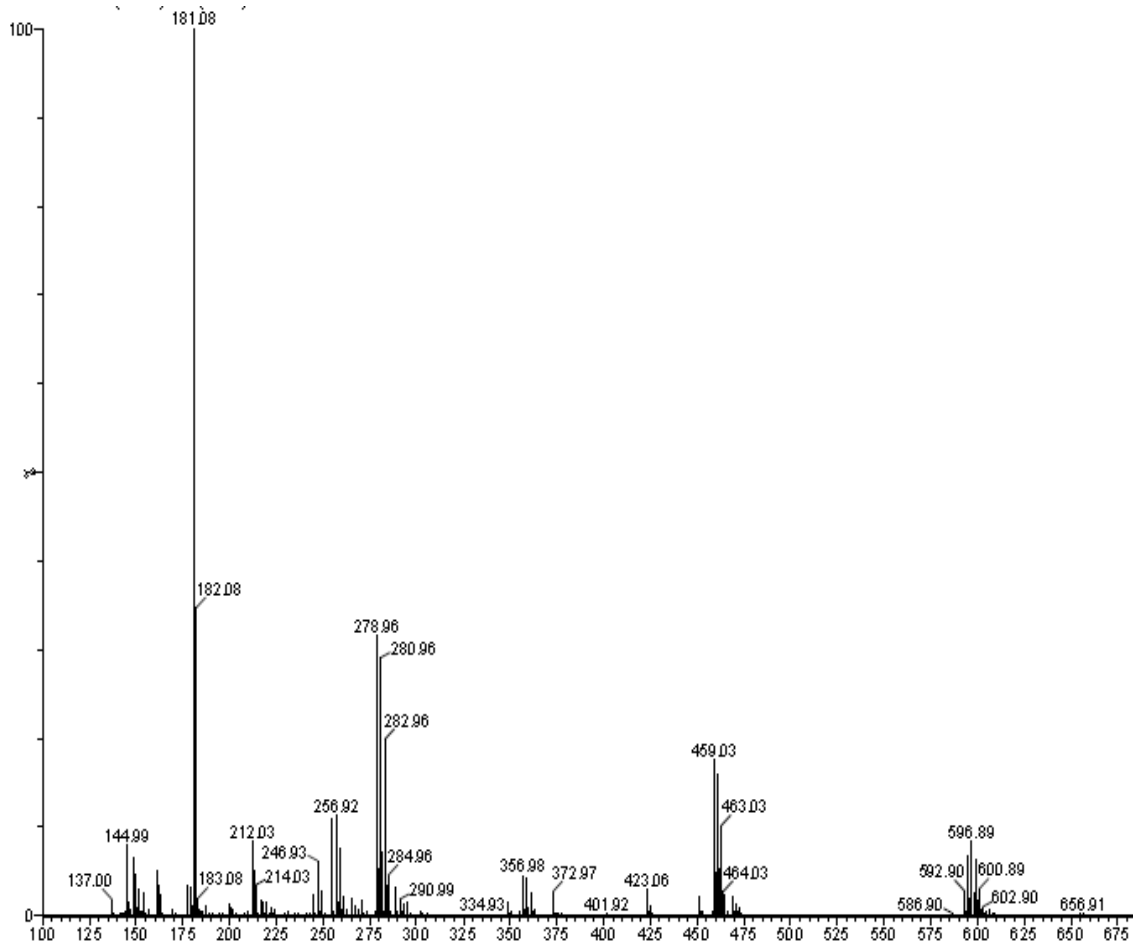

Fig. 77: Mass Spectra of $[Zn(L_5)phen]Cl_2$ (*17*)

m/z	**Loss of**	**Fragment**
595		$[Zn(L_5)phen]Cl$
460	C_6H_5CO, $-OCH_3$	
281	L_5	[Zn(phen)Cl]
246	Cl	[Zn(phen)]
180	Zn	Free phen

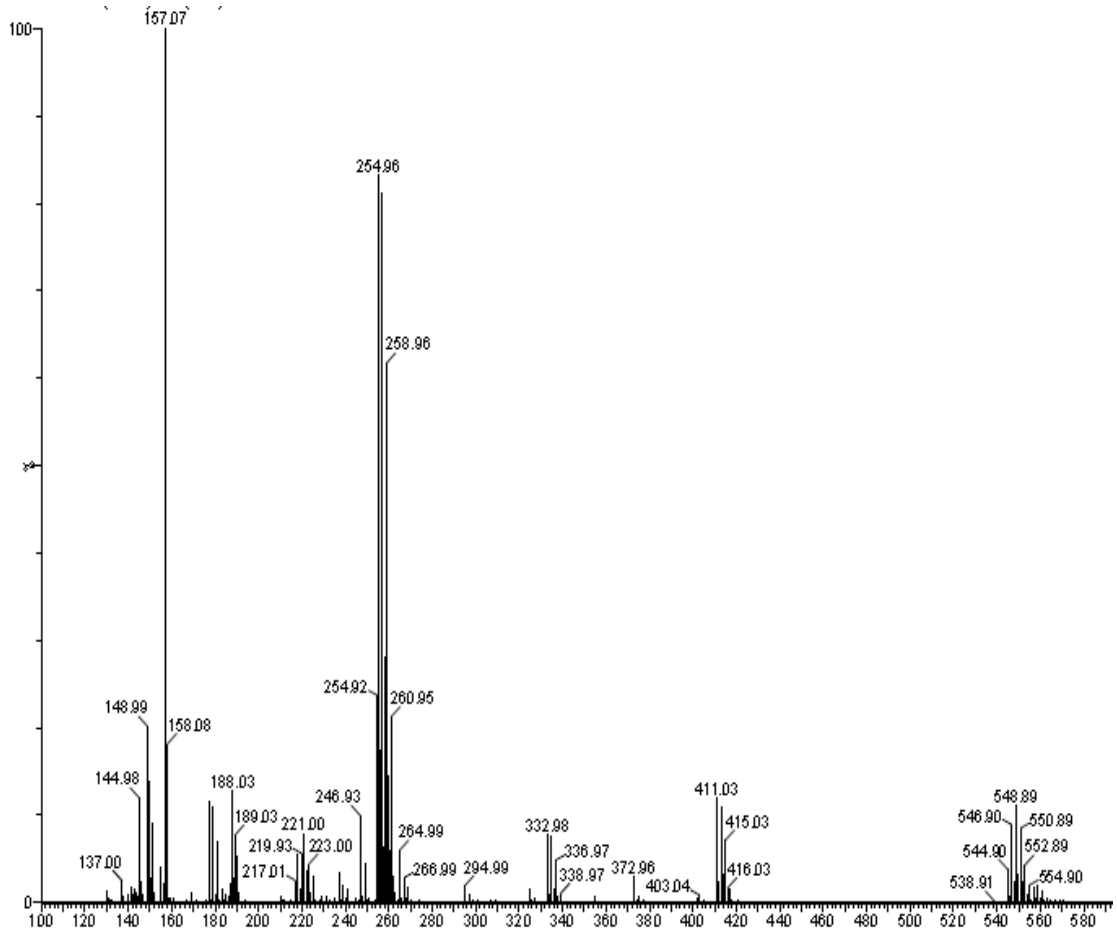

Fig. 78: Mass Spectra of $[Zn(L_5)bpy]Cl_2$ (*18*)

m/z	**Loss of**	**Fragment**
625(Not seen)		$[Zn(L_5)bpy]Cl_2.H_2O$
554	2Cl	$[Zn(L_5)bpy].H_2O$
256	L_5	[Zn(bpy)Cl]
221	Cl	[Zn(bpy)]
156	Zn	Free bpy

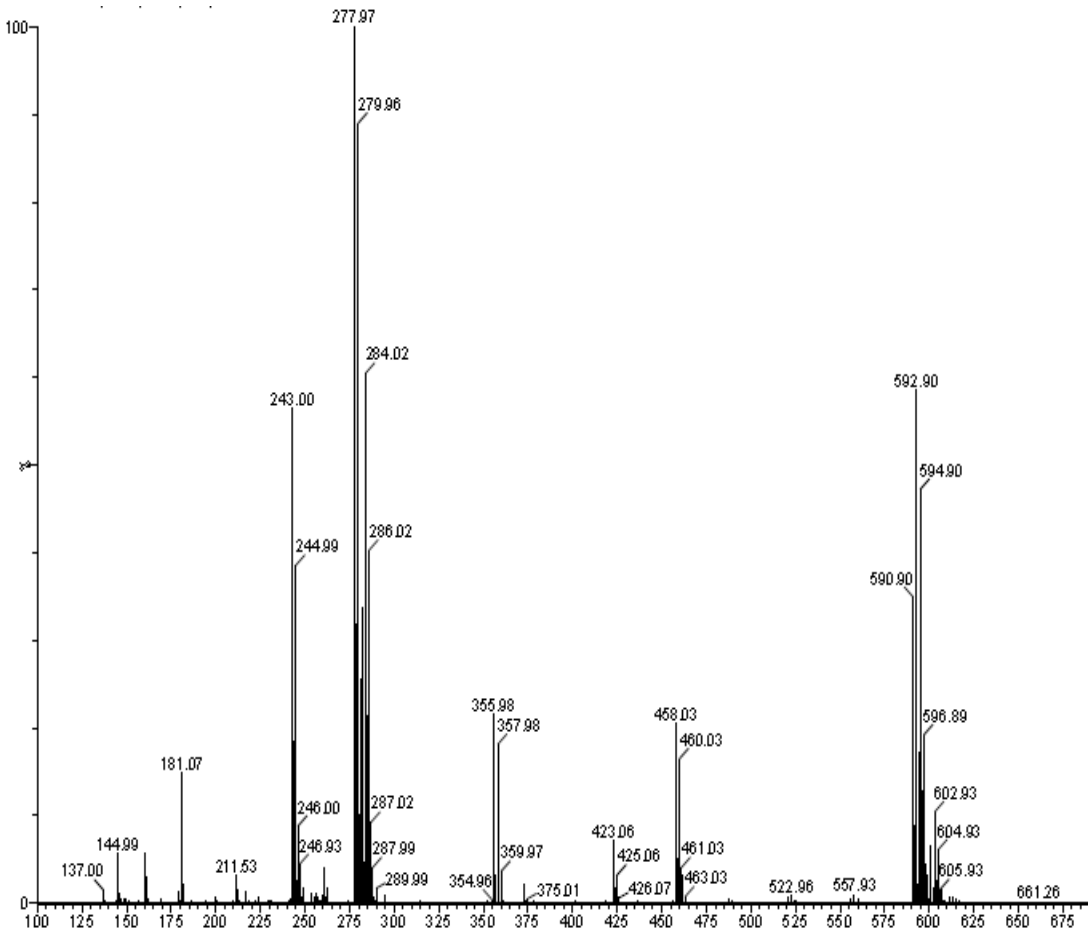

Fig. 79: Mass spectra of $[Cu(L_5)phen]Cl_2$ (*19*)

m/z	**Loss of**	**Fragment**
596		$[Cu(L_5)phen]Cl$
460	C_6H_5CO, $-OCH_3$	
280	L_5	[Cu(phen)Cl]
243	Cl	[Cu(phen)]
180	Cu	Free phen

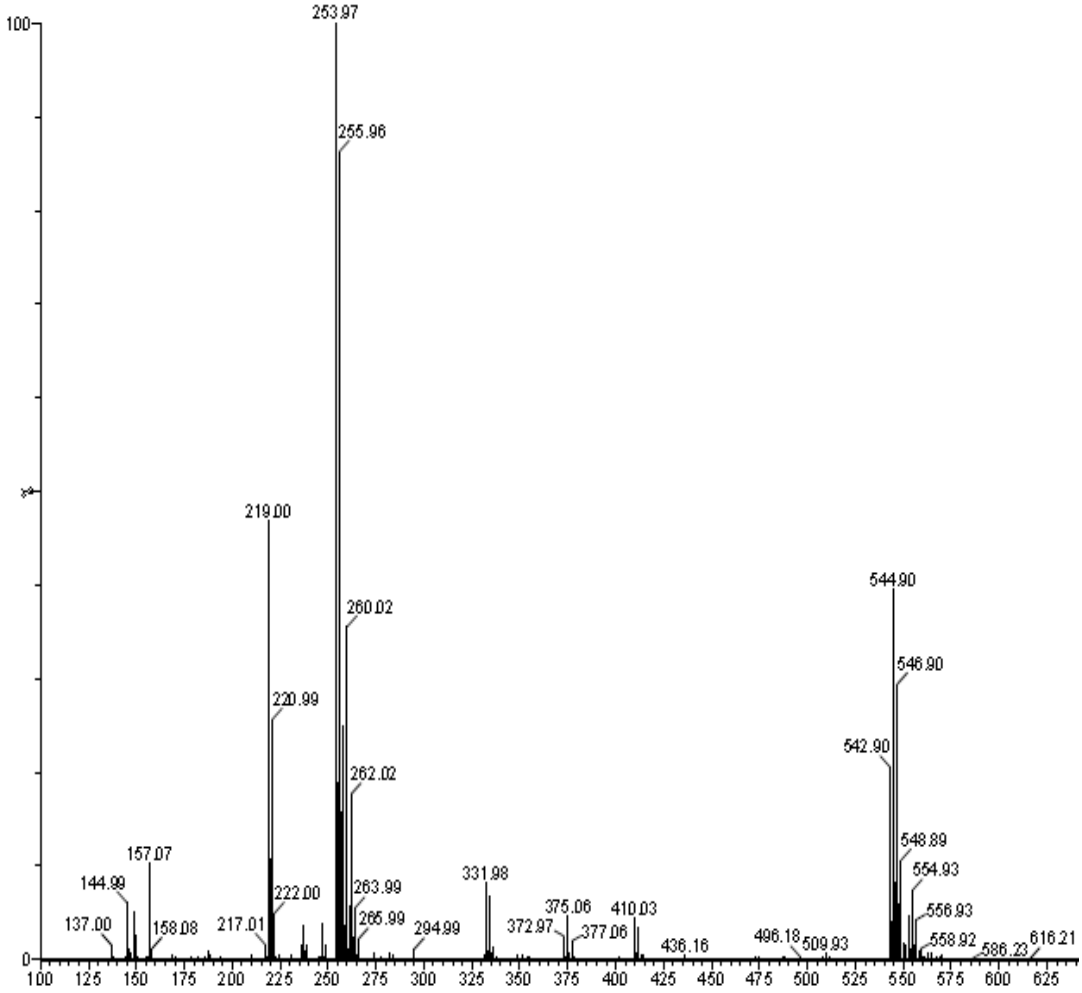

Fig. 80: Mass spectra of $[Cu(L_5)bpy]Cl_2$ (*20)*

m/z	**Loss of**	**Fragment**
623(Not Recorded)		$[Cu(L_5)bpy]Cl_2.H_2O$
552		$[Cu(L_5)bpy]H_2O$
255	L_5	[Cu(bpy)Cl]
220	Cl	[Cu(bpy)]
156	Cu	Free bpy

3.3.4. ^{1}H NMR spectrum

The ^{1}H NMR of the Schiff base ligands was recorded in $CDCl_3$. TMS was used as internal reference. The ^{1}H NMR spectra of the ligands is as follows:

^{1}H NMR of **(L_3)** (400 MHz, $CDCl_3$): 7.28 (d, 1H, Ar-H), 7.15 (d, 1H, Ar-H), 6.99 (t, 2H, Ar-H), 6.86 - 6.72 (m, 9H, Ar-H), 3.86 (s, 3H, -OCH_3)

^{1}H NMR of **(L_4)** (400 MHz, $CDCl_3$): 7.86 (d, 2H, Ar-H), 7.78 (d, 2H, Ar-H), 7.48 (m, 4H, Ar-H), 7.37 (t, 2H, Ar-H), 7.02 (t, 1H, Ar-H), 6.47 (t, 3H, Ar-H), 3.65 (s, 3H, -OCH_3).

^{1}H NMR of **(L_5)** (400 MHz, $CDCl_3$): 7.99 (d, 2H, Ar-H), 7.78 (d, 2H, Ar-H), 7.47 (m, 6H, Ar-H), 6.88 (d, 2H, Ar-H), 6.65 (d, 2H, Ar-H), 3.68 (s, 3H, -OCH_3).

3.4 UV-vis absorption studies of BSA

The same procedure is followed as in section 2.5 of Chapter 2.

Table 18: Values of binding constant (K_b M^{-1})

Complex	**K_b M^{-1}**
$[Zn(L_3)phen]Cl_2$ ***(9)***	-
$[Zn(L_3)bpy]Cl_2$ ***(10)***	-
$[Cu(L_3)phen]Cl_2$ ***(11)***	1.02×10^5
$[Cu(L_3)bpy]Cl_2$ ***(12)***	4.35×10^5
$[Zn(L_4)phen]Cl_2$ ***(13)***	2.50×10^6
$[Zn(L_4)bpy]Cl_2$ ***(14)***	1.14×10^5
$[Cu(L_4)phen]Cl_2$ ***(15)***	-
$[Cu(L_4)bpy]Cl_2$ ***(16)***	5.60×10^6
$[Zn(L_5)phen]Cl_2$ ***(17)***	2.15×10^5
$[Zn(L_5)bpy]Cl_2$ ***(18)***	1.13×10^6
$[Cu(L_5)phen]Cl_2$ ***(19)***	2.06×10^5
$[Cu(L_5)bpy]Cl_2$ ***(20)***	2.70×10^5

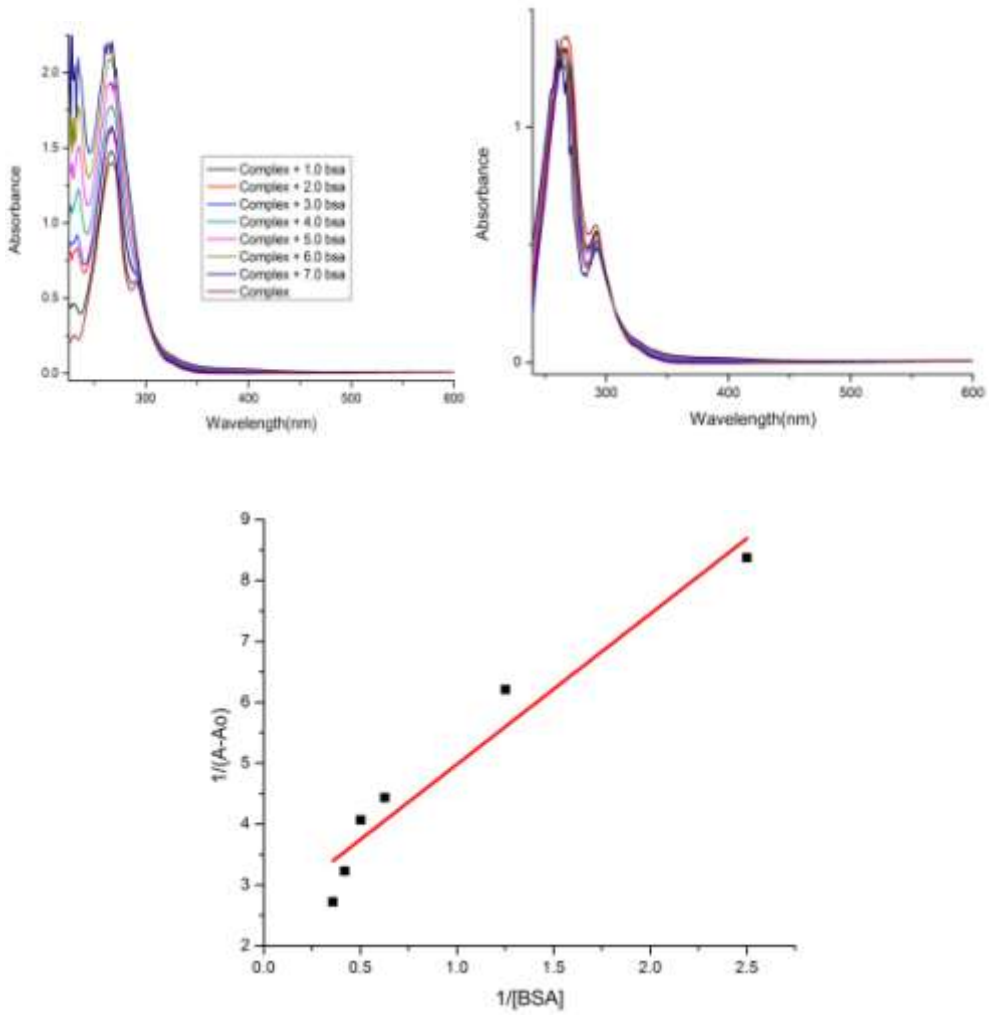

Fig. 81: (A) UV-vis titration graphs of complex $[Cu(L_3)(phen)]Cl_2$ (50 μM) with incremental [BSA] concentration in the range of 0 – 3 μM,

(B) Graph of {[BSA complex with $[Cu(L_3)(phen)]Cl_2$ – [Variant concentrations of [BSA]},

(C) Graph of 1 / ($A-A_0$) vs. 1 / [BSA] concentration

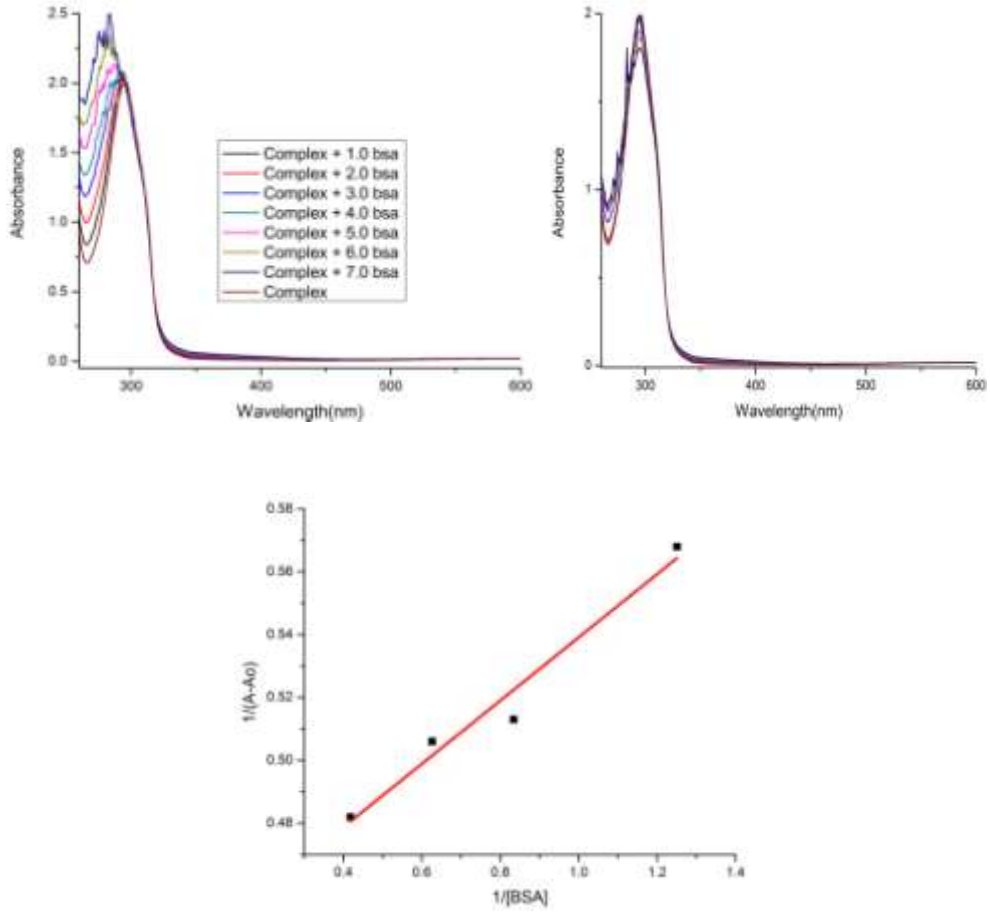

Fig. 82: (A) UV-vis titration graphs of complex $[Cu(L_3)(bpy)]Cl_2$ (50 μM) with incremental [BSA] concentration in the range of 0 – 3 μM,

(B) Graph of {[BSA complex with $[Cu(L_3)(bpy)]Cl_2$ – [Variant concentrations of [BSA]},

(C) Graph of $1 / (A-A_0)$ vs. $1 / [BSA]$ concentration

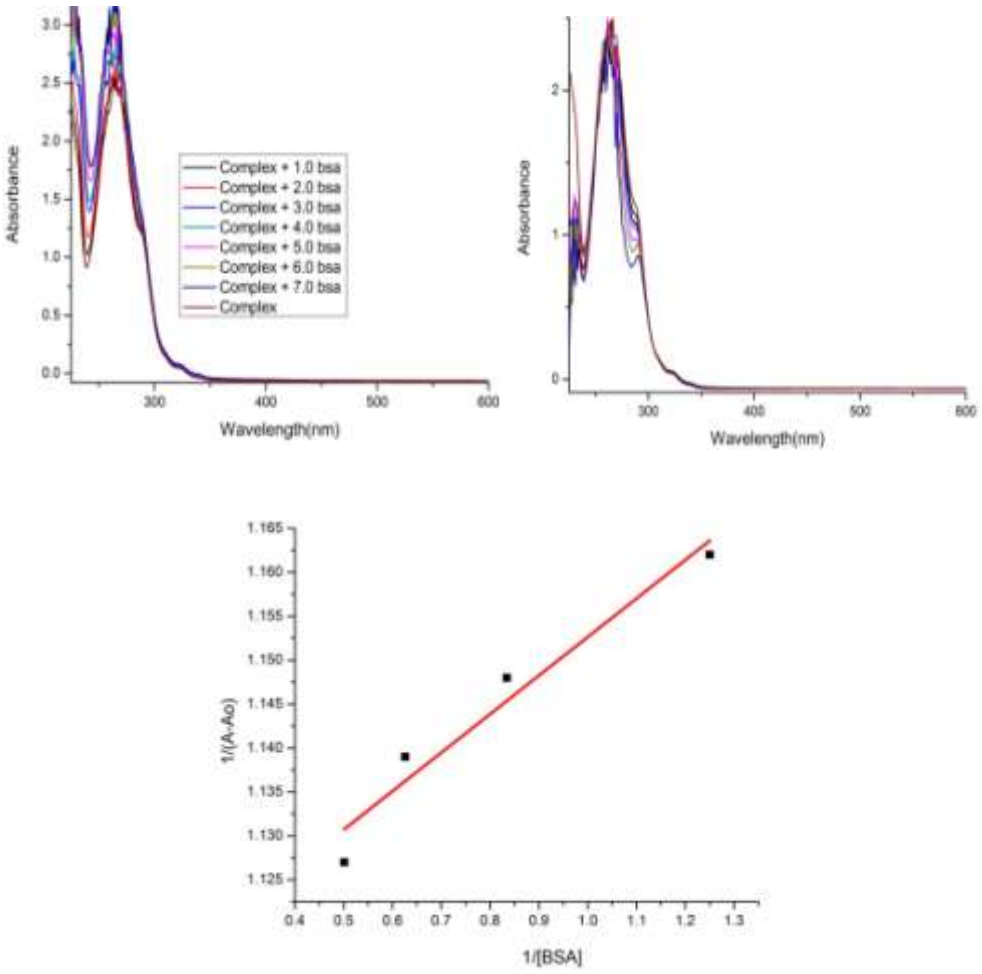

Fig. 83: (A) UV-vis titration graphs of complex $[Zn(L_4)phen]Cl_2$ (50 µM) with incremental [BSA] concentration in the range of 0 – 3 µM,

(B) Graph of {[BSA complex with $[Zn(L_4)phen]Cl_2$ – [Variant concentrations of [BSA]},

(C) Graph of $1 / (A-A_0)$ vs. $1 / [BSA]$ concentration

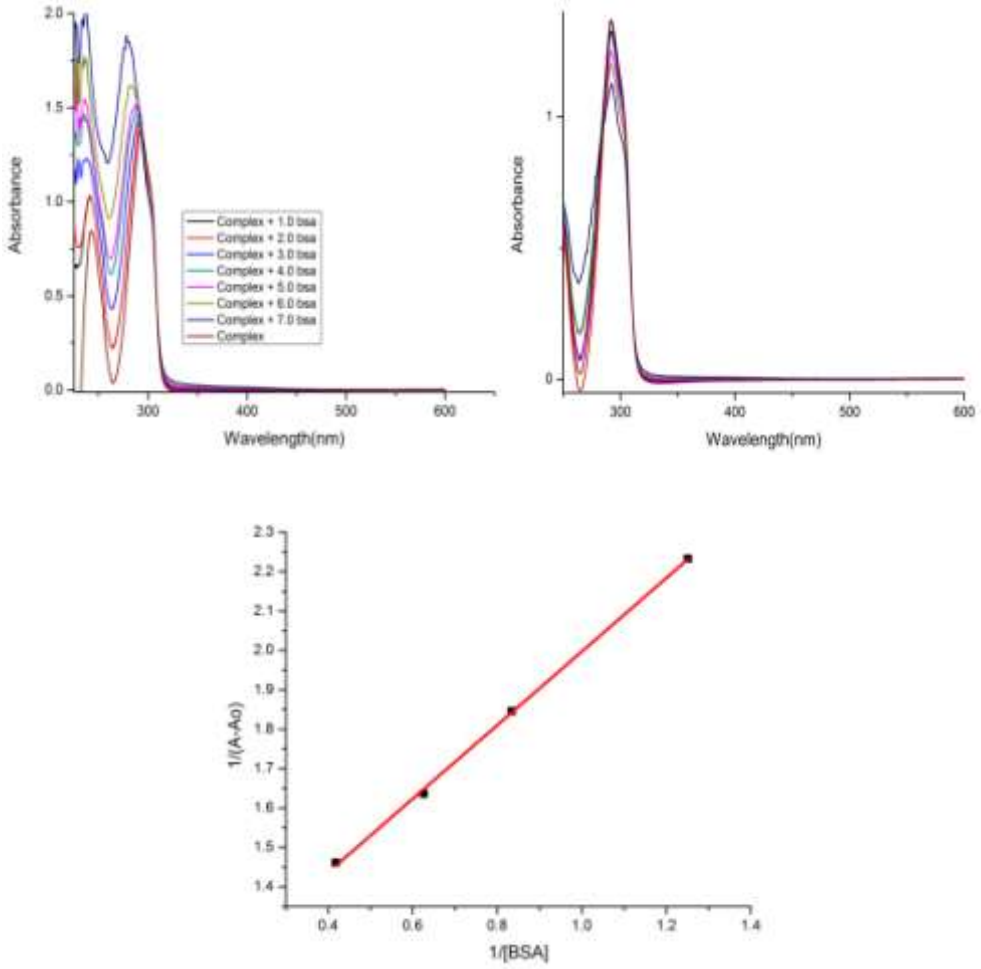

Fig. 84: (A) UV-vis titration graphs of complex $[Zn(L_4)bpy]Cl_2$ (50 μM) with incremental [BSA] concentration in the range of 0 – 3 μM,

(B) Graph of {[BSA complex with $[Zn(L_4)bpy]Cl_2$ – [Variant concentrations of [BSA]},

(C) Graph of $1 / (A-A_0)$ vs. $1 / [BSA]$ concentration

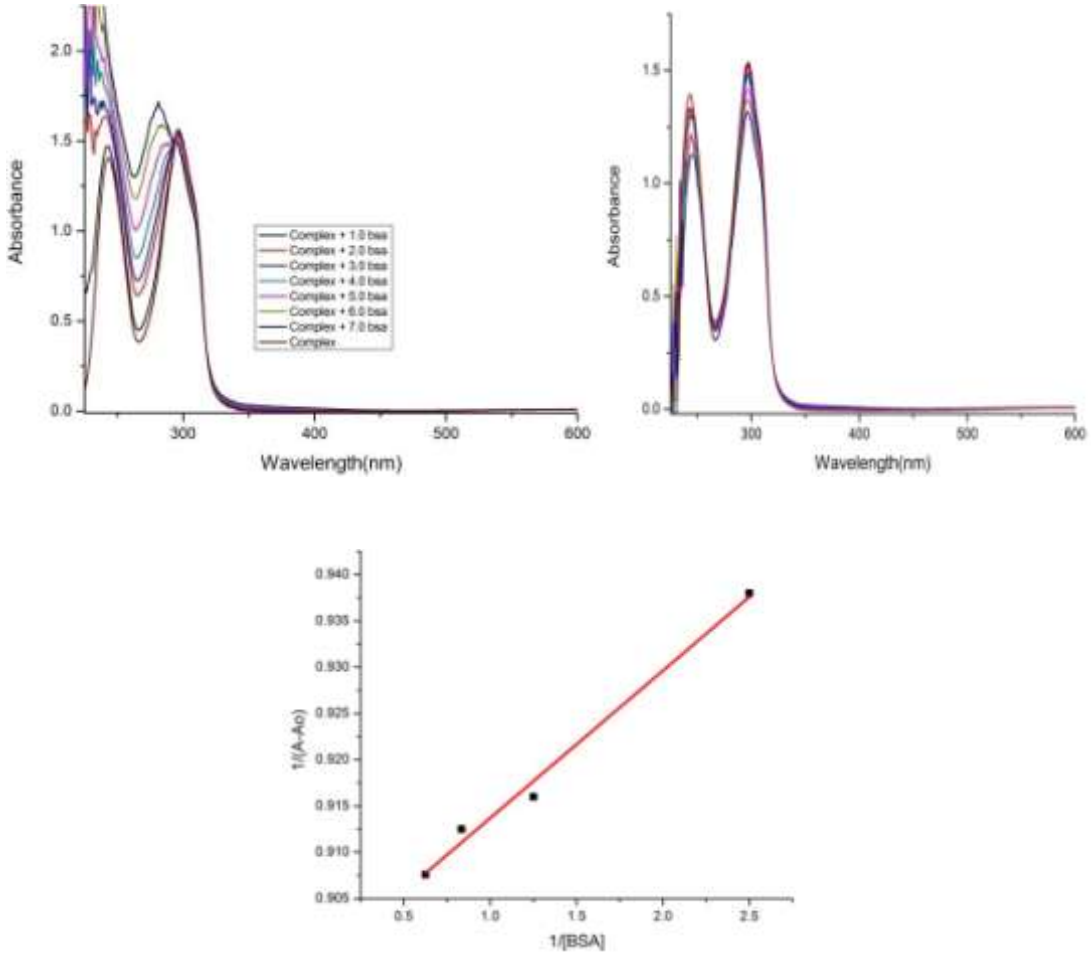

Fig. 85: (A) UV-vis titration graphs of complex $[Cu(L_4)(bpy)]Cl_2$ (50 μM) with incremental [BSA] concentration in the range of 0 – 3 μM,

(B) Graph of {[BSA complex with $[Cu(L_4)(bpy)]Cl_2$ – [Variant concentrations of [BSA]},

(C) Graph of 1 / ($A-A_0$) vs. 1 / [BSA] concentration

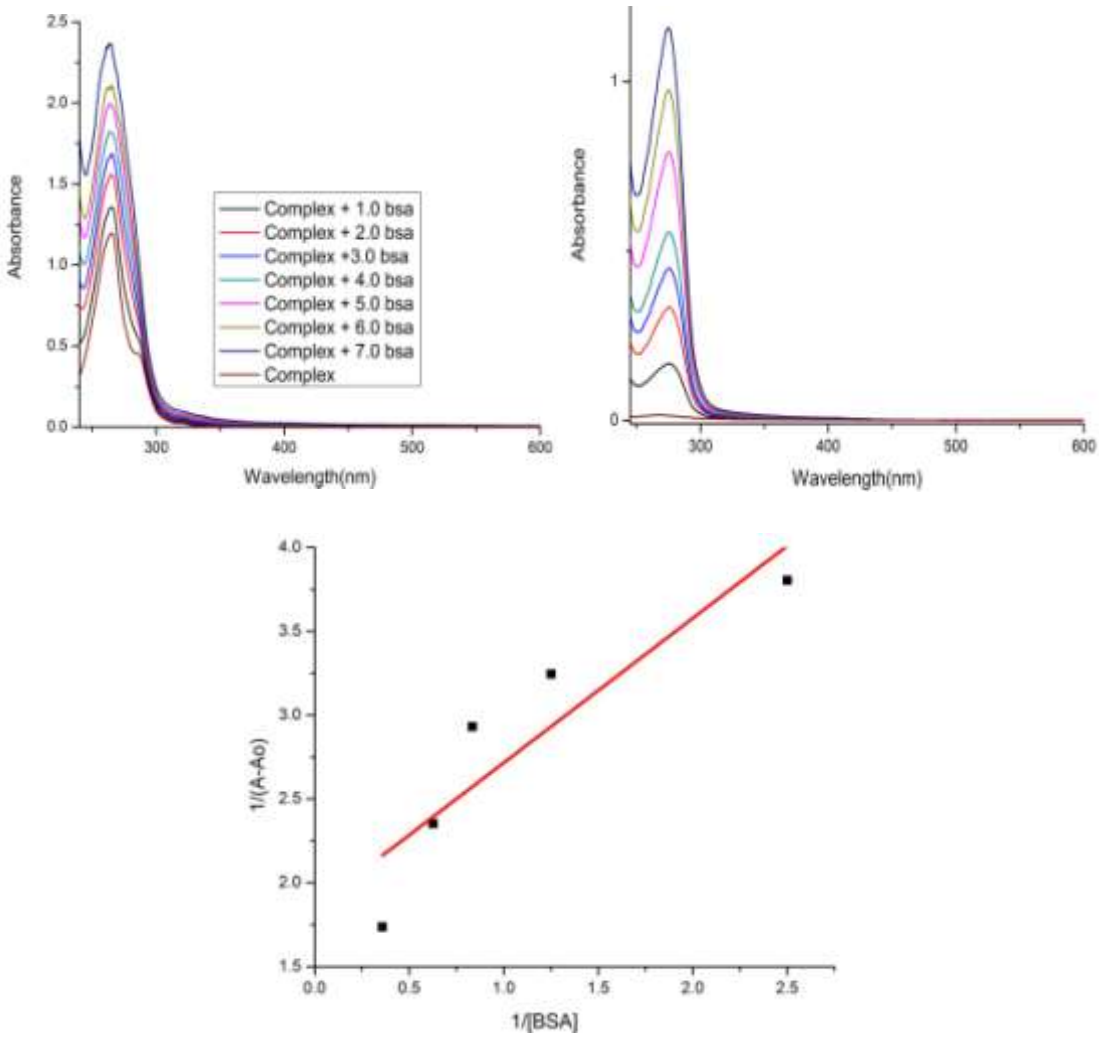

Fig. 86: (A) UV-vis titration graphs of complex $[Zn(L_5)(phen)]Cl_2$ (50 μM)with incremental [BSA] concentration in the range of 0 – 3 μM,

(B) Graph of {[BSA complex with $[Zn(L_5)(phen)]Cl_2$ – [Variant concentrations of [BSA]},

(C) Graph of 1 / ($A-A_0$) vs. 1 / [BSA] concentration

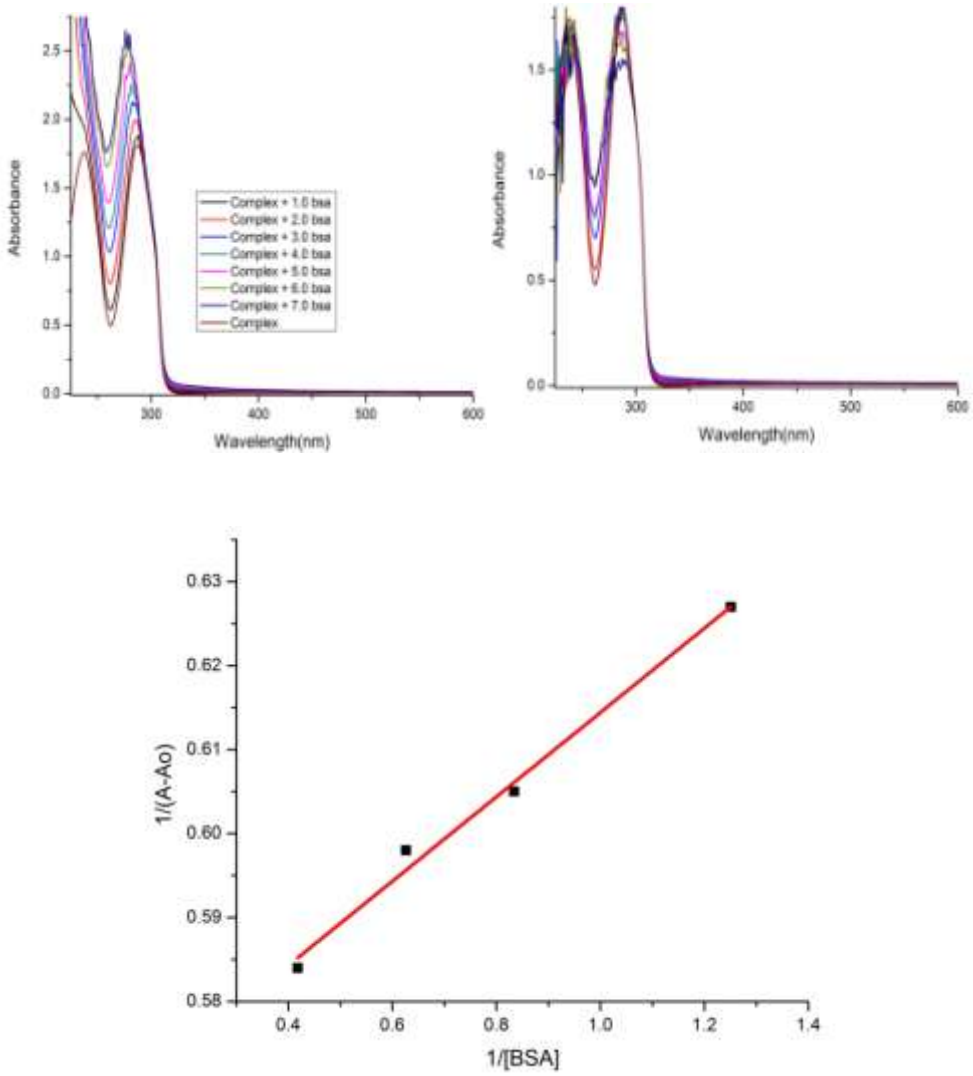

Fig. 87: (A) UV-vis titration graphs of complex $[Zn(L_5)bpy]Cl_2$ (50 µM) with incremental [BSA] concentration in the range of 0 - 3µM,

(B) Graph of {[BSA complex with $[Zn(L_5)bpy]Cl_2$ – [Variant concentrations of [BSA]},

(C) Graph of $1 / (A-A_0)$ vs. $1 / [BSA]$ concentration

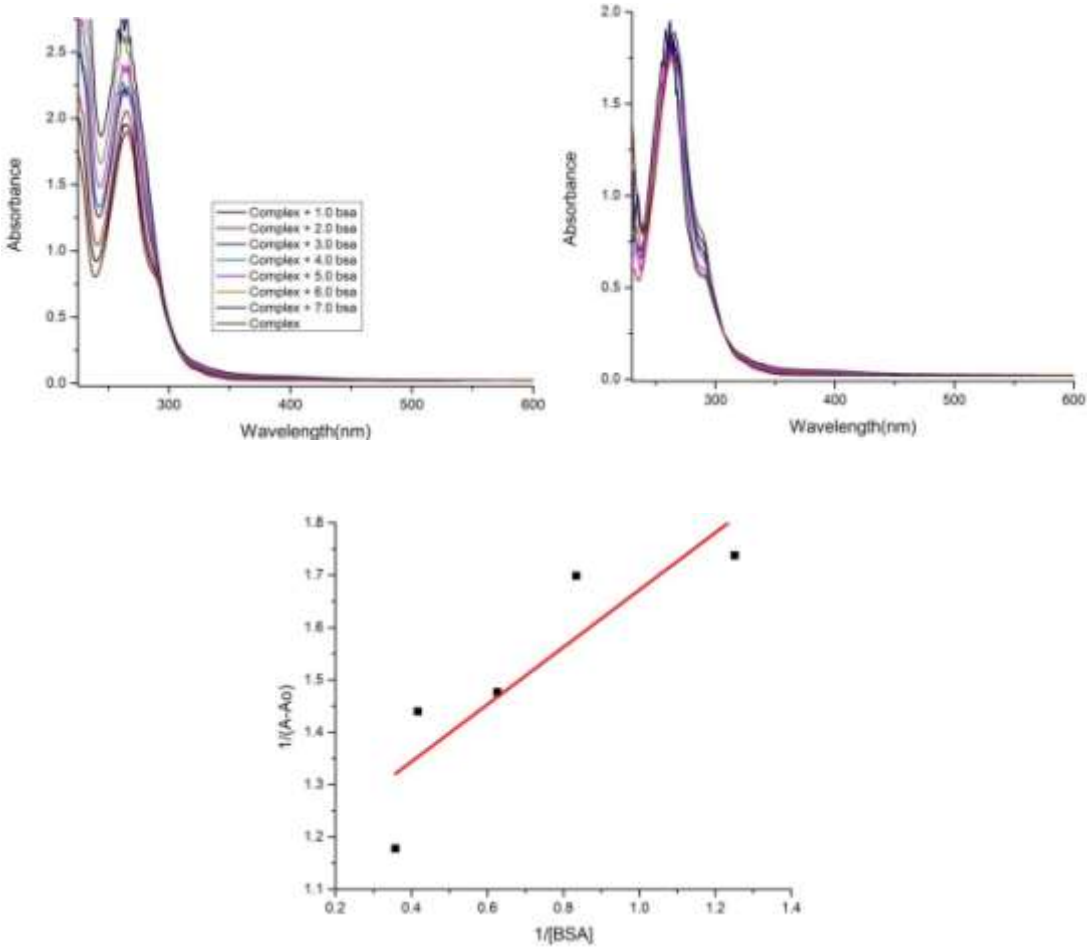

Fig. 88: (A) UV-vis titration graphs of complex $[Cu(L_5)(phen)]Cl_2$ (50 μM) with incremental [BSA] concentration in the range of 0 – 3 μM,

(B) Graph of {[BSA complex with $[Cu(L_5)(phen)]Cl_2$ – [Variant concentrations of [BSA]},

(C) Graph of $1 / (A-A_0)$ vs. $1 / [BSA]$ concentration

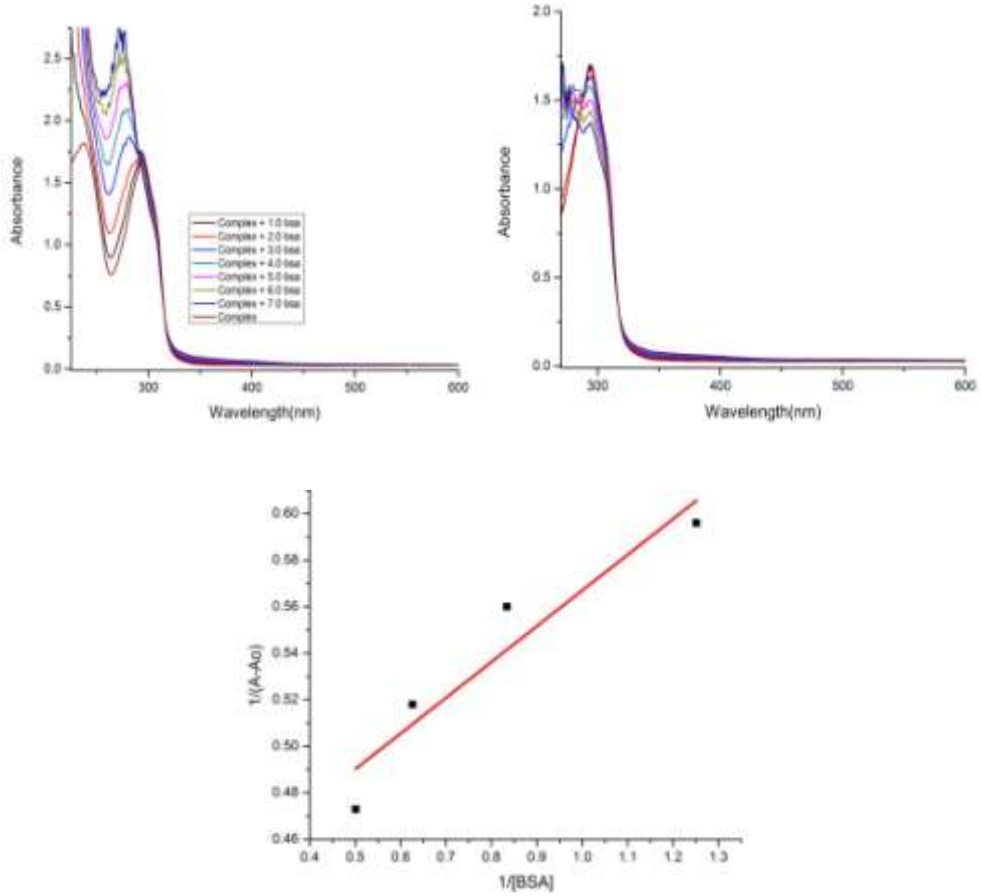

Fig. 89: (A) UV-vis titration graphs of complex $[Cu(L_5)bpy]Cl_2$ (50 µM) with incremental [BSA] concentration in the range of 0 - 3µM,

(B) Graph of {[BSA complex with $[Cu(L_5)bpy]Cl_2$ – [Variant concentrations of [BSA]},

(C) Graph of $1 / (A-A_0)$ vs. $1 / [BSA]$ concentration

3.5 Antimicrobial Assays

The same procedure is followed as in section 2.6 of Chapter 2.

Table 19: Antimicrobial activity of ligand and complexes (Concentration of 5 mg ml^{-1})

Complex	Average Inhibition Zone in diameter (mm) ± SD			
	Antibacterial Activity		Antifungal Activity	
	E. coli **(A)**	***S. aureus*** **(B)**	***A. niger*** **(C)**	***A. fumigatus*** **(D)**
(L_3)	-	-	-	-
$[Zn(L_3)phen]Cl_2$ ***(9)***	20.16±0.29	-	18.16±0.29	43.10±0.23
$[Zn(L_3)bpy]Cl_2$ ***(10)***	-	-	-	18.16±0.29
$[Cu(L_3)phen]Cl_2$ ***(11)***	23.66±0.29	-	32.23±0.25	41.16±0.29
$[Cu(L_3)bpy]Cl_2$ ***(12)***	11.06±0.12	-	19.16±0.29	18.06±0.12
(L_4)	-	-	5.36±0.56	10.05±0.25
$[Zn(L_4)phen]Cl_2$ ***(13)***	20.0±0.10	13.0±0.20	16.90±0.36	38.10±0.26
$[Zn(L_4)bpy]Cl_2$ ***(14)***	-	13.16±0.29	22.96±0.06	32.03±0.25
$[Cu(L_4)phen]Cl_2$ ***(15)***	21.23±0.25	11.83±0.21	36.10±0.36	35.06±0.31
$[Cu(L_4)bpy]Cl_2$ ***(16)***	-	11.23±0.25	20.20±0.20	18.0±.0.50
(L_5)	-	-	-	-
$[Zn(L_5)phen]Cl_2$ ***(17)***	-	18.26±0.25	38.10±0.36	20.23±.25
$[Zn(L_5)bpy]Cl_2$ ***(18)***	-	12.13±0.32	25.90±0.36	17.80±0.26
$[Cu(L_5)phen]Cl_2$ ***(19)***	16.50±0.50	29.33±0.29	37.30±0.61	36.06±0.40
$[Cu(L_5)bpy]Cl_2$ ***(20)***	18.33±0.29	20.16±0.29	27.10±0.36	23.23±0.25
Amikacin	21.50±0.50	24.83±0.76	-	-
Fluconazole	-	-	23.66±0.57	22.66±0.29
DMSO	Nil	Nil	Nil	Nil

Fig. 90: Antimicrobial assay of Schiff base ligand (L_3) and its metal chelate (*9 - 12*) (Alphabet levels are according to table 19.

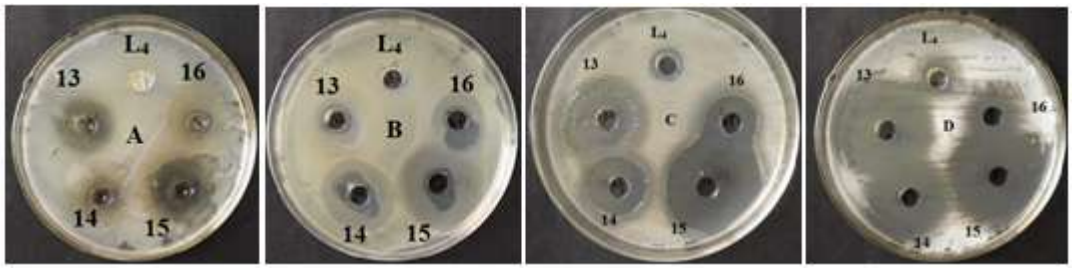

Fig. 91: Antimicrobial assay of Schiff base ligand (L_4) and its metal chelate (*13 - 16*) (Alphabet levels are according to table 19.

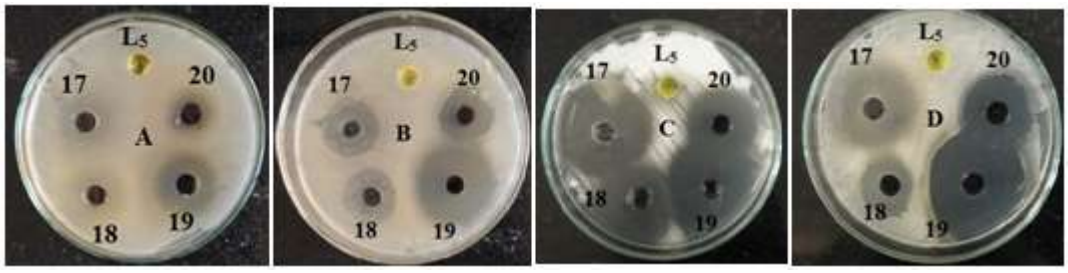

Fig. 92: Antimicrobial assay of Schiff base ligand (L_5) and its metal chelate (*17 - 20*) (Alphabet levels are according to table 19).

3.6 Conclusion

This chapter details about the synthesis of three Schiff bases (**L_3**), (**L_4**) and (**L_5**) and their mixed ligand complexes with zinc(II) and copper(II) metal ions and 1,10-phenanthroline or 2,2' bipyridine as secondary ligand. The reactant for the synthesis of ligands was selected as diketone with different isomers of primary amines. The Schiff base of para isomer precipitates readily while ortho and meta isomer precipitates in a longer time span. In all the reactions, benzil reacted with amine

through one carbonyl group while the second carbonyl group remains unreacted. The reason for the same may be due to steric hindrance caused by bulkier benzyl ring or due to conversion of benzil to benzoin. All the three ligands appear as bidentate coordinating to metal centers through imine nitrogen and carbonyl oxygen. This is supported by presence of peaks in the 400 cm^{-1} region for M-N bond and 600 cm^{-1} region for M-O bond. The decrease and lower shift in band intensity of imine bond and carbonyl bond (up to 60 cm^{-1}) further supports their coordination. Molecular mass of ligand and metal complexes are in consistence with their mass spectral data. Octahedral geometry has been proposed for all the complexes on the basis of evidences shown by their spectral studies where the primary and secondary ligands may occupy equatorial position while weak coordinated anion or water molecule may have occupied the axial position. Serum protein interactions of complexes were then studied by determining the values of binding constants using UV-vis titration technique. The complexes show binding constants in the range of 10^4 - 10^5 M^{-1} which indicates moderate level of binding between the complex and serum proteins. These moderate values of binding constants represent the effectiveness of serum proteins as carrier molecules in delivery of drug at targeted sites. In antimicrobial assays, ligands show least activity while metal complexes show better antifungal activity than antibacterial activity and their antifungal activity against *Aspergillus niger* is the highest. The better activity of metal complexes over ligands may be due to chelation effect.

3.7 Bibliography

[1] Kulandaisamy, A.; Palanimurugan, A. Studies on Schiff base transition metal complexes derived from benzil, *p*-nitroaniline and 2,2-bipyridyl, *J. Chem. Pharm. Res.* **2015**, *7*, 111–119.

[2] Bose, R. N.; Akbar Ali, M. Transition metal complexes of furfural and benzil Schiff bases derived from s-benzyldithiocarbazate, *Polyhedron* **1984**, *3*, 517–522.

[3] Singh, D. P.; Kumar, R.; Malik, V.; Kumar, K. One pot template synthesis and characterization of trivalent transition metal ion complexes derived from diaminopyridine and glyoxal, *Rasayan J. Chem.* **2008**, *1*, 349–354.

[4] Prakash, A.; Adhikari, D. Application of Schiff bases and their metal complexes - A review, **2011**, *3*, 1891–1896.

[5] Sahu, R.; Thakur, D. S.; Kashyap, P. Schiff base: An overview of its medicinal chemistry potential for new drug molecules, *Int. J. Pharm. Sci. Nanotechnol.* **2012**, *5*, 1757–1764.

[6] Jayalakshmi, R.; Rajavel, R. Elaborated studies on Schiff base homo - binuclear Cu(II) and Co(II) complexes, spectral, thermal, P - XRD and biocidal studies, *J. Adv. Appl. Sci. Res.* **2017**, *1*, 1-16.

[7] Ganeshpandian, M.; Loganathan, R.; Ramakrishnan, S.; Riyasdeen, A.; Akbarsha, M. A.; Palaniandavar, M. Interaction of mixed ligand copper(II) complexes with CT DNA and BSA: Effect of primary ligand hydrophobicity on DNA and protein binding and cleavage and anticancer activities, *Polyhedron* **2013**, *52*, 924–938.

[8] Al Zoubi, W. Biological activities of Schiff bases and their complexes: A review of recent works, *Int. J. Org. Chem.* **2013**, *3*, 73–95.

[9] Li, L.; Guo, Q.; Dong, J.; Xu, T.; Li, J. DNA binding, DNA cleavage and BSA interaction of a mixed - ligand copper(II) complex with taurine Schiff base and 1,10-phenanthroline, *J. Photochem. Photobiol. B Biol.* **2013**, *125*, 56–62.

[10] Trnkova, L.; Bousova, I.; Kubi, V.; Drsata, J. Binding of naturally occurring hydroxycinnamic acids to bovine serum albumin, *Nat. Sci.* **2010**, *2*, 563–570.

[11] Jha, N. S.; Kishore, N. Binding of streptomycin with bovine serum albumin: Energetics and conformational aspects, *Thermochim. Acta.* **2009**, *48*, 21–29.

3.8 Annexure

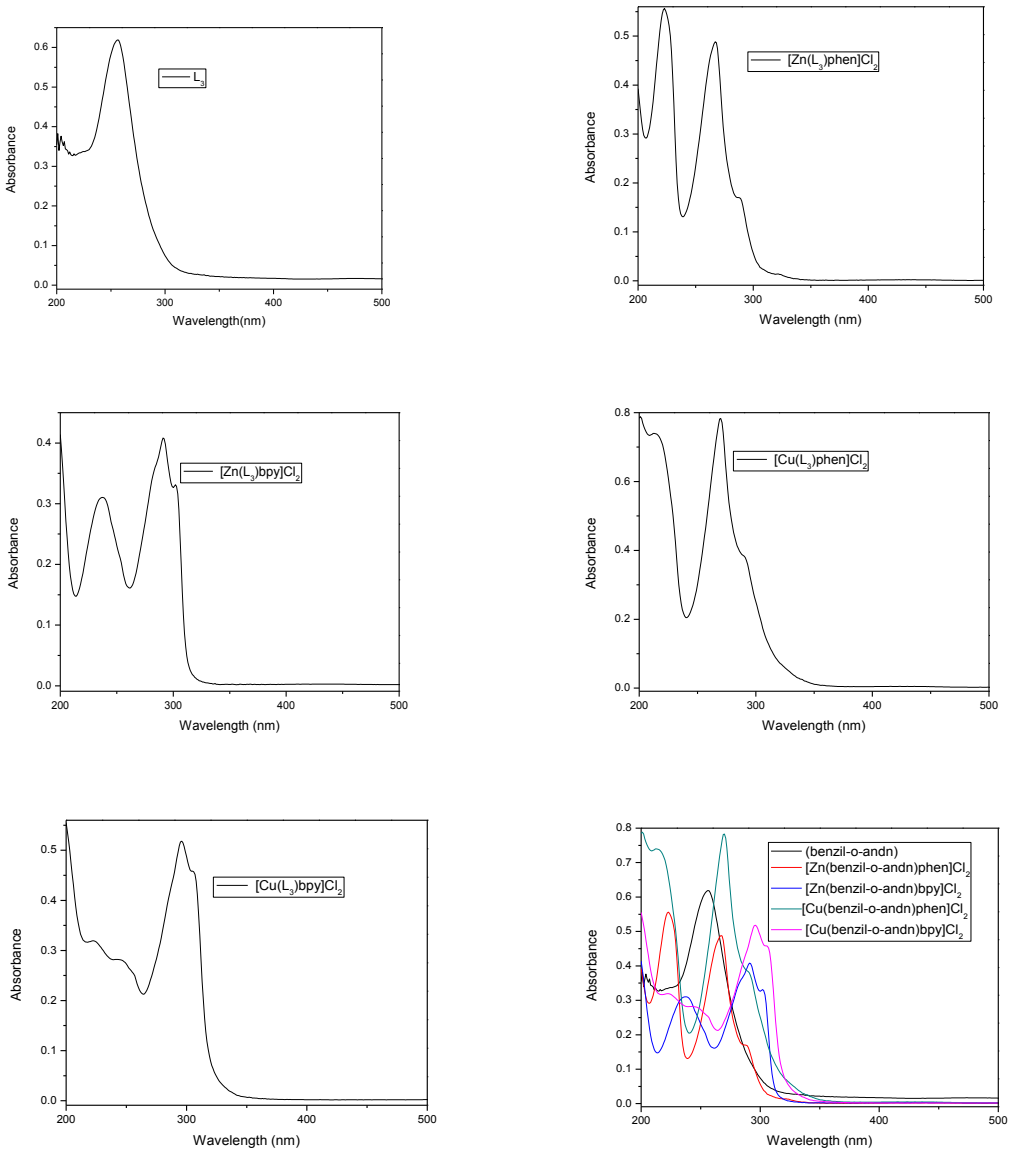

Annexure 3a: UV spectra of (L_3) Schiff base and its metal complexes

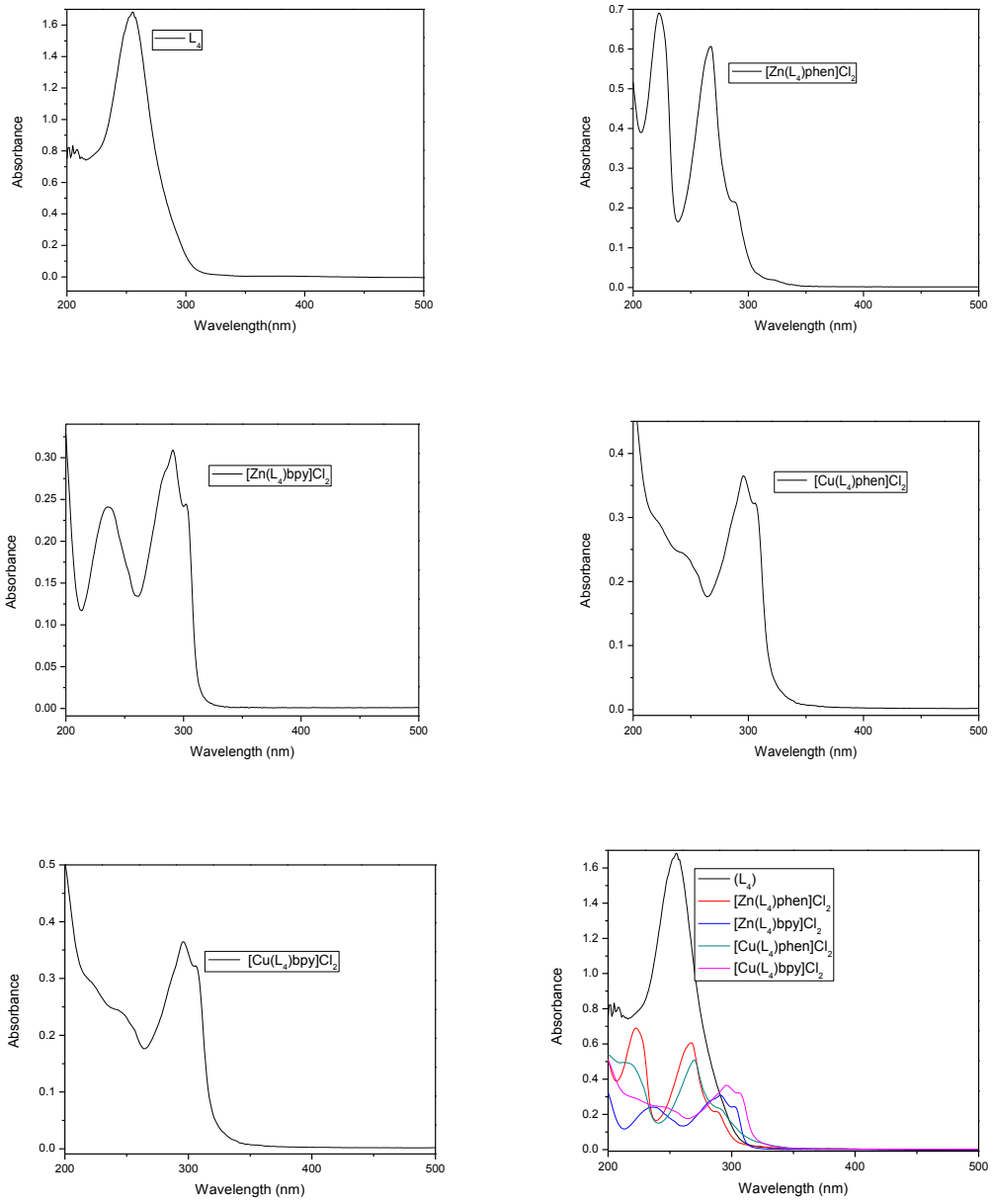

Annexure 3b: UV spectra of (L_4) Schiff base and its metal complexes

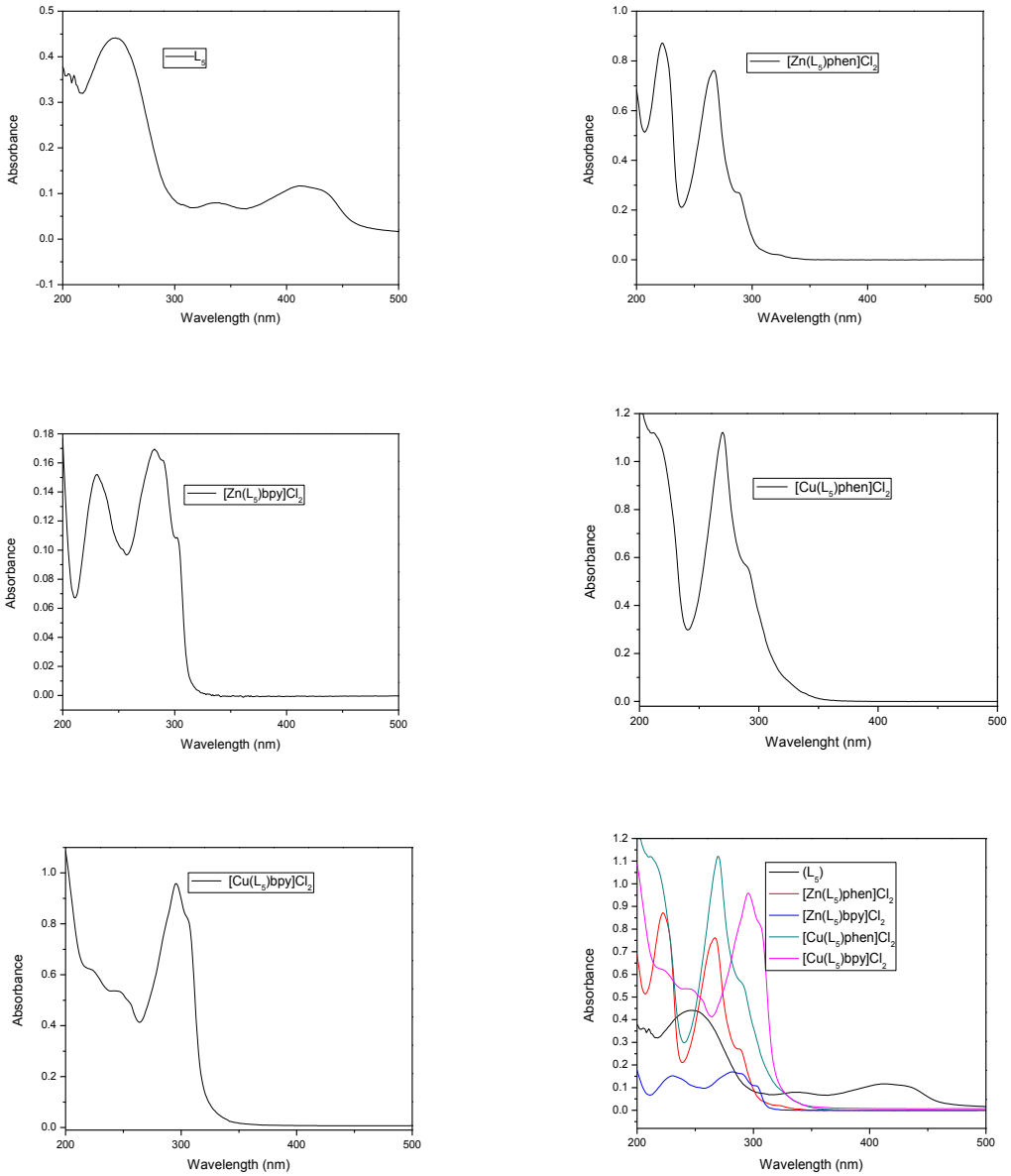

Annexure 3c: UV spectra of (L_5) Schiff base and its metal complexes

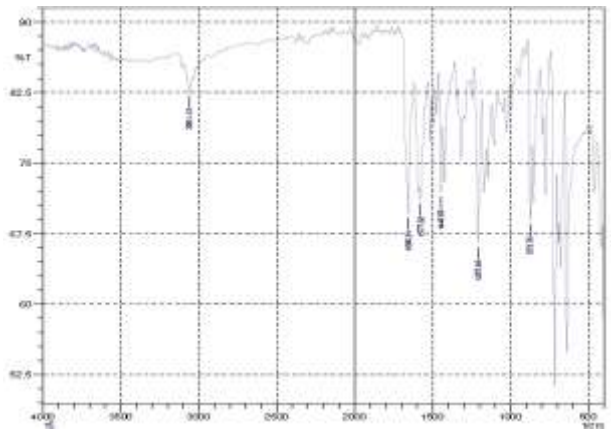

Annexure 3d: IR of (L_3)

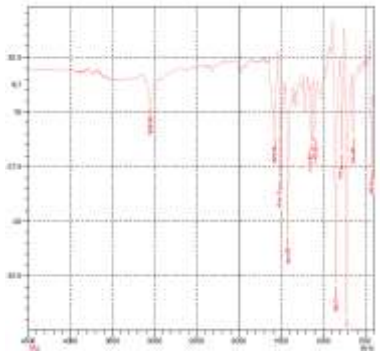

Annexure 3e: IR of [Zn(L_3)phen]Cl_2

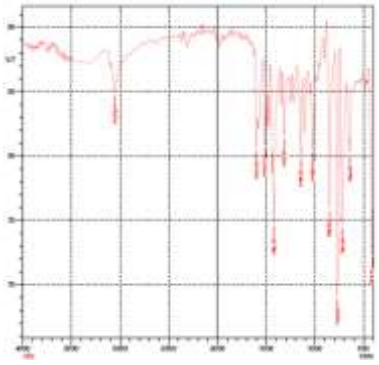

Annexure 3f: IR of [Zn(L_3)bpy]Cl_2

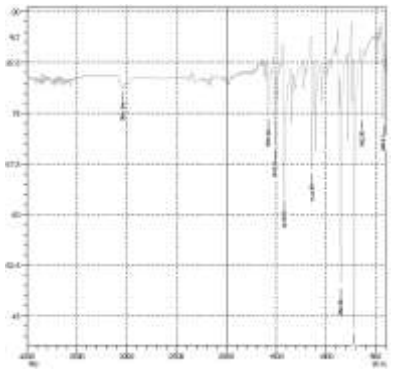

Annexure 3g: IR of [Cu(L_3)phen]Cl_2

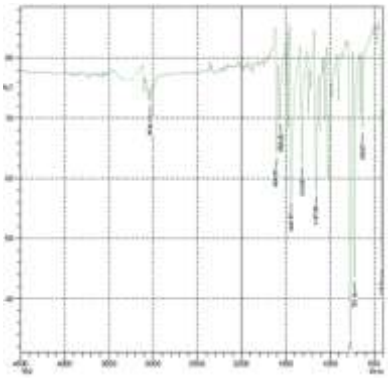

Annexure 3h: IR of [Cu(L_3)bpy]Cl_2

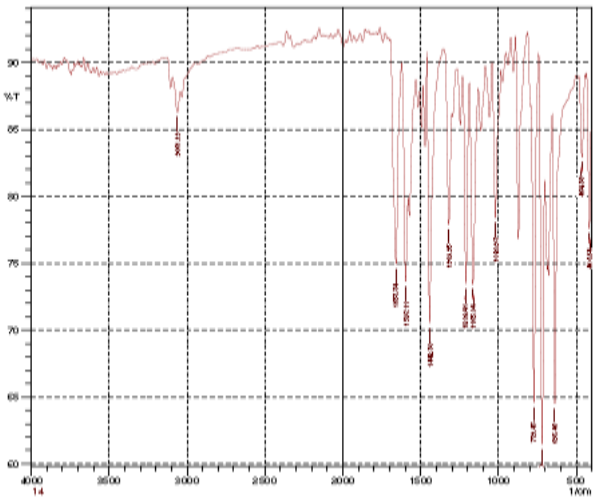

Annexure 3i: IR of L_4

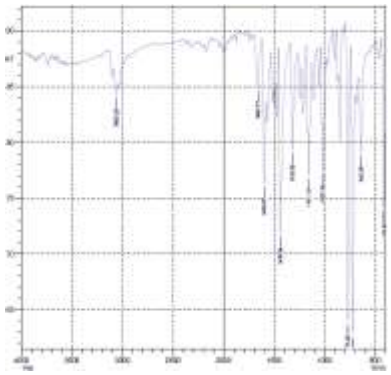

Annexure 3j: IR of $[Zn(L_4)phen]Cl_2$

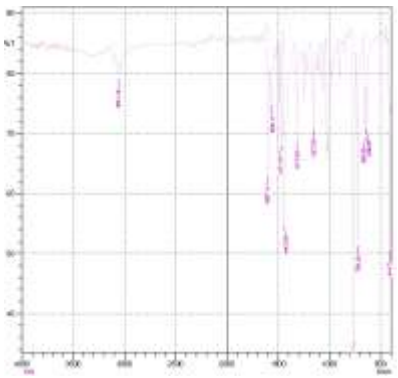

Annexure 3k: IR of $[Zn(L_4)bpy]Cl_2$

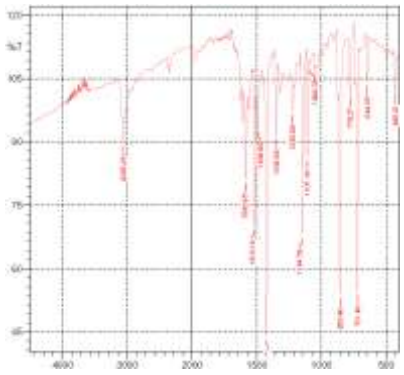

Annexure 3l: IR of $[Cu(L_4)phen]Cl_2$

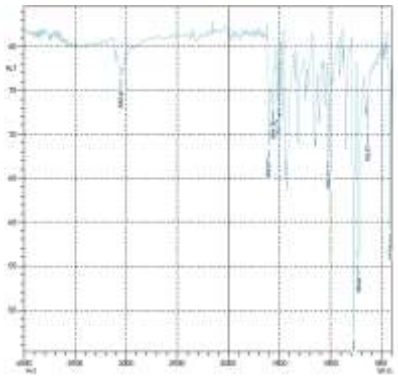

Annexure 3m: IR of $[Cu(L_4)bpy]Cl_2$

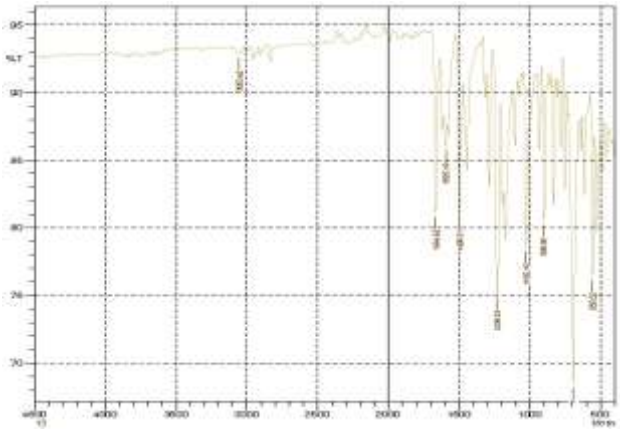

Annexure 3n: IR of (L_5)

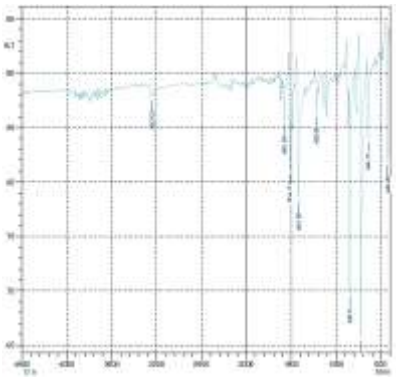

Annexure 3o: IR of [Zn(L_5)phen]Cl_2

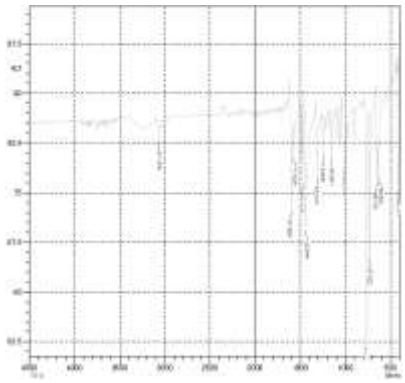

Annexure 3p: IR of [Zn(L_5)bpy]Cl_2

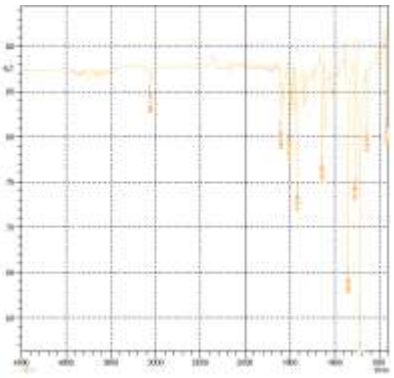

Annexure 3q: IR of [Cu(L_5)phen]Cl

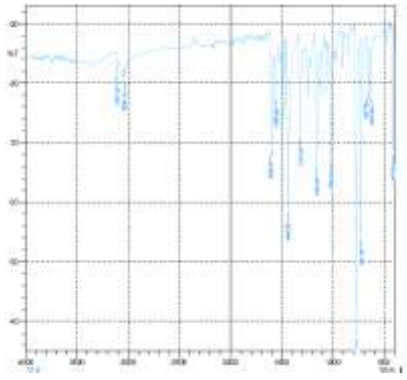

Annexure 3r: IR of [Cu(L_5)bpy]Cl_2

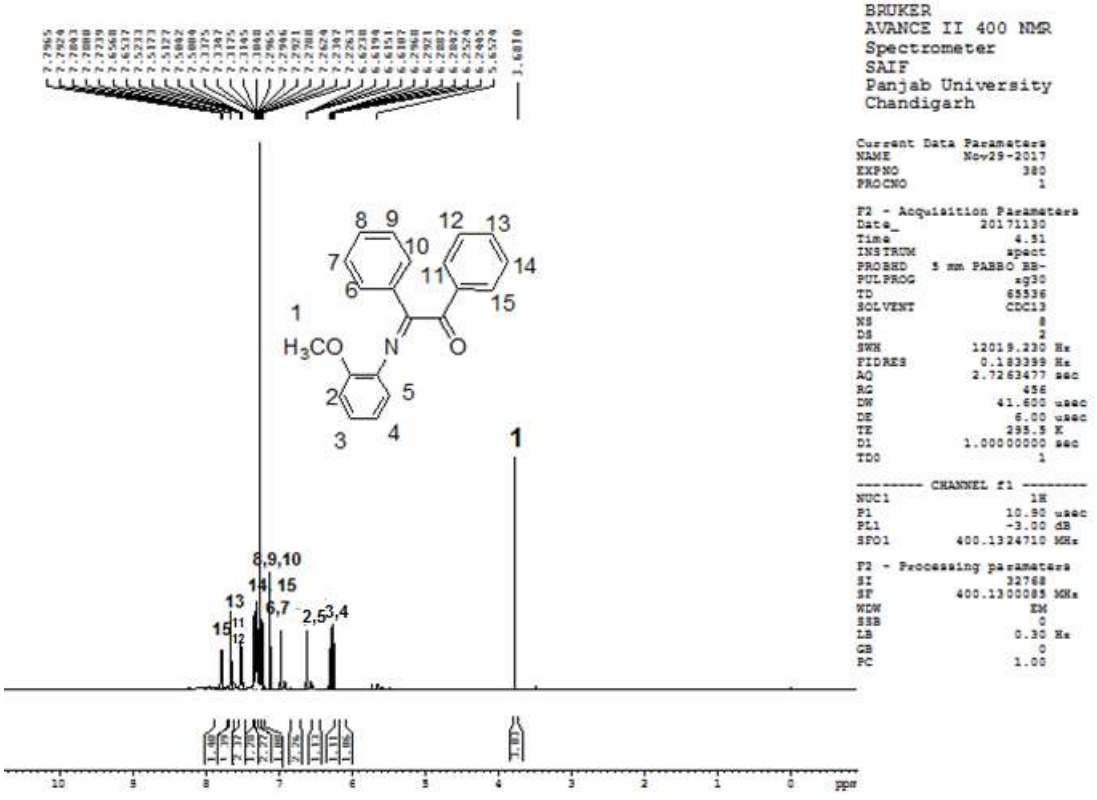

Annexure 3s: NMR spectra of L_3

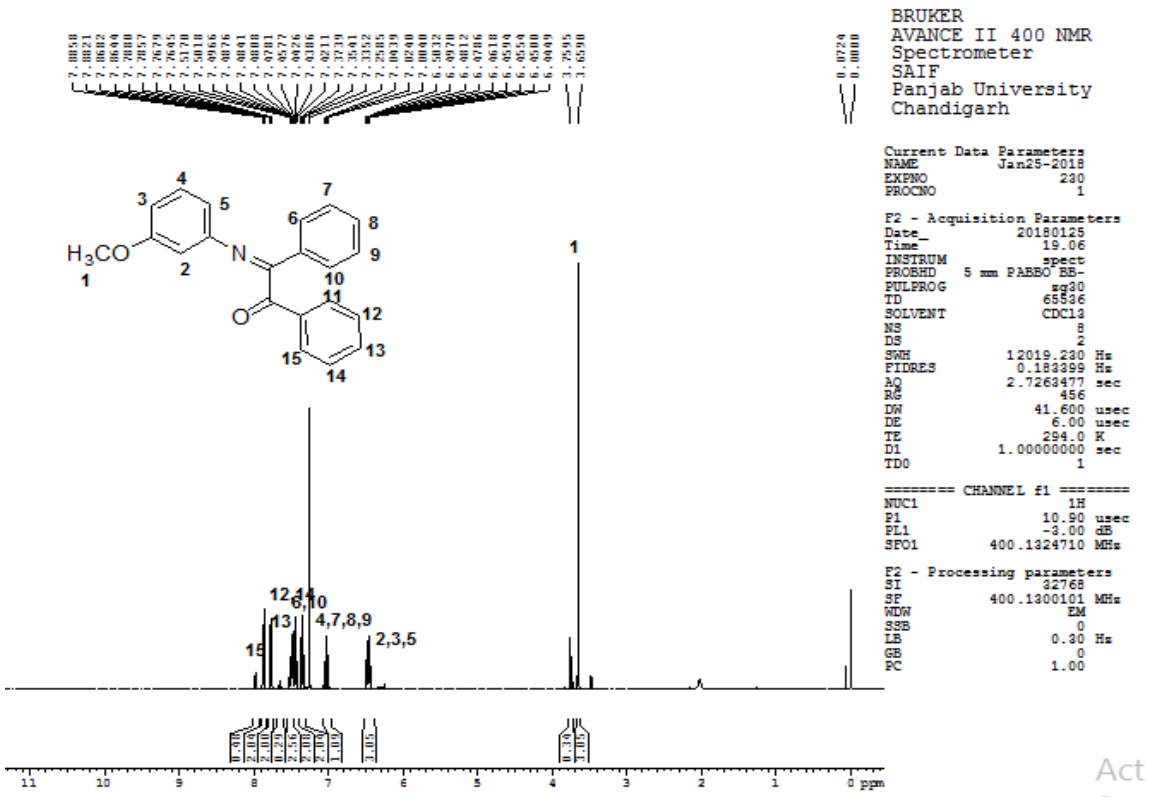

Annexure 3t: NMR spectra of L_4

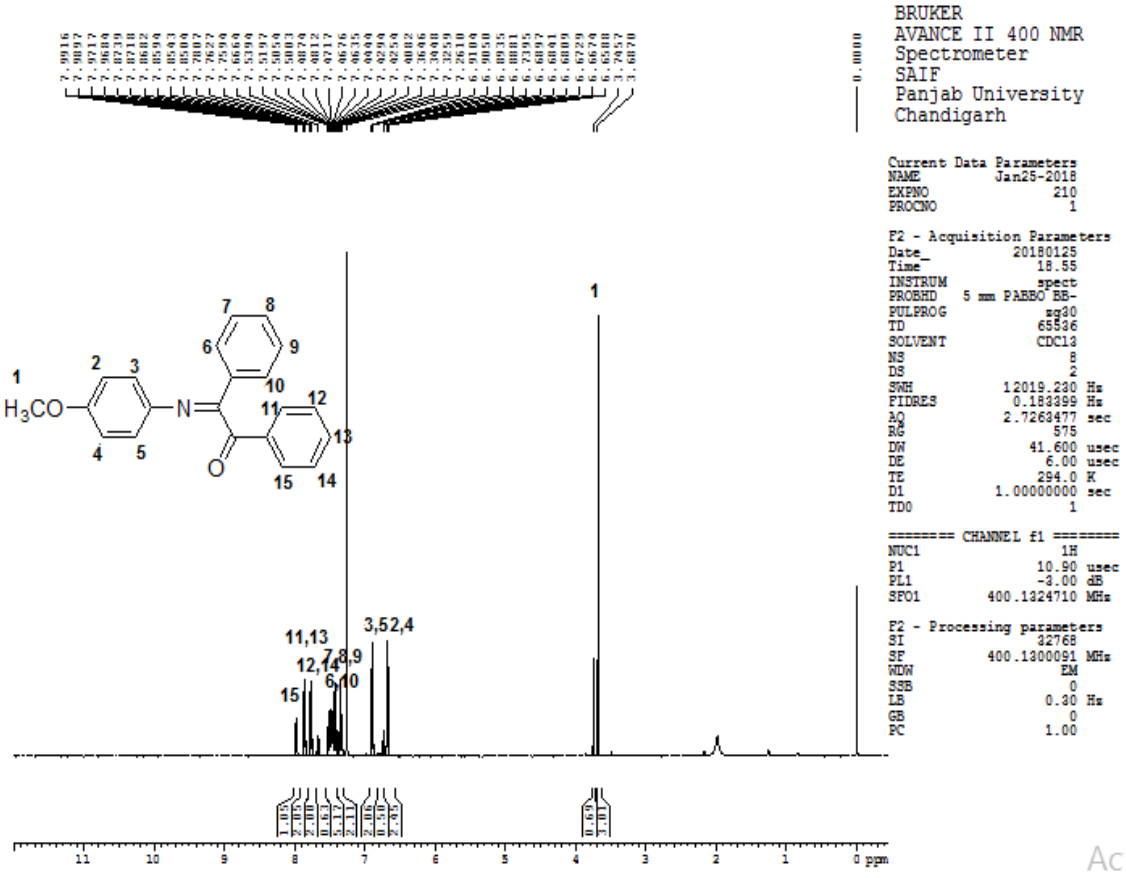

Annexure 3u: NMR spectra of L_5

CHAPTER 4

Synthesis, characterization and biological evaluation studies of Cu(II) and Zn(II) complexes with Schiff base formed by reaction between *o*-aminophenol and glyoxal / diacetyl / benzil and N, N' donor ligands

4.1 Introduction

The aim of the work in this chapter is to synthesize metal complexes of zinc and copper with Schiff base (obtained by the condensation of *o*-aminophenol with glyoxal / diacetyl / benzil) as primary and N, N' donor molecules (1,10-phenanthroline or 2,2'-bipyridine) as secondary ligands. The synthesized complexes were then characterized by various spectroscopic techniques viz. UV-vis, IR, NMR and mass spectral techniques. They were then analyzed for their biological activities against two bacterial species i.e. *Staphylococcus aureus* (gram positive) and *Escherichia coli* (gram negative) and two fungal species i.e. *Aspergillus niger* and *Aspergillus fumigatus* by well diffusion method. The complexes were also analyzed for their interaction with BSA by UV titration method.

4.2 Methodology

4.2.1 Methodology for the synthesis of *o*-aminophenol and glyoxal Schiff base (L_6)

To a stirred and refluxed solution of *o*-aminophenol (4 mmol, 4.37 g) in hot methanol (35 ml) was added drop wise a hot methanolic solution (35 ml) of glyoxal (2 mmol, 2.902 ml). The whole set up was kept in an oil bath for 5 h at 70°C. Precipitates were formed immediately. The solution is further refluxed for 3 h to ensure complete precipitation. The precipitates thus obtained were filtered, washed many times with cold methanol. They were recrystallized using hot methanol as solvent. Yield: 65 %, Color: White, M.P. 165°C, UV (λ_{max}): 231 nm, 290 nm, MS: $[M]^+$ 241, Main IR peaks (cm^{-1}): υ(OH) 3373, υ(C_6H_5 stretch) 3047, υ(C=N) 1606, υ(C-O)1251, ^{1}H NMR (500 MHz, $CDCl_3$) δ = 6.83 (m, 3H, Ar-H), 6.72 (d, 1H, Ar-H), 5.36 (s, 1H, -OH).

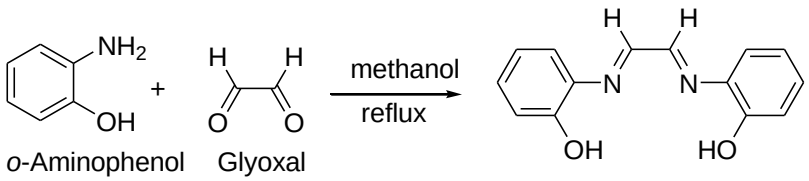

Fig. 93: Scheme for synthesis Schiff base (L_6)

4.2.2 Methodology for the synthesis of $[Zn(L_6)(phen)]Cl_2$ *(21)*

To a hot methanolic solution (30 ml) of Schiff base (1 mmol) **(L_6)** was added methanolic solution (30 ml) of $ZnCl_2$ (1 mmol, 0.136 g) with constant stirring at 70°C. The solution was refluxed for 10 h. A hot methanolic solution of 1,10-phenanthroline (1 mmol or 0.198 g) was added drop wise to above solution with refluxing continuing for further 8 h. Pink precipitates were collected after filtration. Several washings were made with cold methanol. Yield: 80 %, Color: Pink, M.P. Above 280°C, UV (λ_{max}): 221 nm, 265 nm, MS: $[M]^+$ 538, Main IR peaks (cm^{-1}): υ(OH) 3381, υ(C_6H_5 stretch) 3047, υ(C=N) 1583, υ(C-O) 1222, υ(M-O) 648, υ(M-N) 426.

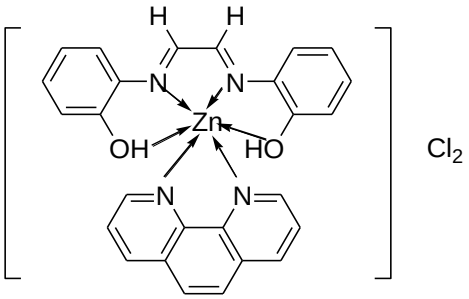

Fig. 94: Proposed geometry of $[Zn(L_6)(phen)]Cl_2$ *(21)*

4.2.3 Methodology for the synthesis of $[Zn(L_6)(bpy)]Cl_2$ *(22)*

To a hot methanolic solution (30 ml) of Schiff base (1 mmol) **(L_6)** was added methanolic solution (30 ml) of $ZnCl_2$ (1 mmol, 0.136 g) with constant stirring at 70°C. The solution was refluxed for 10 h. A hot methanolic solution of 2,2'-bipyridine (1 mmol or 0.156 g) was added drop wise to above solution with refluxing continuing for further 8 h. Pink precipitates were collected after filtration. Several washings were made with cold methanol. Yield: 82 %, Color: Pink, M.P. Above 280°C, UV (λ_{max}):

238 nm, 290 nm, MS: $[M]^+$ 550, Main IR peaks (cm^{-1}): $\upsilon(C_6H_5$ stretch) 3061, υ(C=N) 1597, υ(C-O) 1251, υ(M-O) 636, υ(M-N) 412.

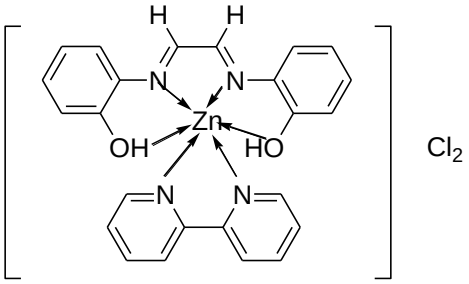

Fig. 95: Proposed geometry of $[Zn(L_6)(bpy)]Cl_2$ *(22)*

4.2.4 Methodology for the synthesis of $[Cu(L_6)(phen)]Cl_2$ *(23)*

To a hot methanolic solution (30 ml) of Schiff base (1 mmol) **(L_6)** was added methanolic solution (30 ml) of $CuCl_2.2H_2O$ (1 mmol, 0.170 g) with constant stirring at 70°C. The solution was refluxed for 10 h. A hot methanolic solution of 1,10-phenanthroline (1mmol or 0.198 g) was added drop wise to above solution with refluxing continuing for further 8 h. Brownish black precipitates were collected after filtration. Several washings were made with cold methanol. Yield: 65 %, Color: Brownish black, M.P. Starts decomposing at 254°C, UV (λ_{max}): 280 nm, MS: $[M]^+$ 572, Main IR peaks (cm^{-1}): $\upsilon(C_6H_5$ stretch) 3057, υ(C=N) 1566, υ(C-O) 1245, υ(M-O) 658, υ(M-N) 417.

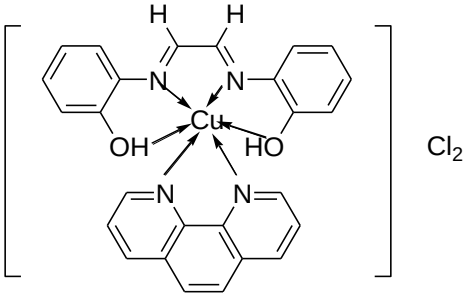

Fig. 96: Proposed geometry of $[Cu(L_6)(phen)]Cl_2$ *(23)*

4.2.5 Methodology for the synthesis of $[Cu(L_6)(bpy)]Cl_2$ *(24)*

To a hot methanolic solution (30 ml) of Schiff base (1mmol) **(L_6)** was added methanolic solution (30 ml) of $CuCl_2.2H_2O$ (1 mmol, 0.170 g) with constant stirring at 70°C. The solution was refluxed for 10 h. A hot methanolic solution of 2,2'-bipyridine (1mmol or 0.156 g) was added drop wise to above solution with refluxing continuing for further 8 h. Brownish black precipitates were collected after filtration. Several washings were made with cold methanol. Yield: 63 %, Color: Brownish black, M.P. Starts decomposing at 258°C, UV (λ_{max}): 301 nm, MS: $[M]^+$ 549, Main IR peaks (cm^{-1}): υ(C_6H_5 stretch) 3053, υ(C=N) 1589, υ(C-O) 1220, υ(M-O) 650, υ(M-N) 426.

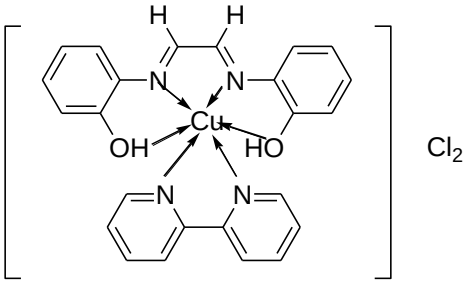

Fig. 97: Proposed geometry of $[Cu(L_6)(bpy)]Cl_2$ *(24)*

4.2.6 Methodology for the synthesis of *o*-aminophenol and diacetyl Schiff base (L_7)

To a stirred and refluxed solution of *o*-aminophenol (4 mmol, 4.37 g) in hot methanol (35 ml) was added drop wise a hot methanolic solution (35 ml) of diacetyl (2 mmol or 1.72 g or 1.75 ml) the whole set up was kept in an oil bath for 5 h at 70°C. Precipitates were formed immediately. The solution is further refluxed for 3 h to ensure complete precipitation. The precipitates thus obtained were filtered, washed many times with cold methanol. They were recrystallized using hot methanol as solvent. Yield: 72 %, Color: White, M.P. 210°C, UV (λ_{max}): 233 nm, 291 nm, MS: $[M]^+$ 269, Main IR peaks (cm^{-1}): υ(OH) 3340, υ(C_6H_5 stretch) 3047, υ(C=N) 1604, υ(C–O) 1222. ^{1}H NMR (500 MHz, $CDCl_3$) δ = 6.83 (s, 1H, Ar-H), 6.77 (s, 2H, Ar-H), 6.69 (d, 1H, Ar-H), 4.71 (s, 1H, -OH).

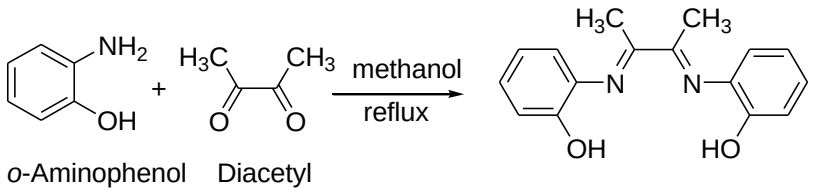

Fig. 98: Scheme for synthesis of diacetyl-*o*-amp Schiff base (L_7)

4.2.7 Methodology for the synthesis of $[Zn(L_7)(phen)]Cl_2$ *(25)*

To a hot methanolic solution (30 ml) of Schiff base (1 mmol) **(L_7)** was added methanolic solution (30 ml) of $ZnCl_2$ (1 mmol, 0.136 g) with constant stirring at 70°C. The solution was refluxed for 10 h. A hot methanolic solution of 1,10-phenanthroline (1 mmol or 0.198 g) was added drop wise to above solution with refluxing continuing for further 8 h. White precipitates were collected after filtration. Several washings were made with cold methanol. Yield: 80 %, Color: White, M.P. Above 280°C, UV (λ_{max}): 221 nm, 266 nm, MS: $[M]^+$ 602, Main IR peaks (cm^{-1}): υ(OH) 3342, υ(C_6H_5 stretch) 3047, υ(C=N) 1581, υ(C-O) 1220, υ(M-O) 643, υ(M-N) 426.

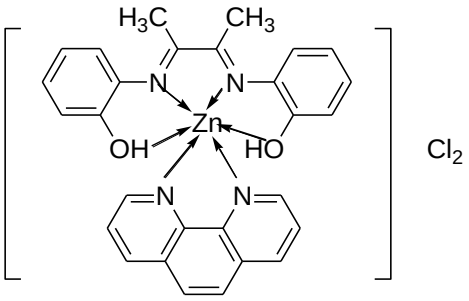

Fig. 99: Proposed geometry of $[Zn(L_7)(phen)]Cl_2$ *(25)*

4.2.8 Methodology for the synthesis of $[Zn(L_7)(bpy)]Cl_2$ *(26)*

To a hot methanolic solution (30 ml) of Schiff base (1 mmol) **(L_7)** was added methanolic solution (30 ml) of $ZnCl_2$ (1 mmol, 0.136 g) with constant stirring at 70°C. The solution was refluxed for 10 h. A hot methanolic solution of 2,2'-bipyridine (1 mmol or 0.156 g) was added drop wise to above solution with refluxing continuing for further 8 h. White precipitates were collected after filtration. Several washings were made with cold methanol. Yield: 81 %, Color: White, M.P. Above 280°C,

UV (λ_{max}): 237 nm, 291 nm, MS: $[M]^+$ 543, Main IR peaks (cm^{-1}): υ(OH) 3200–3400, υ(C_6H_5 stretch) 3061, υ(C=N) 1595, υ(C-O) 1220, υ(M-O) 655, υ(M-N) 414.

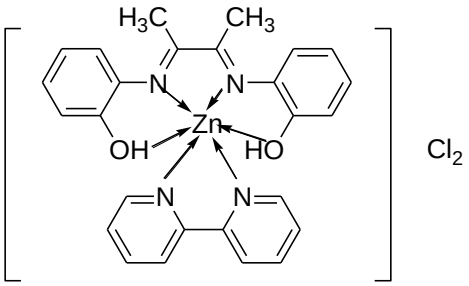

Fig. 100: Proposed geometry of $[Zn(L_7)(bpy)]Cl_2$ *(26)*

4.2.9 Methodology for the synthesis of $[Cu(L_7)(phen)]Cl_2$ *(27)*

To a hot methanolic solution (30 ml) of Schiff base (1 mmol) **(L_7)** was added methanolic solution (30 ml) of $CuCl_2.2H_2O$ (1 mmol, 0.170 g) with constant stirring at 70°C. The solution was refluxed for 10 h. A hot methanolic solution of 1,10-phenanthroline (1 mmol or 0.198 g) was added drop wise to above solution with refluxing continuing for further 8 h. Brown precipitates were collected after filtration. Several washings were made with cold methanol. Yield: 64 %, Color: Brown, M.P. Above 280°C, UV (λ_{max}): 264 nm, 437 nm, MS: $[M]^+$ 672, Main IR peaks (cm^{-1}): υ(OH) 3200-3400, υ(C_6H_5 stretch) 3045, υ(C=N) 1583, υ(M-O) 645, υ(M-N) 426.

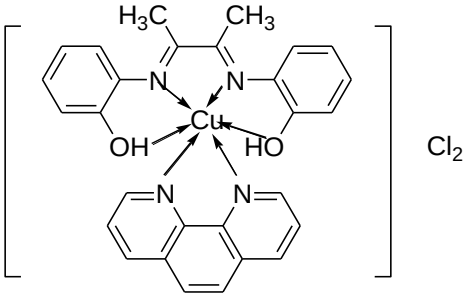

Fig. 101: Proposed geometry of $[Cu(L_7)(phen)]Cl_2$ *(27)*

4.2.10 Methodology for the synthesis of $[Cu(L_7)(bpy)]Cl_2$ *(28)*

To a hot methanolic solution (30 ml) of Schiff base (1 mmol) **(L_7)** was added methanolic solution (30 ml) of $CuCl_2.2H_2O$ (1 mmol, 0.170 g) with constant stirring at 70°C. The solution was refluxed for 10 h. A hot methanolic solution of 2,2'-bipyridyine (1 mmol or 0.156 g) was added drop wise to above solution with refluxing continuing for further 8 h. Brown precipitates were collected after filtration. Several washings were made with cold methanol. Yield: 66 %, Color: Brown, M.P. Above 280°C, UV (λ_{max}): 288 nm, 440 nm, MS: $[M]^+$ 566, Main IR peaks (cm^{-1}): υ (C_6H_5 stretch) 3036, υ(C=N) 1600, υ(M-O) 634, υ(M-N) 416.

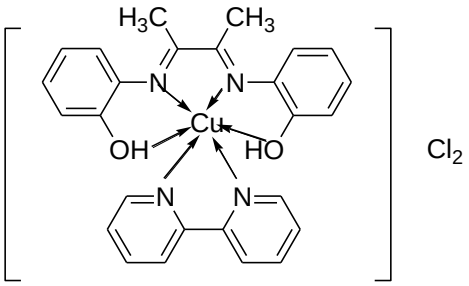

Fig. 102: Proposed geometry of $[Cu(L_7)(bpy)]Cl_2$ *(28)*

4.2.11 Methodology for the synthesis of *o*-aminophenol and benzil Schiff base (L_8)

To a stirred and refluxed solution of *o*-aminophenol (4 mmol, 4.37 g) in hot methanol (35 ml) was added drop wise a hot methanolic solution (35 ml) of benzil (2 mmol or 4.20 g). The whole set up was kept in an oil bath for 5 h at 70°C. The clear solution thus obtained is poured over ice cold water. Immediately light brown precipitates were obtained. The precipitates thus obtained were filtered, washed several times with water and recrystallized from hot chloroform. Yield: 87 %, Color: Brown, M.P. 90°C, UV (λ_{max}): 228 nm, 283 nm, MS: $[M]^+$ 302, Main IR peaks (cm^{-1}): υ(OH) 3200-3400, υ(C_6H_5 stretch) 3061, υ(C=O) 1697, υ(C=N) 1612, υ(C-O) 1234. ^{1}H NMR (500 MHz, $CDCl_3$) δ = 7.86 (m, 1H, Ar-H), 7.72 (d, 1H, Ar-H), 7.65 – 7.52 (m, 3H, Ar-H), 7.44 (m, 1H, Ar-H), 7.36 – 7.16 (m, 5H, Ar-H), 7.11 (t, 1H, Ar-H), 6.99 (d, 1H, Ar-H), 6.93 – 6.82 (m, 1H, Ar-H), 6.62 (s, 1H, Ar-H), 4.00 (s, 1H, -OH).

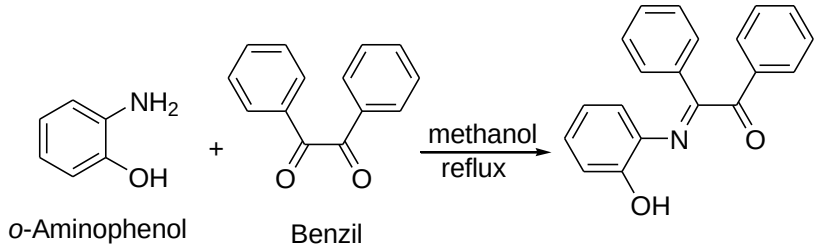

Fig. 103: Scheme for synthesis of Schiff base (L_8)

4.2.12 Methodology for the synthesis of $[Zn(L_8)(phen)]Cl_2$ *(29)*

To a hot methanolic solution (30 ml) of Schiff base (1 mmol) **(L_8)** was added methanolic solution (30 ml) of $ZnCl_2$ (1 mmol, 0.136 g) with constant stirring at 70°C. The solution was refluxed for 10 h. Then a hot methanolic solution of 1,10-phenanthroline (1 mmol or 0.198 g) was added drop wise to above solution with refluxing continuing for further 8 h. Light brown precipitates were collected after filtration. Several washings were made with cold methanol. Yield: 81 %, Color: Light brown, M.P. Above 280°C, UV (λ_{max}): 237 nm, 291 nm, MS: $[M]^+$ 599, Main IR peaks (cm^{-1}): $\upsilon(C_6H_5$ stretch) 3055, υ(C=O) 1622, υ(C=N) 1591, υ(C-O) 1220, υ(M-O) 646, υ(M-N) 428.

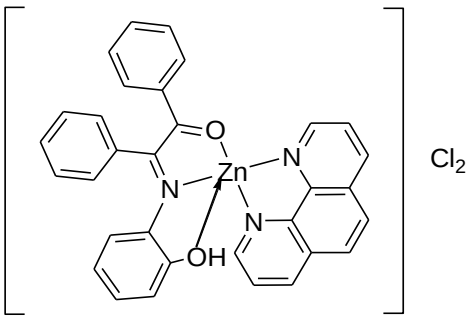

Fig. 104: Proposed geometry of $[Zn(L_8)(phen)]Cl_2$ *(29)*

4.2.13 Methodology for the synthesis of $[Zn(L_8)(bpy)]Cl_2$ *(30)*

To a hot methanolic solution (30 ml) of Schiff base (1mmol) **(L_8)** was added methanolic solution (30 ml) of $ZnCl_2$ (1 mmol, 0.136 g) with constant stirring at 70°C. The solution was refluxed for 10 h. Then a hot methanolic solution of 2,2'-bipyridine (1mmol or 0.156 g) was added drop wise to above solution with refluxing continuing

for further 8 h. Light brown precipitates were collected after filtration. Several washings were made with cold methanol.Yield: 80 %, Color: Light brown, M.P. Above 280°C, UV (λ_{max}): 237 nm, 291 nm, MS: $[M]^+$ 557, Main IR peaks (cm^{-1}): υ(C_6H_5 stretch) 3061, υ(C=O) 1625, υ(C=N) 1597, υ(C-O) 1225, υ(M-O) 646, υ(M-N) 428.

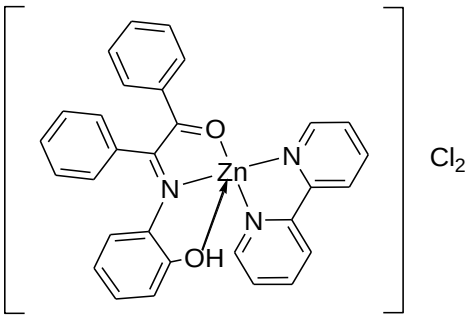

Fig. 105: Proposed geometry of $[Zn(L_8)(bpy)]Cl_2$ *(30)*

4.2.14 Methodology for the synthesis of $[Cu(L_8)(phen)]Cl_2$ *(31)*

To a hot methanolic solution (30 ml) of Schiff base (1 mmol) **(L_8)** was added methanolic solution (30 ml) of $CuCl_2.2H_2O$ (1 mmol, 0.170 g) with constant stirring at 70°C. The solution was refluxed for 10 h. A hot methanolic solution of 1,10-phenanthroline (1 mmol or 0.198 g) was added drop wise to above solution with refluxing continuing for further 8 h. Dark brown precipitates were collected after filtration. Several washings were made with cold methanol. Yield: 68 %, Color: Dark brown, M.P. Starts decomposing at 258°C, UV (λ_{max}): 270 nm, MS: $[M]^+$ 598, Main IR peaks (cm^{-1}): υ(OH) 3200-3400, υ(C_6H_5 stretch) 3039, υ(C=O) 1615, υ(C=N) 1597, υ(C-O) 1220, υ(M-O) 644, υ(M-N) 414.

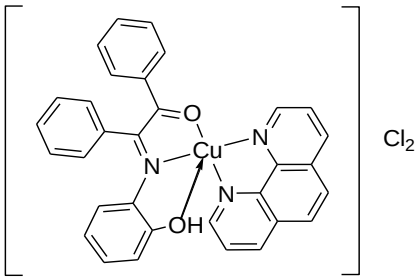

Fig. 106: Proposed geometry of $[Cu(L_8)(phen)]Cl_2$ *(31)*

4.2.15 Methodology for the synthesis of $[Cu(L_8)(bpy)]Cl_2$ *(32)*

To a hot methanolic solution (30 ml) of Schiff base (1 mmol) **(L_8)** was added methanolic solution (30 ml) of $CuCl_2.2H_2O$ (1 mmol, 0.170 g) with constant stirring at 70°C. The solution was refluxed for 10 h. A hot methanolic solution of 2,2'-bipyridine (1 mmol or 0.156 g) was added drop wise to above solution with refluxing continuing further for 8 h. Dark brown precipitates were collected after filtration. Several washings were made with cold methanol. Yield: 65 %, Color: Dark brown, M.P. Starts decomposing at 258°C, UV (λ_{max}): 296 nm, MS: $[M]^+$ 556, Main IR peaks (cm^{-1}): $\upsilon(C_6H_5$ stretch) 3051, υ(C=O) 1625, υ(C=N) 1566, υ(C-O) 1222, υ(M-O) 634, υ(M-N) 410.

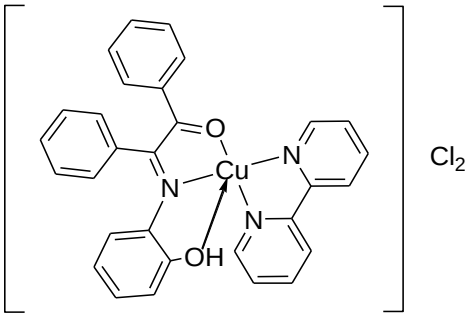

Fig. 107: Proposed geometry of $[Cu(L_8)(bpy)]Cl_2$ *(32)*

4.3 Results and discussions

The Zn^{2+} and Cu^{2+} mixed ligand chelates appear as colored precipitates while ligand **(L_6)** and **(L_7)** appear as white precipitates. All of them were found to be thermally stable and of non hygroscopic nature. They were having fair solubility in water, DMSO, DMF and Tris buffer (pH 7.4).

4.3.1 UV-vis analysis

The UV absorptions occur in the range of 200 - 800 nm at low concentration in water / DMSO. These bands indicates π to π* transitions which confirm binding of 2,2'-bipyridine and 1,10-phenonthroline with metal center of Zn(II) and Cu(II). The UV–vis data of the Schiff base and complexes are as follows (Table 20):

4.3.2 FTIR analysis

In the uncoordinated ligand a strong band appears at 1606 cm^{-1} **(L_6)**, 1604 cm^{-1} **(L_7),** 1612 cm^{-1} **(L_8)** attributing to free azomethine group, but in metal complexes a negative shift up to 1566 cm^{-1} suggests coordination of the imine nitrogen to metal centers. This may occurs due to decrease in bond strength of imine bond and simultaneous increase in bond strength between azomethine nitrogen and metal centre. All the metal complexes show absorption peaks in the region 410 - 428 cm^{-1} corresponding to M-N and 634 - 658 cm^{-1} corresponding to M-O vibrations confirming the bond formation between azomethine nitrogen, phenolic oxygen and metal ion. The ligand formed by condensation of benzil and *o*-aminophenol is half ligand as benzil reacted from one side only. This is further supported by the presence of –C=O- stretch in the region of 1685 cm^{-1} and its shifting to lower values in the metal complexes. Another absorption bands in the range of 3200 - 3400 cm^{-1} in some complexes marks the presence of coordinated or lattice water. IR analyses with selected bond frequencies of all Schiff bases and their corresponding mixed ligand chelates are as follows (Table 20):

Table 20: Selected bond frequencies (cm^{-1}) and UV-vis values of ligands, Zn(II) and Cu(II) mixed ligand chelates

Complex	$\nu_{(M-N)}$ **(cm^{-1})**	$\nu_{(M-O)}$ **(cm^{-1})**	ν**(-C_6H_5) stretch (cm^{-1})**	ν**(-C=N-) stretch (cm^{-1})**	ν**(-C-O) stretch (cm^{-1})**	**OH stretch (cm^{-1})**	π **to** π^* **transition (nm)**
(L_6)	-	-	3047	1606	1251	3373	231, 290
[Zn(L_6)(phen)]Cl_2 ***(21)***	426	648	3047	1583	1222	3381	221, 265
[Zn(L_6)(bpy)]Cl_2 ***(22)***	412	636	3061	1597	1251		238, 290
[Cu(L_6)(phen)]Cl_2 ***(23)***	417	658	3057	1566	1245		280
[Cu(L_6)(bpy)]Cl_2 ***(24)***	426	650	3053	1589	1220		301
(L_7)	-	-	3047	1604	1222	3340	233, 291
[Zn(L_7)(phen)]Cl_2 ***(25)***	426	646	3047	1581	1220	3342	221, 266
[Zn(L_7)(bpy)]Cl_2 ***(26)***	414	655	3061	1595	1220	3200-3400	237, 291
[Cu(L_7)(phen)]Cl_2 ***(27)***	426	645	3045	1583	-	3200-3400	264, 437
[Cu(L_7)(bpy)]Cl_2 ***(28)***	416	634	3036	1600	-	-	288, 440
(L_8)	-	-	3061	1612	1234	3200-3400	228, 283
[Zn(L_8)(phen)]Cl_2 ***(29)***	428	646	3055	1581	1220	-	236, 290
[Zn(L_8)(bpy)]Cl_2 ***(30)***	412	655	3061	1597	1220	-	237, 291
[Cu(L_8)(phen)]Cl_2 ***(31)***	414	644	3039	1581	1220	3200-3400	270
[Cu(L_8)(bpy)]Cl_2 ***(32)***	410	634	3051	1566	1220	-	296

4.3.3 Mass spectral analysis

The molecular ion peaks in mass spectra of ligands was observed at m/z 241 for **L_6**, 269 for **L_7** and 302 for **L_8** which is the parent ion peak of all the three ligands.

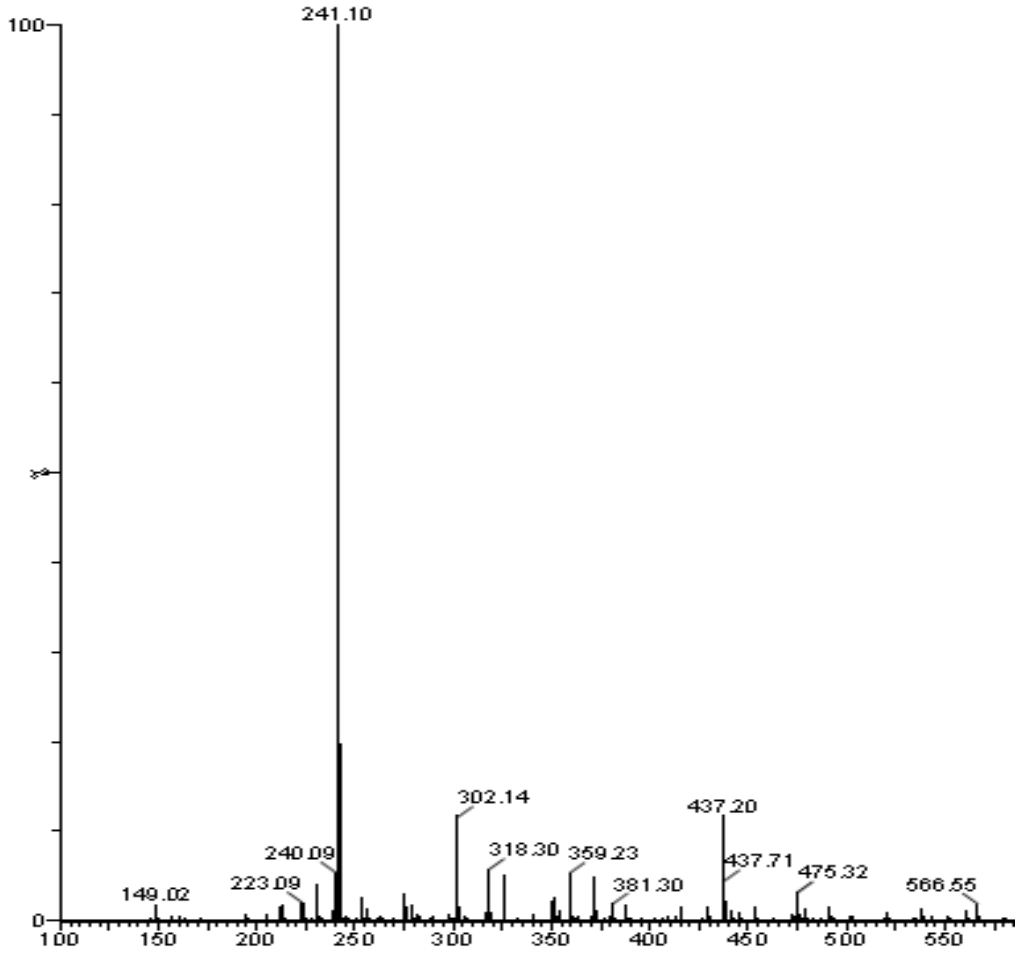

Fig. 108: Mass spectra of (L_6) (Mol. Mass = 240 g)

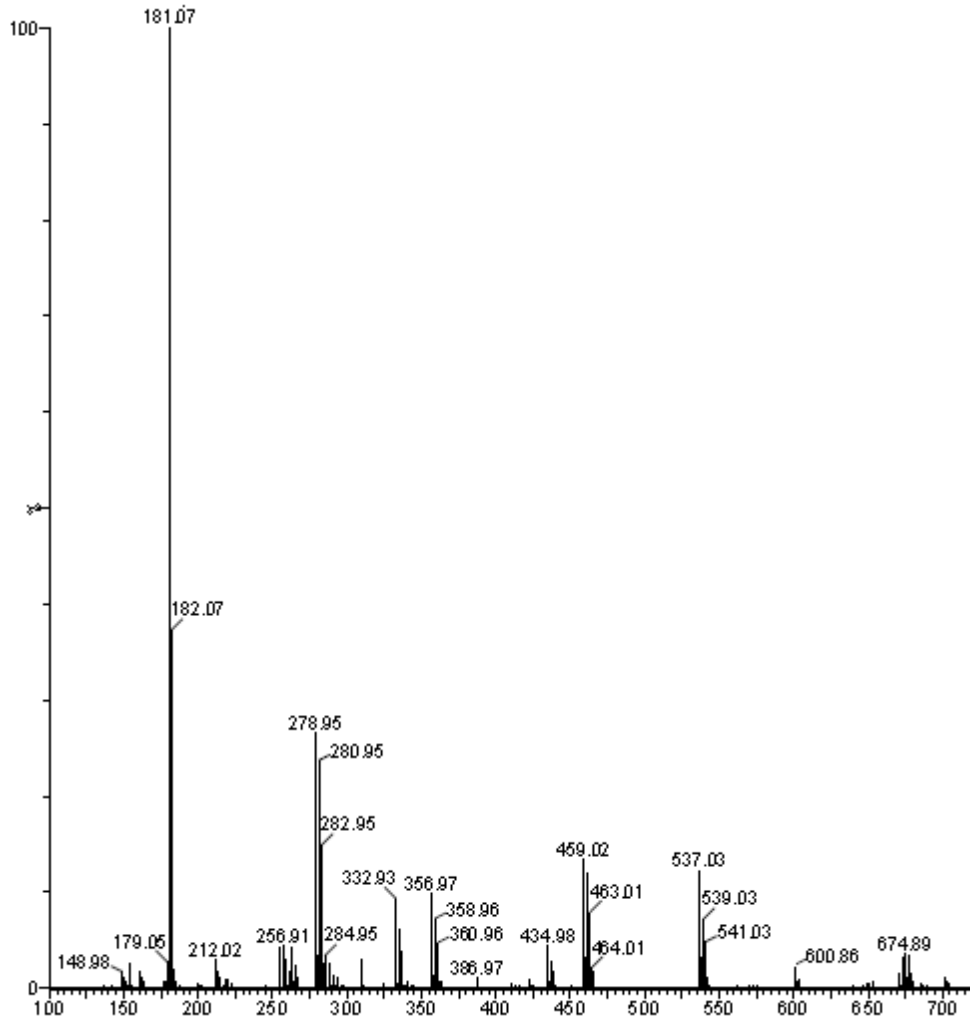

Fig. 109: Mass spectra of $[Zn(L_6)phen]Cl_2$ *(21)*

m/z	**Loss of**	**Fragment**
538		$[Zn(L_6)phen]Cl.H_2O$
460	L_6	$[Zn(phen)_2Cl]$
280	phen	[Zn(phen)Cl]
180	Zn, Cl	Free phen

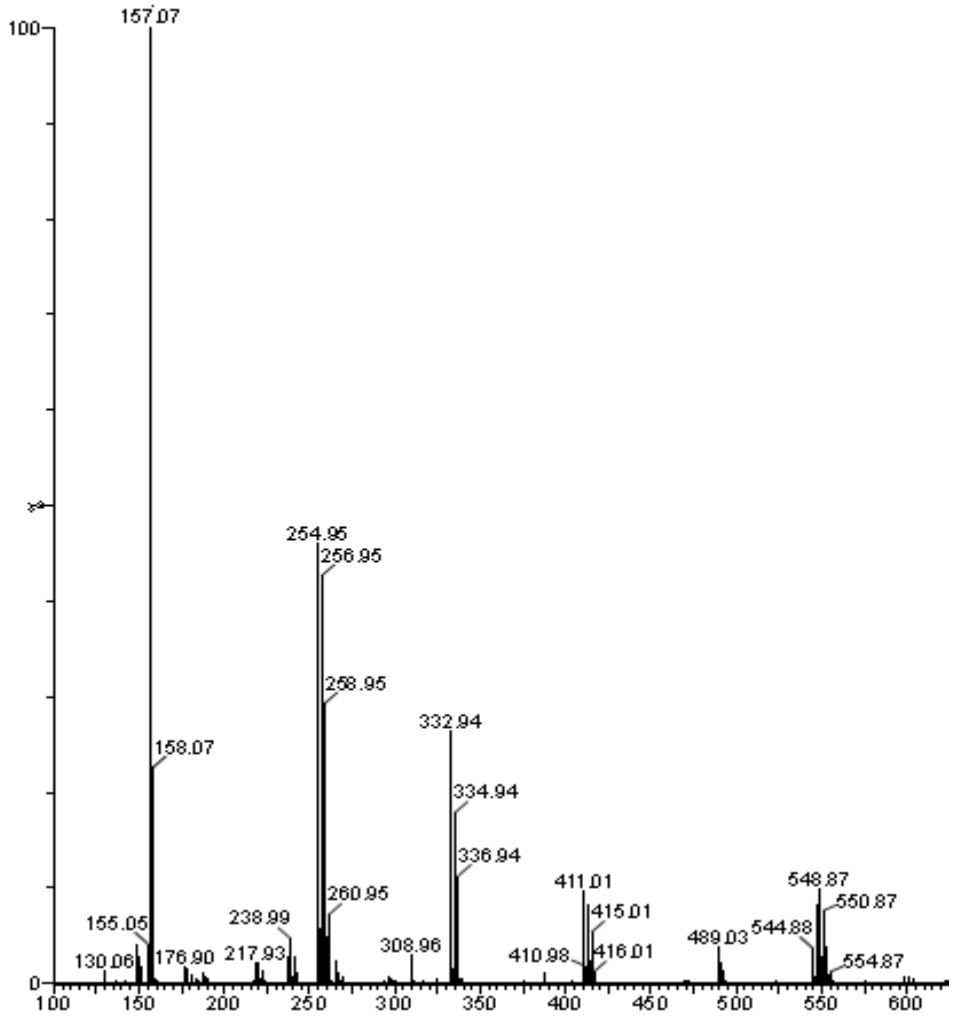

Fig. 110: Mass spectra of $[Zn(L_6)bpy]Cl_2$ *(22)*

m/z	**Loss of**	**Molecular Ion**
550		$[Zn(L_6)bpy]Cl_2.H_2O$
412	L_6	$[Zn(bpy)_2Cl]$
256	bpy	[Zn(bpy)Cl]
156	Zn, Cl	Free bpy

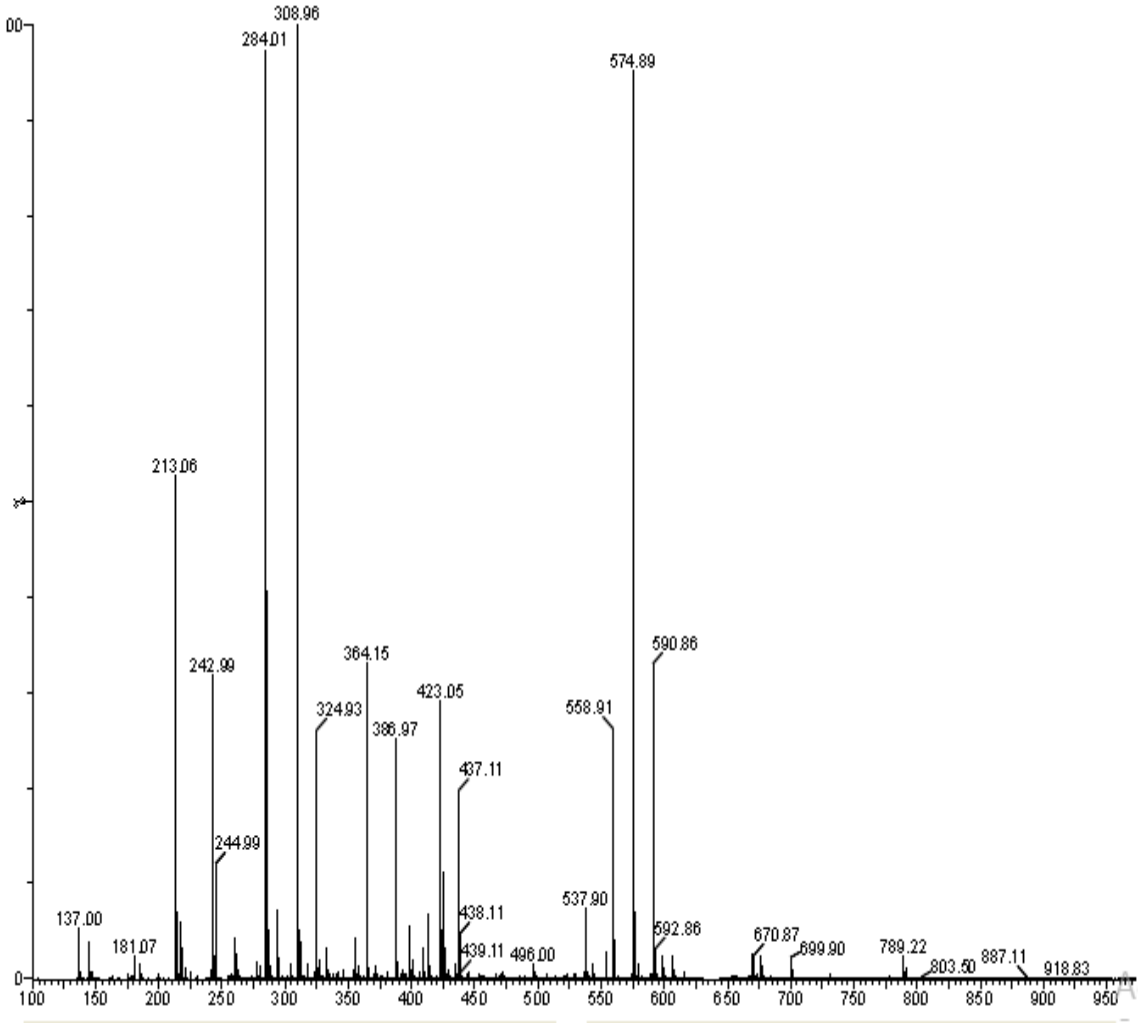

Fig. 111: Mass spectra of $[Cu(L_6)phen]Cl_2$ *(23)*

m/z	**Loss of**	**Molecular Ion**
572		$[Cu(L_6)phen]Cl_2.H_2O$
423	L_6	$[Cu(phen)_2]$
243	phen	[Cu(phen)]

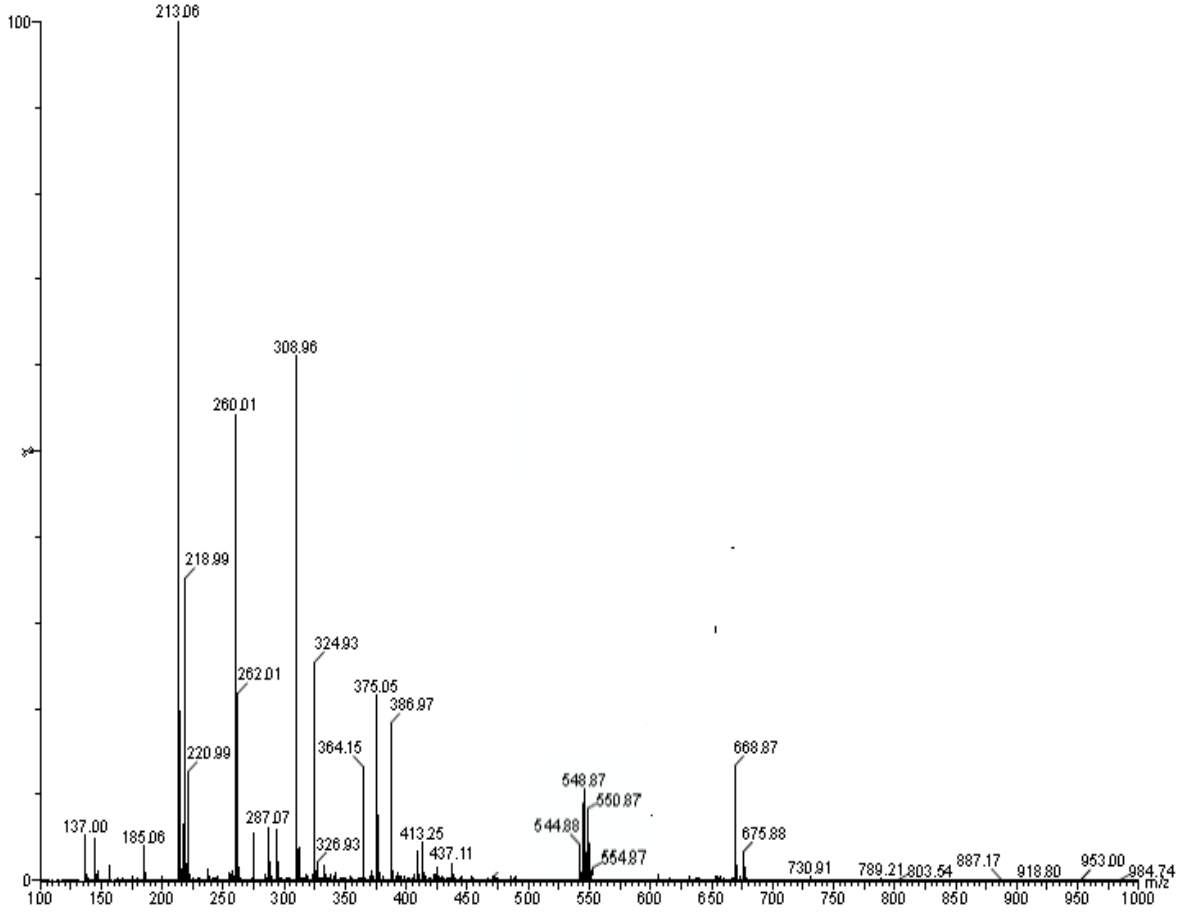

Fig. 112: Mass spectra of $[Cu(L_6)bpy]Cl_2$ *(24)*

m/z	**Loss of**	**Fragment**
549		$[Cu(L_6)bpy]Cl_2.H_2O$
411	L_6	$[Cu(bpy)_2Cl]$
375	Cl	$[Cu(bpy)_2]$
220	bpy	[Cu(bpy)]

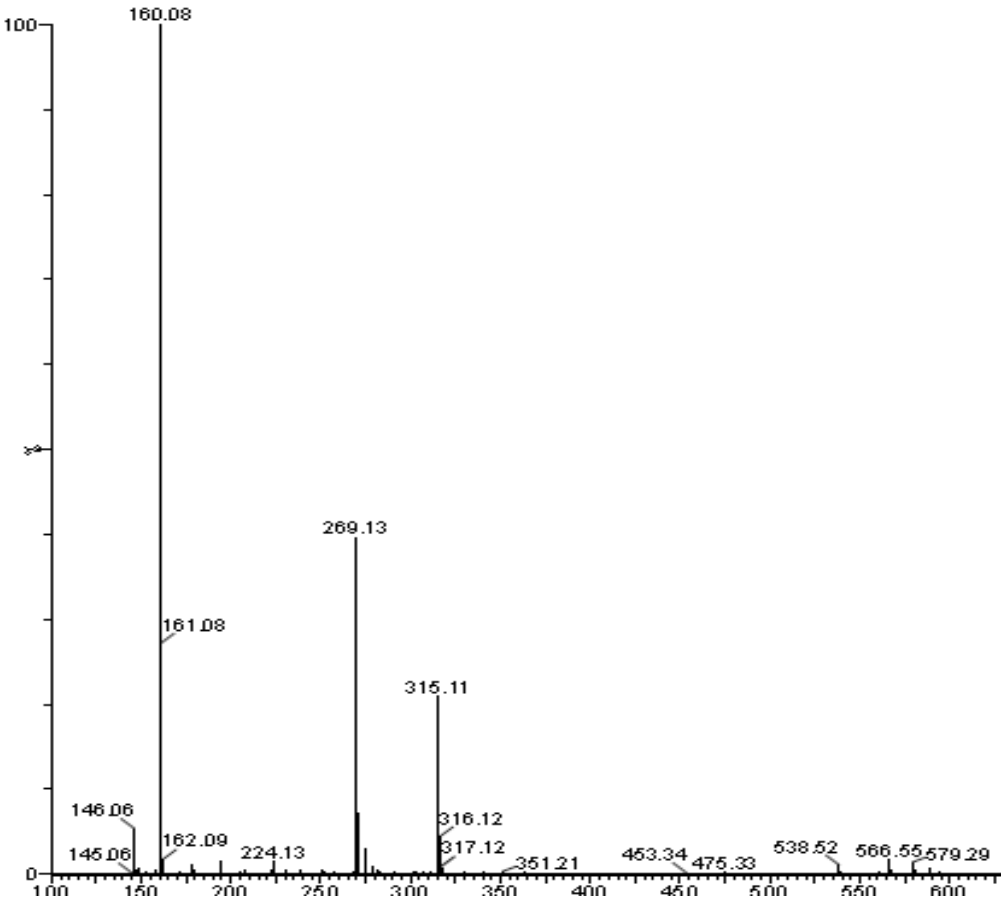

Fig. 113: Mass spectra of (L_7) (Mol. Mass = 268 g)

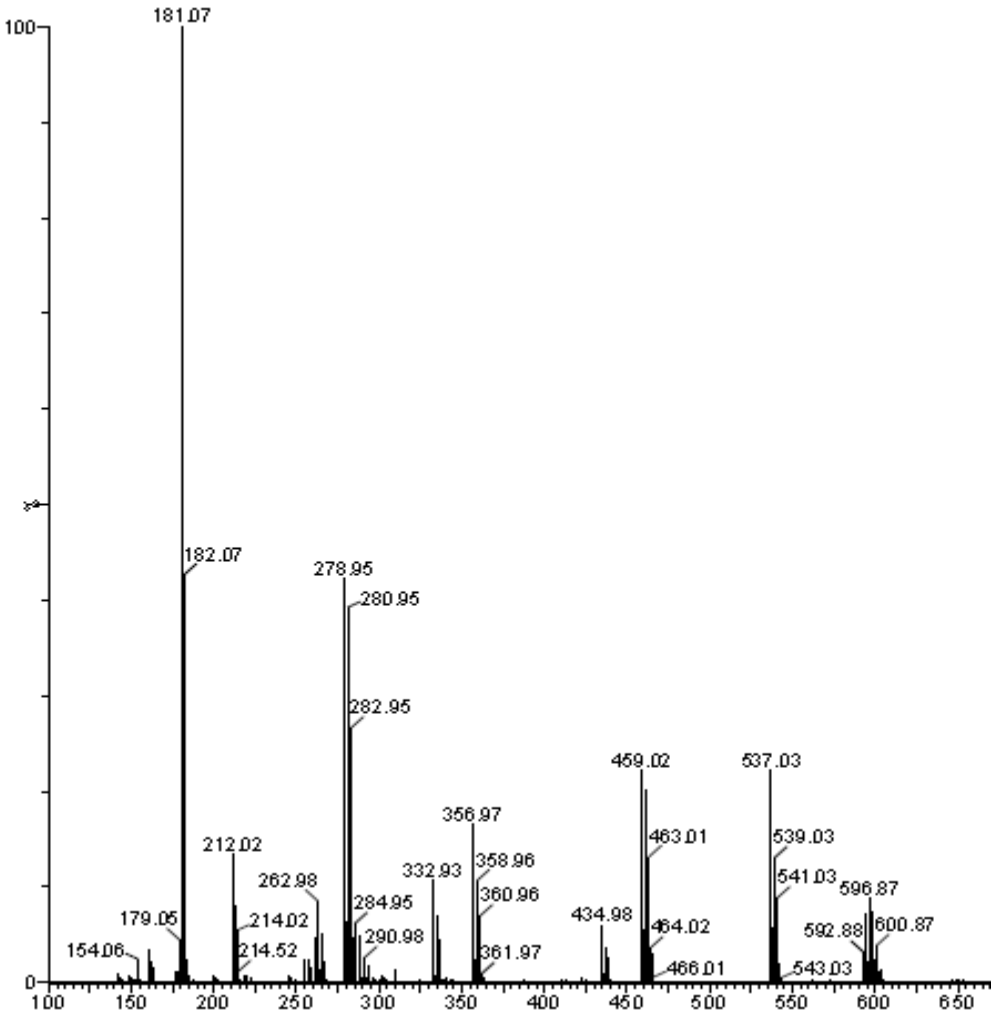

Fig. 114: Mass spectra of [Zn(L_7)phen]Cl_2 *(25)*

m/z	**Loss of**	**Molecular Ion**
602		[Zn(L_7)phen]$Cl_2.H_2O$
459	L_7	[Zn$(phen)_2$Cl]
279	phen	[Zn(phen)Cl]
180	Zn, Cl	Free phen

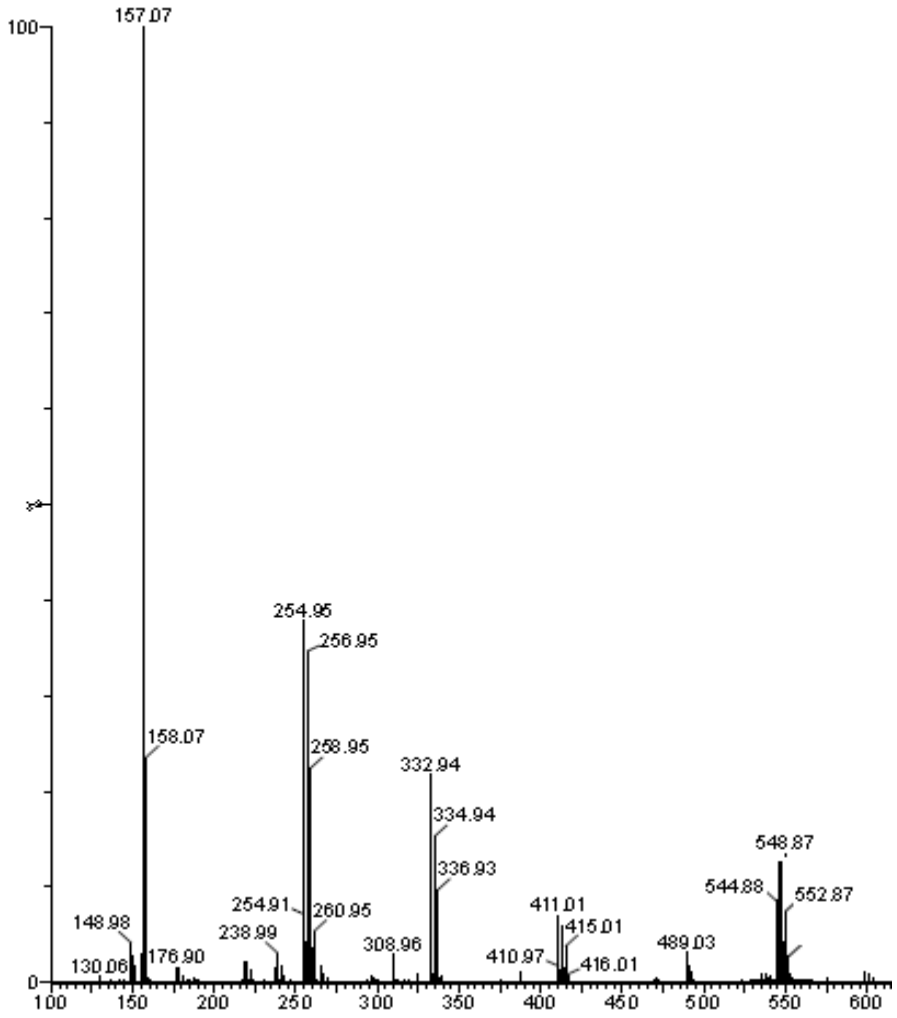

Fig. 115: Mass spectra of $[Zn(L_7)bpy]Cl_2$ *(26)*

m/z	**Loss of**	**Molecular Ion**
543		$[Zn(L_7)(bpy)]Cl.H_2O$
411	L_7, H_2O	$[Zn(bpy)_2Cl]$
255	bpy	[Zn(bpy)Cl]
156	Zn, Cl	Free bpy

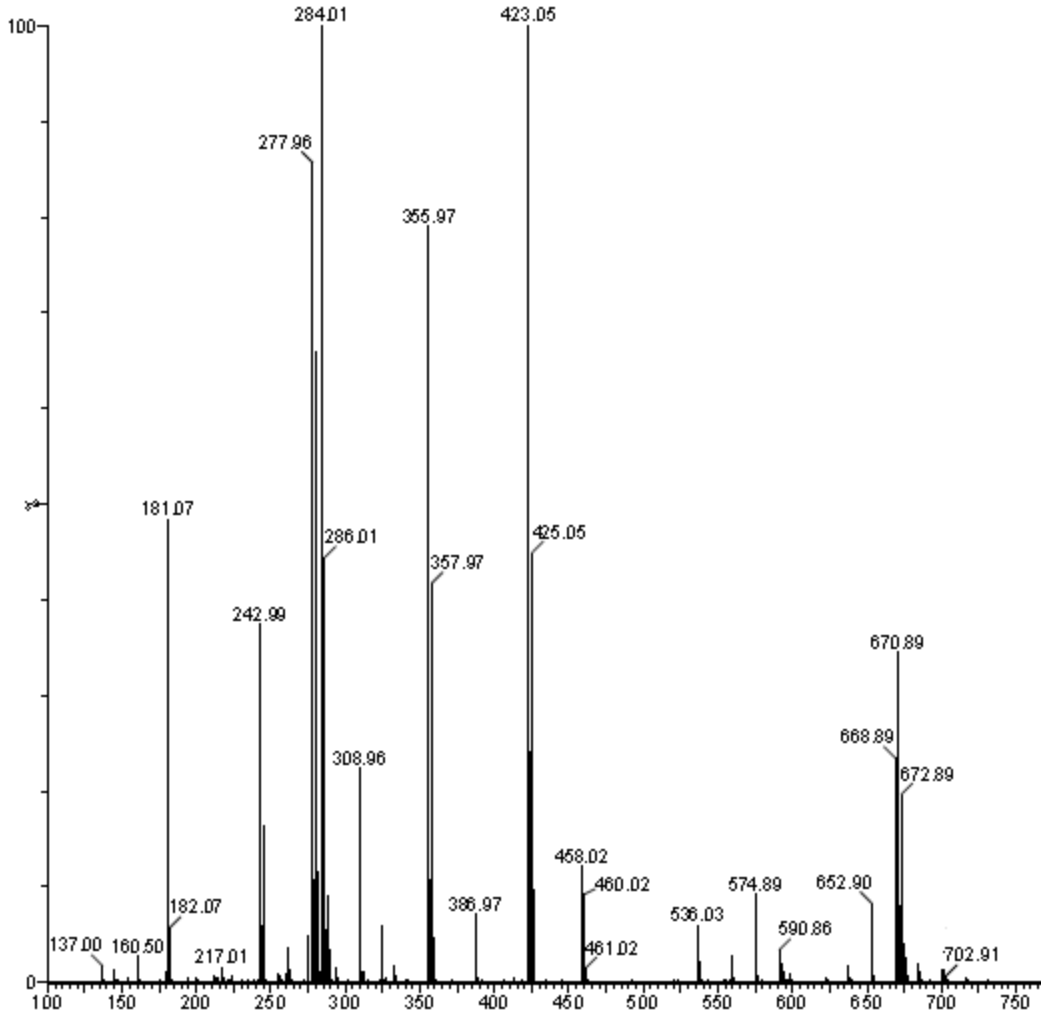

Fig. 116: Mass spectra of $[Cu(L_7)phen]Cl_2$ *(27)*

m/z	**Loss of**	**Molecular Ion**
672		$[Cu(L_7)(phen)]Cl_2.5H_2O$
458	L_7, Cl, H_2O	$[Cu(phen)_2Cl]$
423	Cl	$[Cu(phen)_2]$
278	phen	[Cu(phen)Cl]
180	Cu, Cl	Free phen

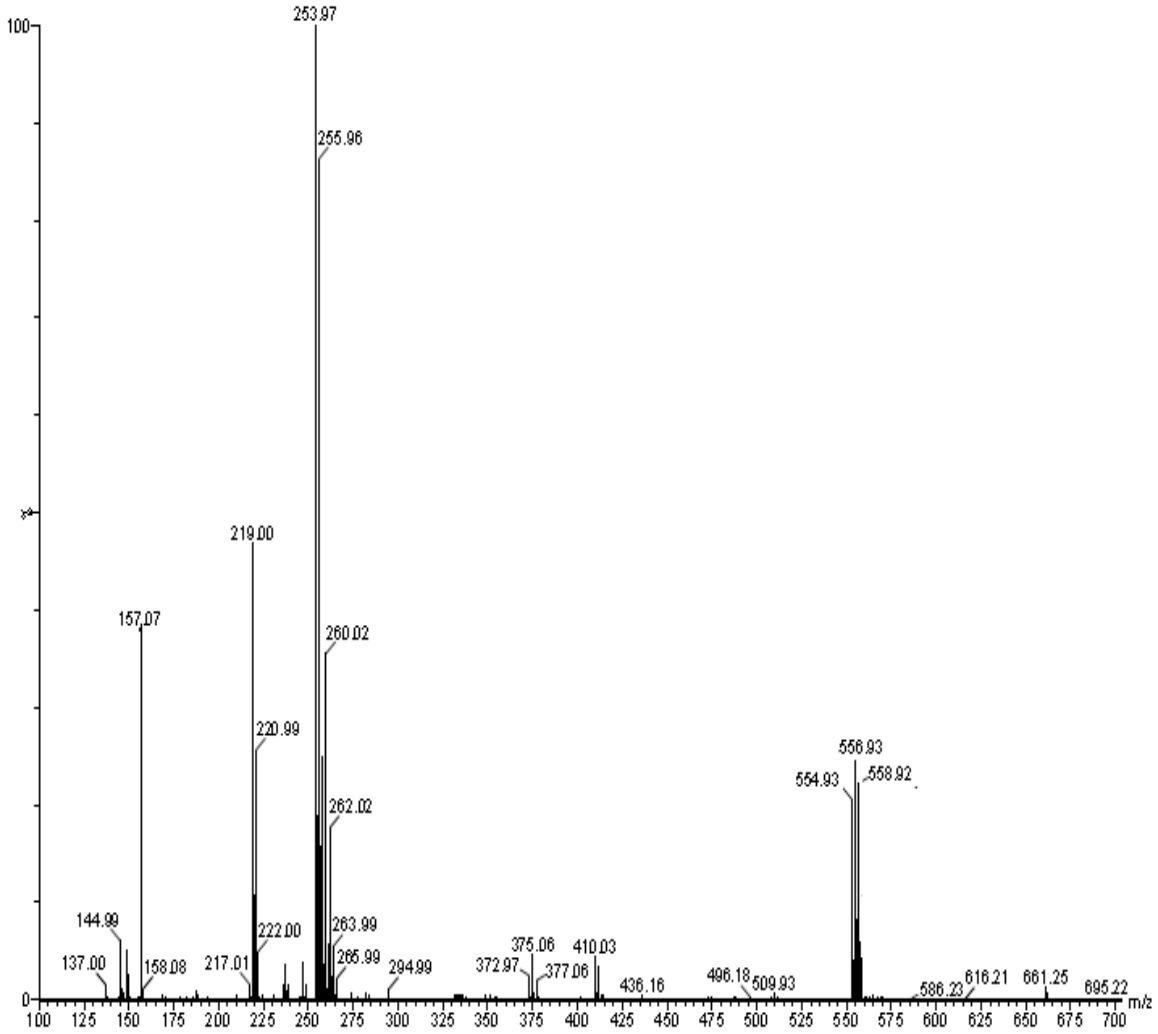

Fig. 117: Mass spectra of $[Cu(L_7)bpy]Cl_2$ *(28)*

m/z	**Loss of**	**Molecular Ion**
558		$[Cu(L_7)(bpy)]Cl_2$
255	bpy	[Cu(bpy)Cl]
156	Cu, Cl	Free bpy

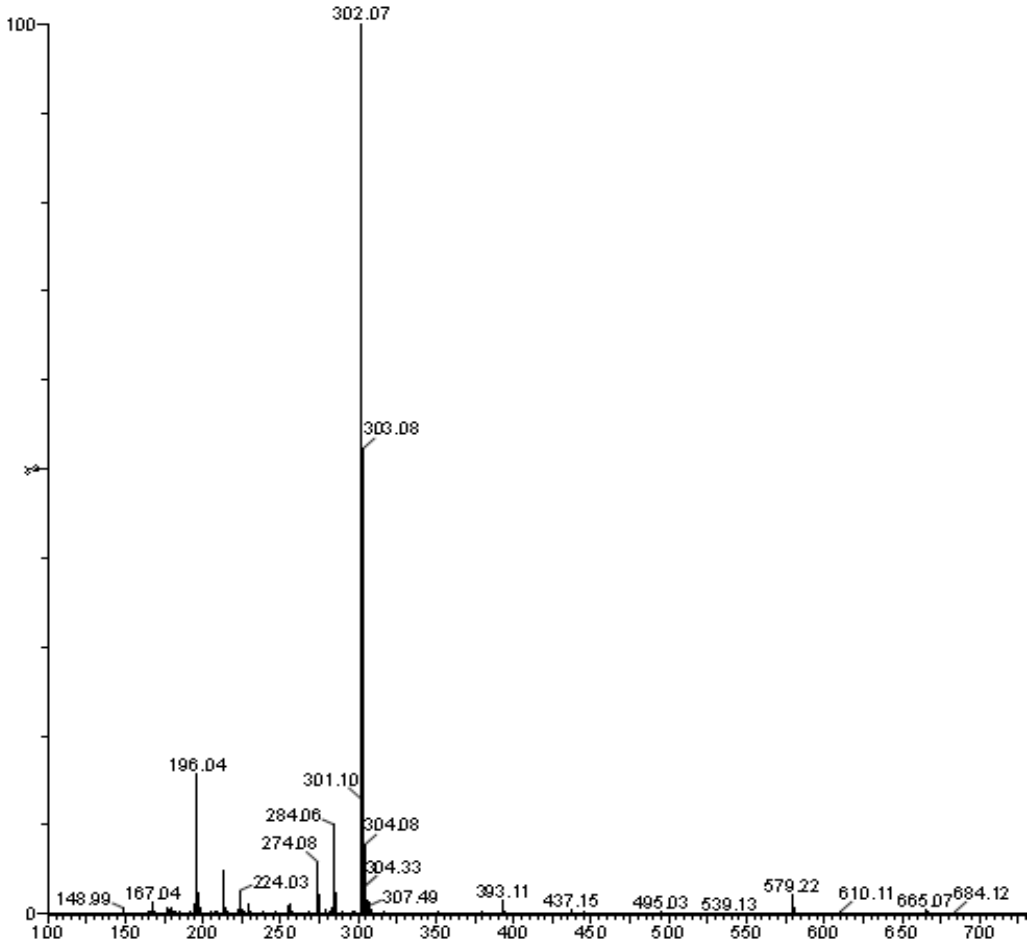

Fig. 118: Mass spectra of (L_8) (Mol. Mass = 301 g)

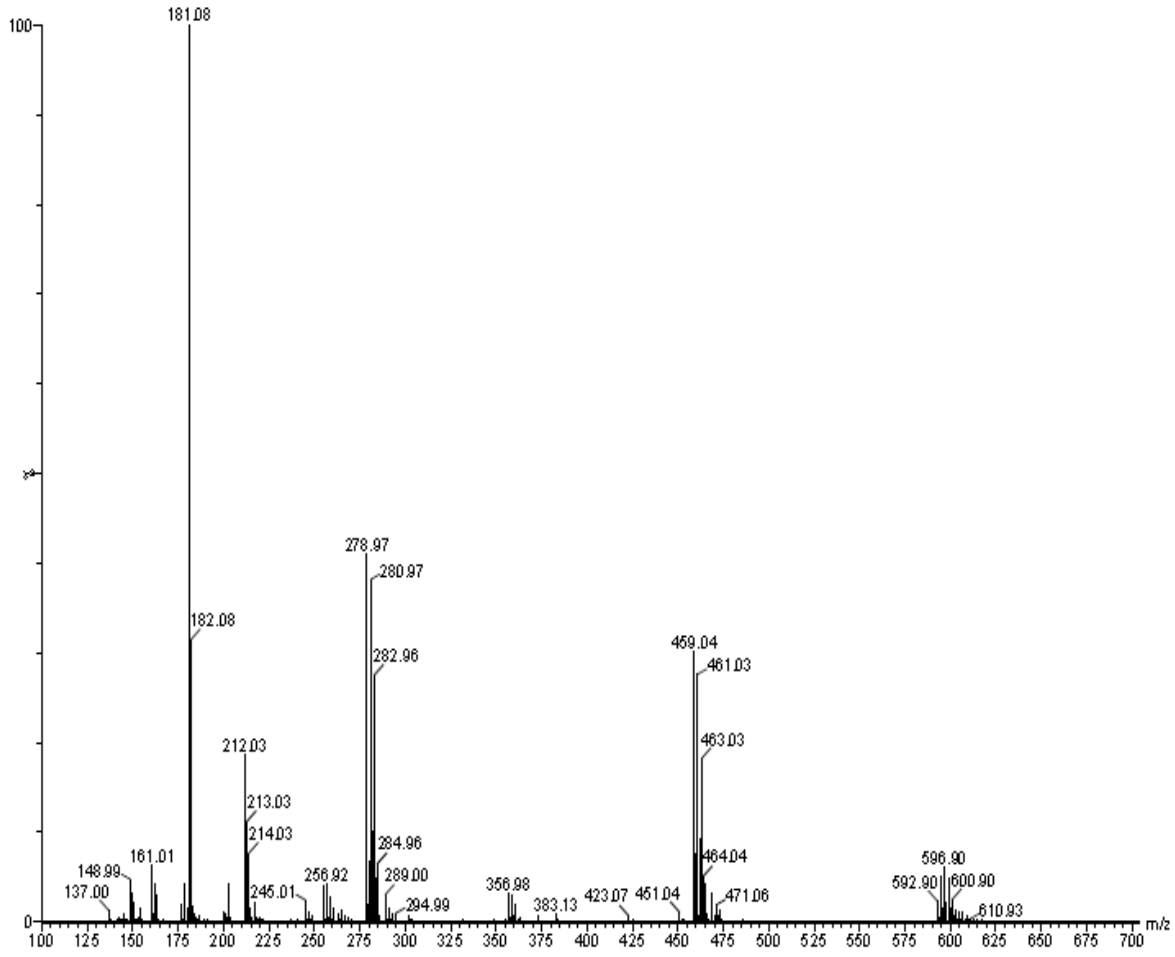

Fig. 119: Mass spectra of $[Zn(L_8)(phen)]Cl_2$ *(29)*

m/z	**Loss of**	**Molecular Ion**
599		$[Zn(L_8)(phen)Cl].H_2O$
460	L_8, H_2O	$[Zn(phen)_2Cl]$
280	phen	[Zn(phen)Cl]
180	Zn, Cl	Free phen

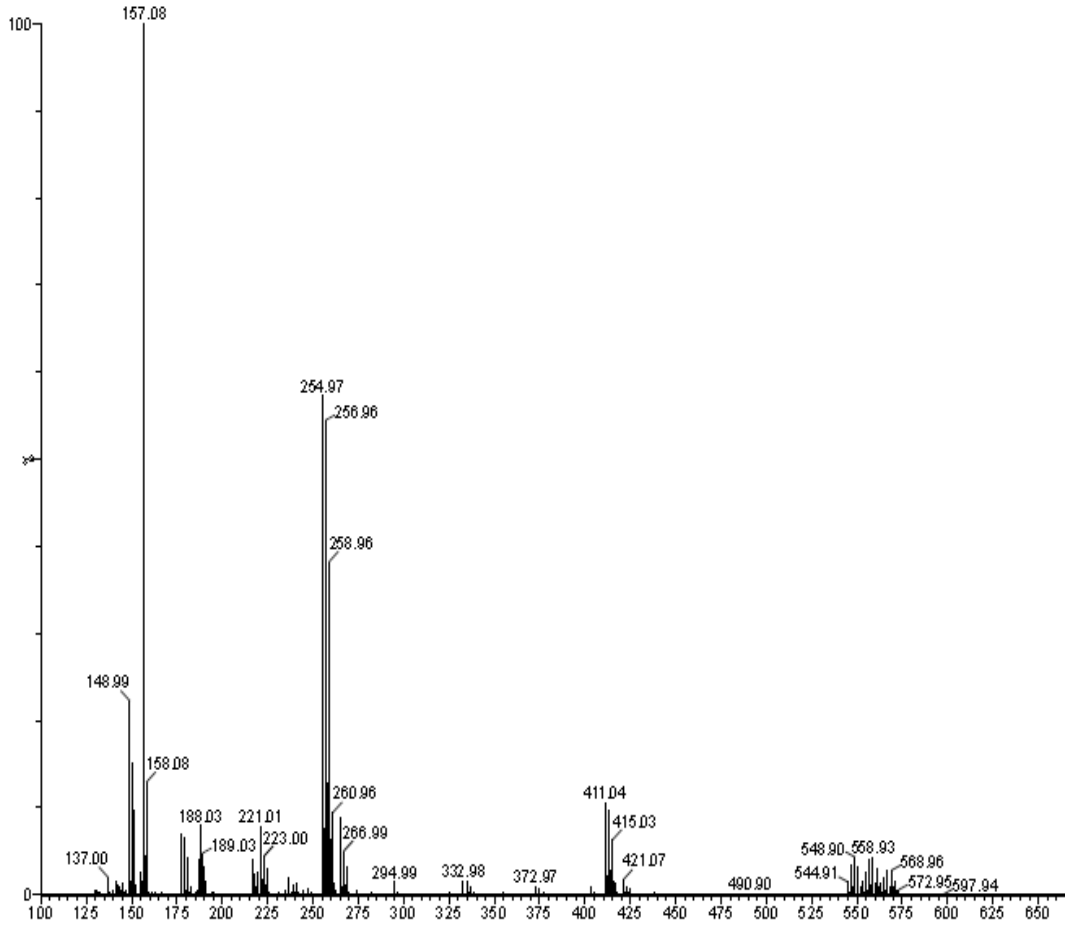

Fig. 120: Mass spectra of $[Zn(L_8)(bpy)]Cl_2$ *(30)*

m/z	**Loss of**	**Molecular Ion**
557		$[Zn(L_8)(bpy)Cl]$
412	L_8	$[Zn(bpy)_2Cl]$
256	bpy	[Zn(bpy)Cl]
156	Zn, Cl	Free bpy

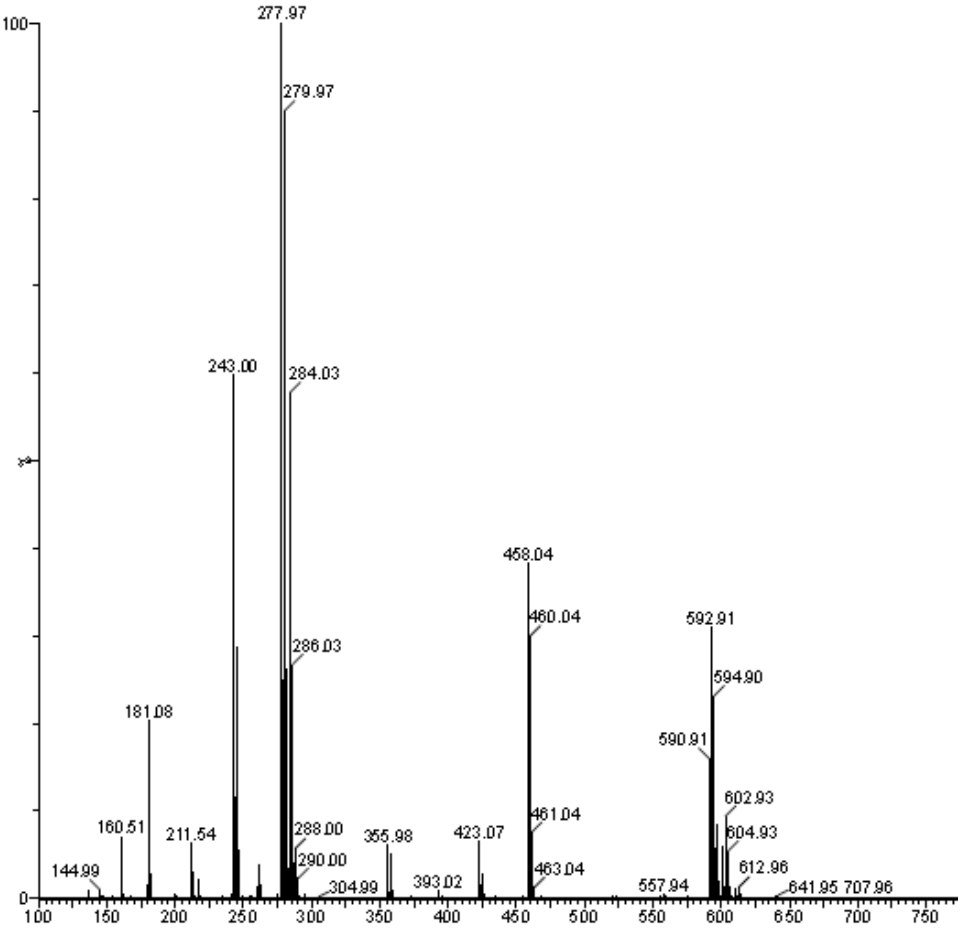

Fig. 121: Mass spectra of $[Cu(L_8)(phen)]Cl_2$ *(31)*

m/z	**Loss of**	**Molecular Ion**
598		$[Cu(L_8)(phen)Cl].H_2O$
459	L_8	$[Cu(phen)_2Cl]$
279	phen	[Cu(phen)Cl]
180	Cu	Free phen

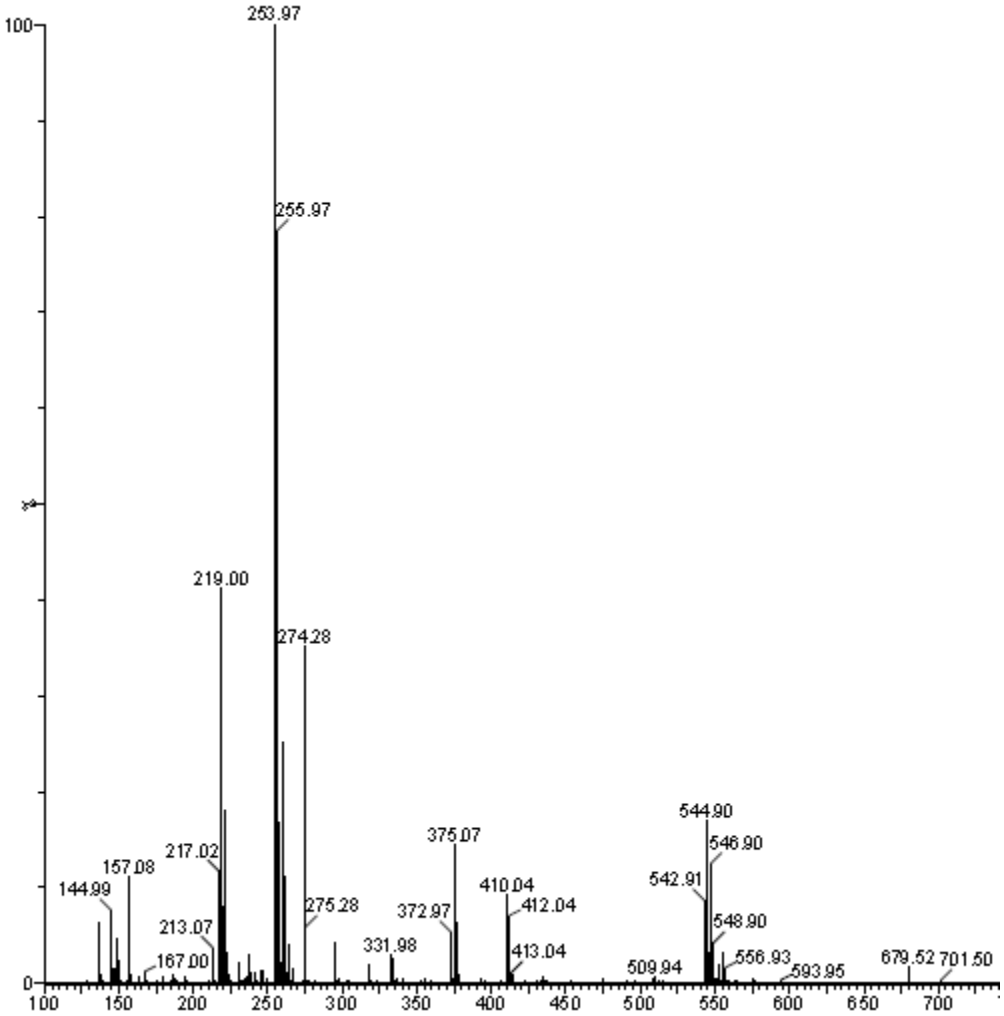

Fig. 122: Mass spectra of $[Cu(L_8)(bpy)]Cl_2$ *(32)*

m/z	**Loss of**	**Molecular Ion**
556		$[Cu(L_8)(bpy)Cl]$
411	L_8	$[Cu(bpy)_2Cl]$
255	bpy	[Cu(bpy)Cl]
219	Cl	[Cu(bpy)]

4.3.4. ^{1}H NMR spectrum

The ^{1}H NMR of the Schiff base ligands was recorded in chloroform. TMS was used as reference. A signal around 4.0 - 5.36 is assigned to phenolic group. The multiplet in the range of 6.9 - 7.3 was assigned to protons of aromatic rings. The ^{1}H NMR spectral assignments of the ligands is as follows:

NMR of **(L_6)** (500 MHz, $CDCl_3$): ^{1}H NMR (500 MHz, $CDCl_3$) δ 6.83 (m, 3H, Ar-H), 6.72 (d, 1H, Ar-H), 5.36 (s, 1H, -OH).

NMR of **(L_7)** (500 MHz, $CDCl_3$): ^{1}H NMR (500 MHz, $CDCl_3$) δ 6.83 (s, 1H, Ar-H), 6.77 (s, 2H, Ar-H), 6.69 (d, 1H, Ar-H), 4.71 (s, 1H, -OH).

NMR of **(L_8)** (500 MHz, $CDCl_3$): ^{1}H NMR (500 MHz, $CDCl_3$) δ 7.86 (m, 1H, Ar-H), 7.72 (d, 1H, Ar-H), 7.65 – 7.52 (m, 3H, Ar-H), 7.44 (m, 1H, Ar-H), 7.36 – 7.16 (m, 5H, Ar-H), 7.11 (t, 1H, Ar-H), 6.99 (d, 1H, Ar-H), 6.93 – 6.82 (m, 1H, Ar-H), 6.62 (s, 1H, Ar-H), 4.00 (s, 1H, -OH).

4.4 UV-vis absorption studies of BSA

The same procedure is followed as in section 2.5 of Chapter 2 (Table 21).

Table 21: Values of binding constant (K_b M^{-1})

Complex	**K_b M^{-1}**
$[Zn(L_6)(phen)]Cl_2$ ***(21)***	3.5×10^4
$[Zn(L_6)(bpy)]Cl_2$ ***(22)***	1.1×10^4
$[Cu(L_6)(phen)]Cl_2$ ***(23)***	-
$[Cu(L_6)(bpy)]Cl_2$ ***(24)***	-
$[Zn(L_7)(phen)]Cl_2$ ***(25)***	5.8×10^4
$[Zn(L_7)(bpy)]Cl_2$ ***(26)***	5.1×10^5
$[Cu(L_7)(phen)]Cl_2$ ***(27)***	-
$[Cu(L_7)(bpy)]Cl_2$ ***(28)***	-
$[Zn(L_8)(phen)]Cl_2$ ***(29)***	4.9×10^4
$[Zn(L_8)(bpy)]Cl_2$ ***(30)***	1.2×10^5
$[Cu(L_8)(phen)]Cl_2$ ***(31)***	-
$[Cu(L_8)(bpy)]Cl_2$ ***(32)***	-

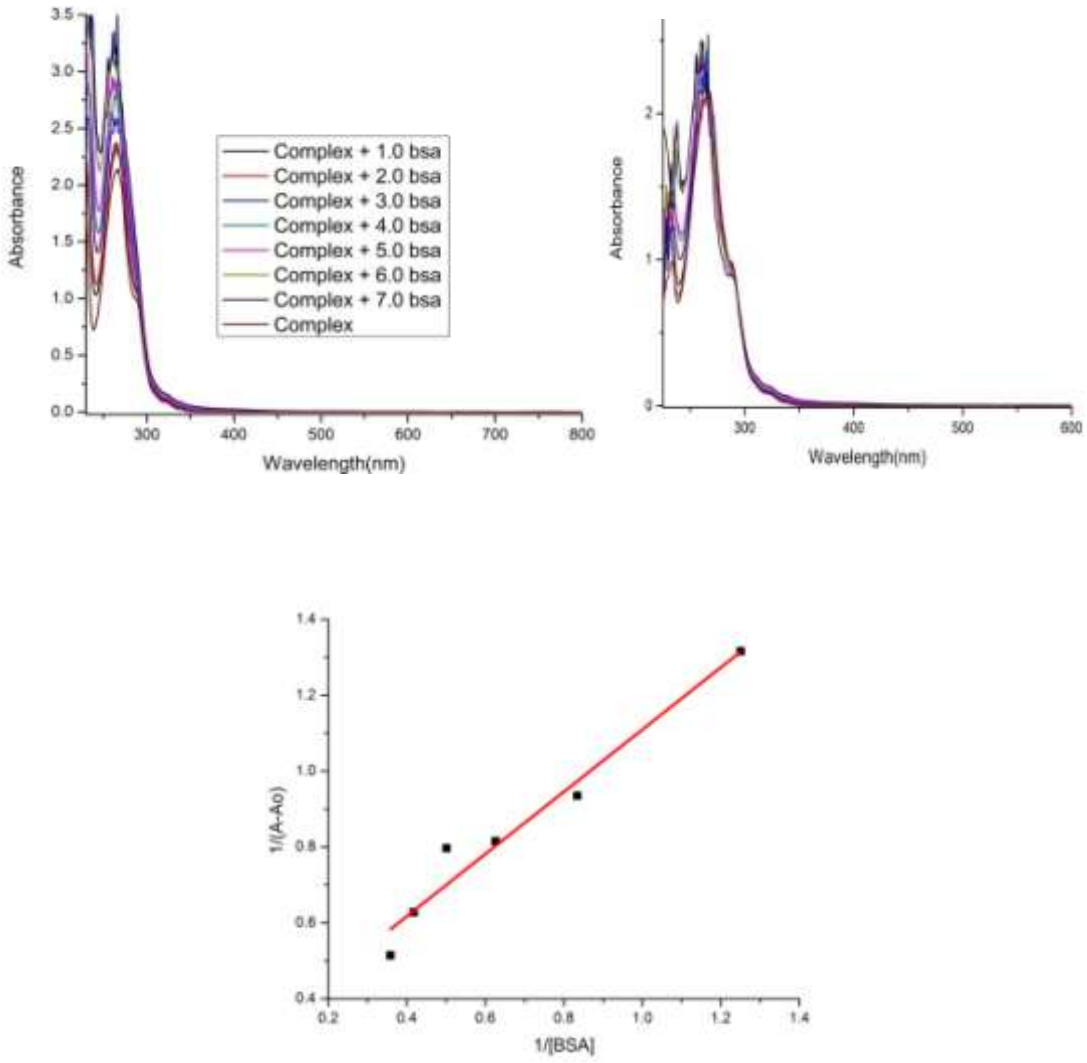

Fig. 123: (A) UV-vis titration graphs of complex $[Zn(L_6)(phen)]Cl_2$ (50 μM) with incremental [BSA] concentration in the range of 0 - 3 μM,

(B) Graph of {[BSA complex with $[Zn(L_6)(phen)]Cl_2$ – [Variant concentrations of [BSA]},

(C) Graph of 1 / ($A-A_0$) vs. 1 / [BSA] concentration

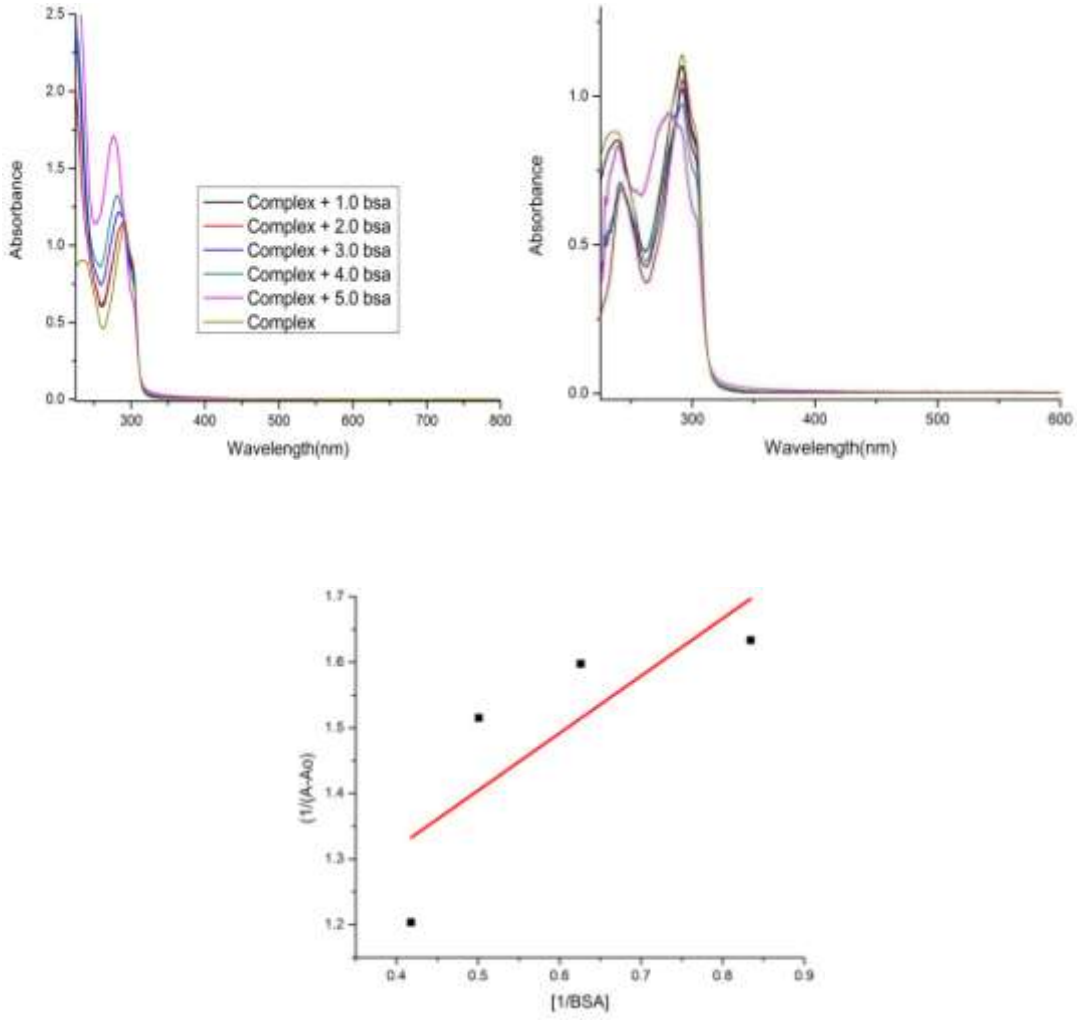

Fig. 124: (A) UV-vis titration graphs of complex $[Zn(L_6)(bpy)]Cl_2$ (50 μM) with incremental [BSA] concentration in the range of 0 – 3 μM,

(B) Graph of {[BSA complex with $[Zn(L_6)(bpy)]Cl_2$ – [Variant concentrations of [BSA]},

(C) Graph of 1 / ($A-A_0$) vs. 1 / [BSA] concentration

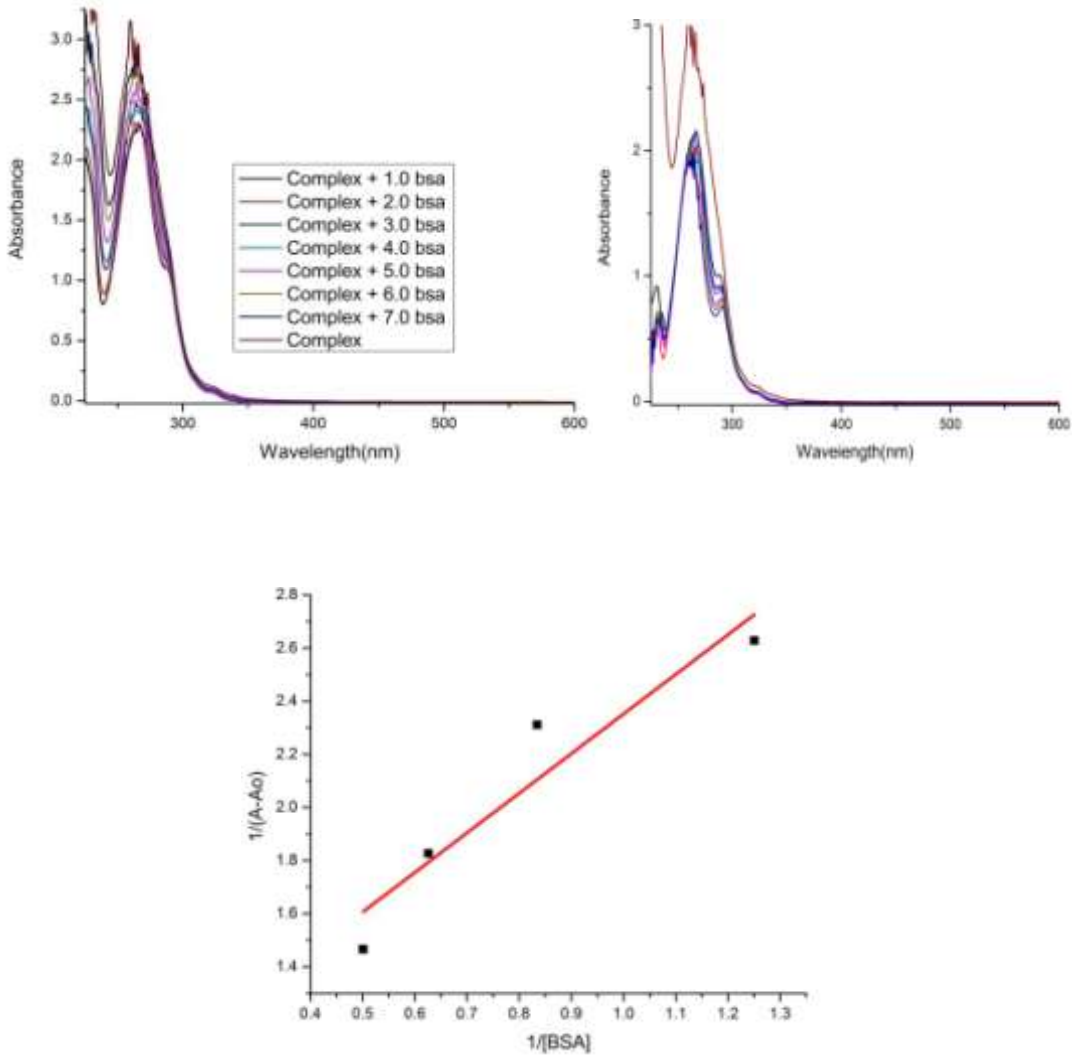

Fig.125: (A) UV-vis titration graphs of complex $[Zn(L_7)(phen)]Cl_2$ (50 μM) with incremental [BSA] concentration in the range of 0 – 3 μM,

(B) Graph of {[BSA complex with $[Zn(L_7)(phen)]Cl_2$ – [Variant concentrations of [BSA]},

(C) Graph of 1 / ($A-A_0$) vs. 1 / [BSA] concentration

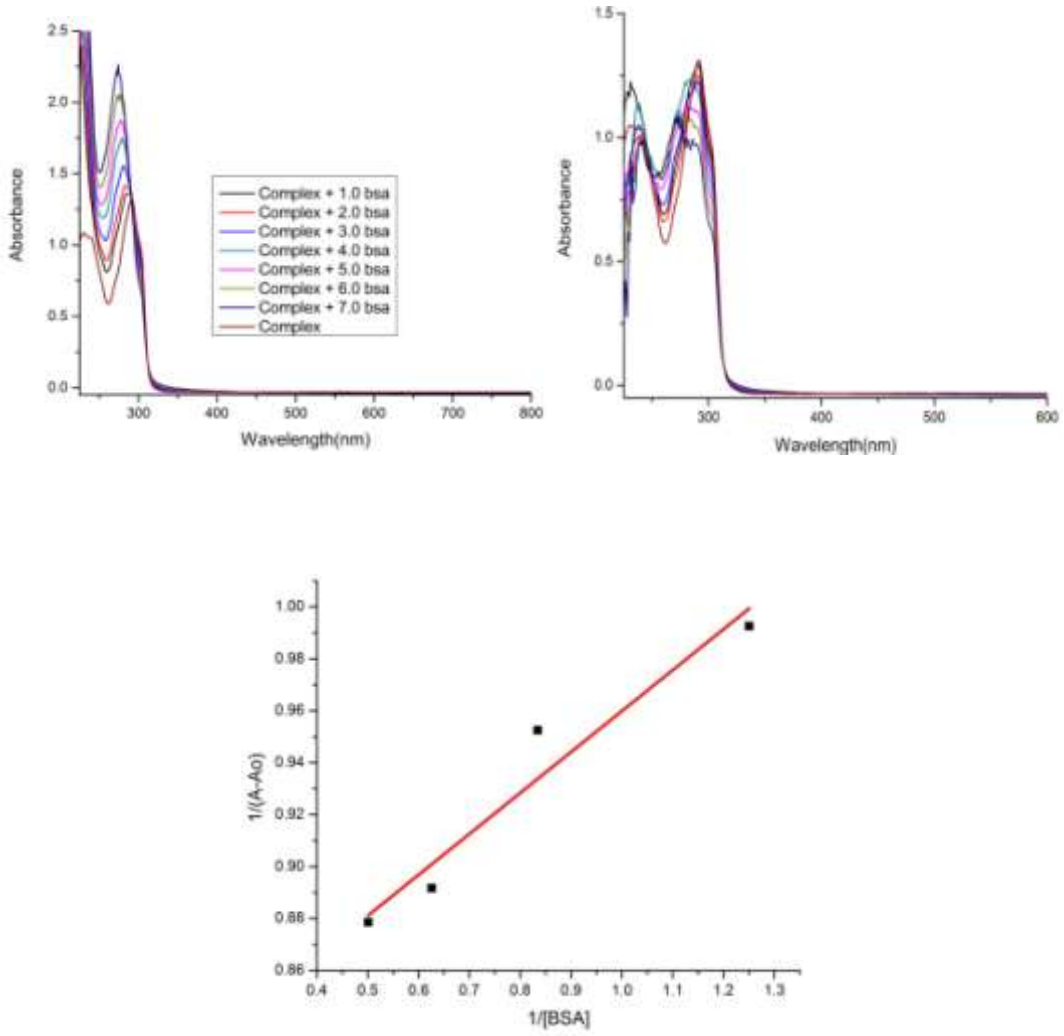

Fig. 126: (A) UV-vis titration graphs of complex $[Zn(L_7)(bpy)]Cl_2$ (50 μM) with incremental [BSA] concentration in the range of 0 – 3 μM,

(B) Graph of {[BSA complex with $[Zn(L_7)(bpy)]Cl_2$ – [Variant concentrations of [BSA]},

(C) Graph of 1 / ($A-A_0$) vs. 1 / [BSA] concentration

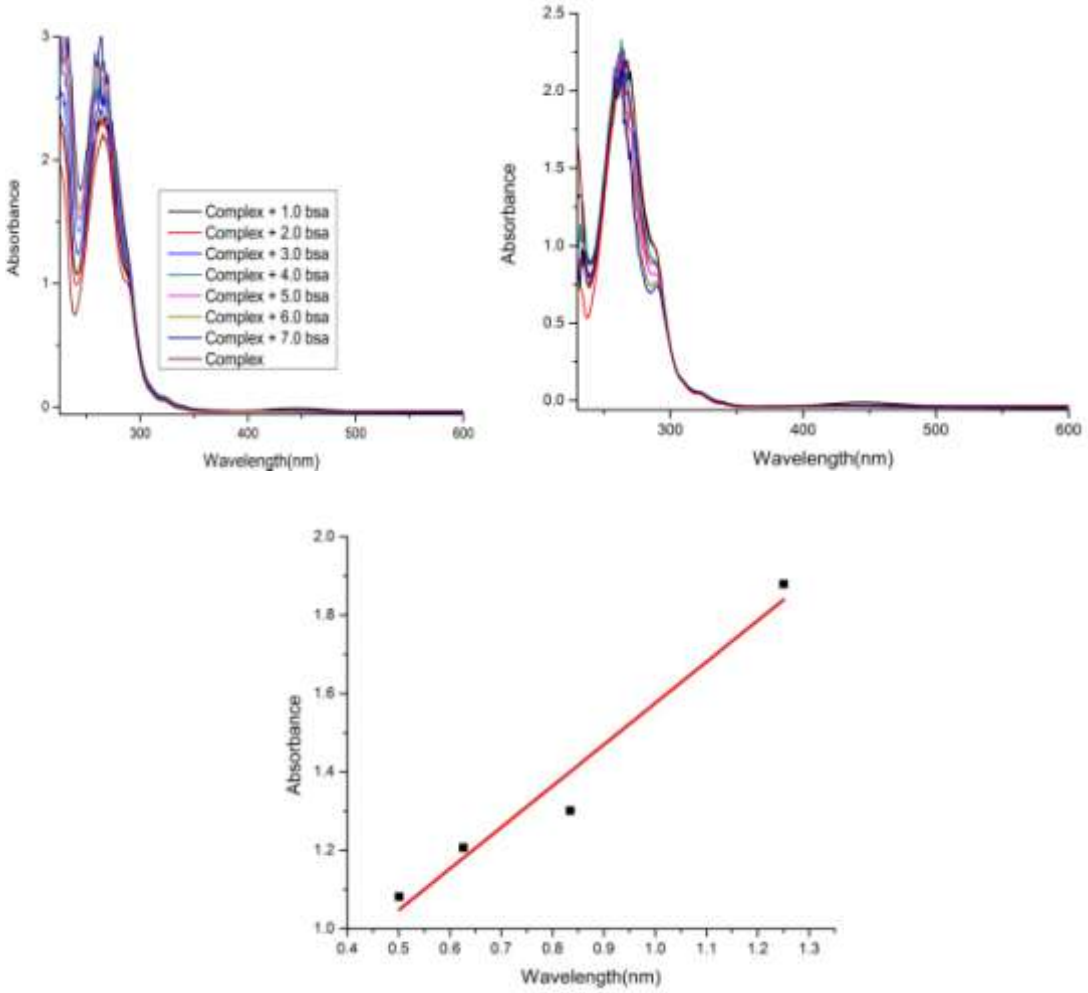

Fig. 127: (A) UV-vis titration graphs of complex $[Zn(L_8)(phen)]Cl_2$ (50 μM) with incremental [BSA] concentration in the range of 0 – 3 μM,

(B) Graph of {[BSA complex with $[Zn(L_8)(phen)]Cl_2$ – [Variant concentrations of [BSA]},

(C) Graph of 1 / ($A-A_0$) vs. 1 / [BSA] concentration

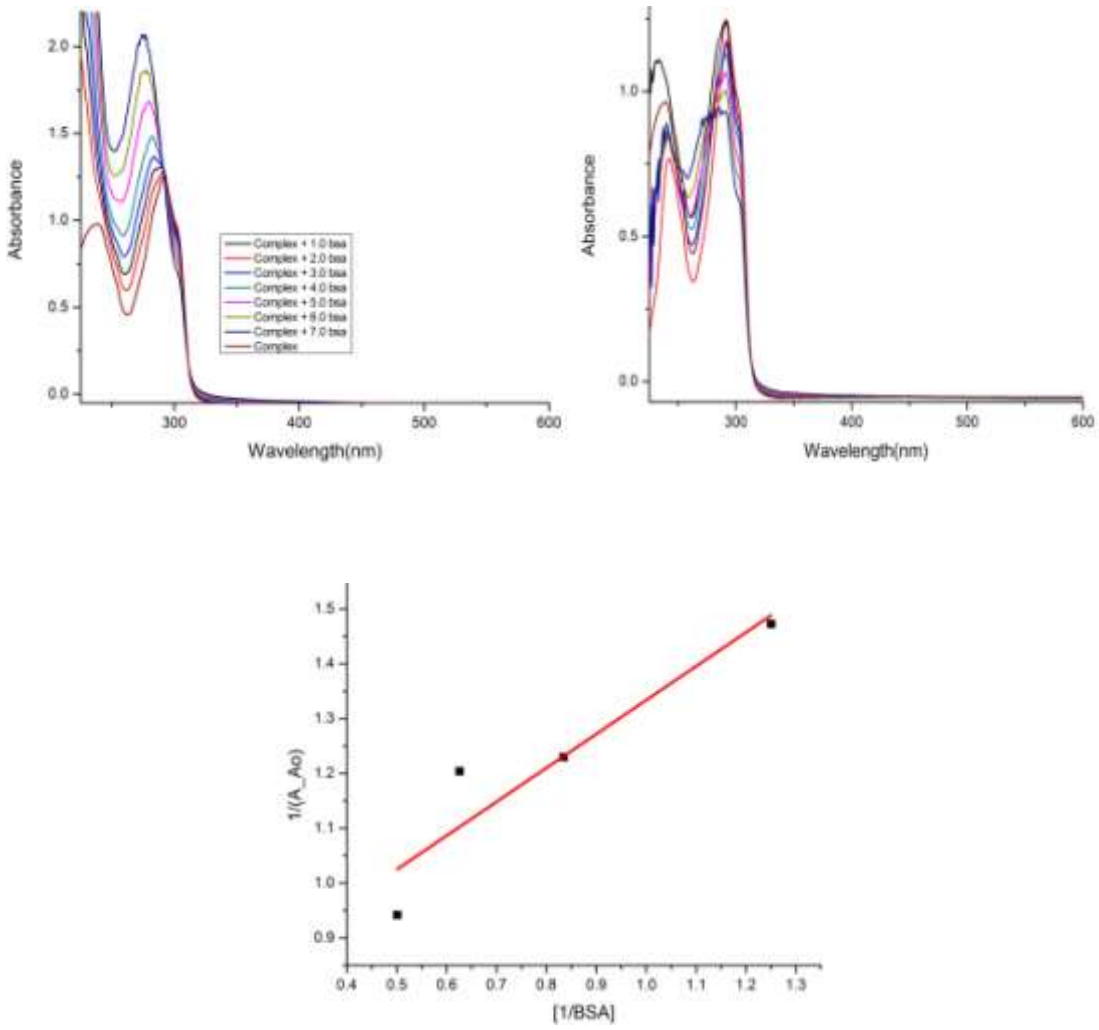

Fig. 128: (A) UV-vis titration graphs of complex $[Zn(L_8)(bpy)]Cl_2$ (50 μM) with incremental [BSA] concentration in the range of 0 – 3 μM,

(B) Graph of {[BSA complex with $[Zn(L_8)(bpy)]Cl_2$ – [Variant concentrations of [BSA]},

(C) Graph of 1 / (A-A_0) vs. 1 / [BSA] concentration

4.5 Antimicrobial assays

The same procedure is followed as in section 2.6 of Chapter 2.

Table 22: Antimicrobial activity of ligand and complexes (Concentration of 5 mg ml^{-1})

Complex	Average Inhibition Zone in diameter (mm) ± SD			
	Antibacterial Activity		Antifungal Activity	
	E. coli **(A)**	***S. aureus*** **(B)**	***A. niger*** **(C)**	***A. fumigatus*** **(D)**
(glyoxal-*o*-aminophenol) (L_6)	04.16±0.29	7.33±0.15	-	-
$[Zn(L_6)(phen)]Cl_2$ ***(21)***	26.10±0.36	18.1±0.36	18.33±0.29	11.9±0.17
$[Zn(L_6)(bpy)]Cl_2$ ***(22)***	11.76±0.25	32.33±0.29	15.66±0.29	28.16±0.29
$[Cu(L_6)(phen)]Cl_2$ ***(23)***	13.33±0.29	19.87±0.23	-	32.16±0.29
$[Cu(L_6)(bpy)]Cl_2$ ***(24)***	22.23±0.25	14.9±0.36	05.06±0.11	20.16±0.29
(diacetyl-*o*-aminophenol) (L_7)	-	-	-	-
$[Zn(L_7)(phen)]Cl_2$ ***(25)***	-	31.83±0.29	20.5±0.50	37.83±0.29
$[Zn(L_7)(bpy)]Cl_2$ ***(26)***	-	11.66±0.29	12.06±0.40	26.06±0.11
$[Cu(L_7)(phen)]Cl_2$ ***(27)***	-	28.33±0.29	31.0±0.50	33.33±0.29
$[Cu(L_7)(bpy)]Cl_2$ ***(28)***	-	12.06±0.40	22.16±0.29	-
(benzil-*o*-aminophenol) (L_8)	-	-	17.9±0.17	11.16±0.76
$[Zn(L_8)(phen)]Cl_2$ ***(29)***	18.17±0.29	27.83±0.29	18.33±0.29	35.16±0.29
$[Zn(L_8)(bpy)]Cl_2$ ***(30)***	-	14.9±0.40	-	21.66±0.58
$[Cu(L_8)(phen)]Cl_2$ ***(31)***	26.06±0.40	30.33±0.29	33.76±0.25	38.15±0.21
$[Cu(L_8)(bpy)]Cl_2$ ***(32)***	-	11.66±0.29	23.83±0.29	15.33±0.29
Amikacin	21.5±0.50	24.83±0.76	-	-
Fluconazole	-	-	23.66±0.57	22.66±0.29
DMSO	Nil	Nil	Nil	Nil

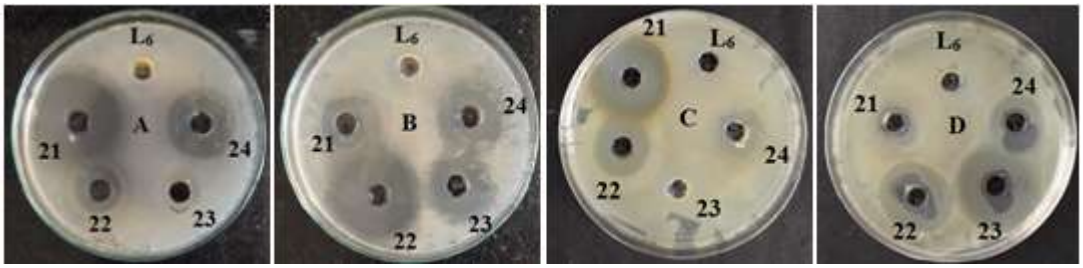

Fig. 129: Antimicrobial assay of Schiff base ligand (L_6) and its metal chelate (*21 - 24*) (Alphabet levels are according to table 22)

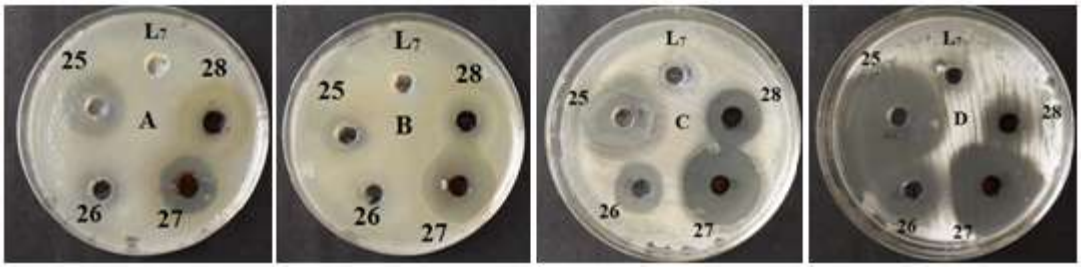

Fig. 130: Antimicrobial assay of Schiff base ligand (L_7) and its metal chelate (*25 - 28*) (Alphabet levels are according to table 22)

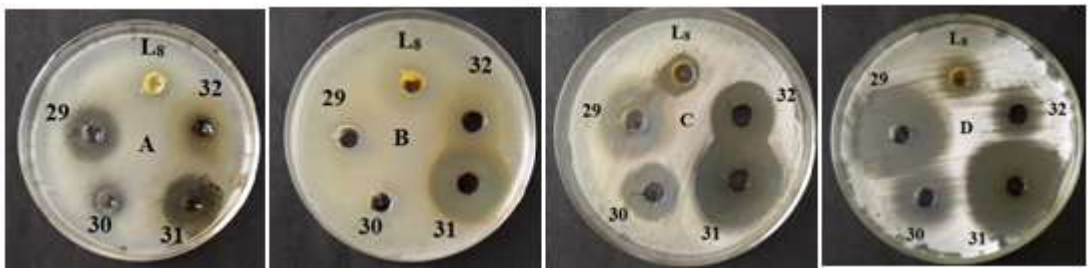

Fig. 131: Antimicrobial assay of Schiff base ligand (L_8) and its metal chelate (*29 - 32*) (Alphabet levels are according to table 22)

4.6 Conclusion

This chapter details about the synthesis of three Schiff bases (**L_6**), (**L_7**), (**L_8**) and their mixed ligand complexes with zinc(II) and copper(II) metal ions. The ligands are synthesized with a new strategy of funtionalization of diketones rather than the usual approach of diamines as starting materials. The ligands should be able to provide a different coordination approach from the existing ones due to different stereo-chemical positioning of the ligating atoms. Although the approach was to create symmetrically disubstituted ligands but in case of benzil the substitution occurred only from one side only creating a unsymmetrical ligand. The steric bulk of the phenyl ring over methyl or hydrogen could be the reason for substitution from one side only. Both ligand and complexes were found to be stable thermally and are of non- hygroscopic nature. The ligands (**L_6**), (**L_7**) appear as tetradentate coordinating to metal centers through imine nitrogen and hydroxyl group while the ligand (**L_8**) appears as tridentate ligand coordinating the metal through imine nitrogen, hydroxyl group and carbonyl oxygen. This is supported by shifting in the peaks of imine nitrogen, carbonyl group [in case of (**L_8**)] and appearance of new peaks in the 400 cm^{-1} region for M-N bond and 600 cm^{-1} region for M-O bond. Molecular mass of ligand and metal complexes are in consistence with their mass fragmentation data. Octahedral geometry has been proposed for all the complexes on the basis of evidences shown by their spectral studies. Serum protein interactions of complexes were then studied by determining the values of binding constants using UV-vis titration technique. All the Zn(II) complexes show binding constants in the range of 10^4 - 10^5 M^{-1} while no Cu(II) complex shows solubility in tris buffer. These values indicate that they bind to serum proteins in a modest manner. The results of antimicrobial assays indicate that mixed ligand metal chelates are more biologically active as compared to their Schiff base ligand where ligands show least activity while the antibacterial activities of ***(21), (23)*** and ***(25)*** are greater as compared to standard drug amikacin and antifungal activity of ***(31)*** was highest as compared to standard drug fluconazole.

4.7 Bibliography

[1] Akila, E.; Usharani, M.; Ramachandran, S.; Jayaseelan, P.; Velraj, G.; Rajavel, R. Tetradentate - arm Schiff base derived from the condensation reaction of 3,3′-dihydroxybenzidine, glyoxal / diacetyl and 2-aminophenol: Designing, structural elucidation and properties of their binuclear metal(II) complexes, *Arab. J. Chem.* **2017**, *10*, S2950–S2960.

[2] Chaudhary, N. K. In vitro antibacterial studies of some transition metal complexes of Schiff base derived from 2-aminophenol and furan-2-carbaldehyde, *Arch. Appl. Sci. Res.* **2013**, *5*, 227–231.

[3] Owolabi, S. A. Synthesis, characterization and antimicrobial activity of copper (II) complexes of some hydroxybenzaldimines and their derivatives, Ph.D. Dissertation, Rhodes University, **2012**.

[4] El - Ajaily, M. M.; Maihub, A. A.; Mahanta, U. K.; Badhei, G.; Mohapatra, R. K.; Das, P. K. Mixed ligand complexes containing Schiff bases and their biological activities: A short review, *Rasayan J. Chem.* **2018**, *11*, 166–174.

[5] de Fatima, A.; Martins, C. V. B.; Modolo, L. V.; da Silva, C. M.; Alves, R. B.; da Silva, D. L.; de Resende, M. A. Schiff bases: A short review of their antimicrobial activities, *J. Adv. Res.* **2010**, *2*, 1–8.

[6] Selvi, E. T.; Mahalakshmi, S. Synthesis and characterisation of new heterocyclic Schiff base ligand derived from 4-amino antipyrine, *Int. J. Adv. Res. Dev.* **2017**, *2*, 51–56.

[7] Bose, R. N.; Akbar Ali, M. Transition metal complexes of furfural and benzil Schiff bases derived from s-benzyldithiocarbazate, *Polyhedron* **1984**, *3*, 517–522.

[8] Wang, T.; Zhao, Z.; Hua, J.; Zhang, J. Characterization of the interaction between reserpine and bovine serum albumin: Spectroscopic approaches, *Indian J. Biochem. Biophys.* **2011**, *48*, 388–394.

[9] Yasseen, Z. G. On the interactions of bovine serum albumin with some surfactants: New insights from conductivity studies, *J. Chem. Pharm. Res.* **2012**, *4*, 3361–3367.

[10] Jha, N. S.; Kishore, N. Binding of streptomycin with bovine serum albumin: Energetics and conformational aspects, *Thermochim. Acta.* **2009**, *48*, *2*21–29.

[11] Peyrin, E.; Guillaume, Y. C.; Guinchard, C. Characterization of solute binding at human serum albumin site II and its geometry using a biochromatographic approach, *Biophys. J.* **1999**, *77*, 1206–1212.

[12] Trnkova, L.; Bousova, I.; Kubicek, V.; Drsata, Binding of naturally occurring hydroxycinnamic acids to bovine serum albumin, *J. Nat. Sci.* **2010**, *2*, 563–570.

4.9 Annexure

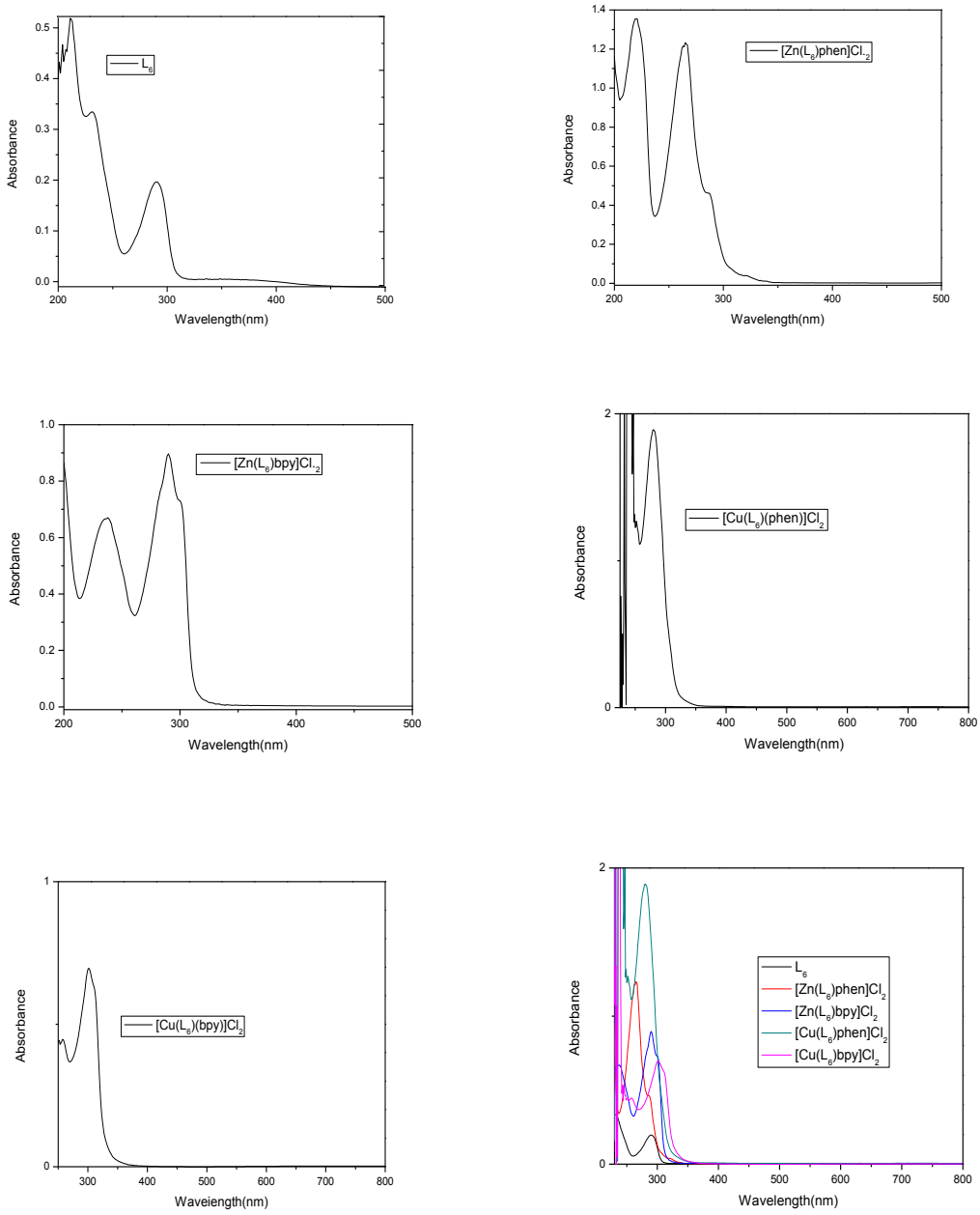

Annexure 4a: UV spectra of (L_6) Schiff base and its metal complexes

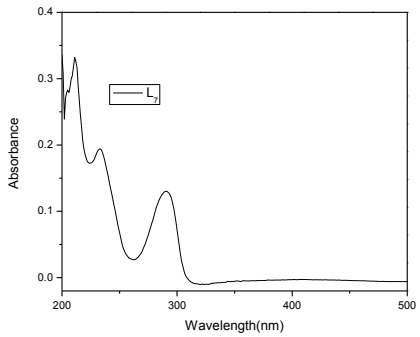

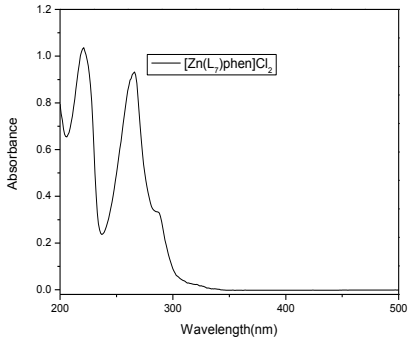

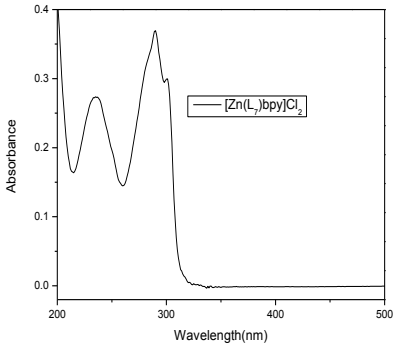

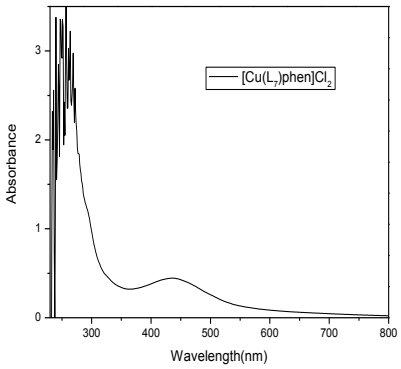

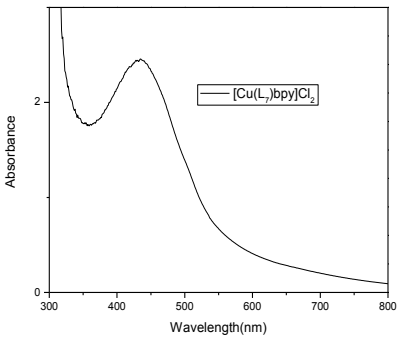

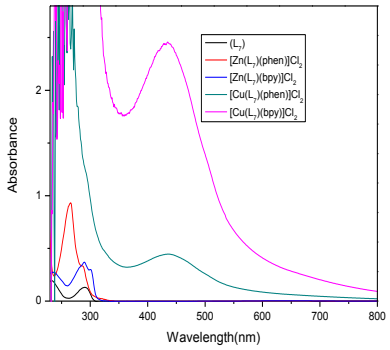

Annexure 4b: UV spectra of (L_7) Schiff base and its metal complexes

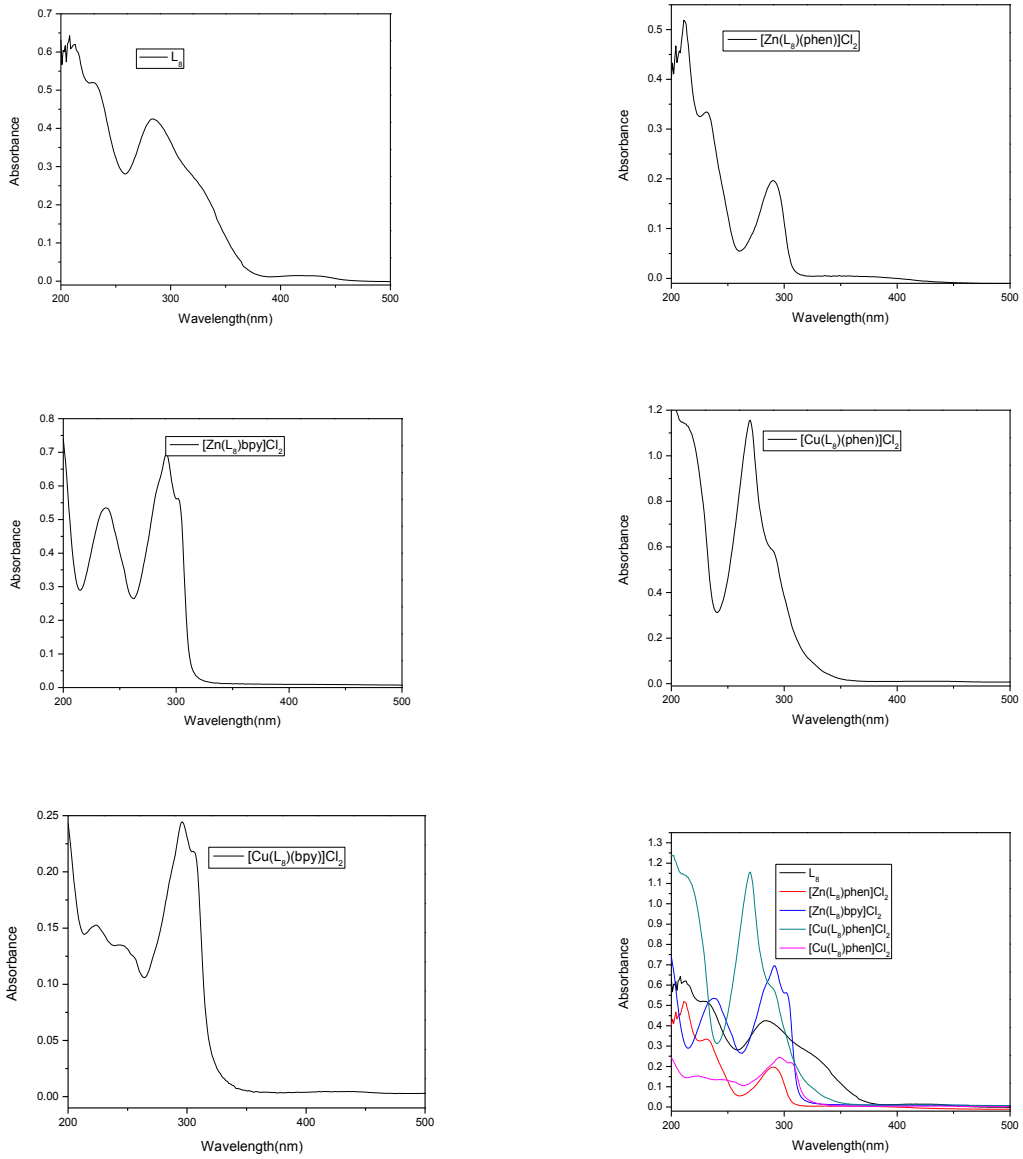

Annexure 4c: UV spectra of (L_8) Schiff base and its metal complexes

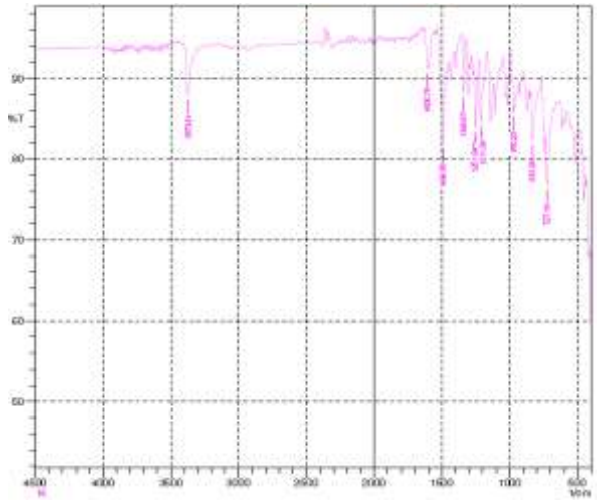

Annexure 4d: IR spectra of (L_6)

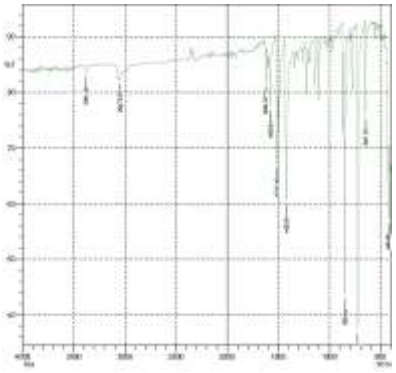

Annexure 4e: IR spectra of [$Zn(L_6)(phen)Cl_2$]

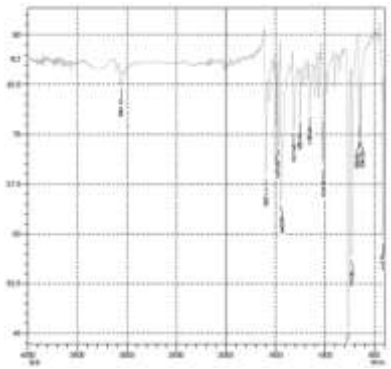

Annexure 4f: IR spectra of [$Zn(L_6)(bpy)Cl_2$]

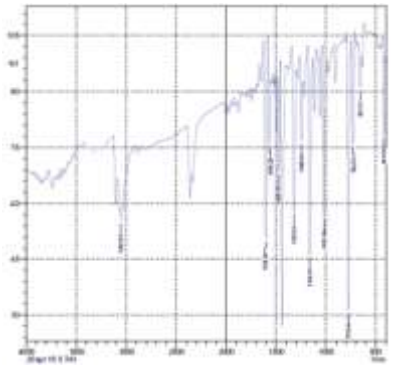

Annexure 4g: IR spectra of [$Cu(L_6)(phen)Cl_2$]

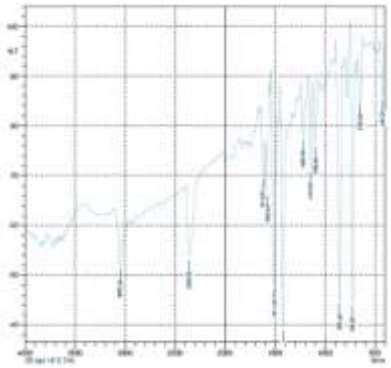

Annexure 4h: IR spectra of [$Cu(L_6)(bpy)Cl_2$]

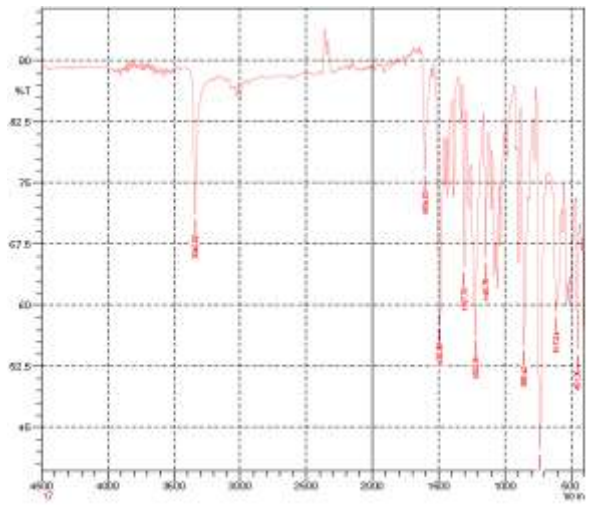

Annexure 4i: IR spectra of (L_7)

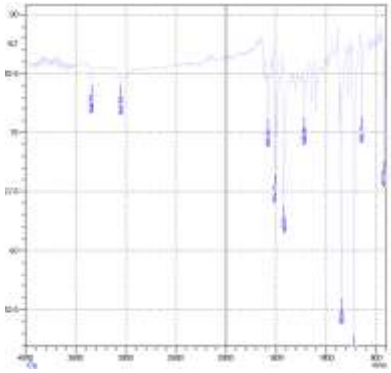

Annexure 4j: IR spectra of [Zn(L_7)(phen)Cl_2]

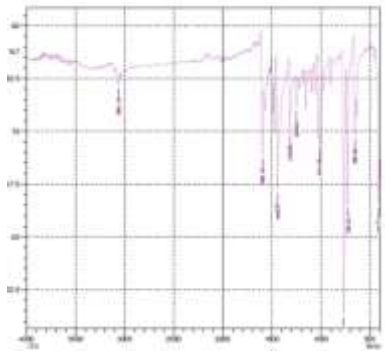

Annexure 4k: IR spectra of [Zn(L_7)(bpy)Cl_2]

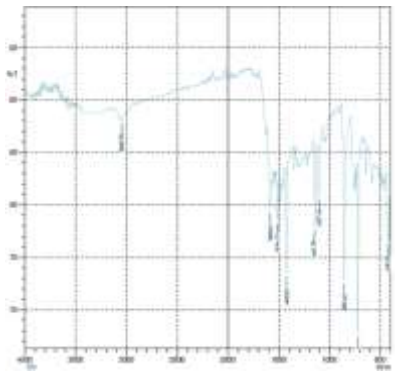

Annexure 4l: IR spectra of [Cu(L_7)(phen)Cl_2]

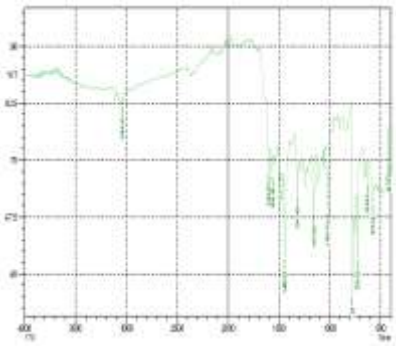

Annexure 4m: IR spectra of [Cu(L_7)(bpy)Cl_2]

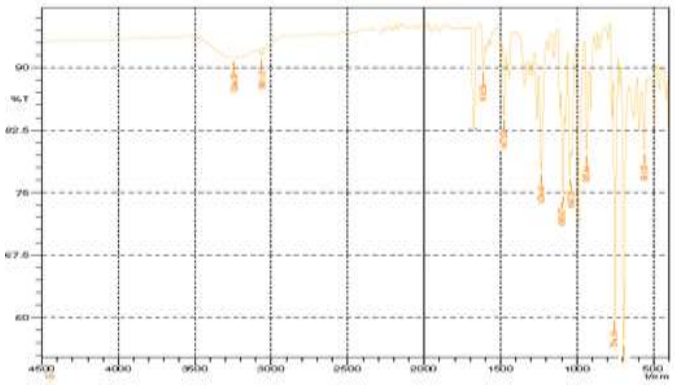

Annexure 4n: IR of (L_8)

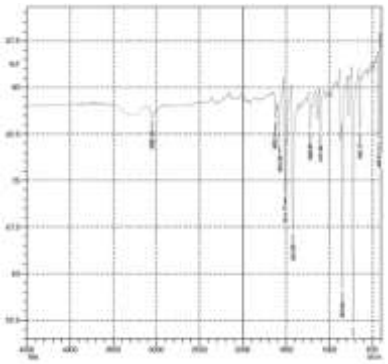

Annexure 4o: IR spectra of [Zn(L_8)(phen)Cl].H_2O

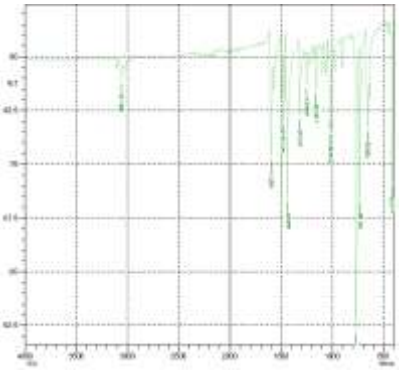

Annexure 4p: IR spectra of [Zn(L_8)(bpy)Cl].H_2O

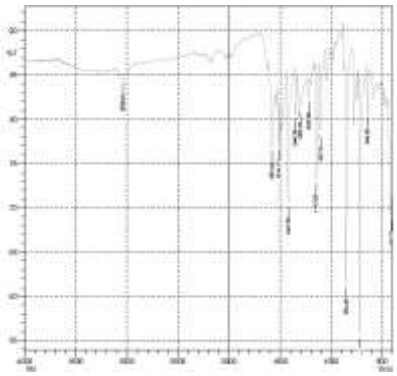

Annexure 4q: IR spectra of [Cu(L_8)(phen)Cl].H_2O

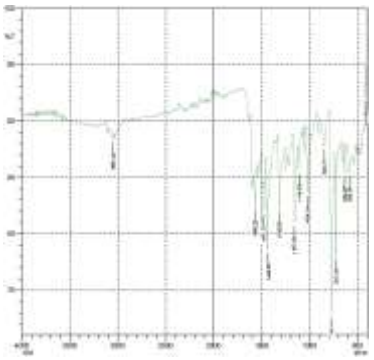

Annexure 4r: IR spectra of [Cu(L_8)(bpy)Cl].H_2O

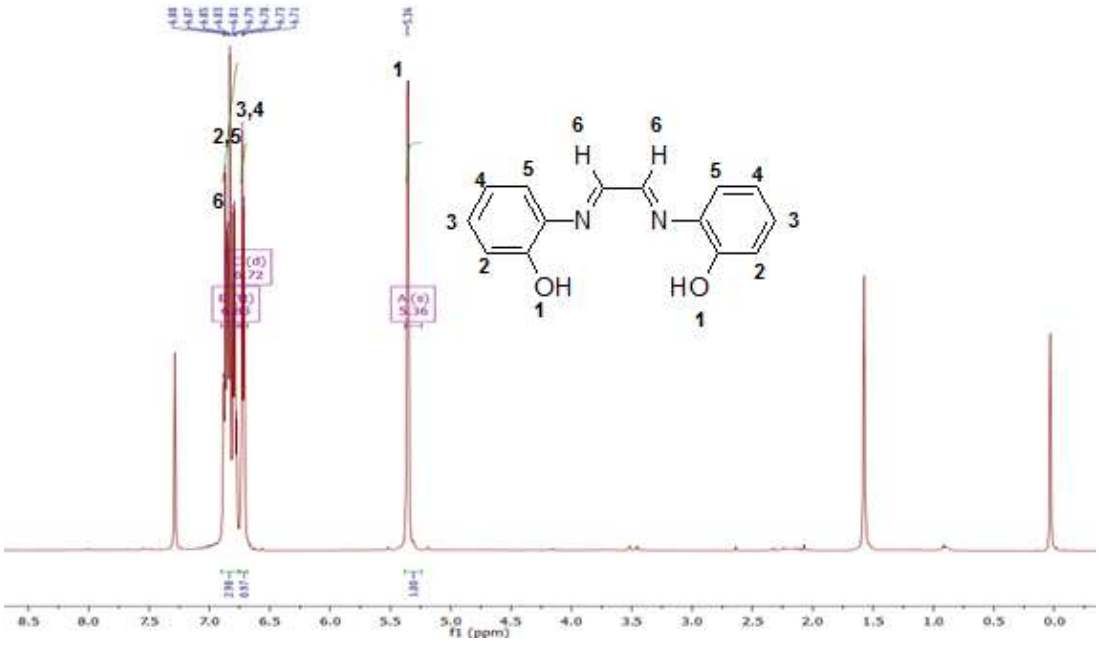

Annexure 4s: NMR of (L_6)

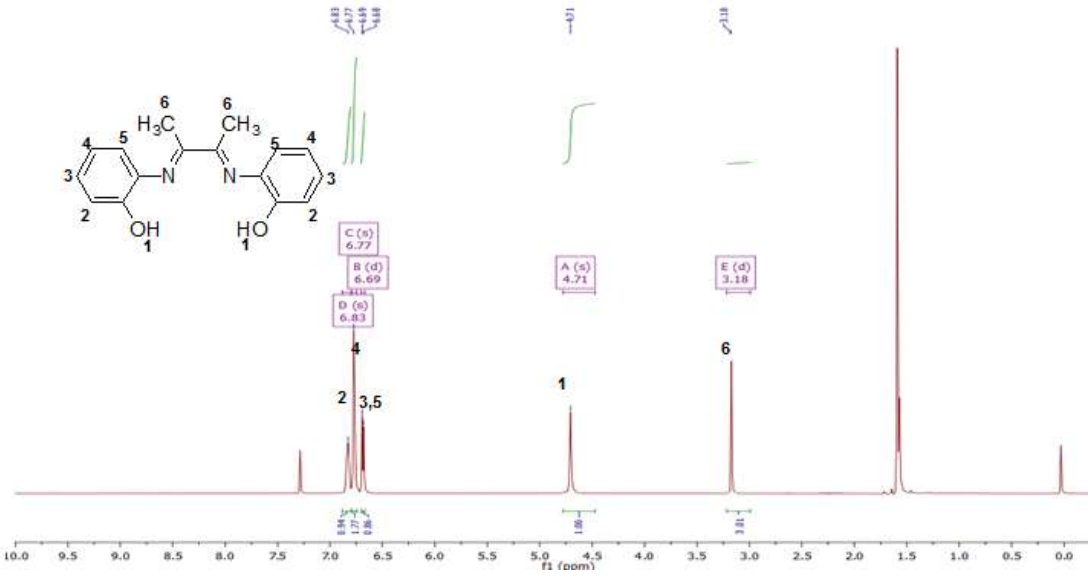

Annexure 4t: NMR of (L_7)

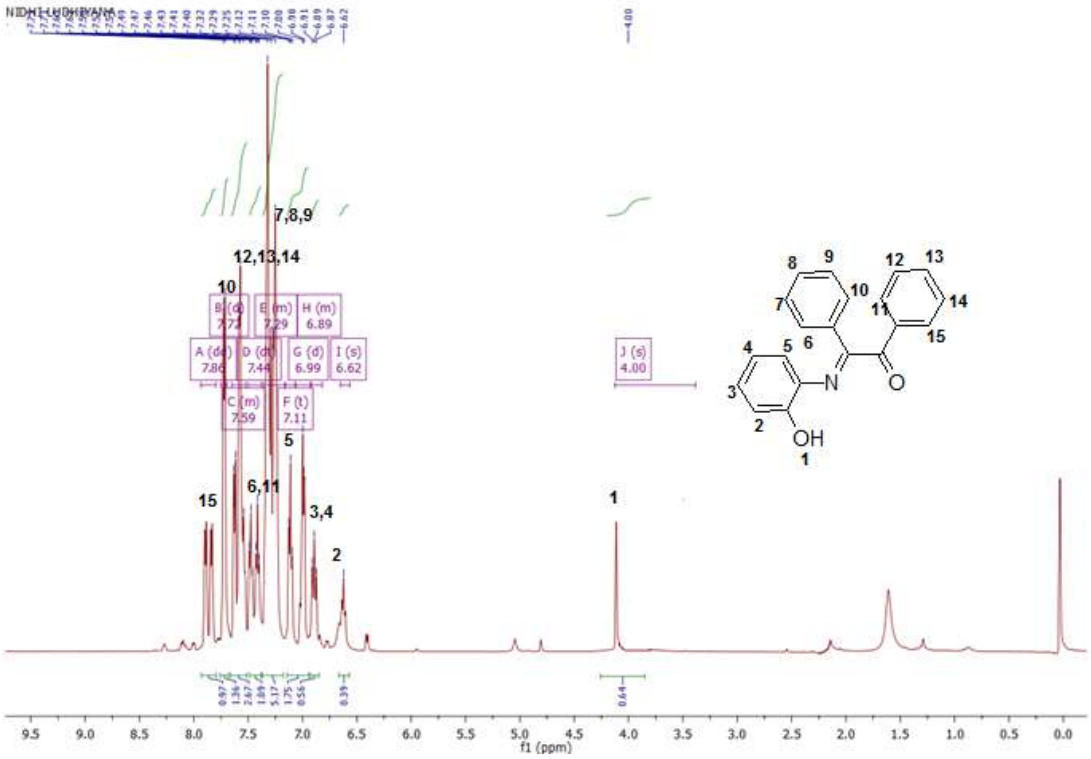

Annexure 4u: NMR of (L_8)

Chapter 5

Synthesis, characterization and biological activity of mixed ligand complexes of Zn(II) and Cu(II) metal ions with salicylic acid / 3,5-dinitrosalicylic acid as primary ligand and N, N' donor as secondary ligands

5.1 Introduction

The aim of the work in this chapter is to synthesize mixed ligand metal complexes of zinc and copper with salicylic acid / 3,5-dinitrosalicylic acid as primary and N, N' donor molecules (1,10- phenanthroline or 2,2'-bipyridine) as secondary ligands. The synthesized complexes were then characterized by various spectroscopic techniques viz. UV-vis, IR, NMR and mass spectral techniques. They were then analyzed for their biological activities against two bacterial species i.e. *Staphylococcus aureus* (gram positive) and *Escherichia coli* (gram negative) and two fungal species i.e. *Aspergillus niger* and *Aspergillus fumigatus* by well diffusion method. The complexes were also analyzed for their interaction with BSA by UV titration method.

5.2 Methodology

5.2.1 General scheme for the synthesis of metal complexes

The complexes were prepared by the following methodology:

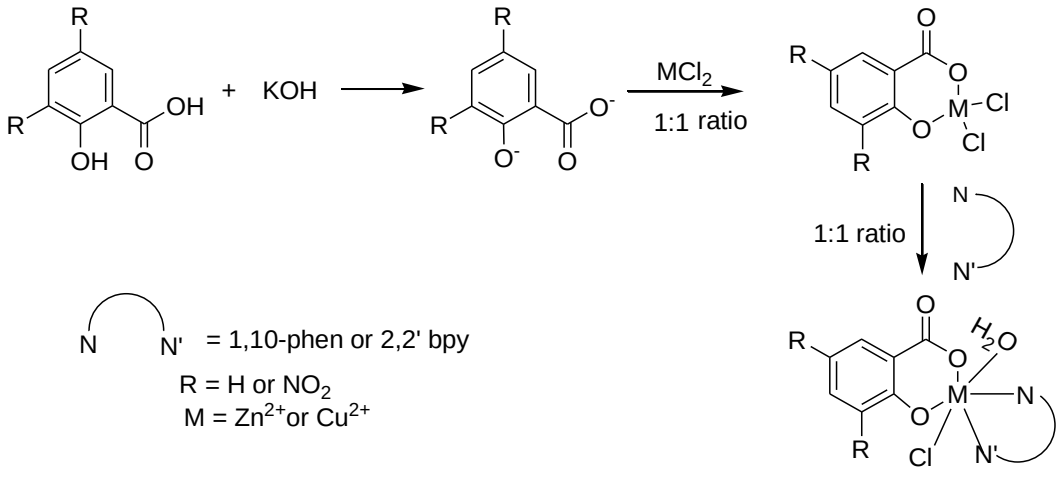

Fig. 132: General scheme for the preparation of the complexes

5.2.2 Methodology for the synthesis of [Zn(sal)(phen)]Cl *(33)*

0.552 g (0.004 mol) of salicylic acid and 0.22 g (0.004 mol) of KOH was dissolved separately in methanol (25 ml), two solutions were mixed and allowed to stir for 15 minutes. To this solution was added 0.545 g (0.004 mol) of $ZnCl_2$ in 25 ml methanol. The reaction mixture was refluxed for 2 h with constant stirring at 50ºC. A 20 ml methanolic solution of 0.792 g (0.004 mol) of 1,10-phenanthroline was added to reaction mixture and the solution mixture was refluxed for 3 h with constant stirring. The precipitates formed were filtered, washed with cold methanol and dried in desiccator for 3 - 4 days. Yield: 79 %, Color: Dull white, M.P. 175 - 177°C, UV (λ_{max}): 264 nm, MS: $[M]^+$ 436, Main IR peaks (cm^{-1}): υ(C_6H_5 stretch) 3057, υ(C-O) 1625, υ(M-O) 503, υ(M-N) 472.

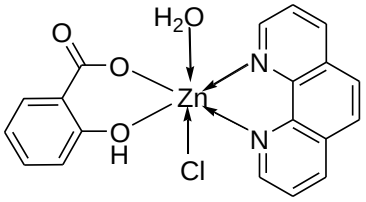

Fig. 133: Proposed geometry of [Zn(sal)(phen)]Cl *(33)*

5.2.3 Methodology for the synthesis of [Zn(sal)(bpy)]Cl *(34)*

0.552 g (0.004 mol) of salicylic acid and 0.22 g (0.004 mol) of KOH was dissolved separately in methanol (25 ml), two solutions were mixed and allowed to stir for 15 minutes. To this solution was added 0.545 g (0.004 mol) of $ZnCl_2$ in 25 ml methanol. The reaction mixture was refluxed for 2 h with constant stirring at 50ºC. A 20 ml methanolic solution of 0.625 g (0.004 mol) of 2,2'-bipyridine was added to reaction mixture and the solution mixture was refluxed for 3 h with constant stirring. The precipitates formed were filtered, washed with cold methanol and dried in desiccator for 3 - 4 days. Yield: 84 %, Color: White, M.P. Starts decomposing at 230°C, UV (λ_{max}): 245 nm, MS: $[M]^+$ 567, Main IR peaks (cm^{-1}): υ(C_6H_5 stretch) 3031, υ(C-O) 1627, υ(M-O) 560, υ(M-N) 412.

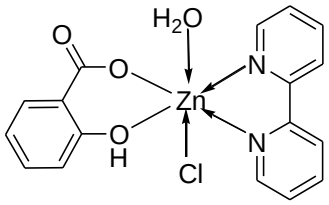

Fig. 134: Proposed geometry of [Zn(sal)(bpy)]Cl *(34)*

5.2.4 Methodology for the synthesis of [Zn(DNSA)(phen)]Cl *(35)*

0.912 g (0.004 mol) of 3,5-dinitrosalicylic acid and 0.22 g (0.004 mol) of KOH separately in methanol (25 ml), two solutions were mixed and allowed to stir for 15 minutes. To this solution was added 0.545 g (0.004 mol) of $ZnCl_2$ in 25 ml methanol. The reaction mixture was refluxed for 3 h with constant stirring at 50ºC. A 20 ml methanolic solution of 0.792 g (0.004 mol) of 1,10-phenanthroline was added to reaction mixture and the solution mixture was refluxed for 3 h with constant stirring. The precipitates formed were filtered, washed with cold methanol and dried in desiccator for 3 - 4 days. Yield: 81 %, Color: Brownish yellow, M.P. 198 - 200°C, UV (λ_{max}): 280 nm, 364 nm, MS: $[M]^+$ 545, Main IR peaks (cm^{-1}): $\upsilon(C_6H_5$ stretch) 3051, υ(C-O) 1622, $\upsilon(NO_2)$ 1518, υ(M-O) 507, υ(M-N) 490.

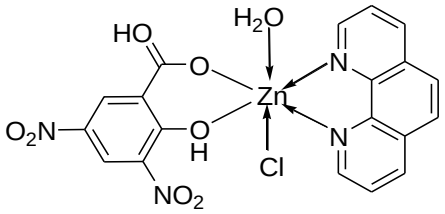

Fig. 135: Proposed geometry of [Zn(DNSA)(phen)]Cl *(35)*

5.2.5 Methodology for the synthesis of [Zn(DNSA)(bpy)]Cl *(36)*

0.912 g (0.004 mol) of 3,5-dinitrosalicylic acid and 0.22 g (0.004 mol) of KOH separately in methanol (25 ml), two solutions were mixed and allowed to stir for 15 minutes. To this solution was added 0.545 g (0.004 mol) of $ZnCl_2$ in 25 ml methanol. The reaction mixture was refluxed for 3 h with constant stirring at 50ºC. A 20 ml methanolic solution of 0.625 g (0.004 mol) of 2,2'-bipyridine was added to

reaction mixture and the solution mixture was refluxed for 3 h with constant stirring. The precipitates formed were filtered, washed and dried in desiccator for 3 - 4 days. Yield: 86 %, Color: Brownish yellow, M.P. 220 - 222°C, UV (λ_{max}): 276 nm, 363 nm, MS: $[M]^+$ 658, Main IR peaks (cm^{-1}): υ(C_6H_5 stretch) 3071, υ(C-O) 1656, υ(NO_2) 1525, υ(M-O) 544, υ(M-N) 493.

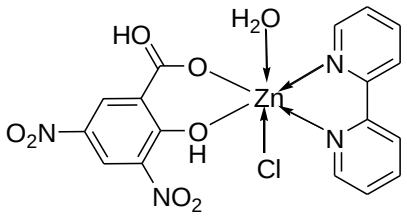

Fig. 136: Proposed geometry of [Zn(DNSA)(bpy)]Cl *(36)*

5.2.6 Methodology for the synthesis of [Cu(sal)(phen)]Cl *(37)*

0.552 g (0.004 mol) of salicylic acid and 0.22 g (0.004 mol) of KOH was dissolved separately in methanol (25 ml), two solutions were mixed and allowed to stir for 15 minutes. To this solution was added 0.682g (0.004 mol) of $CuCl_2.2H_2O$ in 25 ml methanol. The reaction mixture was refluxed for 2 h with constant stirring at 50ºC. A 20 ml methanolic solution of 0.792 g (0.004 mol) of 1,10-phenanthroline was added to reaction mixture and the solution mixture was refluxed for 3 h with constant stirring. The precipitates formed were filtered, washed with cold methanol and dried in desiccator for 3 - 4 days. Yield: 82 %, Color: Green, M.P. 235 - 236°C, UV (λ_{max}): 294 nm, MS: $[M]^+$ 613, Main IR peaks (cm^{-1}): υ(OH) 3200-3400; υ(C_6H_5 stretch) 3053, υ(C-O) 1600, υ(M-O) 642, υ(M-N) 440.

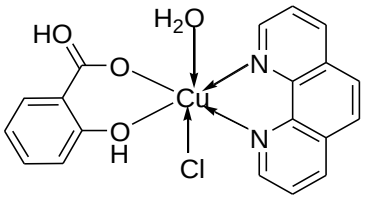

Fig. 137: Proposed geometry of [Cu(sal)(phen)]Cl *(37)*

5.2.7 Methodology for the synthesis of [Cu(sal)(bpy)]Cl *(38)*

0.552 g (0.004 mol) of salicylic acid and 0.22 g (0.004 mol) of KOH was dissolved separately in methanol (25 ml), two solutions were mixed and allowed to stir for 15 minutes. To this solution was added 0.682g (0.004 mol) of $CuCl_2.2H_2O$ in 25 ml methanol. The reaction mixture was refluxed for 2 h with constant stirring at 50ºC. A 20 ml methanolic solution of 0.625 g (0.004 mol) of 2,2'-bipyridine was added to reaction mixture and the solution mixture was refluxed for 3 h with constant stirring. The precipitates formed were filtered, washed and dried in desiccator for 3 - 4 days. Yield: 80 %, Color: Green, M.P. 220 - 222°C, UV (λ_{max}): 268 nm, MS: $[M]^+$ 548, Main IR peaks (cm^{-1}): υ(OH) 3200–3400, υ(C_6H_5 stretch) 3057, υ(C-O) 1624, υ(NO_2) 1514, υ(M-O) 646, υ(M-N) 430.

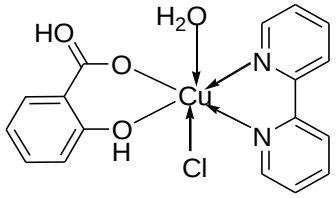

Fig. 138: Proposed geometry of [Cu(sal)(bpy)]Cl *(38)*

5.2.8 Methodology for the synthesis of [Cu(DNSA)(phen)]Cl *(39)*

0.912 g (0.004 mol) of 3,5-dinitrosalicylic acid and 0.22 g (0.004 mol) of KOH separately in methanol (25 ml), two solutions were mixed and allowed to stir for 15 minutes. To this solution was added 0.682g (0.004 mol) of $CuCl_2.2H_2O$ in 25 ml methanol. The reaction mixture was refluxed for 3 h with constant stirring at 50ºC. A 20 ml methanolic solution of 0.792 g (0.004 mol) of 1,10-phenanthroline was added to reaction mixture and the solution mixture was refluxed for 3 h with constant stirring. The precipitates formed were filtered, washed with cold methanol and dried in desiccator for 3 - 4 days. Yield: 80 %, Color: Green, M.P. 244 - 245°C, UV (λ_{max}): 271 nm, 367 nm, MS: $[M]^+$ 596, Main IR peaks (cm^{-1}): υ(OH) 3200–3400, υ(C_6H_5 stretch) 3032, υ(C-O) 1599, υ(NO_2) 1514, υ(M-O) 636, υ(M-N) 416.

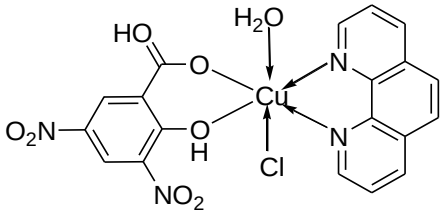

Fig. 139: Proposed geometry of [Cu(DNSA)(phen)]Cl *(39)*

5.2.9 Methodology for the synthesis of [Cu(DNSA)(bpy)]Cl *(40)*

0.912 g (0.004 mol) of 3,5-dinitrosalicylic acid and 0.22 g (0.004 mol) of KOH separately in methanol (25 ml), two solutions were mixed and allowed to stir for 15 minutes. To this solution was added 0.682g (0.004 mol) of $CuCl_2.2H_2O$ in 20 ml methanol and 5 ml water solvent mixture. The reaction mixture was refluxed for 3 h with constant stirring at 50ºC. A 20 ml methanolic solution of 0.625 g (0.004 mol) of 2,2'-bipyridine was added to reaction mixture and the solution mixture was refluxed for 3 h with constant stirring. The precipitates formed were filtered, washed with cold methanol and dried in desiccator for 3 - 4 days. Yield: 81 %, Color: Green, M.P. 228 - 230°C, UV (λ_{max}): 301 nm, 356 nm, MS: $[M]^+$ 554, Main IR peaks (cm^{-1}): υ(OH) 3200–3400, υ(C_6H_5 stretch) 3034, υ(C-O) 1645, υ(NO_2) 1521, υ(M-O) 661, υ(M-N) 416.

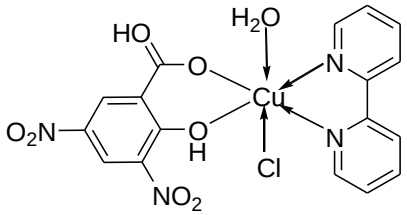

Fig. 140: Proposed geometry of [Cu(DNSA)(bpy)]Cl *(40)*

5.3 Results and discussions

The Cu^{2+} mixed ligand chelates appear as colored precipitates while Zn^{2+} complexes appear as white precipitates. All of them were found to be thermally stable and of non hygroscopic nature. They were having fair solubility in water, DMSO, DMF and Tris buffer (pH 7.4).

5.3.1 UV-vis analysis

The results of the UV-vis absorption studies of metal complexes were recorded in the range of 200 - 800 nm at low concentrations using water / DMSO as solvent. The bands observed indicates π to π^* and n to π^* transitions which confirm binding of 1,10-phenanthroline or 2,2'-bipyridine with metal centers.

5.3.2 FTIR analysis

The significant peak of carbonyl stretch in the range of 1599 - 1656 cm^{-1} as compared to 1670 cm^{-1} in the free salicylic acid molecule showed the bonding nature of carboxylic acid group. Another absorption peaks in the 1510 cm^{-1} region of metal complexes are due to $-NO_2$ stretching vibrations. The characteristic absorption bands at 410 - 490 cm^{-1} suggest coordination of M-N bond and at 500 - 650 cm^{-1} represents M-O bonds in the complexes. A broad band in the region of 3200 - 3400 cm^{-1} suggests presence of coordinated or lattice water (Table 23).

Table 23: Selected bond frequencies (cm^{-1}) of synthesized complexes

Complex	$\nu_{(C=O)}$ **(cm^{-1})**	$\nu_{(M-N)}$ **(cm^{-1})**	$\nu_{(M-O)aryl}$ **(cm^{-1})**	**C_6H_5 stretch (cm^{-1})**	**ν (NO_2) of 3,5 DNSA (cm^{-1})**	**Lattice / Coordinated water**	**π to π* transition (nm)**	**n to π* transition (nm)**
[Zn(sal)(phen)]Cl ***(33)***	1625	472	503	3057	-	-	264	-
[Zn(sal)(bpy)]Cl ***(34)***	1627	412	560	3031	-	-	245	-
[Zn(DNSA)(phen)]Cl (***35)***	1622	490	507	3051	1518	-	280	364
[Zn(DNSA)(bpy)]Cl ***(36)***	1656	493	544	3071	1525	-	276	363
[Cu(sal)(phen)]Cl ***(37)***	1600	440	642	3053	-	3200-3400	294	-
[Cu(sal)(bpy)]Cl ***(38)***	1624	430	646	3057	1514	3200-3400	268	-
[Cu(DNSA)(phen)]Cl ***(39)***	1599	416	636	3032	-	3200-3400	271	367
[Cu(DNSA)(bpy)]Cl ***(40)***	1645	416	661	3034	1521	3200-3400	301	356

5.3.3 Mass spectral analysis

The mass fragmentation pattern of the complexes has been tabulated as follows:

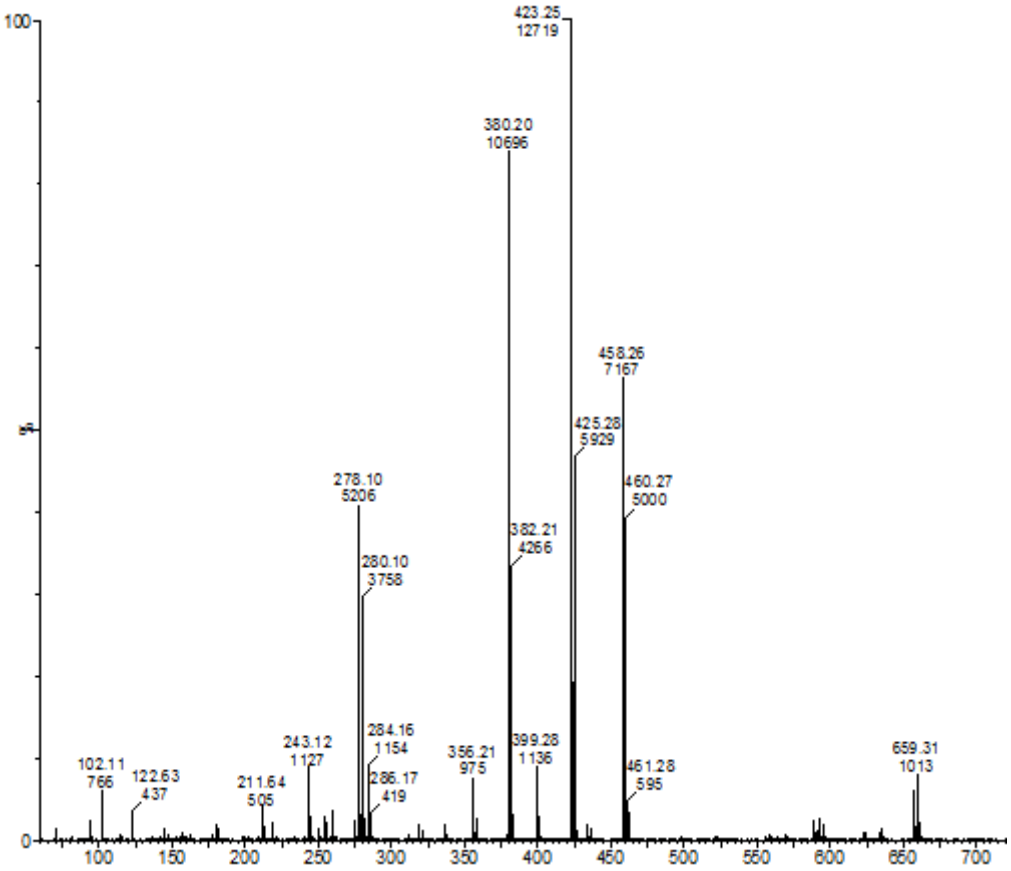

Fig. 141: Mass spectra of [Zn(sal)(phen)]Cl *(33)*

m/z	**Loss of**	**Fragment**
596		[Zn(sal)(phen)$_2$Cl]
425	Sal, Cl	[Zn(phen)$_2$]
381		[Zn(sal)(phen)]
245	phen	[Zn(phen)]

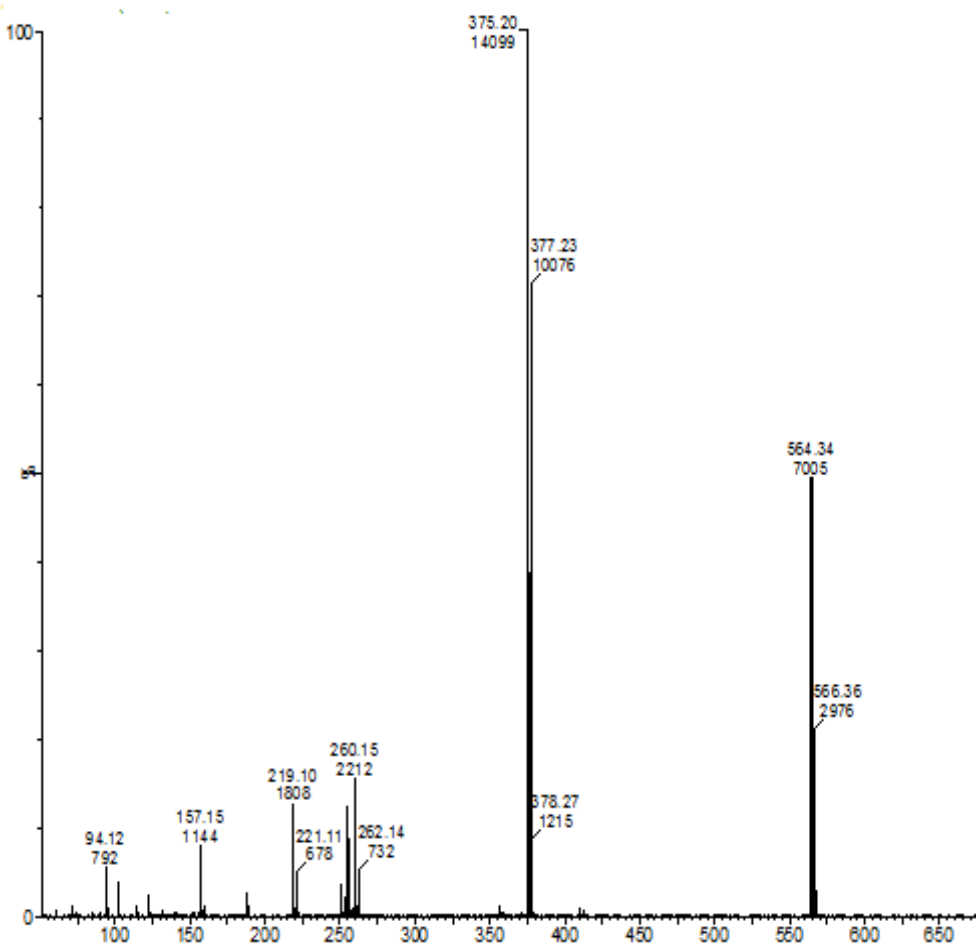

Fig.142: Mass spectra of [Zn(sal)(bpy)]Cl *(34)*

m/z	**Loss of**	**Fragment**
567		$[Zn(sal)(bpy)_2Cl].H_2O$
376	sal	$[Zn(sal)(bpy)H_2O]$
221	Cl	[Zn(bpy)]
156		Free bpy

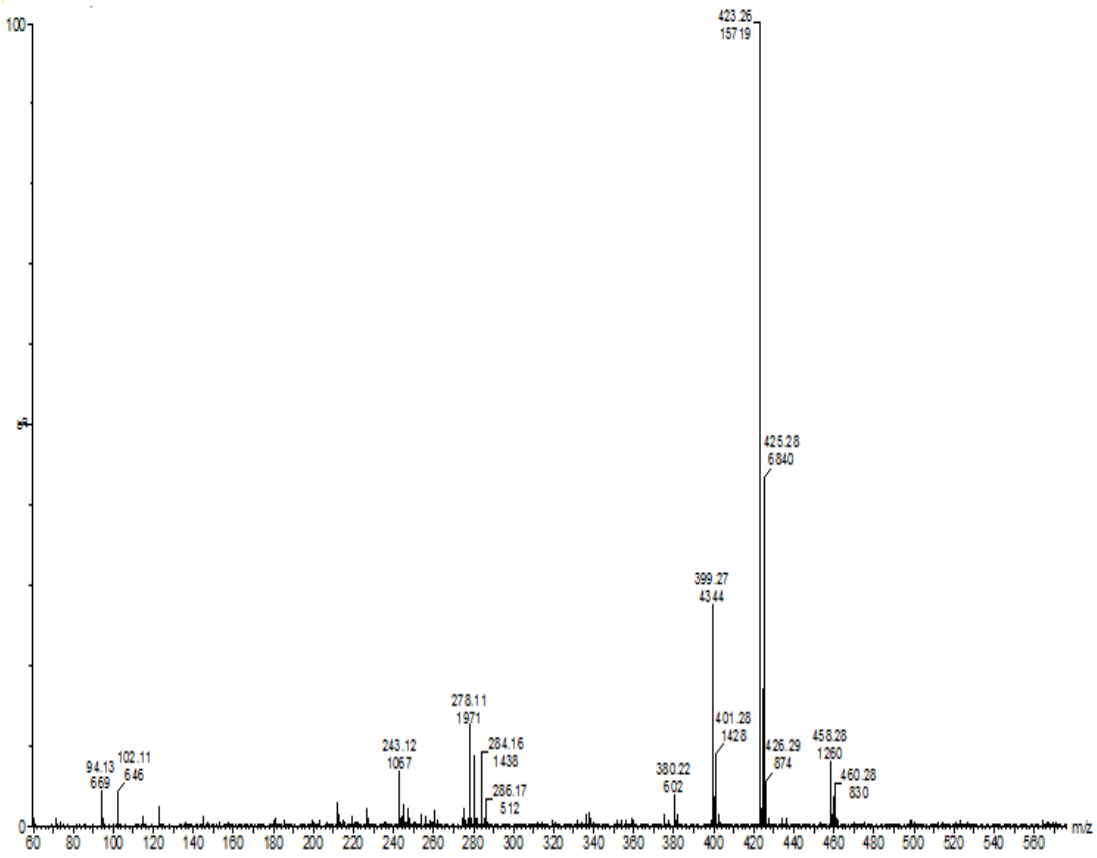

Fig. 143: Mass spectra of [Zn(DNSA)(phen)]Cl *(35)*

m/z	**Loss of**	**Fragment**
507		[Zn(DNSA)(phen)Cl]
425	2 H_2O, NO_2	[Zn(DNSA)(phen)]
245		[Zn(phen)]

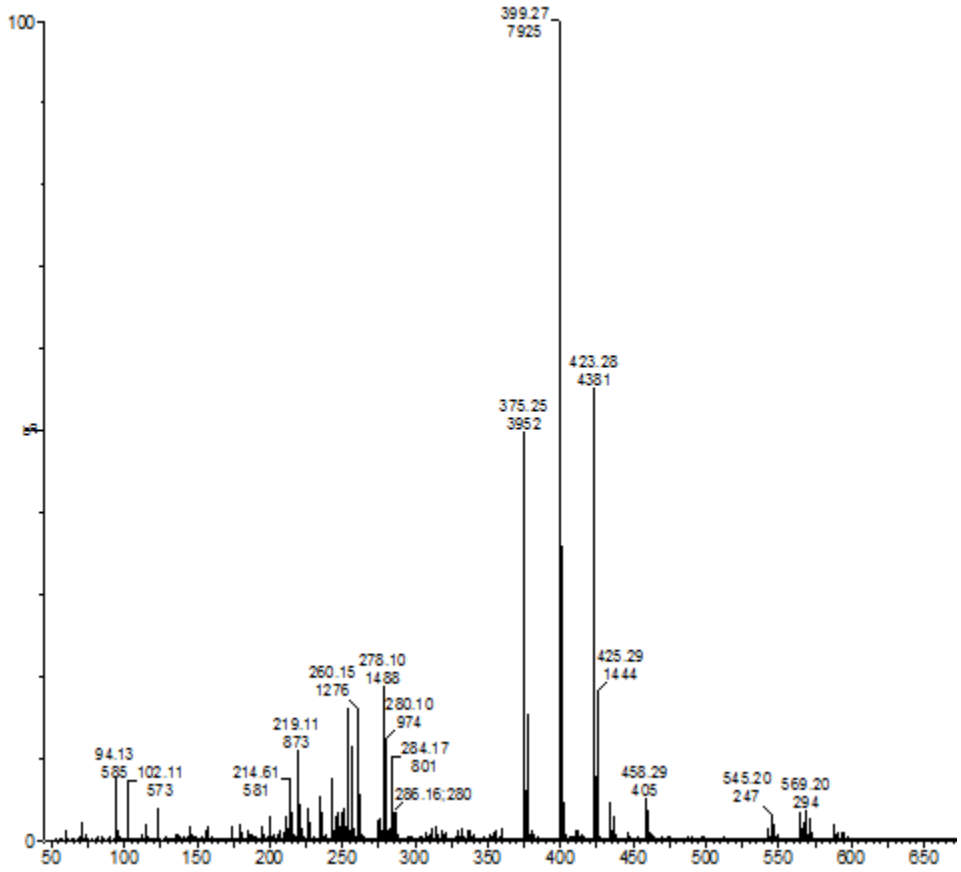

Fig. 144: Mass spectra of [Zn(DNSA)(bpy)]Cl *(36)*

m/z	**Loss of**	**Fragment**
483		[Zn(DNSA)(bpy)Cl]
401	Cl, NO_2	[Zn(DNSA)(bpy)]
377	DNSA	$[Zn(bpy)_2]$
221	bpy	[Zn(bpy)]

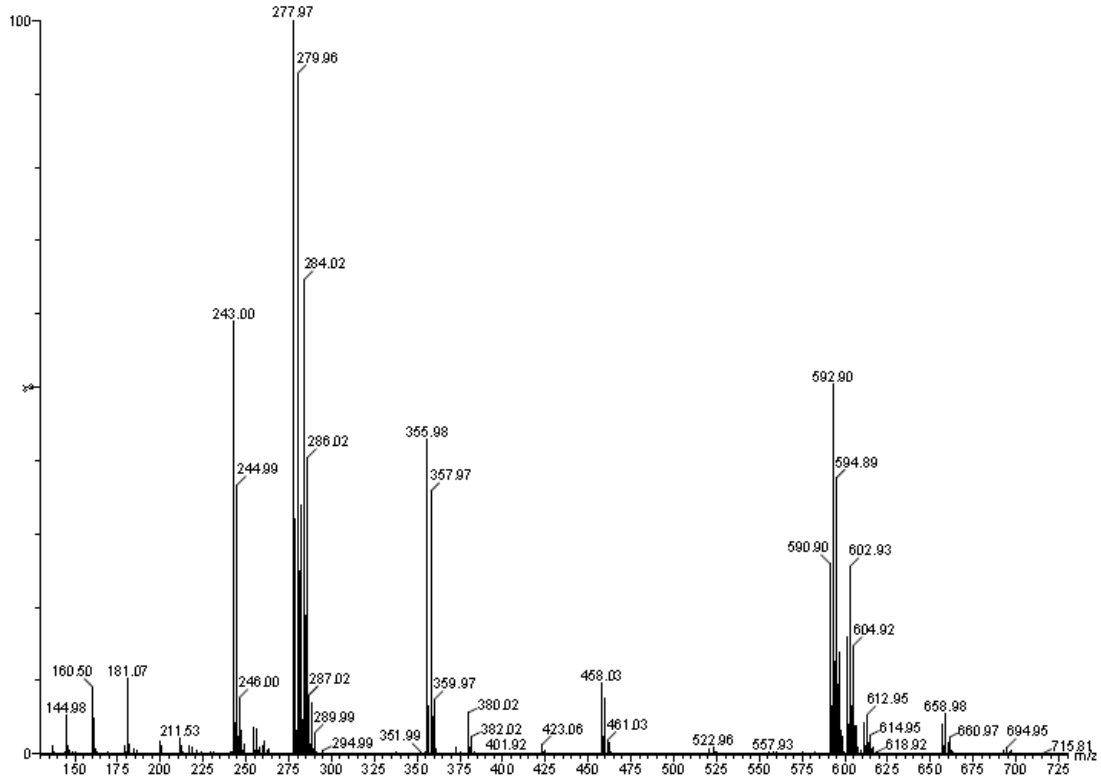

Fig. 145: Mass spectra of [Cu(sal)(phen)]Cl *(37)*

m/z	**Loss of**	**Fragment**
596		[Cu(sal)$(phen)_2$Cl]
355		[Cu$(sal)_2H_2O$]
279	phen	[Cu(phen)Cl]
243	Cl	[Cu(phen)]
180	Cu	Free phen

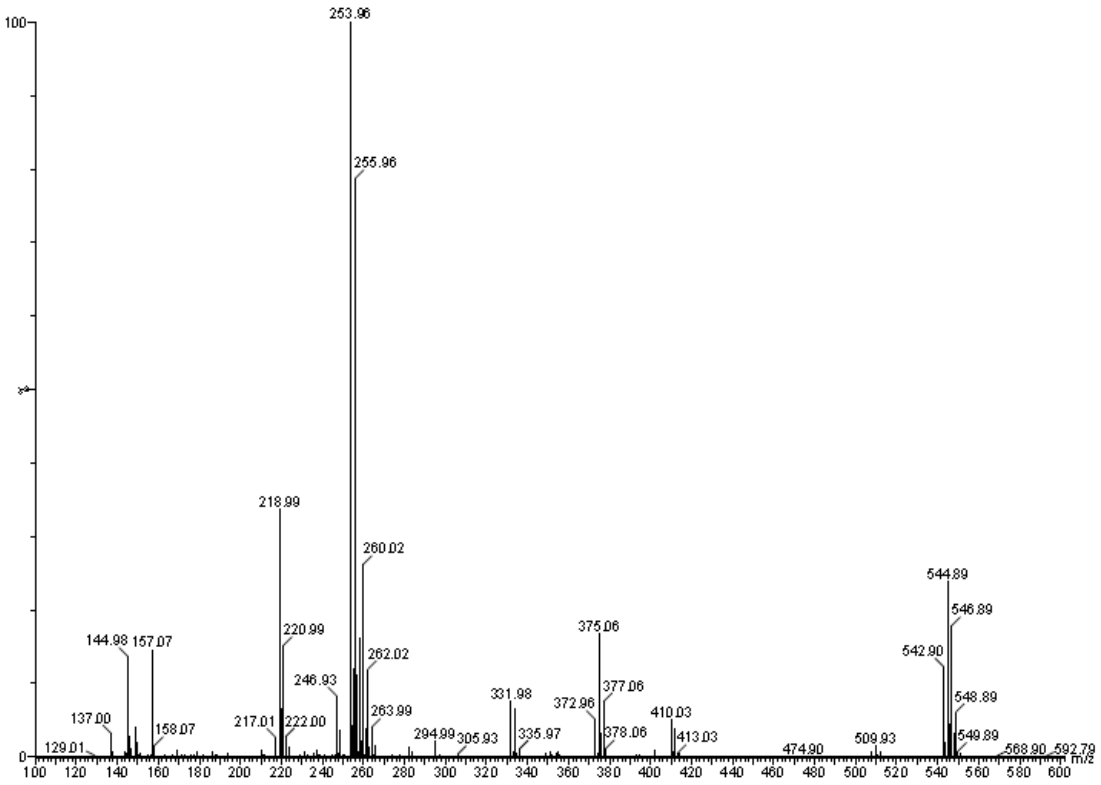

Fig. 146: Mass spectra of [Cu(sal)(bpy)]Cl *(38)*

m/z	**Loss of**	**Fragment**
548		$[Cu(sal)(bpy)_2Cl]$
411	sal	$[Cu(bpy)_2\ Cl]$
255	bpy	[Cu(bpy)Cl]
219	Cl	[Cu(bpy)]
156	Cu	Free bpy

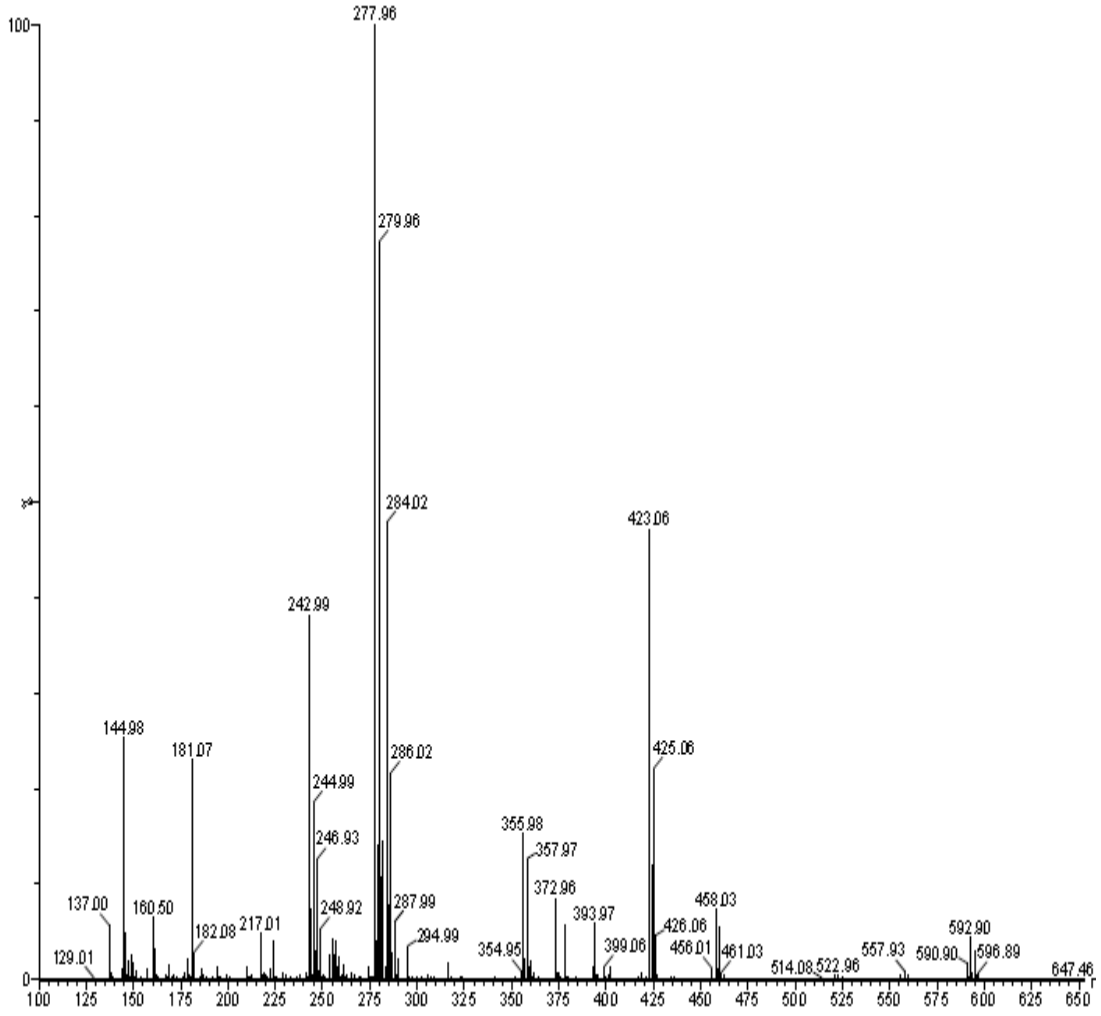

Fig. 147: Mass spectra of [Cu(DNSA)(phen)Cl] ***(39)***

m/z	**Loss of**	**Fragment**
506		[Cu(DNSA)(phen)Cl]
423	NO_2, H_2O	[Cu(DNSA)(phen)]
279		[Cu(phen)Cl]
243	phen	[Cu(phen)]
180	Cu	Free phen

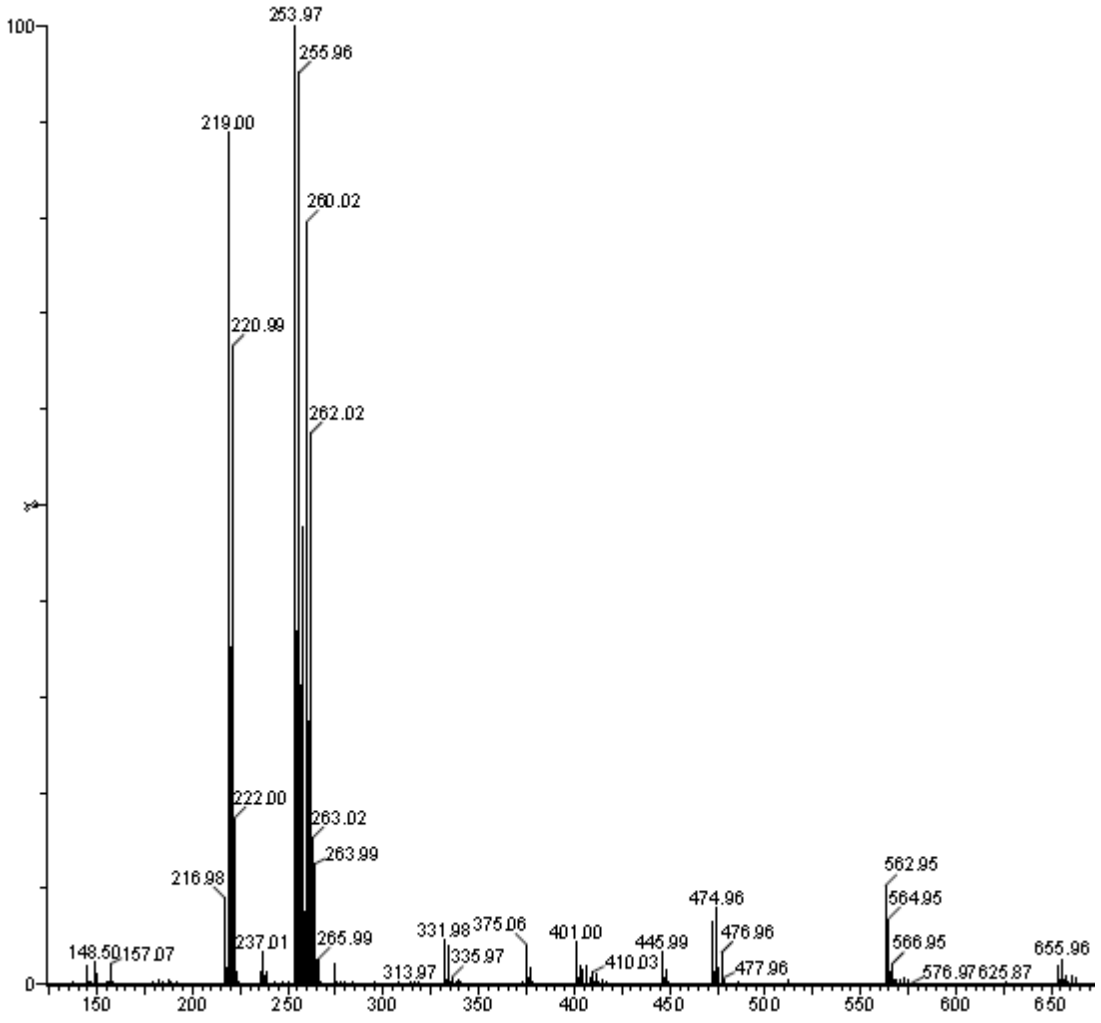

Fig. 148: Mass spectra of [Cu(DNSA)(bpy)]Cl *(40)*

m/z	**Loss of**	**Fragment**
482		[Cu(DNSA)(bpy)]Cl
255	DNSA	[Cu(bpy)Cl]
219	Cl	[Cu(bpy)]
156	Cu	Free bpy

5.4 UV-vis absorption studies of BSA

The same procedure is followed as in section 2.5 of Chapter 2.

Table 24: Values of binding constant (K_b M^{-1})

Complex	**K_b M^{-1}**
[Zn(sal)(phen)]Cl ***(33)***	-
[Zn(sal)(bpy)]Cl ***(34)***	2.35×10^5
[Zn(DNSA)(phen)]Cl (***35)***	2.46×10^5
[Zn(DNSA)(bpy)]Cl ***(36)***	3.80×10^4
[Cu(sal)(phen)]Cl ***(37)***	3.60×10^5
[Cu(sal)(bpy)]Cl ***(38)***	1.25×10^5
[Cu(DNSA)(phen)]Cl ***(39)***	4.80×10^4
[Cu(DNSA)(bpy)]Cl ***(40)***	9.60×10^4

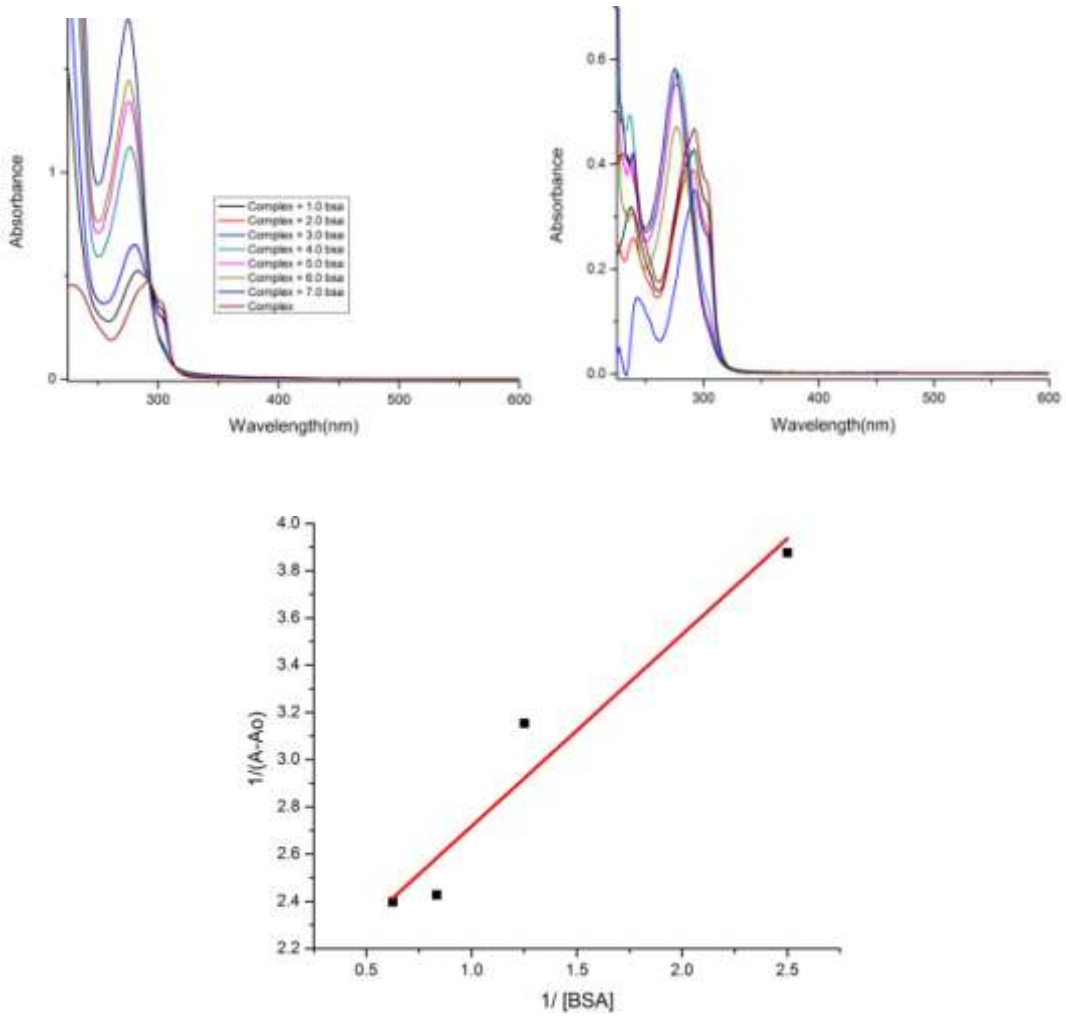

Fig. 149: A) UV-vis titration graphs of complex [Zn(sal)(bpy)]Cl (50 μM) with incremental [BSA] concentration in the range of 0 – 3 μM,

(B) Graph of {[BSA complex with [Zn(sal)(bpy)]Cl – [Variant concentrations of [BSA]},

(C) Graph of 1 / (A-A_0) vs. 1 / [BSA] concentration

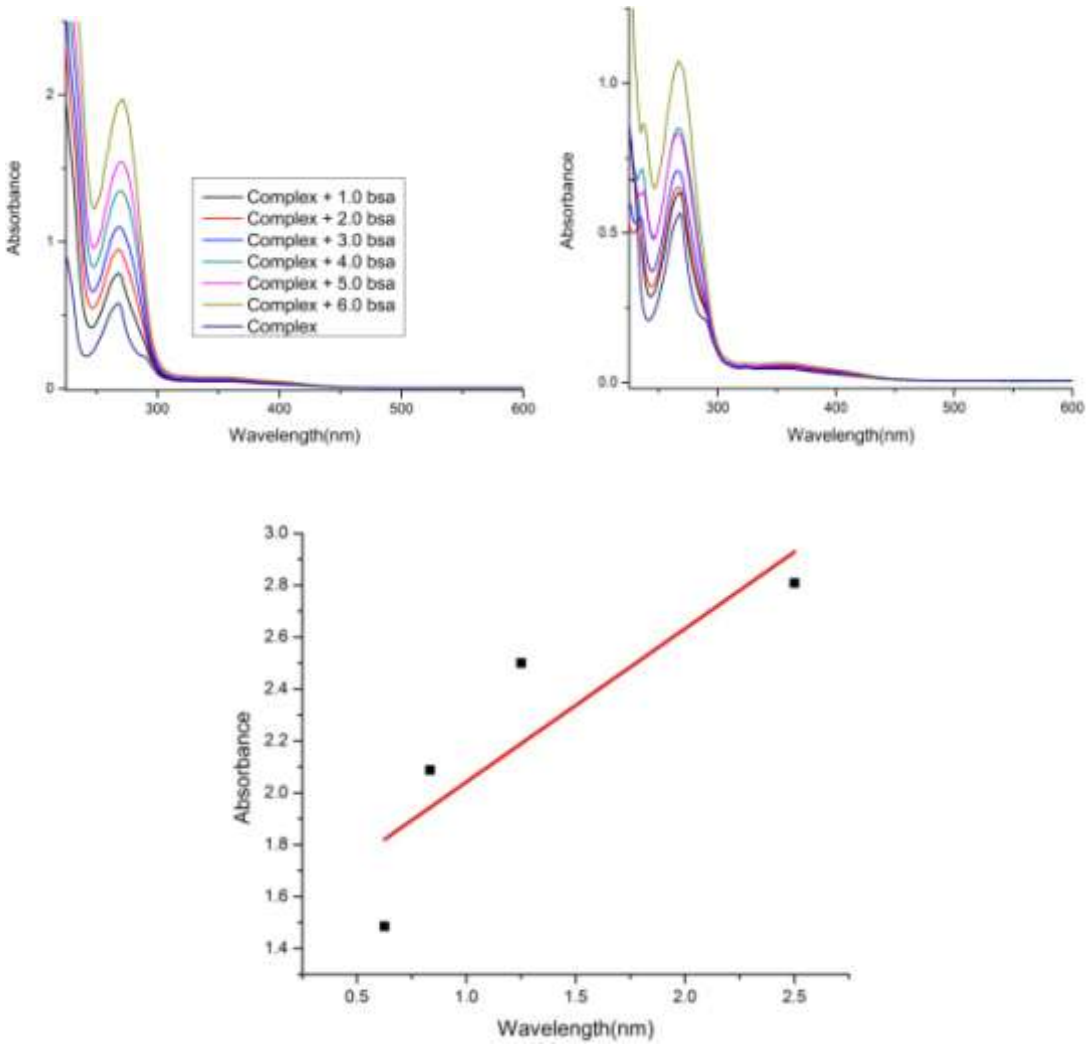

Fig. 150: (A) UV-vis titration graphs of complex [Zn(DNSA)(phen)]Cl (50 μM) with incremental [BSA] concentration in the range of 0 – 3 μM,

(B) Graph of {[BSA complex with [Zn(DNSA)(phen)]Cl – [Variant concentrations of [BSA]},

(C) Graph of 1 / (A-A_0) vs. 1 / [BSA] concentration

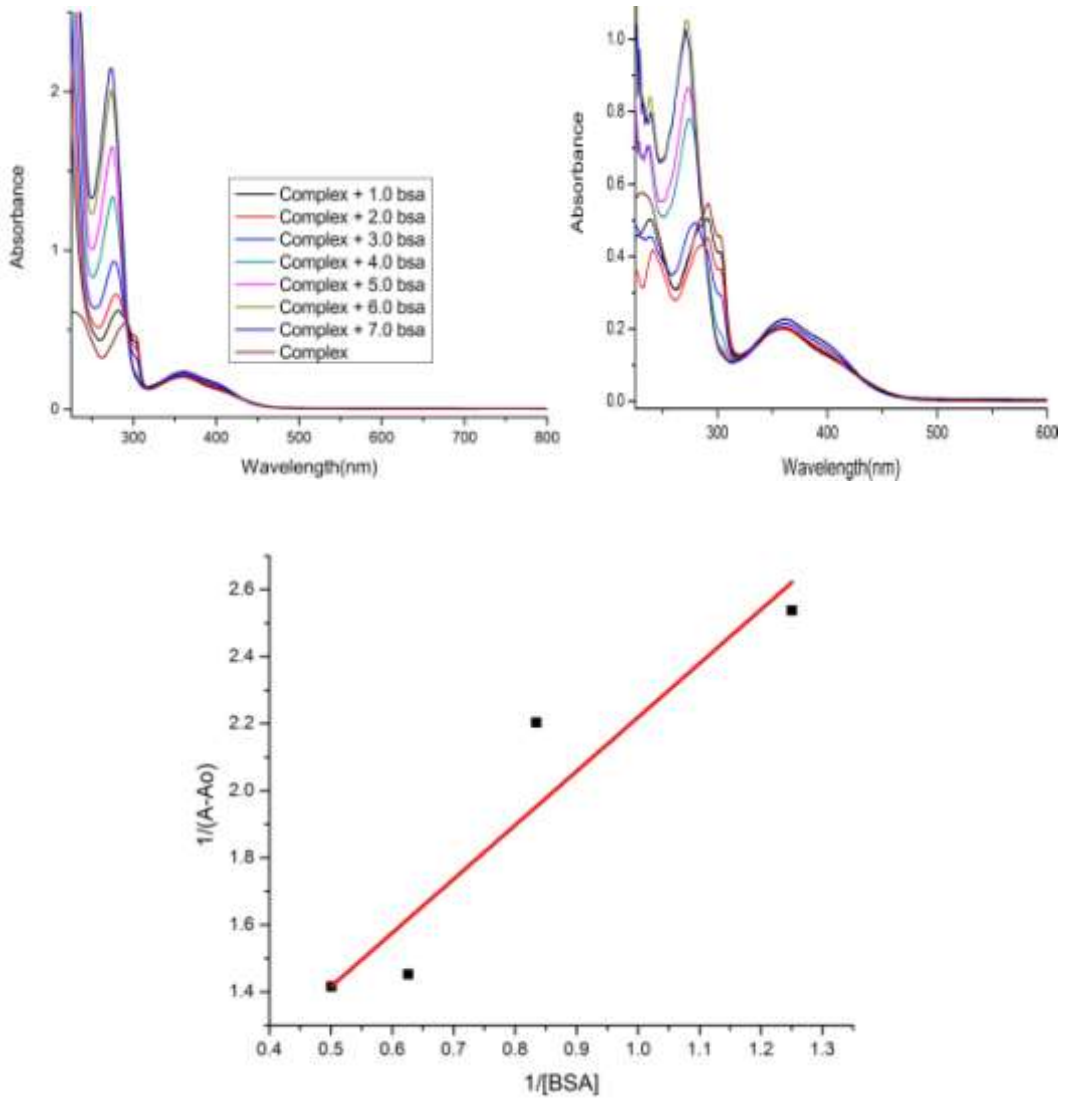

Fig. 151: (A) UV-vis titration graphs of complex [Zn(DNSA)(bpy)]Cl (50 μM) with incremental [BSA] concentration in the range of 0 – 3 μM,

(B) Graph of {[BSA complex with [Zn(DNSA)(bpy)]Cl – [Variant concentrations of [BSA]},

(C) Graph of 1 / (A-A_0) vs. 1 / [BSA] concentration

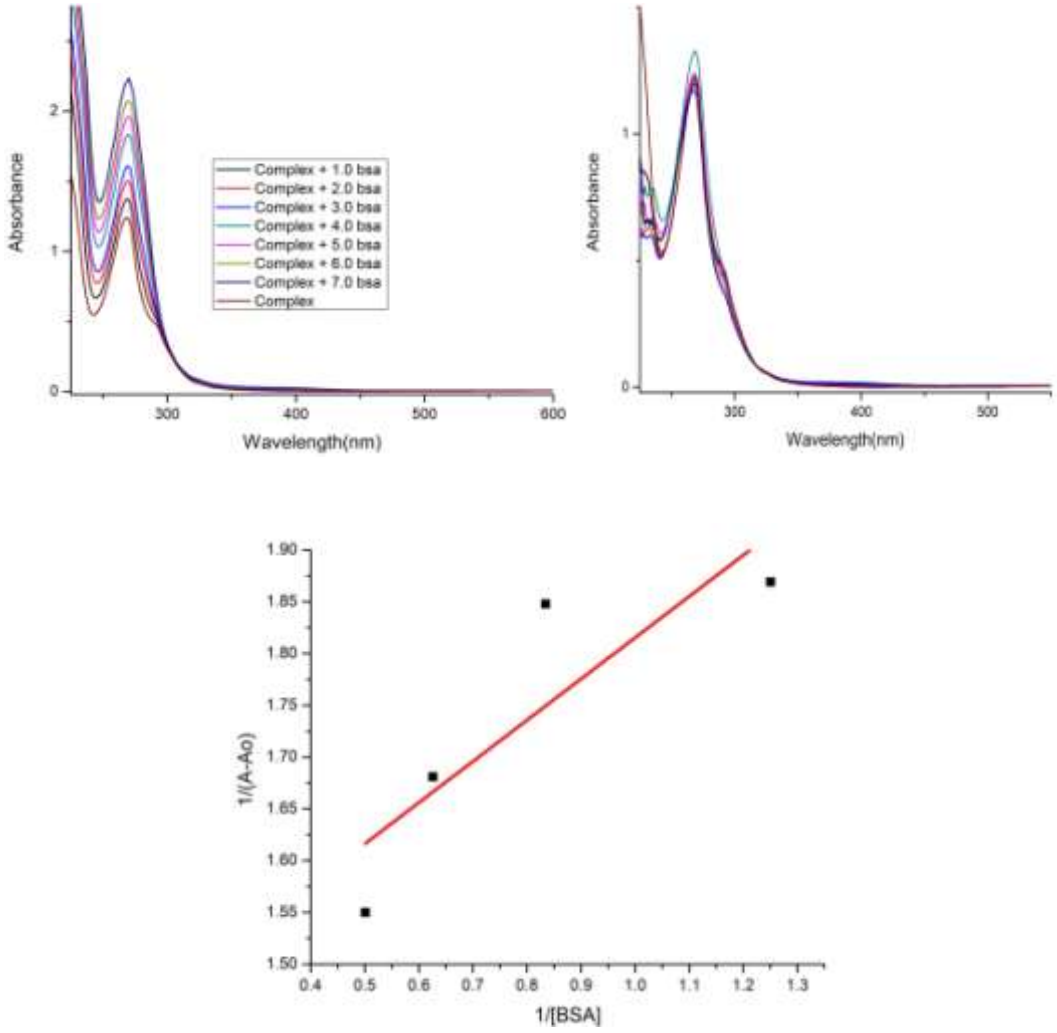

Fig. 152: (A) UV-vis titration graphs of complex [Cu(sal)(phen)]Cl (50 μM) with incremental [BSA] concentration in the range of 0 – 3 μM,

(B) Graph of {[BSA complex with [Cu(sal)(phen)]Cl – [Variant concentrations of [BSA]},

(C) Graph of 1 / (A-A_0) vs. 1 / [BSA] concentration

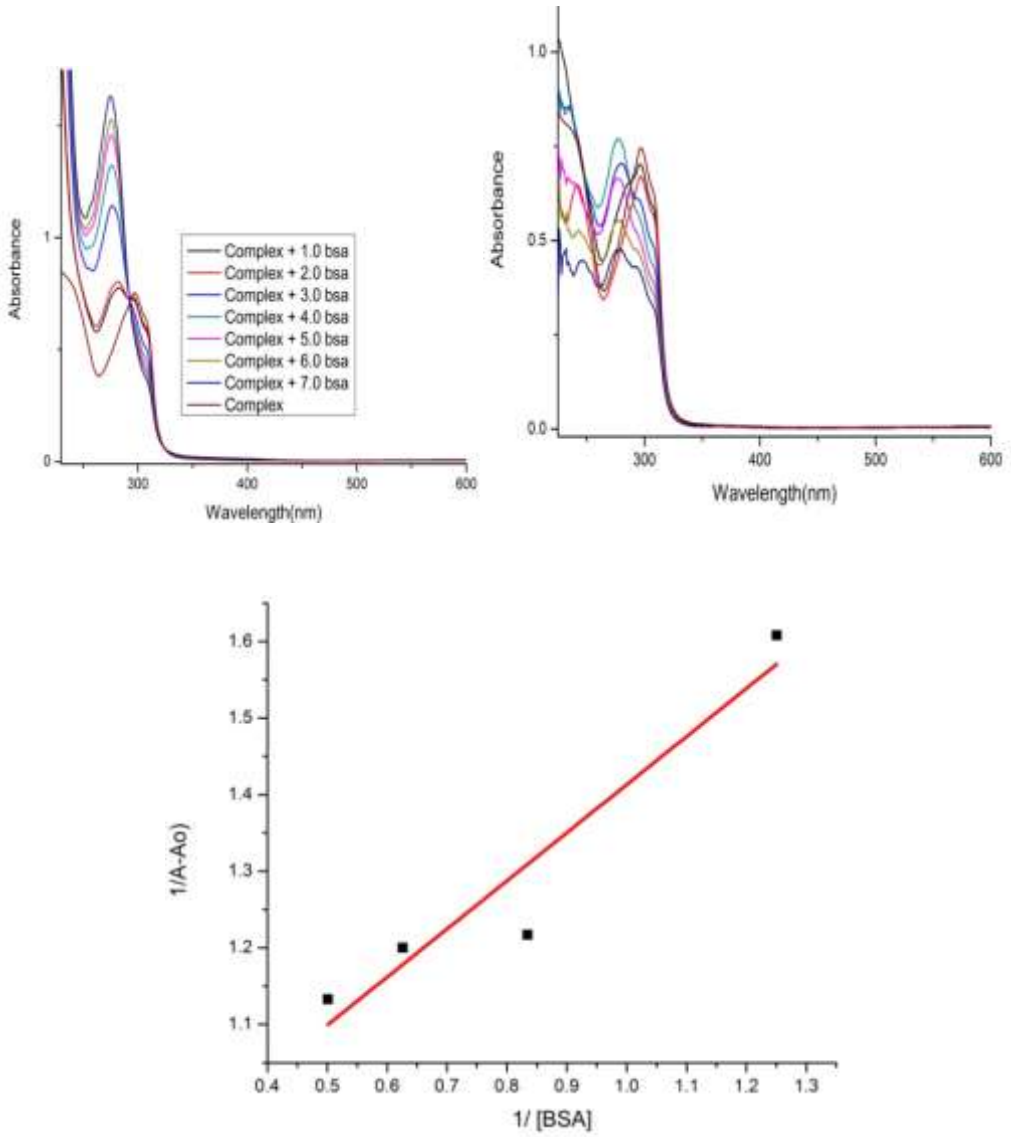

Fig. 153: (A) UV-vis titration graphs of complex [Cu(sal)(bpy)]Cl (50 μM) with incremental [BSA] concentration in the range of 0 - 3 μM,

(B) Graph of {[BSA complex with [Cu(sal)(bpy)]Cl – [Variant concentrations of [BSA]},

(C) Graph of 1 / (A-A_0) vs. 1 / [BSA] concentration

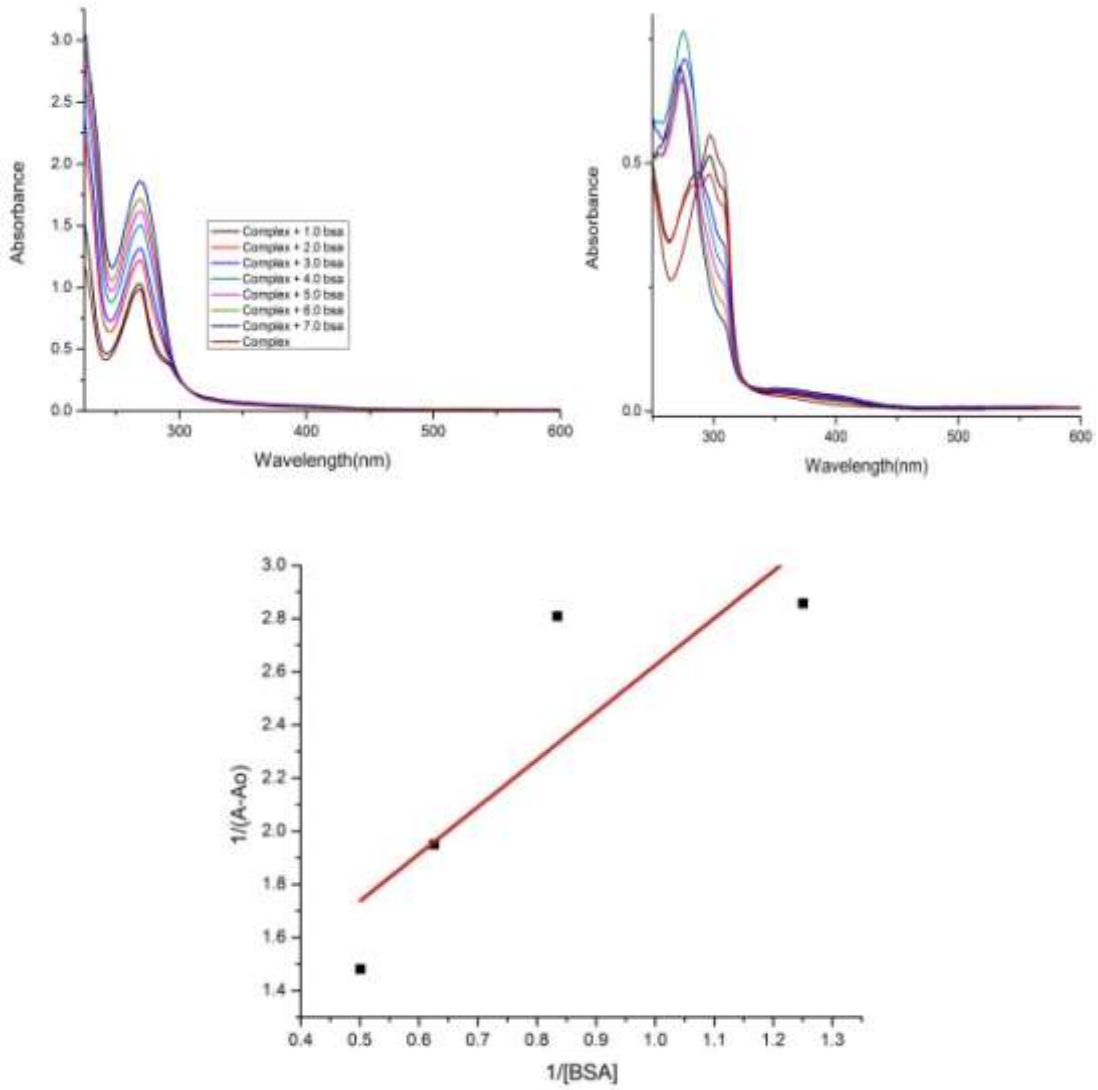

Fig. 154: (A) UV-vis titration graphs of complex [Cu(DNSA)(phen)]Cl (50 μM) with incremental [BSA] concentration in the range of 0 – 3 μM,

(B) Graph of {[BSA complex with [Cu(DNSA)(phen)]Cl – [Variant concentrations of [BSA]},

(C) Graph of 1 / (A-A_0) vs. 1 / [BSA] concentration

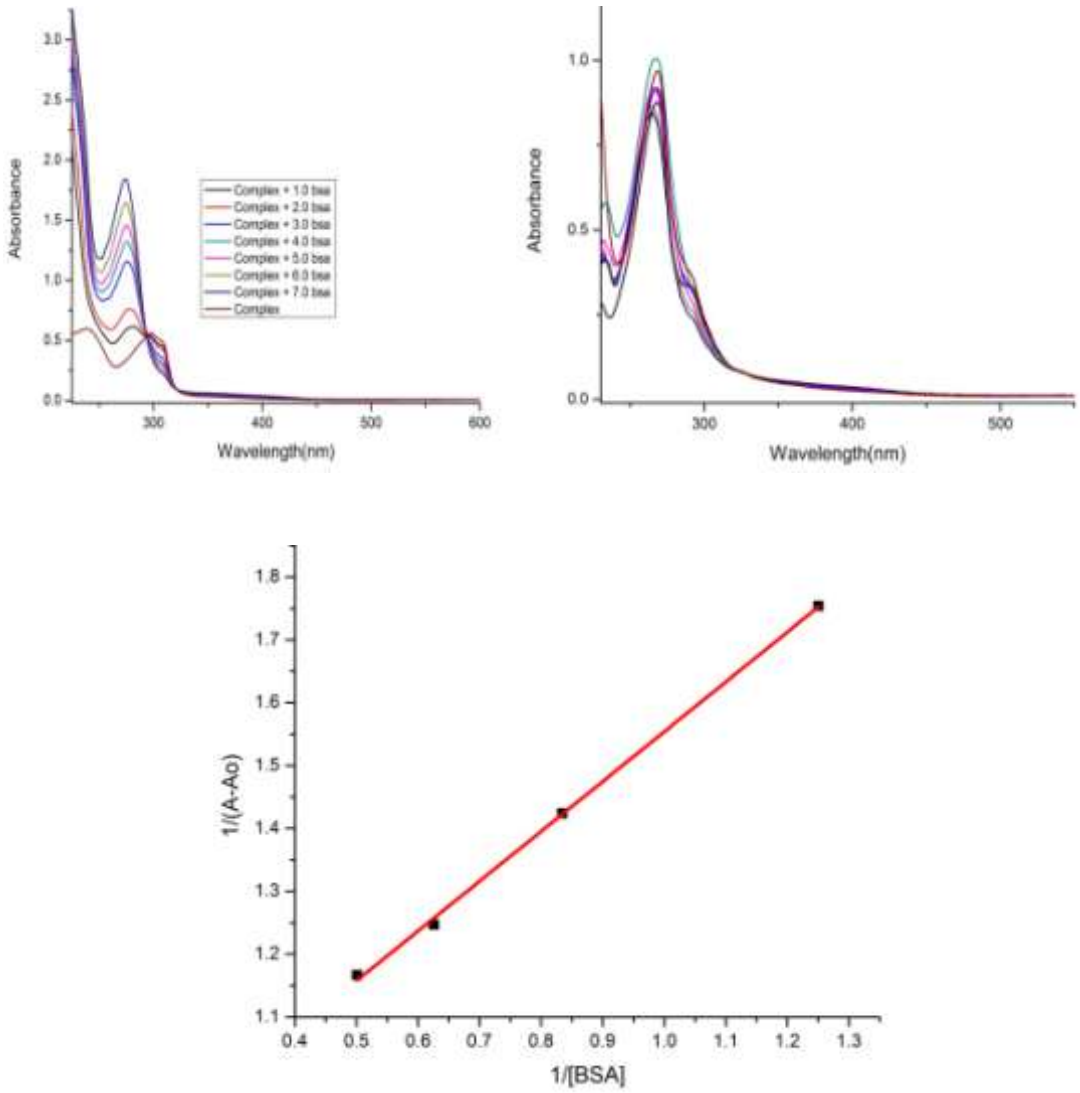

Fig. 155: (A) UV-vis titration graphs of complex [Cu(DNSA)(bpy)]Cl (50 μM) with incremental [BSA] concentration in the range of 0 – 3 μM,

(B) Graph of {[BSA complex with [Cu(DNSA)(bpy)]Cl – [Variant concentrations of [BSA]},

(C) Graph of 1 / (A-A_0) vs. 1 / [BSA] concentration.

5.5 Antimicrobial Activity

The same procedure is followed as in section 2.6 of Chapter 2.

Table 25: Antimicrobial activity of mixed ligand complexes(Concentration of 5 mg ml^{-1})

Complex	Average Inhibition Zone in diameter (mm) ± SD			
	Antibacterial Activity		Antifungal Activity	
	E. coli **(A)**	***S. aureus*** **(B)**	***A. niger*** **(C)**	***A. fumigatus*** **(D)**
[Zn(sal)(phen)]Cl ***(33)***	8.16±0.29	30.33±0.29	7.66±0.29	34.83±0.29
[Zn(sal)(bpy)]Cl ***(34)***	11.83±0.57	31.16±0.29	8.80±0.50	38.16±0.29
[Zn(DNSA)(phen)]Cl (***35)***	-	11.83±0.29	13.66±0.29	21.33±0.29
[Zn(DNSA)(bpy)]Cl ***(36)***	-	11.66±0.57	14.83±0.76	19.33±0.29
[Cu(sal)(phen)]Cl ***(37)***	25.10±0.36	32.16±0.29	40.33±0.29	33.33±0.29
[Cu(sal)(bpy)]Cl ***(38)***	19.83±0.29	30.0±0.50	20.16±0.29	16.0±0.50
[Cu(DNSA)(phen)]Cl ***(39)***	11.50±0.50	8.33±0.50	19.66±0.29	33.0±0.50
[Cu(DNSA)(bpy)]Cl ***(40)***	-	22.16±0.29	24.83±0.29	12.16±0.29
Amikacin	21.50±0.50	24.83±0.76	-	-
Fluconazole	-	-	23.66±0.57	22.66±0.29
DMSO	Nil	Nil	Nil	Nil

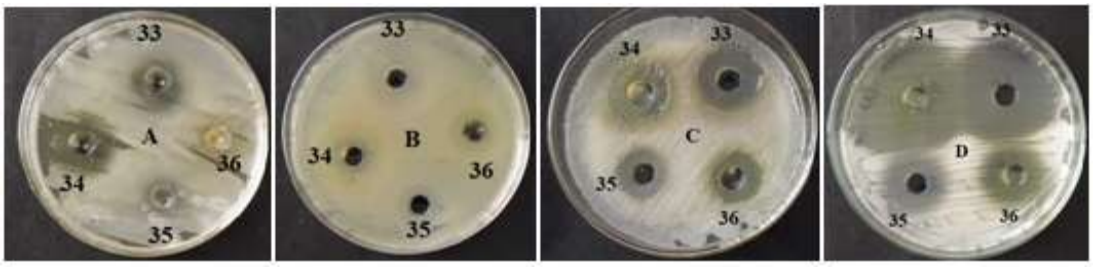

Fig. 156: Antimicrobial activity of mixed ligand complexes of zinc (*33* - *36*) (Alphabetical levels are according to table 25)

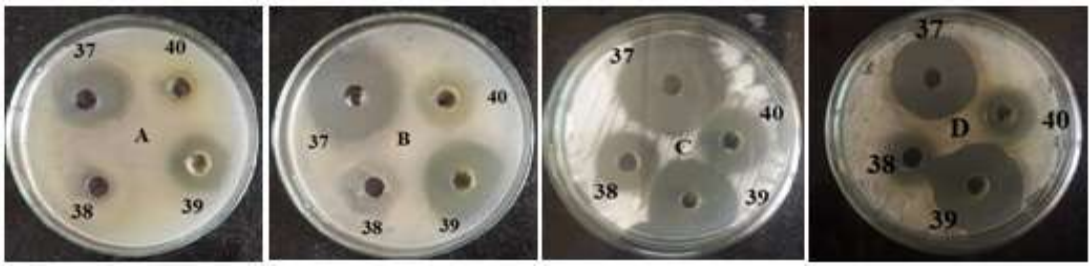

Fig. 157: Antimicrobial activity of mixed ligand complexes of copper (*37* - *40*) (Alphabetical levels are according to table 25)

5.6 Conclusion

In the present study, eight complexes of zinc / copper with salicylic acid or 3,5-dinitrosalicylic acid as primary ligand and 1,10-phenanthroline / 2,2'-bipyridine as secondary ligands have been reported. These complexes are characterized by UV-vis, FTIR and mass analysis to determine the mode of binding between metal and ligand. The C-H, C=O, M-N and M-O peaks in the IR spectra confirmed the synthesis of the complexes. The binding of phenanthroline and 2,2'-bipyridine to the metal complex is supported by n to π^* and π to π^* transitions in the UV spectra. On the basis of spectral studies, octahedral geometries have been proposed for all the complexes where salicylic acid / 3,5-dinitrosalicylic acid and secondary ligands i.e. diimine occupy the equatorial positions and axial positions may be occupied weekly by either anion or water molecules. Serum protein interaction of these complexes was studied by determining the values of binding constants using UV-vis titration techniques. The complexes bind moderately with binding constant value in the range of 10^4 - 10^5 M^{-1}. It is important to note here that the moderate affinity binding is consistent with the

role of serum proteins as carrier molecules for the delivery of the parent drug and its derivatives to target tissues. The antimicrobial activities of complex with salicylic acid as ligand are better as compared to complexes with 3,5-dinitrosalicylic acid as primary ligand. This may be due to – I effect of NO_2 group which decrease the charge density on ligand resulting in less charge transfer to free d - orbitals of metal ions. Thus polarity of the metal ion is reduced to a lesser extent which further decreases its antimicrobial activities.

5.7 Bibliography

[1] Mahmoud, W. H.; Mohamed, G. G.; El - Dessouky, M. M. I. M. Synthesis, characterization and in vitro biological activity of mixed transition metal complexes of lornoxicam with 1,10-phenanthroline, *Int. J. Electrochem. Sci.* **2014**, *9*, 1415–1438.

[2] Rosu, T.; Negoiu, M.; Circu, V. Complex combinations of Cu (II) with mixed ligands, *Analele Univ. Din Bucureşti – Chim.* **2005**, *I – II*, 153–159.

[3] Gurumoorthy, P.; Ravichandran, J.; Rahiman, A. K. Mixed - ligand binuclear copper(II) complex of 5-methylsalicylaldehyde and 2,2′-bipyridyl: Synthesis, crystal structure, DNA binding and nuclease activity, *J. Chem. Sci.* **2014**, *126*, 783–792.

[4] Choudhary, A.; Sharma, R.; Nagar, M. Synthesis, characterization and antimicrobial activity of mixed ligand complexes of Co(II) and Cu(II) with N, O / S donor ligands and amino acids, *Int. Res. J. Pharm. Pharmacol.* **2011**, *1*, 2251–176.

[5] Adelaide, O. M.; James, O. O. Antimicrobial, DNA cleavage and antitumoral properties of some transition metal complexes of 1,10-phenanthroline and 2,2'–bipyridine: A review, *Int. J. Res. Pharm. Biomed. Sci.* **2013**, *4*, 1160–1171.

[6] Shoaib, K.; Rehman, W.; Mohammad, B.; Ali, S. Synthesis, characterization and biological applications of transition metal complexes of [NO] donor Schiff bases, *J. Proteomics Bioinform.* **2013**, *6*, 153–157.

[7] Carrette, T. Effect of natural complexing agents on zinc accumulation in navy beans, Ph.D. Dissertation, Universiteit Gent, **2013**.

[8] Sreekanth, B.; Gopinath, S.; Pillai, V.; Shareef, I.; Reddy, J.; Vishnuvardhan, T.; Murali, K.; Sridhara, V. DNA binding and antimicrobial studies on Co(III) and Fe(II) metal complexes containing mixed ligands, *Res. J. Pharm. Biol. Chem. Sci.* **2013**, *4*, 217–225.

[9] Gomleksiz, M.; Alkan, C.; Erdem, B. Synthesis, characterization and antibacterial activity of imidazole derivatives of 1,10-phenanthroline and their Cu(II), Co(II) and Ni(II) complexes, *S. Afr. J. Chem.* **2013**, *66*, 107–112.

[10] Devereux, M.; Shea, D. O.; Mccann, M.; Geraghty, M.; Sullivan, L. O.; Mason, J. Insights into the mode of action of the anti-candida activity of 1,10-phenanthroline and its metal chelates, *Met. Based Drugs* **2000**, *7*, 185–193.

[11] Chen, X.; Liu, Y.; Peng, M.; Shi, S.; Zhang, Y. Differential effects of Cu(II) and Fe(III) on the binding of omeprazole and pantoprazole to bovine serum albumin: Toxic effect of metal ions on drugs, *J. Pharm. Biomed. Anal.* **2011**, *56*, 1064–1068.

[12] Bourassa, P.; Kanakis, C. D.; Tarantilis, P.; Pollissiou, M. G.; Tajmir - Riahi, H. A. Resveratrol, genistein, and curcumin bind bovine serum albumin, *J. Phys. Chem. B.* **2010**, *114*, 3348–3354.

[13] Souaya, E. R.; Khalil, M. M. H.; Ismail, E. H.; Bendas, E. R.; Neaz, O. S. Synthesis and characterization of ternary complexes of certain hydroxyl acids and their biological applications, *Res. J. Pharm. Biol. Chem. Sci. Synth.* **2014**, *5*, 18–30.

[14] Gunagi, S.; Nandibewoor, S.; Chimatadar, S. Interaction between a antiretroviral drug – Navirapine with bovine serum albumin: A fluorescence quenching and fourier transformation infrared spectroscopy study, *Res. J. Pharm. Biol. Chem. Sci.* **2011**, *2*, 814–826.

[15] Yiase, S. G.; Adejo, S. O.; Gbertyo, J. A.; Edeh, J. Synthesis, characterization and antimicrobial studies of salicylic acid complexes of some transition metals, *J. Appl. Chem.* **2014**, *7*, 4–10.

5.9 Annexure

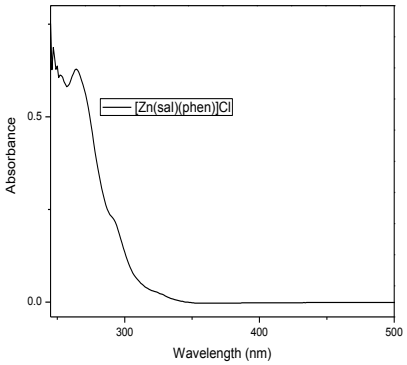

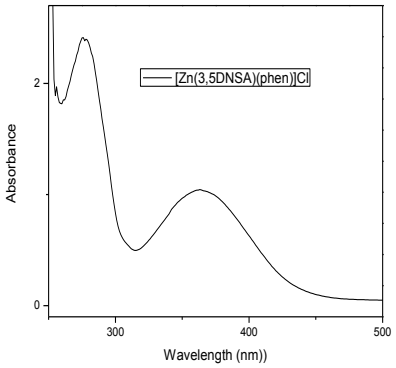

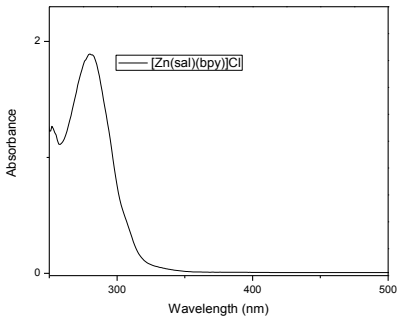

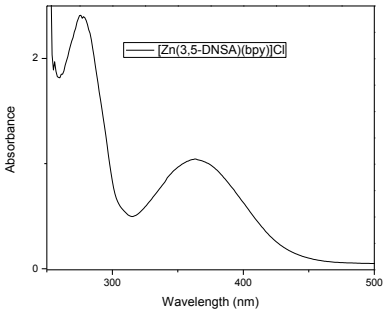

Annexure 5a: UV spectra of mixed ligand complexes of zinc

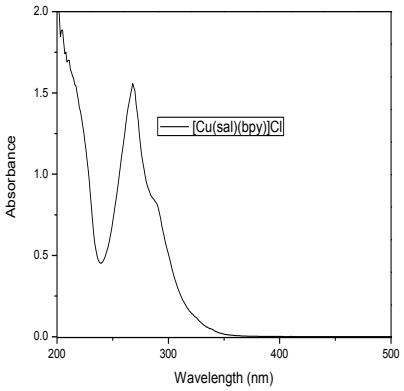

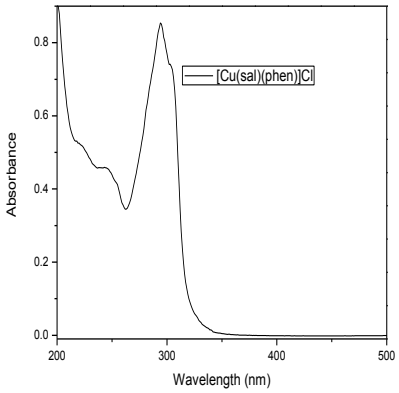

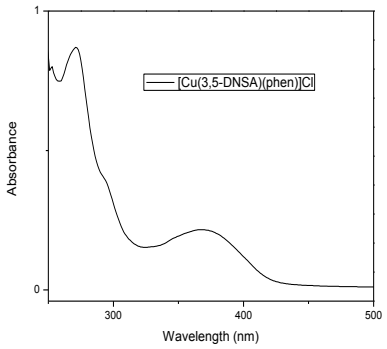

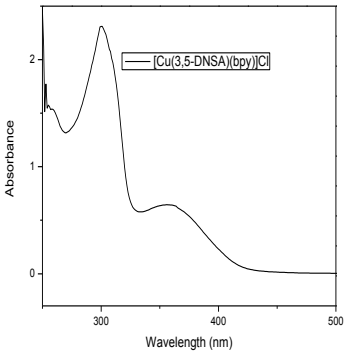

Annexure 5b: UV spectra of mixed ligand complexes of copper

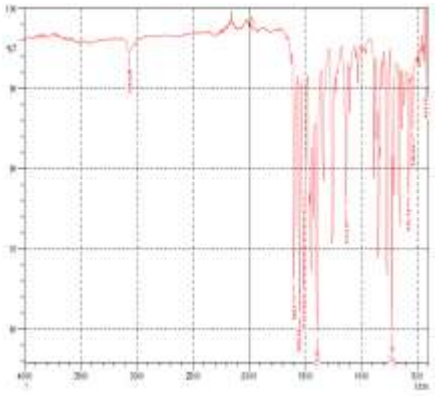

Annexure 5c: IR spectra of [Zn(sal)(phen)]Cl

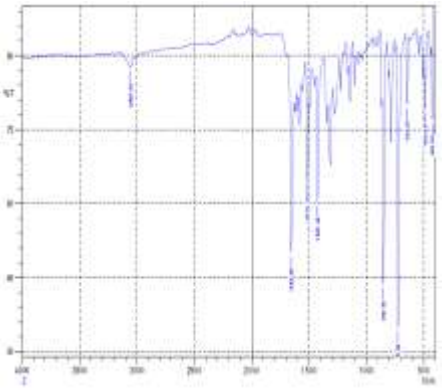

Annexure 5d: IR spectra of [Zn(DNSA)(phen)]Cl

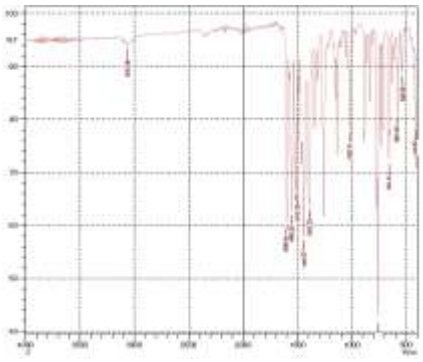

Annexure 5e: IR spectra of [Zn(sal)(bpy)]Cl

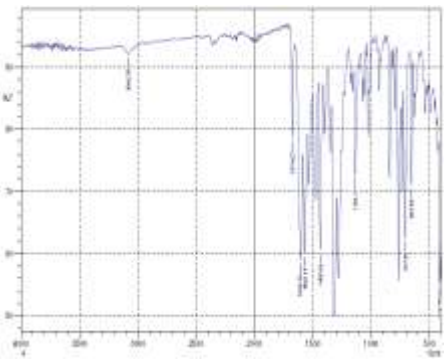

Annexure 5f: IR spectra of [Zn(DNSA)(bpy)]Cl

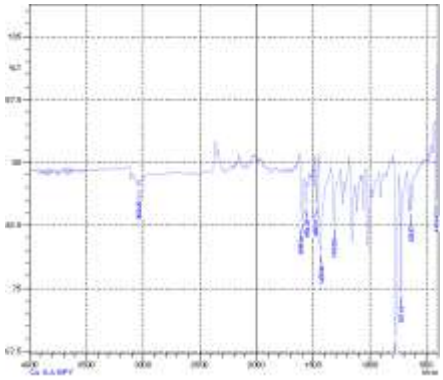

Annexure 5g: IR spectra of [Cu(DNSA)(bpy)]Cl

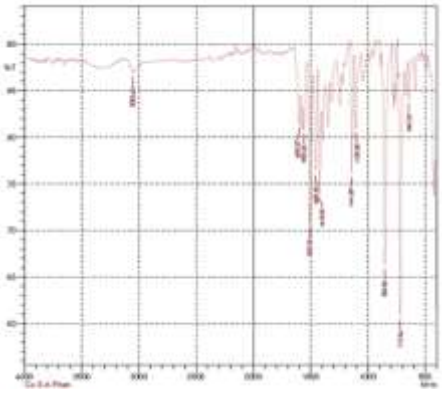

Annexure 5h: IR spectra of [Cu(sal)(phen)]Cl

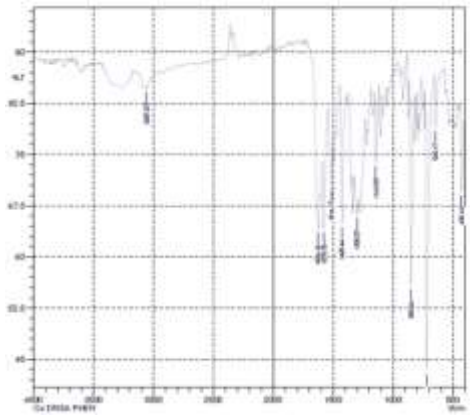

Annexure 5i: IR spectra of [Cu(DNSA)(phen)]Cl

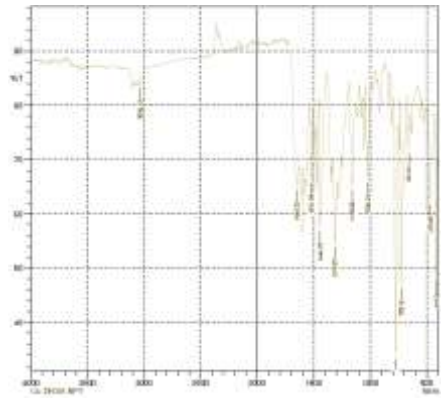

Annexure 5j: IR spectra of [Cu(DNSA)(bpy)]Cl